Formulation and evaluation of a post-processing algorithm for generating seamless, high resolution ensemble precipitation forecasts

by

Clive Pierce, Tamas Hirsch and Andrew C. Bennett

Met Office, Exeter, UK

Forecasting R&D Technical Report 550

November 2010

This page is intentionally blank.

© Crown copyright 2010

Contents

To update the table of contents, right click and select ‘Update field’

Executive Summary i

i. Background i

ii. Objectives i

iii. Potential benefits i

iv. Deliverables ii

v. Conclusions ii

Technical achievements ii

Scientific achievements iii

Scientific challenges to be addressed iii

vi. Recommendations iv

1. Introduction 1

1.1. Background 1

1.2. The user requirement and project scope 1

Design constraints 2

Use of UKV control and ensemble forecasts 2

Performance assessment criteria 2

1.3. Findings of the interim case study report 3

2. The challenges posed: key concepts and issues to address 4

2.1. Use of observations of precipitation 4

2.2. Choice of model domain, projection and resolution 4

2.3. A cascade modelling framework 5

Justification for the use of a cascade model 5

A description of the STEPS cascade model 6

Effects of the mixed, positively skewed distribution of rain rate 7

The form of decomposition used 7

© Crown copyright 2010

2.4. Issues surrounding the blending algorithm formulation, calibration, verification and implementation 7

2.4.1. Issues surrounding blending algorithm formulation 7

Formulation of an algorithm for generating ensembles of blended forecasts **.... 7**

Impact of differences in NWP modelled distributions of precipitation rate and those inferred from weather radar **..... 8**

2.4.2. Spatial and temporal variations in model skill – implications for blending algorithm performance 9

2.4.3. Calibration of the blended ensembles 9

2.4.4. Behaviour of the blended forecasts 10

2.4.5. Generation of synthetic precipitation fields with appropriate space-time statistical properties 11

The importance of noise in the blending algorithm **..... 11**

How to create synthetic precipitation fields with a given target spatial distribution **..... 11**

Implications of using spatially homogeneous noise **..... 12**

Choice of target distribution for noise generation **..... 12**

2.4.6. Choice of blended forecast configurations for evaluation 13

2.4.7. The choice of criteria used to assess the skill and realism of the blended forecasts 14

2.4.8. Operational constraints and implications for the blending algorithm. 14

3. Descriptions of the source models, pertinent aspects of their formulation and configurations used for high resolution ensemble runs 16

3.1. Overview 16

3.2. STEPS extrapolation nowcasts 16

3.3. Variable (1.5 km) resolution configuration of the UM 16

3.4. MOGREPS-R 17

3.5. Configurations of MOGREPS-R and UM: 1.5 models used for high resolution ensemble case studies 17

4. An algorithm for generating a seamless blend of model forecasts 20

4.1. Blending of the component forecasts 20

Choice of blended forecast configurations **..... 20**

© Crown copyright 2010

A MOGREPS-R downscaler 20

Formulation of a blended forecast incorporating an extrapolation nowcast, a UKV ensemble forecast and noise 21

Formulation of a blended forecast incorporating an extrapolation nowcast, UKV and MOGREPS-R ensemble forecasts and noise 23

Generation of control member blends 24

4.2. The extrapolation nowcast 25

4.3. Formulation of the noise 26

A parametric noise generator for downscaling and perturbing MOGREPS-R precipitation forecasts 26

A non-parametric noise generator for perturbing extrapolation and UKV precipitation forecasts 27

Temporal updating of the non-parametric and parametric noise fields 27

4.4. Advection of the noise and extrapolation cascades 28

4.5. Algorithm calibration 29

Overview 29

Estimation of $\hat{f}_k^{h,p}$ *and* $\hat{f}_k^{m,p}$ 29

Estimation of $\hat{r}_k^m(t+t_l)$ *and* $\hat{r}_k^h(t+t_l)$ 31

4.6. Configurations of the blending algorithms evaluated in this report 37

Use of spatially varying target means and variances 37

Control member forecast configurations 37

Ensemble members forecast configurations 38

4.7. Software design 38

The benefits of object-oriented programming 38

Design of the STEPS source code 39

Design of source code for blending a nowcast with multiple forecast components and noise 39

Unit testing 40

5. Evaluation of two configurations of blending algorithm 42

5.1. Approach 42

© Crown copyright 2010

5.2. Descriptions of the case study events 43

5.2.1. Case study selection 43

5.2.2. Case study 1 – 5–6 September 2008 43

***Synopsis* 43**

***Features of relevance to the blending algorithms* 44**

5.2.3. Case study 2 – 29 October 2008 46

***Synopsis* 46**

***Features of relevance to the blending algorithms* 47**

5.2.4. Case study 3– 18-19 November 2009 49

***Synopsis* 49**

***Features of relevance to the blending algorithms* 50**

5.2.5. Case study 4– 17 February 2010 52

***Synopsis* 52**

***Features of relevance to the blending algorithms* 53**

5.2.6. Case study 5– 25 March 2010 54

***Synopsis* 54**

***Features of relevance to the blending algorithms* 55**

5.3. Performance of the noise generation algorithms 57

5.3.1. Overview 57

5.3.2. Verification criteria 58

5.3.3. Performance of the non-parametric noise generator 58

***Generation of noise fields that evolve seamlessly from one target distribution to another* 58**

5.3.4. Performance of the parametric noise generator 65

5.4. Performance of the blending algorithms 69

5.4.1. Configurations of blended forecasts evaluated 69

5.4.2. Scope of the performance assessment 70

5.4.3. Verification criteria and their application 71

© Crown copyright 2010

Tests to demonstrate the generation of plausible, seamless blended forecasts 71

Tests to demonstrate the generation of skilful, blended control member and ensemble forecasts 71

The Fractions Skill Score 71

Measures of ensemble forecast skill 73

Brier Skill Score, resolution score and reliability score 74

Reliability (Attributes) diagram 75

Relative Operating Characteristic 76

Spread-Skill 77

5.4.4. Can the blending algorithms generate plausible, seamless blended forecasts? 79

A case study based evaluation of control member blends 79

Case study 5 – 25/03/2010 79

Case study 2 – 29/10/2008 89

Case study based evaluation of ensemble member blends 97

Case study 5 – 25/03/2010 97

Case study 2 – 29/10/2008 109

5.4.5. Can the blending algorithms generate skilful blended control and ensemble forecasts? 117

Requirements 117

Are the scale selective blended forecasts optimal over a range of scales 118

Control member blended forecasts 118

Ensembles of blended forecasts 120

Are the ensembles of blended forecasts well calibrated and do they demonstrate useful skill 125

Overview 125

Reliability (Attributes) plots 125

Brier Skill Score, resolution and reliability scores 129

ROC plots 133

Spread-skill 137

© Crown copyright 2010

6. Summary **143**

Formulation and behaviour of the various blending algorithm configurations **143**

Formulation of the noise generators **143**

Forecast evaluation – method of approach **144**

Performance of the noise generators **145**

Performance characteristics of the source models **145**

Performance of the control member blended forecasts **146**

The performances of ensembles of blended forecasts **147**

7. Conclusions **148**

7.1. Achievements **148**

Algorithm design, formulation and calibration **148**

Software design and functionality **148**

Performance of the noise generators **148**

Performance of two configurations of blended forecasts **149**

7.2. Challenges **149**

Impact of differing radar and model forecast distributions of precipitation rate **149**

Impact of co-existing widespread precipitation and showers **150**

Formulation and use of the noise in the blending **150**

Evaluation of the blended forecasts **150**

8. Recommendations **151**

9. References **152**

10. Appendices **155**

10.1. Appendix A.1 Case study oriented verification for the control member blended forecasts **155**

Case study 1 – 05/09/2008 ..... **155**

Case study 3 – 19/11/2009 ..... **162**

Case study 4 – 17/02/2010 ..... **169**

© Crown copyright 2010

10.2. Appendix A.2 Case study oriented verification for ensembles of blended forecasts..... 176

***Case study 1 – 05/09/2008* 176**

***Case study 3 – 19/11/2009* 184**

***Case study 4 – 17/02/2010* 192**

© Crown copyright 2010

Executive Summary

i. Background

This project, entitled "*Blending convective scale NWP with ensemble nowcasting*", is funded by the Public Weather Service and Environment Agency and DEFRA sponsored Flood and Coastal Risk R&D programme. It aims to integrate recent developments in storm scale Numerical Weather Prediction and nowcasting to produce a seamless, high resolution ensemble precipitation forecast suitable for driving hydrological models and for use by hydrologists and meteorologists for fluvial and pluvial flood prediction.

Current production strategy in the Met Office aims to deliver to customers *seamless* forecasts incorporating the best available (most skilful) model predictions (nowcasts, Numerical Weather Prediction model forecasts) at any given lead time. In support of this strategy, the "*Blending convective scale NWP with nowcast ensembles*" project has formulated, developed and evaluated a post-processing algorithm for generating seamless, high resolution (≤2km, 15 minute), ensemble precipitation forecasts with a range of several days.

This report reviews the key scientific challenges posed by the user requirements, details the formulation of several alternative configurations of blending algorithm and describes calibration work on these configurations. An in-depth, case study based appraisal of blended control member and ensemble forecasts is presented. This is followed by a summary of findings, conclusions and recommendations.

ii. Objectives

The objectives of the project were three fold:

- to formulate a blending algorithm for the generation of high resolution precipitation ensembles with a maximum range of two days;
- to compare the skill and realism of the forecasts produced by the blending algorithm with those of the individual source models;
- to synthesize results on algorithm performance, draw conclusions on benefits and make recommendations for possible improvements and operational implementation.

iii. Potential benefits

The blending algorithms described in this report offer the following potential benefits to operational hydro-meteorology:

- they provide the capability to generate seamless, high resolution (≤ 2 km) precipitation forecasts which optimally combine the skilful information content of radar based precipitation nowcasts and a range of NWP precipitation forecasts, whilst quantifying and conveying associated forecast uncertainty through the generation of ensembles (multiple forecast scenarios);
- they afford a means of handling configuration changes to operational NWP models so that these are made transparent to end users;

© Crown copyright 2010

- their seamless, high resolution precipitation forecasts are expected to provide earlier and improved warnings of heavy and extreme precipitation leading to earlier and superior pluvial and fluvial flood forecasts and warnings;

- their capability to generate large ensembles cheaply should facilitate the adoption of best practice, risk based approaches to pluvial and fluvial flood forecasting and warning.

iv. Deliverables

The project has delivered the following:

- a case study oriented archive of precipitation observations (radar, rain gauge) and forecasts from the regional configuration of the Met Office Global and Regional Ensemble Prediction System (MOGREPS-R), and the 4 km and 1.5 km configurations of the Unified Model (hereafter the UK4 and UKV respectively);

- an interim report reviewing the performance of source model precipitation forecasts from MOGREPS-R, the UK4 and UKV;

- a formulation paper describing a number of alternative, blending algorithm configurations and reviewing the associated scientific and technical challenges entailed in their development and implementation;

- C++ source code capable of generating high resolution (2km, 15 minute) control and ensemble precipitation forecasts by combining two or more precipitation forecasts (from Numerical Weather Prediction models or extrapolation nowcasts) with synthetically generated precipitation fields;

- FORTRAN-90 source code for evaluating the performance of the blended control and ensemble forecasts and their component model forecasts against radar and rain gauge observations of precipitation;

- This R&D report, incorporating a discussion of the scientific challenges, a description of and justification for the blending algorithms developed, a summary of the findings of a case study oriented evaluation of four configurations of blended forecasts, conclusions and recommendations.

v. Conclusions

Technical achievements

- The project has successfully developed, tested and evaluated object-oriented C++ software capable of generating the following products: 1) control and ensemble extrapolation precipitation nowcasts, 2) control and ensemble blends of an extrapolation nowcast and one or more NWP model precipitation forecasts, 3) ensembles of downscaled NWP model precipitation forecasts; 4) time series of synthetic precipitation fields (noise) with space-time statistical properties inferred from radar and/or a high resolution configuration of the Met Office's Unified Model.

© Crown copyright 2010

Scientific achievements

- A case study oriented performance appraisal of Met Office Numerical Weather Prediction model forecasts has confirmed that there are significant variations in the performance of MOGREPS-R and high resolution configurations of the UM between events as a function of spatial scale and forecast lead time. These findings support the use of a cascade modelling framework which allows the scale selective blending of these model forecasts to take account for scale and time dependent variations in forecast skill.

- It has been shown that a *non-parametric* noise generator based upon a scheme implemented within the Short Term Ensemble Prediction System (STEPS) is capable of producing synthetic precipitation fields whose space-time statistical properties evolve reliably and seamlessly from those of a weather radar inferred distribution of precipitation rate to those of a UKV precipitation forecast.

- Three configurations of blended forecasts have been formulated. Two of these have been evaluated: a downscaled MOGREPS-R precipitation forecast and a blend of a deterministic extrapolation nowcast, a UKV control forecast and non-parametric noise. Control (unperturbed) and ensemble (perturbed) forecasts have been generated from each configuration.

- In the case studies involving a single precipitation regime (widespread rain or showers) the blending algorithms and non-parametric noise generator can produce blended control and ensemble forecasts which evolve optimally and seamlessly from an extrapolation nowcast to a UKV forecast. In these circumstances, it has been shown that perturbed (ensemble), blended forecasts are well calibrated and are therefore a useful predictor of the skill of the control forecast.Scientific challenges to be addressed.

Scientific challenges to be addressed

- Evaluation of two experimental, ensemble runs of the UKV model has shown that UKV ensemble precipitation forecasts were over spread: the spread about the ensemble mean was found to be larger than the error in the ensemble mean measured relative to quality controlled radar and rain gauge observations. This behaviour is thought to be due to an excess of spread at the convective scales since UKV forecasts exhibit a tendency to over predict heavy convective precipitation relative to radar observations.

- A MOGREPS-R downscaling algorithm exploiting a *parametric* noise generation method demonstrated limited skill in adding plausible fine scale structures to coarse resolution MOGREPS-R precipitation forecasts. The variable performance of the algorithm is attributed to deficiencies in the noise generator. Reliable, high resolution target distributions for the noise beyond the range of the UKV model are needed to resolve this issue. Extension of the UKV control forecast to T+48h would suffice. This would enable the *non-parametric* noise generator to be used for downscaling.

- In cases involving co-existing widespread (frontal) and showery precipitation, the performances of the two blending algorithm configurations tended to be inferior. On these occasions, unrealistic fine scale precipitation structures were observed in the blended forecasts. This behaviour is largely due to the

© Crown copyright 2010

use of a spatially homogenous distribution for the noise. It is believed that performance can be improved substantially by modelling the distributions of widespread rain and showers separately. Further R&D is needed in this area.

vi. Recommendations

- The performances of the *non-parametric* noise generator and blended forecasts incorporating non-parametric noise are encouraging and justify further R&D to address outstanding issues related to the noise formulation, choice of target distribution for noise generation and cascade design. The implementation of a blended control and ensemble forecast with a range similar to that of the UKV (36 hours) is achievable with modest additional investment.

- With some enhancement to the formulation of the non-parametric noise, it is expected that at least one configuration of the blending algorithm – a combination of non-parametric noise, an extrapolation nowcast and UKV forecast – will perform on a par with the Short Term Ensemble Prediction System. It is recommended that improvements to the non-parametric noise generator be made in the remaining months of FY 10/11 with a view to conducting an operational trial of this blended forecast configuration in spring 2011.

- Given the above mentioned enhancement of the non-parametric noise generator, it should be straightforward to implement a MOGREPS-R downscaler with satisfactory levels of performance. This would be limited to the range of the UKV because the latter is required to provide a suitable target distribution for the noise.

- The project has identified systematic discrepancies between UKV forecast distributions of precipitation rate and those inferred from weather radar. There is evidence to suggest that these discrepancies may have been the cause of excessive ensemble spread in two experimental UKV ensemble precipitation forecasts supplied by the Convective-scale Ensembles Project. This finding warrants further investigation.

© Crown copyright 2010

1. Introduction

1.1. Background

The Environment Agency, responsible for fluvial (river) flood warning in England and Wales, has a requirement for precipitation forecasts with a horizontal resolution of at least 2 km and a range of at least several days. At present, no single Numerical Weather Prediction model forecast can satisfy this requirement and products with this specification are created subjectively by combining outputs from a precipitation nowcast with several NWP model precipitation forecasts, each having different performance characteristics. The resulting forecast loses spatial resolution at forecast ranges beyond 36 hours ahead because the longer range configurations of the Unified Model are run at coarser horizontal grid lengths.

The *Storm scale numerical modelling* project (Roberts, 2005) examined the ability of a 1 km, convective scale configuration of the Unified Model to predict convective rainfall. It concluded that a significant increase in forecast accuracy was achievable and that the benefits for fluvial and pluvial flood prediction could be enhanced further by post-processing the output to take account of forecast uncertainty.

Concurrent developments in nowcasting research led to the introduction of a new, ensemble precipitation nowcasting model, the Short Term Ensemble Prediction System (Bowler *et al*., 2006), in 2007. STEPS scale-selectively blends extrapolated observations with the most recent forecast from the 4 km configuration of the UM and a time series of synthetically generated precipitation fields (noise) with space-time statistical properties inferred from weather radar. The noise component serves to account for uncertainties in the evolution of the extrapolation and NWP forecast components and also to downscale the NWP forecast.

This project, entitled "*Blending convective scale NWP with ensemble nowcasting*", aims to integrate these developments to produce a seamless, high resolution ensemble precipitation forecast suitable for driving hydrological models and for use by hydrologists and meteorologists for fluvial and pluvial flood prediction and warning. The work is jointly funded by the Met Office's Public Weather Service programme and the Environment Agency and DEFRA sponsored Flood and Coastal Risk R&D programme.

1.2. The user requirement and project scope

The objectives of the project as defined in the Project Initiation Document are three fold:

- to formulate a blending algorithm for the generation of high resolution (≤ 2km) precipitation ensembles with a maximum range of two days;
- to compare the skill and realism of the forecasts produced by the blending algorithm with those of the individual source models;
- to synthesize results on algorithm performance, draw conclusions on its benefits and make recommendations for possible improvements and operational implementation.

© Crown copyright 2010

Design constraints

The first project objective implies the need to integrate precipitation forecasts from at least three sources: an observation (radar and satellite) based extrapolation nowcast, an ensemble of forecasts from the variable (≥1.5km) resolution configuration of the UM, and an ensemble of forecasts from the regional (24 km, North Atlantic and European) configuration of MOGREPS. There may be a future requirement to extend the range of the blended, downscaled forecasts using the global configuration of MOGREPS. Thus, the blending algorithm must be sufficiently flexible in design to allow the integration of a range of model forecasts with differing resolutions and performance characteristics.

Use of UKV control and ensemble forecasts

At the inception of the project, the focus of the proposed blending algorithm was placed on the combination of a single UKV model forecast with ensembles of extrapolation nowcasts and MOGREPS-R forecasts. However, following a year-long suspension of the project due to staff shortages in the JCHMR, the Board reviewed the project scope and recommended a change of emphasis. This prioritised the generation of blended precipitation forecasts incorporating ensembles of UKV precipitation forecasts: intervening developments in the *Convective Scale Ensembles* project had demonstrated a means of generating MOGREPS-R driven UKV ensembles, and 24 member ensemble UKV precipitation forecasts for two extreme precipitation events (5 September and 29 October 2008) were now available for the testing and evaluation of the blending algorithm.

When work on the project re-commenced in 2009, it was recognized that the limited availability of UKV ensemble precipitation forecasts would shape and constrain the ways in which the capabilities of the blending algorithm could be demonstrated and appraised. On their own, the UKV ensemble forecasts generated by the *Convective Scale Ensembles* project would not afford sufficient evidence to appraise all aspects of blending algorithm performance. Consequently, further case study data have been compiled from operational archives. The latter do not incorporate UKV ensembles but only quasi-operational UKV control runs driven using analyses and boundary conditions downscaled from the North Atlantic and European (12 km) configuration of the UM.

Performance assessment criteria

Evaluations of two, key aspects of blending algorithm performance have been given priority in this project. The first is concerned with demonstrating that the character of the blended precipitation forecasts is plausible and that their skill is at least as good as the individual forecast components which contribute to the blend (i.e. the extrapolation nowcast, a 1.5 km resolution UKV forecast, and a 24 km resolution MOGREPS-R forecast). The second aspect of performance relevant to demonstrating the viability of the algorithm relates to the skill of the blended ensembles. It must be shown that these ensembles are well calibrated and skilful relative to the control (unperturbed) forecasts.

© Crown copyright 2010

1.3. Findings of the interim case study report

In common with previous R&D projects such as the *Storm scale numerical modelling* project, case study investigations in 2008 (Pierce *et al*., ibid.) confirmed that there are significant variations in the performance of Numerical Weather Prediction models including MOGREPS-R and the variable resolution (1.5 km) configuration of the Unified Model (hereafter, the UKV model) between events and as a function of scale. These findings make the case for using a cascade based modelling framework which allows the blending of the component model forecasts to take account of scale dependent variations in forecast skill between model runs.

In order to produce a seamless forecast evolution, both in the blended control (unperturbed) forecast and in the blended ensemble forecasts, two alternative blending techniques were proposed. These assumed that a single UKV forecast (control run) would be available for blending with a given MOGREPS-R ensemble forecast, comprising a control member and 23 perturbed ensemble members. The first approach involved perturbing the position of large scales features in the UKV forecast to coincide with equivalent features in each MOGREPS-R ensemble member.

The second approach involved using the UKV control forecast to generate noise for perturbing the UKV forecast and downscaling each MOGREPS-R ensemble member. This technique was justified on the grounds that the UKV model is capable of generating forecast precipitation fields which exhibit structures similar to those seen in radar inferred precipitation fields over a wide range of scales. Owing to parallel advances in the generation of UKV ensembles by the *Convective-scale ensembles* project, this latter technique, rather than one focused on the application of large scale perturbations to a single UKV forecast, has been given priority in the blending algorithm formulation.

© Crown copyright 2010

2. The challenges posed: key concepts and issues to address

2.1. Use of observations of precipitation

The second objective in section 1.2 implies that we have knowledge of the true space-time distribution of instantaneous precipitation rate at the earth's surface. Clearly, this is not the case: our two main observation sources for precipitation are weather radar and rain gauge. Each is subject to significant, but very different sources of errors and their limitations in relation to quantitative precipitation estimation, forecasting and verification have been extensively reviewed in the literature (Joss and Waldvogel, 1990).

For the purposes of this project, radar is invaluable despite its many limitations. It is the only observation source providing an instantaneous, contiguous estimate of the spatial distribution of precipitation, albeit above the earth's surface. As such radar data form the starting point for extrapolation based precipitation nowcasts, are employed to model the space-time probability density function of instantaneous rain rate, and provide a means of assessing the extent to which the blended ensemble forecasts and their components are capable of representing observed precipitation structures over a wide range of scales.

Nonetheless, the importance of rain gauge data as an independent, surface observation source should not be underestimated. In this work we have used rain gauge data to evaluate some aspects of the performance of the blended ensembles alongside surface estimates of rain rate from the quality controlled Radarnet-IV radar composites.

2.2. Choice of model domain, projection and resolution

Currently, the Environment Agency receives a range of precipitation forecast products from the Met Office. The majority of these, including analyses of surface rain rate and STEPS (Bowler *et al*., 2006) precipitation nowcasts, are generated by the UK Post-Processing (UKPP) system. This system is dedicated to post-processing outputs from the 4km and variable (1.5 km) resolution configurations of the UM (hereafter, the UK4 and UKV respectively). At the time of writing (June 2010), the UKV is under going operational trials and is expect to supersede the UK4 as the operational, high resolution model for the UK by the end of 2010.

Figure 1 shows the geographical extent of the UK4 and UKV model domains and the sub-area within this for which operational, UKPP products are produced. This inner area becomes a rectangle with a width of 1096 km and a height of 1408 km when re-projected onto the Ordnance Survey's National Grid projection – a Tranverse-Mercator projection[1] employed for all UKPP products.

Given the project's intention of developing a blending algorithm formulation to supersede STEPS, it is appropriate to recommend the use of the existing UKPP domain and horizontal resolution (2km) for all blended precipitation forecasts. For the duration of the project, this choice has facilitated the

[1] The O.S. National Grid Projection is based upon the Airy, 1830 ellipsoid with a true origin at 2°W, 4 9° N (400 km E, -100 km N).

© Crown copyright 2010

development, testing and evaluation of the algorithm and is expected to simplify future, operational implementation because ingestion of existing operational radar and UKPP products should not require any additional software development.

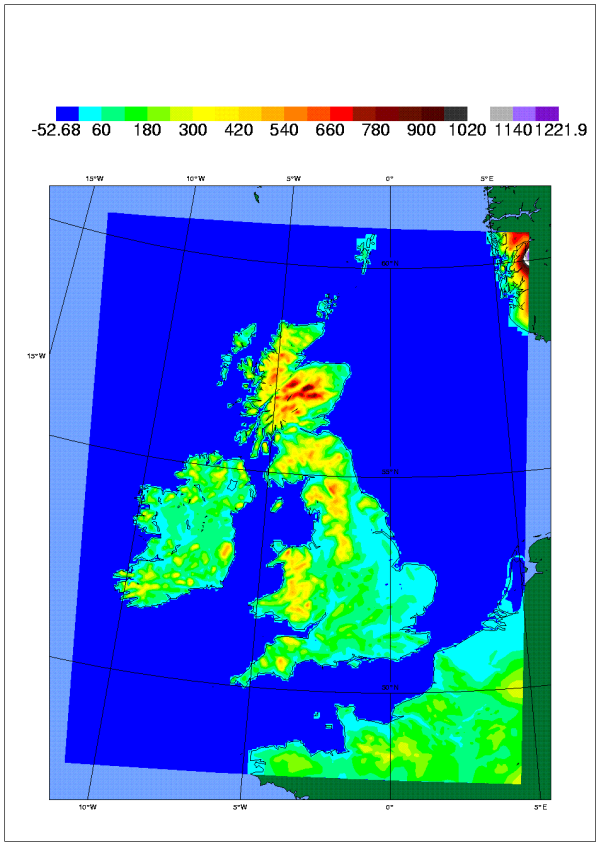

Figure 1 The geographical extent of the UK4 and UKV model domains with an inner, shaded area representing the UKPP domain.

2.3. A cascade modelling framework

Justification for the use of a cascade model

In this project we have chosen to exploit the cascade modelling framework utilised in STEPS. Cascade models provide an effective means of representing several fundamental properties of precipitation fields relating to their organisation in space and time. Firstly, precipitation fields exhibit so called *fractal* properties. This implies that they are not, as intuition might suggest, comprised of a collection of discrete objects each with a characteristic length scale (e.g. showers and fronts); rather, they are composed of structures on a continuum of scales ranging from the synoptic (~1000 km) down to scales finer than those of individual convective (shower) clouds (e.g. Marsan and Schertzer, 1996). Secondly, empirical studies have shown that a power law relationship exists between the typical life time of precipitation structures and their degree of spatial coherence (Schertzer *et al*., 1997, Zawadzki *et al*.,1994).Thus, synoptic scale bands of frontal precipitation are, on average, much longer lived than individual showers.

© Crown copyright 2010

A description of the STEPS cascade model

The cascade model exploited in this work and in STEPS comprises 8 levels. A field of instantaneous rain rate (estimated from radar or generated by a NWP model), with dimensions of *L* by *L* grid points, is decomposed into 8 component fields (levels) representing the variability in the field originating from a discrete set of horizontal scales, $L_k = 2^{N-1} \diagup 2^k$, where the largest scale represented is 512 km. Expressed in units of rain rate (e.g. mm h^{-1}), the cascade takes the form:

$$R_{i,j}(t) = \prod_{k=0}^{N-1} X_{k,i,j}(t) \text{ for } i=1,..,L,\ j=1,..,L,\ L=2^{N-1} \quad (1),$$

where *N* is the number of component levels in the cascade, and the k^{th} field in the cascade, $X_k(t)$, represents the variability in the original field with frequencies, ω_k, in the range $\frac{2^{k-1}}{L} < \omega_k < \frac{2^k}{L}\ pixel^{-1}$ at time, *t*.

From a modelling perspective, it is more convenient to work in units of $10\log_{10}(R+c)$ or decibels of rain rate (hereafter, *dBR*) because the log transformation produces a probability distribution closer to a Normal distribution, and the addition of *c* (an arbitrary small, positive number) simplifies the treatment of no-rain areas. In *dBR,* the cascade becomes additive:

$$dBR_{i,j}(t) = \sum_{k=0}^{N-1} X_{k,i,j}(t) \text{ for } i=1,..,L,\ j=1,..,L,\ L=2^{N-1} \quad (2),$$

where N=8.

The field of surface rain rate expressed in dBR is transformed into the frequency domain by means of a Fast Fourier Transform. Each level, $X_k(t)$, of the cascade is retrieved using a Gaussian window based band-pass filter to pass the appropriate frequencies. An inverse transform is performed to return each Fourier component of the original field back into the spatial domain. Finally, the cascade levels are normalised using

$$Y_{k,i,j}(t) = \frac{X_{k,i,j}(t) - \mu_k(t)}{\sigma_k(t)} \quad (3),$$

where $\mu_k(t)$ and $\sigma_k(t)$ are the mean and standard deviation of the k^{th} level respectively. The $Y_{k,i,j}(t)$ are referred to as the component levels of the cascade where the subscripts, *i* and *j*, are references to grid point values in a cascade level field.

Decomposed fields of this form can be generated from radar inferred precipitation fields (denoted by $Y^e_{k,i,j}(t)$, where the superscript, *e*, refers to extrapolated radar), and UKV ($Y^h_{k,i,j}(t)$, where superscript, *h*, is shorthand for high resolution) and MOGREPS-R ($Y^m_{k,i,j}(t)$) forecasts. These cascade level fields form the building blocks of the blended ensembles and will be referred

© Crown copyright 2010

to throughout this report in relation to the blending algorithm formulation and noise (synthetic rainfall) generation. In the following sections note that the subscripts, *i* and *j*, are omitted from cascade based formulae to simplify presentation.

Effects of the mixed, positively skewed distribution of rain rate

Precipitation fields exhibit a mixed distribution comprising dry areas with a precipitation rate of 0 mm/h and wet areas with a positively skewed distribution of non-zero values. The conversion of precipitation fields to units of $10\log_{10}(R+c)$ removes the zeros and reduces the skewness. However, as a consequence of this conversion and the use of a threshold, *c*, some of the variability in the original precipitation field will be lost, resulting in increased variability at the smallest scales (bottom of the cascade). This effect is an unavoidable consequence of the discontinuous nature of precipitation fields and must be accounted for when generating cascades of noise (Bowler *et al*., 2006).

The form of decomposition used

The FFT based decomposition described here and used in STEPS is just one of a number of viable cascade decomposition algorithms. Other forms are described in the literature. For example, Perica and Foufoula-Georgiou (1996) used a Haar wavelet decomposition to downscale precipitation forecasts from a mesoscale NWP model. However, there is little to be gained from using alternative forms of decomposition such as the wavelet. All such algorithms suffer from limitations in relation to space-frequency localisation or ringing (Mallat, 1989), and the existing algorithm is computationally efficient.

2.4. Issues surrounding the blending algorithm formulation, calibration, verification and implementation

2.4.1. Issues surrounding blending algorithm formulation

Formulation of an algorithm for generating ensembles of blended forecasts

The formulation paper (Pierce, 2007) proposes a number of alternative, cascade based blending algorithms of the form:

$$Y_k^p(t+t_l) = \sum_{c=1}^{N} w_k^c(t+t_l) Y_k^{c,p}(t+t_l) + w_k^n(t+t_l) Y_k^{n,p}(t+t_l) \qquad (4),$$

where the blended, normalised cascade level field for level, *k*, for ensemble member, *p*, denoted by $Y_k^p(t+t_l)$, is a weighted sum of *N* cascades of component forecast fields, c_1 to c_N (where *N* ranges between 1 and 3) and a cascade of noise. The weights, $w_k^{c=1,N}(t+t_l)$, are a function of the skill of these forecast components, estimated on each cascade level (scale). The noise cascade, $Y_k^{n,p}(t+t_l)$, serves to perturb precipitation features which lack skill and adds structure to the blended forecasts at scales which lack it. The weights assigned to the

© Crown copyright 2010

cascade level noise fields are designed to preserve the standard deviation of the blended cascade level forecast fields.

$Y_k^p(t+t_l)$ is collapsed back into a single field in units of *dBR* using

$$dBR_{i,j}^p(t+t_l) = \mu^p(t+t_l) + \sum_{k=0}^{N-1} \sigma_k^p(t+t_l) \cdot Y_{k,i,j}^p(t+t_l) \quad (5),$$

where the field mean of the collapsed, blended cascade for the p^{th} ensemble member, $\mu^p(t+t_l)$, is a weighted blend of the field means of the component forecasts, c_1 to c_N

$$\mu^p(t+t_l) = \sum_{c=1}^{N} \left[\frac{w_k^c(t+t_l)}{\sum_{c=1}^{N} w_k^c(t+t_l)} \mu^c(t+t_l) \right] \quad (6),$$

and the standard deviations of the cascade level, blended forecast fields, $\sigma_k^p(t+t_l)$, are a weighted combination of the standard deviations of the same components forecasts

$$\sigma_k^p(t+t_l) = \sum_{c=1}^{N} \left[\frac{w_k^c(t+t_l)}{\sum_{c=1}^{N} w_k^c(t+t_l)} \sigma_k^{c,p}(t+t_l) \right] \quad (7).$$

The collapsed, blended forecast field is converted back to rainfall rate and the threshold previously applied when converting to dBR is subtracted (see section 2.3 above).

Impact of differences in NWP modelled distributions of precipitation rate and those inferred from weather radar

The precipitation forecast fields generated by NWP models, including the UM, lack structure (variance) at scales below those adequately resolved (see for example Harris *et al*., 2001). Bowler *et al*. (ibid.) proposed adjusting the cascade level standard deviations of the NWP precipitation forecasts to correct for biases relative to radar. They computed a climatology of the ratio of radar and NWP model cascade level standard deviations

$$\hat{f}_k^{NWP} = \left\langle \frac{\sigma_k^r}{\sigma_k^{NWP}} \right\rangle \quad (8),$$

where σ_k^r denotes the standard deviation of decomposed radar data for cascade level, *k*, and σ_k^{NWP} denotes the standard deviation of an equivalent, time synchronous NWP model forecast. For the calibration of STEPS, this expression was evaluated using a month's worth of data by selecting only samples for which more than 5% of the area of radar coverage was wet. A similar approach has been adopted for adjustment of the cascade level standard deviations of MOGREPS-R ($\sigma_k^{m,p}$) and UKV ($\sigma_k^{h,p}$) precipitation forecasts in two configurations of

© Crown copyright 2010

the blending algorithm (see section 2(v) below for further details). In these cases, the adjustments, $\hat{f}_k^{h,p}$ and $\hat{f}_k^{m,p}$, are identical for all ensemble members and have been estimated using a month's worth of UKV and MOGREPS-R control member forecasts.

2.4.2. Spatial and temporal variations in model skill – implications for blending algorithm performance

In STEPS, single, field wide estimates of the current skills of the cascade level extrapolation nowcast and UKV forecast fields are used to calculate the weights assigned to them in the blend. However, evidence from various case study investigations (e.g. Golding *et al*., 2005) demonstrates that the skill of high resolution configurations of the Unified Model can vary geographically over a modelling domain at any given point in time. This is consistent with the intuition that the scale of the predominant forcings responsible for generating precipitation may vary regionally according to the presence or absence of any synoptic scale or mesoscale weather systems.

The implication is that the skill of the component models in the blended ensemble may need to be estimated on a grid rather than as a domain average skill, since the latter cannot reflect any regional variations in the performance of the UM or the extrapolation nowcast. This issue is a challenging one to address in the context of the proposed blending methodology, since the blending of cascades using spatially varying weights will be computationally expensive.

Furthermore, there is the related issue of how to compute model skill climatologies. It would seem unlikely that a spatially varying model skill climatology can be justified, except perhaps in regions of complex orography where local, surface forcings routinely play a significant role in the generation of precipitation. Therefore, spatially varying estimates of current forecast skill should probably relax to a single, field wide skill climatology with advancing lead time.

The reliance on cascade level skill climatologies for each model forecast component at longer forecast lead times raises an important question: whether or not the use of such climatologies will be adequate to produce skilful, blended ensembles with appropriate spread. In other words: to what extent does the skill of a forecast on a given cascade level deviate from climatology in space and time? If substantial deviations between actual skill and estimated skill arise, the performance of the blended ensemble forecasts will be adversely affected.

2.4.3. Calibration of the blended ensembles

For a well calibrated ensemble forecast, the ensemble spread should provide an accurate prediction of the error in the ensemble mean at any given instant (Bowler *et al*., 2007). In ensemble NWP, the spread in the evolution of different members of an ensemble forecast arises from the cumulative effects of initial condition perturbations applied to the analysis (the starting point for a NWP forecast) and, in some cases (e.g. MOGREPS), from stochastic perturbations applied to tuneable

© Crown copyright 2010

parameters in the various parameterisation schemes. Spread-skill can vary between model runs and post-processing of NWP ensembles is often required to produce well calibrated forecast probabilities for areas of point locations.

By contrast, the spread in the blended ensembles generated using (4) can be controlled (increased) directly by perturbing the cascade of blended forecasts with different proportions of noise. Noise is injected into each level of the cascade to represent that fraction of the variance in the radar inferred precipitation field not explained by the component forecasts (extrapolation, UKV and MOGREPS-R). A new estimate of this unexplained variance will be produced on each cascade level every time the blending algorithm is run, from estimates of the current skill of each model forecast on each level. As a result, the spread in the blended ensembles will vary in response to these variations in the estimated skill of the component forecasts. Thus, the calibration of the blended ensembles is an intrinsic part of the blending algorithm design.

2.4.4. Behaviour of the blended forecasts

The relationship between ensemble spread and model skill as a function scale (cascade level) is central to understanding the behaviour of (4). The estimated skill of the component forecasts in the blend on each cascade level will determine the contribution made by the noise on the hierarchy of scales represented by the cascade, and consequently, the degree to which the component forecasts at each scale are perturbed. Since NWP model forecast skill tends to decline markedly with decreasing scale below about 100 km (Bowler *et al*., 2006; Roberts and Lean, 2008), the influence of the noise will increase substantially towards the bottom of the cascade. As a result, differences between blended ensemble forecast members will be greatest at these scales.

Verification of MOGREPS-R precipitation ensembles confirms that the prediction of synoptic precipitation features is generally well handled: reliability diagrams for 6h rain accumulation > 0.3 mm show the performance of MOGREPS-R T+36 h ensemble forecasts to be close to perfect reliability in the winter months (Bowler *et al*., 2007). Similar behaviour is expected of the MOGREPS-R driven UKV ensembles evaluated in this project since they are *downscale* ensembles. This implies that the MOGREPS-R and UKV ensembles probably already have sufficient spread (at least on average in the winter months) at the top cascade level (~500 km); hence, there should be little need to perturb the blended forecasts at this scale, at least at lead times shorter than 36 hours.

In the context of generating high resolution, ensemble precipitation forecasts, the adequate representation of ensemble spread at the convective and meso scales (< ~100 km) is essential. MOGREPS-R cannot resolve convection explicitly, and although the UKV does resolve convection, it lacks skill in predicting the evolution of individual showers (Robert and Lean, ibid.). Thus, in the short range (< 36 hours), the bulk of the uncertainty in MOGREPS-R and UKV

© Crown copyright 2010

precipitation forecasts normally derives from uncertainties in the evolution of convective and mesoscale precipitation features. The injection of noise with appropriate space-time statistical properties, $Y_{k,i,j}^{n,p}(t+t_l)$, into the blended cascade is intended to address these deficiencies: it serves to downscale the MOGREPS-R and UKV precipitation forecasts adding variance (structure) at scales which lack it, and also to perturb features with low skill.

2.4.5. Generation of synthetic precipitation fields with appropriate space-time statistical properties

The importance of noise in the blending algorithm

If the blended forecast evolution is to be seamless and plausible, then the space-time statistical properties of the noise must be formulated in such a way that when the noise is combined with the other forecast components, the resulting, composite distribution of rain rate is not substantially different in character from the radar or UKV forecast distributions. This should be achievable if the target distributions used to generate the noise are a radar based UKPP rain analysis or a UKV precipitation forecast. However, there is no obvious high resolution, target field for use in downscaling MOGREPS-R ensemble precipitation forecasts beyond the forecast range of the UKV model runs (36 hours). This issue is discussed below.

How to create synthetic precipitation fields with a given target spatial distribution

Synthetic precipitation fields (noise) can be generated using a similar FFT decomposition to that employed by the cascade model (see section 2.3 above). The FFT of a radar based UKPP rain analysis or UKV precipitation forecast (referred to as the target field) can be used to create fields which exhibit structures similar to those of radar or UKV forecast precipitation fields. Two approaches to noise generation have been developed for use in STEPS. Both have been employed in the blending algorithm configurations evaluated in this report, and are described in more detail below.

The first (parametric) technique, assumes that the Power Spectral Density (PSD) of the target precipitation field can be approximated by a power law relationship between frequency and PSD. This approach has the advantage that the variance (variability) at any given spatial scale can be inferred even if there is insufficient information content in the target field at this scale. However, the power law assumption provides only an approximation of the PSD of the true precipitation field: if the latter deviates from this so called *scaling behaviour*, this cannot be replicated by the noise. Furthermore, reliance on a radially averaged PSD constrains the noise to be isotropic in form (i.e. only spherical structures can be produced).

A second approach involves using the FFT of the target distribution as a filter. This has the advantage that the PSD of the target field can be replicated without making any assumptions about the shape of the PSD. This non-parametric technique is also capable of generating

© Crown copyright 2010

noise which reproduces any anisotropic structures in the target field. Thus, if the target precipitation field contains a band of precipitation associated with a weather front, similarly shaped structures will be generated in the noise.

Both parametric and non-parametric noise generators produce synthetic precipitation fields with spatially uniform (homogenous) statistical properties. The implications of this limitation are discussed below.

Implications of using spatially homogeneous noise

Given the size of the UKPP domain (1096 km E-W by 1408 km N-S) there are likely to be numerous occasions when frontal precipitation and showers co-exist in different areas. In these circumstances, spatially homogeneous noise can only represent the average spatial statistical properties of frontal and convective precipitation; it cannot generate a mixture of features with the distinct characteristics of either of these precipitation types. This limitation may result in the addition of unrealistic perturbations to the component forecasts in the blend, resulting, for example, in too much variance being injected in frontal precipitation bands. However, any viable solution to this problem, such as maintaining separate noise cascades representative of fronts and showers, is likely to prove computationally expensive.

Choice of target distribution for noise generation

In STEPS, the most recent UKPP rain analysis provides the target distribution for the noise fields used to generate ensembles with a range of 6 hours. For longer forecast lead times, reliance on a target distribution inferred from radar observations is unlikely to be appropriate. In this project, the additional use of UKV precipitation forecasts to generate UKV like noise fields for longer forecast lead times is recommended. This is justified on the grounds that the power spectra of UKV precipitation forecasts are similar to those of precipitation fields inferred from weather radar (Pierce *et al*., 2008). However, this provides only a partial solution to the noise generation problem since UKV forecasts are not available beyond T+36h and noise fields will be required to downscale MOGREPS-R forecasts with a range of at least 48 hours.

A 2km resolution target distribution for downscaling MOGREPS-R ensemble precipitation forecasts could be based upon the last available (T+36h) UKV forecast, but such an approach would not be sufficiently robust if the character of the precipitation field were to evolve significantly between T+36h and T+48h. One alternative could involve using a climatological target distribution representative of fronts or showers. However, this might be even more prone to error in situations where the precipitation field is evolving rapidly; it would also require a reliable method for identifying and discriminating frontal and showery precipitation. A third technique involves estimating the desired power spectrum of the noise using the 24 km resolution MOGREPS-R ensemble precipitation forecasts as the target field. The Power Spectral Density at all relevant scales is approximated by fitting

© Crown copyright 2010

a straight line with constant slope to the PSD of the MOGREPS-R forecasts.

This last solution, referred to as the *parametric* noise generation method in section 4.3 below, is appealing because it exploits the information content of the forecast field to be downscaled. However, it is unclear just how robust this technique will prove. In STEPS, its use is confined to situations when there is insufficient precipitation to establish a sensible noise distribution by other means (a *non-parametric* noise generator is used when precipitation covers more than 5% of the UKPP domain).

2.4.6. Choice of blended forecast configurations for evaluation

The formulation paper (Pierce *et al*., 2007) considers a number of alternative configurations of blended forecasts. These include blends of an extrapolation nowcast, a single control or ensemble member UKV forecast and noise, with and without a MOGREPS-R control or ensemble member forecast, and a standalone MOGREPS-R downscaler. Although the ultimate aim is to generate blended ensembles from representative members of clustered UKV and MOGREPS-R ensemble forecasts, the evaluations of two configurations of blending algorithm presented in this report are focused on blends incorporating UKV and MOGREPS-R control member forecasts. This has been necessary because UKV ensemble forecasts were available for only two case study events.

As discussed in section 4.3 below, several different noise generation techniques, referred to as *parametric* and *non-parametric*, are proposed for perturbing and downscaling the blended forecasts. This is because there is no obvious 2km resolution target distribution of rain rate for noise generation beyond the forecast range of the UKV model (T+36h), whereas, at shorter lead times, either the 2km resolution, radar based UKPP rain analyses or 2 km interpolated UKV forecasts can be employed as the target. Thus, the noise generation method recommended for downscaling and perturbing MOGREPS-R forecasts beyond T+36h (the *parametric* method) is distinct from that recommended for a similar treatment of UKV and extrapolation forecasts at shorter lead times (the *non-parametric* method).

Given this dichotomy of approaches to noise generation, it is appropriate to evaluate blended forecasts incorporating an extrapolation nowcast, a UKV forecast and non-parametric noise separately from blended forecasts incorporating a MOGREPS-R forecast and parametric noise. Note that the evaluation of blends of extrapolation, UKV, MOGREPS-R and noise has been excluded in this work. This is because the MOGREPS-R driven UKV ensemble runs supplied by the *Convective-scale ensembles* project are *downscale* ensembles generated without UKV initial condition perturbations. Consequently, the evolution of each UKV ensemble member in each of the two case studies provided (5 September 2008 and 29 October 2008) closely follows its MOGREP-R counterpart for the duration of the forecast.

© Crown copyright 2010

2.4.7. The choice of criteria used to assess the skill and realism of the blended forecasts

This report focuses on two, key aspects of the performance of the blended forecasts:

- *the capability to generate plausible, seamless blends of extrapolation, UKV and downscaled MOGREPS-R precipitation forecasts*:

  this entails demonstrating a smooth evolution of the blended precipitation forecasts in terms of field statistics such as mean, variance, raining fraction and power spectral density

- *the capability to generate skilful blended control member and ensemble forecasts*;

  this involves establishing whether the blended forecasts are optimal on the hierarchy of scales represented by the cascade model: this will be the case if they are at least as skilful as constituent model forecasts at these scales.

It must also be demonstrated that ensembles of blended forecasts are: 1) reliable (the forecast probabilities of events are similar to the observed frequencies of those same events); 2) have resolution or sharpness (forecast probabilities exhibit a range of values other than climatology); 3) exhibit an increase (decrease) in spread about the ensemble mean with increasing (decreasing) error in the ensemble mean. A fuller explanation of these aspects of ensemble performance can be found in section 5.4.3 below.

2.4.8. Operational constraints and implications for the blending algorithm

In an operational context, the cost of generating UKV ensembles of more than a few members is likely to be prohibitive. Consequently, clustering techniques will be needed to identify a subset of MOGREPS-R members which approximate the spread of the full MOGREPS-R ensembles. These members will provide lateral boundary conditions for running small UKV ensembles.

Blended, 2 km, ensemble precipitation forecasts of 50 members or more are likely to be needed by users including the Environment Agency[2]. Thus, multiple blended ensemble forecasts will need to be generated from each UKV ensemble forecast member and its associated MOGREPS-R forecast member using multiple realisations of noise. Given that the synoptic scale spread could be under represented by ensembles of no more than 6 members, the injected

[2] In ensemble NWP an ensemble size of approximately 50 members is thought be sufficient to capture the full range of possible solutions at the synoptic and meso-scales. However, when considering high resolution ensembles resolving individual showers, there may be a requirement for even larger ensemble sizes to capture the wide range of possible solutions in the distribution of convective precipitation.

© Crown copyright 2010

noise may be needed to perturb synoptic scale precipitation features as well as the mesoscale and convective scales.

© Crown copyright 2010

3. Descriptions of the source models, pertinent aspects of their formulation and configurations used for high resolution ensemble runs

3.1. Overview

This section briefly reviews pertinent aspects of the formulations of the source models used by the blending algorithm: STEPS extrapolation nowcasts, the 1.5 km configuration of the Unified Model (UKV), and MOGREPS-R.

3.2. STEPS extrapolation nowcasts

STEPS (Bowler *et al*., 2006) exploits a cascade model representation of precipitation fields to generate a high resolution (2 km) ensemble of precipitation nowcasts with a range of 6 hours. These ensembles are a blend of an extrapolated UKPP rain analysis derived from weather radar and satellite observations, NWP precipitation forecasts from the 4 km configuration of the UM and noise with space-time statistical properties inferred from weather radar. Errors in the extrapolation nowcast are assumed to originate from two sources: errors in the predicted motion of the precipitation field and errors in its evolution, measured in a Lagrangian reference frame moving with the precipitation field.

An extrapolation nowcast is produced using an extrapolation velocity field diagnosed from a time sequential pair of UKPP rain analyses using optical flow techniques (Bowler and Pierce, 2002). The errors in this velocity field are modelled by adding perturbations to the *u* and *v* components of the velocities. These perturbations are statistically homogeneous in space and uncorrelated with the diagnosed velocities. At each nowcast time step, the extrapolation and noise cascades must be advected using a perturbed velocity field because their evolution is modelled in a Lagrangian reference frame.

The method employed to model errors in the evolution of the extrapolated precipitation field reflects the need to account for the observed dependency of this rate of evolution on the horizontal length scale of precipitation features. Field evolution is modelled separately on each level in the cascade. A hierarchy of second order Auto-Regressive (AR-2) models – one for each cascade level – is used to establish the rate of evolution as function of scale (Bowler *et al*., ibid). The purpose of this approach is to limit the useful range of the extrapolation forecast in a scale dependent fashion and according to an objective measure of nowcast skill.

3.3. Variable (1.5 km) resolution configuration of the UM

The Unified Model is a non-hydrostatic model with semi-Lagrangian advection and semi-implicit time integration (Davies *et al*., 2005). Sub-grid parameterisations include those for clouds and precipitation (Wilson and Ballard, 1999), radiation (Edwards and Slingo, 1990), surface exchange (MOSES II – Cox et al., 1999), non-local boundary layer (Lock *et al*., 2000) and convection (Gregory and Rowntree, 1990). The horizontal coordinate

© Crown copyright 2010

system uses an Arakawa C grid, and the vertical coordinate is a terrain following, hybrid height coordinate with a Charney-Philips vertical staggering.

Currently, the variable resolution UM is run four times daily at 03Z, 09Z, 15Z and 21Z with 70 levels and a forecast range of 36 hours. The convection scheme is disabled so that convection can only be resolved explicitly. The scale of the explicitly resolved convection is controlled by restricting the amount of atmospheric shear using a fixed ∇^4 horizontal diffusivity (Roberts and Lean, 2008).

3.4. MOGREPS-R

MOGREPS is run in two configurations, one global, the other regional. The regional configuration, MOGREPS-R, also known as the North Atlantic and European (NAE) configuration, is run with 70 levels and a horizontal resolution of 24 km (18 km as of spring 2010). A 24 member ensemble with a range of 54 hours is produced (an unperturbed control and 23 perturbed members) twice daily at 06Z and 18Z. The NAE takes its Lateral Boundary Conditions (LBCs) and initial condition perturbations from a 6 hour forecast of the global ensemble. The initial condition perturbations are generated using an Ensemble Transform Kalman Filter (ETKF) (Bishop *et al*., 2001). In this approach, the perturbations generated for each cycle are a linear combination of the forecast perturbations from the previous cycle. This allows the perturbations to be orthogonalised. This is expected to lead to improved performance over error breeding (Wang and Bishop, 2003).

MOGREPS-R addresses the uncertainty arising from model error through the addition of stochastic perturbations to tuneable parameters in a number of the parameterisation schemes. Under this Random Parameters scheme, tuneable parameters are allowed to vary smoothly from time step to time step in a random fashion within the error bounds of the empirical estimation of the parameter values. The uncertainties in the initial conditions and model are not independent since the impact of stochastic tuneable parameters is propagated into the initial condition perturbations of the next cycle through the ETKF.

3.5. Configurations of MOGREPS-R and UM: 1.5 models used for high resolution ensemble case studies

For the two cases for which MOGREPS-R driven UKV ensembles were generated by the Convective-scale Ensembles Project (5-6th September 2008 and 29th October 2008), the MOGREPS-R ensemble was run from 0600 GMT. The UKV ensemble was embedded within the MOGREPS-R ensemble and run from 1200 GMT. This involved retrieving the operational North Atlantic and European (12 km) model analysis for 0600 GMT, and twenty-four (control and 23 perturbed member) T+7 hour forecasts and twenty-four boundary files (with a range of T+54h) from the global (90 km) MOGREPS ensemble run for 0000 GMT. The global ensemble was created using the Ensemble Transform Kalman Filter (ETKF).

The following steps were then performed (see Figure 2).

1. The NAE control analysis valid at 0600 GMT and the MOGREPS-G ensemble forecasts (control forecast + 23 members) valid at 0700 GMT

© Crown copyright 2010

were re-projected and interpolated on to the MOGREPS-R coordinate system and model domain.

2. Each of the 23 MOGREPS-G ensemble members, now interpolated to a horizontal resolution of 24 km were subtracted from the equivalent MOGREPS-G control forecast to give 23 perturbation fields containing the differences between each global ensemble member and the global control.

3. The 23 sets of perturbations for 0700 GMT were then added into the NAE control forecast (now at 24 km, originally at 12 km) over the period 0600 GMT to 0900 GMT to generate the 23 perturbed members. The Incremental Analysis Update (IAU) system was used.

4. These 23 perturbed MOGREPS-R members were run from 0900 GMT as forecasts for a minimum of 23 hours (30 hours for 5-6 September 2008) using boundary files from the global ensemble. Similarly, the NAE control forecast was run for the same period using the boundary file from the global control forecast.

5. Data dumps containing all fields required to run the NAE control and 23 perturbed MOGREPS-R members were output at 1200 GMT. Boundary files were also output spanning the full duration of the NAE and MOGREPS-R forecasts. These data were re-projected on to the UKV domain and coordinate system in preparation for running an equivalent 24 member UKV ensemble.

6. The 24 member UKV ensemble was run from 1200 GMT to the end of the MOGREPS-R ensemble forecast.

With the exception of the data dumps for the UKV ensemble runs, steps 1 to 5 are standard in the operational MOGREPS system and were run using the Suite Control System. The running of a UKV ensemble (step 6) is new functionality. Consequently, each UKV ensemble member was run individually outside the SCS.

© Crown copyright 2010

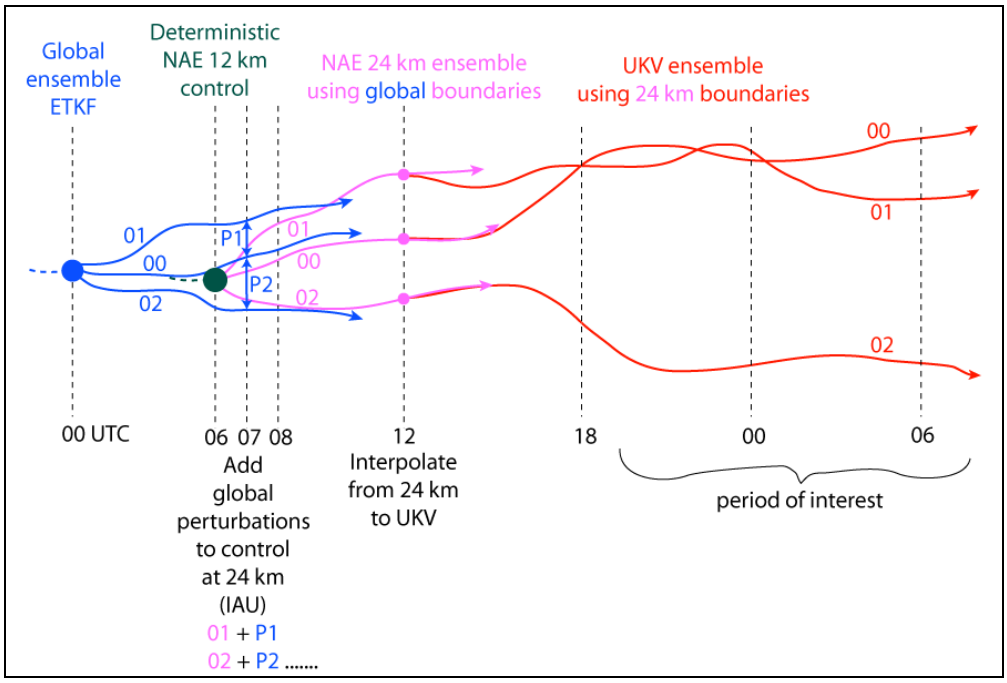

Figure 2 Graphical representation of the generation of MOGREPS-R driven UKV ensembles for the case studies events of 5-6th September 2008 and 29th October 2008.

© Crown copyright 2010

4. An algorithm for generating a seamless blend of model forecasts

4.1. Blending of the component forecasts

Choice of blended forecast configurations

The formulation paper (Pierce *et al*., 2007) proposes a number of alternative blending formulations based around cascade decomposed forecasts. This section of the report focuses on descriptions of a MOGREPS-R downscaler and a blended forecast combining an extrapolation nowcast, a UKV control member or ensemble forecast member and noise. A description of a blend incorporating an extrapolation nowcast, ensemble forecasts from the UKV and MOGREPS-R and noise follows, because the ultimate aim of these cascade-based blending techniques is to produce seamless forecasts with a range of at least several days. However, the evaluation of this type of configuration cannot be justified until quasi-operational UKV ensemble forecasts become available. To date, the experimental UKV ensembles generated by the *Convective-scale Ensembles Project* and employed in this study have been *downscale* ensembles with forecast solutions very similar to their driving model (MOGREPS-R) forecasts. In addition, the separate evaluation of forecast blends incorporating non-parametric and parametric noise is desirable since it will enable an independent assessment of their performance.

A MOGREPS-R downscaler

The simplest of the blended forecasts described in the formulation paper is a MOGREPS-R downscaler

$$Y_k^{\,p}(t+t_l) = w_k^{m,p}(t+t_l)Y_k^{\,m,p}(t+t_l) + w_k^{n,p}(t+t_l)Y_k^{\,n,p}(t+t_l) \qquad (9),$$

where $Y_k^{\,p}(t+t_l)$ is the blended cascade incorporating the *p*'th member of a MOGREPS-R ensemble forecast, $Y_k^{\,m,p}(t+t_l)$, and the *p*'th realisation of noise, $Y_k^{\,n,p}(t+t_l)$. The weight given to the MOGREPS-R cascade in this blend is

$$w_k^m(t+t_l) = \bar{r}_k^m(t+t_l) \qquad (10),$$

where the correlation coefficient , $\bar{r}_k^m(t+t_l)$, is an ensemble mean which tends from a current estimate, $\sum_{p=1}^{N} r_k^{m,p}(t) \Big/ N$, to a climatology, $\hat{r}_k^m(t+t_l) = \sum_{p=0}^{N} \hat{r}_k^{m,p}(t+t_l) \Big/ N$, which is a function of forecast lead time. The relaxation of the current skill to climatology is consistent with the measured auto-correlation of $\sum_{p=0}^{N} r_k^{m,p}(t) \Big/ N$ over time (Bowler *et al*., ibid.).

The RMS error of an ensemble forecast from a perturbed ensemble member is larger than that of the control forecast by a factor of $\sim\sqrt{2}$. If one used the correlation coefficient of each perturbed member as an estimate of its current skill, more weight would be given to the noise component when blending with perturbed members. This is incorrect since each perturbed ensemble member

© Crown copyright 2010

will already account for some of the forecast uncertainty. The weights must be formulated such that they do not degrade the skill of the ensemble mean.

The weight assigned to the noise component in (9), $w_k^{n,p}$, is the fraction of the variance unexplained by MOGREPS-R ensemble forecast

$$w_k^{n,p}(t+t_l) = \sqrt{1 - w_k^{m,p}(t+t_l)^2} \quad (11).$$

The formulation of the noise component is described in section 4.3 below.

The blended cascades valid at a given time step, $t+t_l$, are collapsed back into a single field using

$$dBR_{i,j}^{p}(t+t_l) = \mu^{p}(t+t_l) + \sum_{k=0}^{N-1} \sigma_k^{p}(t+t_l) \cdot Y_{k,i,j}^{p}(t+t_l) \quad (12),$$

where $\mu^{p}(t+t_l)$ is the field mean of the *p*'th member of the MOGREPS-R ensemble forecast, $\mu^{m,p}(t+t_l)$, and $\sigma_k^{p}(t+t_l)$ are the standard deviations, $\sigma_k^{m,p}(t+t_l)$, of the same ensemble member after an adjustment, $\hat{f}_k^{m,p}$, to account for time averaged biases between $\sigma_k^{m,p}$ and the equivalent values derived from radar based UKPP rain analyses (σ_k^{r})

$$\hat{f}_k^{m,p} = \left\langle \frac{\sigma_k^{r}}{\sigma_k^{m,p}} \right\rangle \quad (13).$$

The resultant, collapsed field in units of $10\log_{10}(R+c)$ is then converted back to rainfall rate and the threshold, *c*, subtracted (see section 2.3 above).

Formulation of a blended forecast incorporating an extrapolation nowcast, a UKV ensemble forecast and noise

A natural extension of the STEPS nowcast, incorporating an extrapolation based precipitation nowcast, a single NWP precipitation forecast and noise is to generate a blend incorporating a UM ensemble precipitation forecast, in this case from the variable resolution (1.5 km) configuration of the UM

$$Y_k^{p}(t+t_l) = w_k^{e}(t+t_l)Y_k^{e}(t+t_l) + w_k^{h,p}(t+t_l)Y_k^{h,p}(t+t_l) + w_k^{n,p}(t+t_l)Y_k^{n,p}(t+t_l) \quad (14),$$

where $Y_k^{e}(t+t_l)$ is the extrapolation cascade, $Y_k^{h,p}(t+t_l)$ and $Y_k^{n,p}(t+t_l)$ are the UKV ensemble forecast and noise cascades for ensemble member, *p*, and $Y_k^{p}(t+t_l)$ is the blended cascade. Bowler *et al*. (ibid.) formulated weights for a blend of two forecast components and noise as follows.

$$w_k^{e}(t+t_l) = r_k^{e}(t+t_l)\sqrt{\frac{\lambda_k^{e}(t+t_l)}{\lambda_k^{e}(t+t_l) + \lambda_k^{m,p}(t+t_l)}} \quad (15),$$

© Crown copyright 2010

$$w_k^{h,p}(t+t_l) = \bar{r}_k^{h,p}(t+t_l)\sqrt{\frac{\lambda_k^h(t+t_l)}{\lambda_k^e(t+t_l)+\lambda_k^{h,p}(t+t_l)}} \quad (16).$$

$\lambda_k^e(t+t_l)$ and $\lambda_k^{h,p}(t+t_l)$ are the ratios of the explained variance to unexplained variance for the extrapolation nowcast and the *p*'th member of the UKV ensemble forecast respectively

$$\lambda_k^e(t+t_l) = \frac{r_k^e(t+t_l)^2}{1-r_k^e(t+t_l)^2} \quad \text{and} \quad \lambda_k^{m,p}(t+t_l) = \frac{\bar{r}_k^{h,p}(t+t_l)^2}{1-\bar{r}_k^{h,p}(t+t_l)^2} \quad (17).$$

$r_k^e(t+t_l)$ is the correlation coefficient between each level of the extrapolation cascade valid at, $t+t_i$, and the radar based UKPP rain analysis. $\bar{r}_k^{h,p}(t+t_l)$ is an ensemble mean correlation coefficient which tends from a current estimate, $\sum_{p=0}^{N} r_k^{h,p}(t) \Big/ N$, to a climatology, $\hat{r}_k^h(t+t_l) = \sum_{p=0}^{N} \hat{r}_k^{h,p}(t+t_l) \Big/ N$, which is a function of forecast lead time. The relaxation of the current skill to climatology is consistent with the measured auto-correlation of $\sum_{p=0}^{N} r_k^{h,p}(t) \Big/ N$ over time.

Thus, $w_k^e(t+t_l)$ and $w_k^{h,p}(t+t_l)$ tend towards values dictated by the climatological skill of the extrapolation nowcast and ensemble of UKV forecasts. Since the extrapolation nowcast cascade is updated using a hierarchy of AR-2 models, its climatological skill on each level of the cascade is estimated from climatologies of the AR-2 auto-correlation coefficients (see sub-section 4.2 below).

The weights assigned to the noise cascade are designed such that they preserve the variance on each cascade level

$$w_k^{n,p}(t+t_l) = \sqrt{1-w_k^{h,p}(t+t_l)^2 - w_k^e(t+t_l)^2} \quad (18).$$

The blended forecast field valid at time step, $t+t_l$, is re-constituted using equation (7) where

$$\mu^p(t+t_l) = \frac{w_k^e(t+t_l)}{w_k^e(t+t_l)+w_k^{m,p}(t+t_l)}\mu^e(t+t_l) + \frac{w_k^{h,p}(t+t_l)}{w_k^e(t+t_l)+w_k^{h,p}(t+t_l)}\mu^{h,p}(t+t_l) \quad (19),$$

and

$$\sigma_k^p(t+t_l) = \frac{w_k^e(t+t_l)}{w_k^e(t+t_l)+w_k^{m,p}(t+t_l)}\sigma_k^e(t+t_l) + \frac{w_k^{h,p}(t+t_l)}{w_k^e(t+t_l)+w_k^{h,p}(t+t_l)}\sigma_k^{h,p}(t+t_l) \quad (20).$$

$\sigma_k^{h,p}$ is the standard deviation of the *p*'th member of the UKV ensemble precipitation forecast after adjustment to account for time averaged biases between $\sigma_k^{h,p}$ and the equivalent values derived from radar based UKPP rain analyses (σ_k^r):

$$\hat{f}_k^{h,p} = \left\langle \frac{\sigma_k^r}{\sigma_k^{h,p}} \right\rangle \quad (21).$$

© Crown copyright 2010

This approach to blending assumes that the extrapolation nowcast and UKV forecast cascades are uncorrelated.

A more rigorous approach requires consideration of the covariation between the component forecasts. Accounting for the covariance of $Y_k^e(t+t_l)$ and $Y_k^{m,p}(t+t_l)$, denoted by $\mathrm{cov}_k^{e/m,p}(t+t_l)$, gives

$$\sigma_k^p(t+t_l) = a_k^p \cdot \sigma_k^{m,p}(t+t_l) + b_k^p \cdot \sigma_k^e(t+t_l) - \sqrt{2 \cdot a_k^p \cdot b_k^p \cdot \mathrm{cov}_k^{e/m,p}(t+t_l)} \quad (22),$$

where

$$a_k^p = \frac{w_k^{h,p}(t+t_l)}{w_k^e(t+t_l) + w_k^{h,p}(t+t_l)} \text{ and } b_k^p = \frac{w_k^e(t+t_l)}{w_k^e(t+t_l) + w_k^{m,p}(t+t_l)} \quad (23).$$

Formulation of a blended forecast incorporating an extrapolation nowcast, UKV and MOGREPS-R ensemble forecasts and noise

It is straightforward to envisage an extension of (9) to incorporate a third forecast component

$$Y_k^p(t+t_l) = w_k^e(t+t_l)Y_k^e(t+t_l) + w_k^{h,p}(t+t_l)Y_k^{h,p}(t+t_l) + w_k^{m,p}(t+t_l)Y_k^{m,p}(t+t_l) + w_k^{n,p}(t+t_l)Y_k^{n,p}(t+t_l) \quad (24),$$

where $Y_k^e(t+t_l)$ is the extrapolation nowcast cascade, $Y_k^{h,p}(t+t_l)$ and $Y_k^{m,p}(t+t_l)$ are cascades generated from the p^{th} ensemble members of UKV and MOGREPS-R ensemble forecasts respectively, $Y_k^{n,p}(t+t_l)$ is the decomposed, p^{th} realisation of an ensemble of noise fields, and $Y_k^p(t+t_l)$ is the resultant blend valid at time, $t+t_l$, where t is the data time (starting point) of the blended forecast and t_l is the forecast lead time.

The weights are given by:

$$w_k^e(t+t_l) = r_k^e(t+t_l)\sqrt{\frac{\lambda_k^e(t+t_l)}{\lambda_k^e(t+t_l) + \lambda_k^{m,p}(t+t_l) + \lambda_k^{h,p}(t+t_l)}} \quad (25),$$

$$w_k^{h,p}(t+t_l) = \bar{r}_k^{h,p}(t+t_l)\sqrt{\frac{\lambda_k^{h,p}(t+t_l)}{\lambda_k^e(t+t_l) + \lambda_k^{m,p}(t+t_l) + \lambda_k^{h,p}(t+t_l)}} \quad (26),$$

$$w_k^{m,p}(t+t_l) = \bar{r}_k^{m,p}(t+t_l)\sqrt{\frac{\lambda_k^{m,p}(t+t_l)}{\lambda_k^e(t+t_l) + \lambda_k^{m,p}(t+t_l) + \lambda_k^{h,p}(t+t_l)}} \quad (27),$$

$$w_k^{n,p}(t+t_l) = \sqrt{1 - w_k^{m,p}(t+t_l)^2 - w_k^{h,p}(t+t_l)^2 - w_k^e(t+t_l)^2} \quad (28),$$

and

© Crown copyright 2010

$$\lambda_k^e(t+t_l)=\frac{r_k^e(t+t_l)^2}{1-r_k^e(t+t_l)^2},\ \lambda_k^{h,p}(t+t_l)=\frac{\bar{r}_k^{h,p}(t+t_l)^2}{1-\bar{r}_k^{h,p}(t+t_l)^2}\ \text{and}\ \lambda_k^{m,p}(t+t_l)=\frac{\bar{r}_k^{m,p}(t+t_l)^2}{1-\bar{r}_k^{m,p}(t+t_l)^2} \quad (29).$$

The correlation coefficients, $\bar{r}_k^{m,p}(t+t_l)$ and $\bar{r}_k^{h,p}(t+t_l)$ are ensemble means representing the average skills of UKV and MOGREPS-R ensemble forecasts incorporating their control runs. With advancing forecast lead time, $\bar{r}_k^{m,p}(t+t_l)$ and $\bar{r}_k^{h,p}(t+t_l)$ tend from current estimates, $\sum_{p=0}^{N} r_k^{h,p}(t) \Big/ N$ and $\sum_{p=0}^{N} r_k^{m,p}(t) \Big/ N$, to climatologies, $\hat{r}_k^h(t+t_l)=\sum_{p=0}^{N} \hat{r}_k^{h,p}(t+t_l) \Big/ N$ and $\hat{r}_k^m(t+t_l)=\sum_{p=0}^{N} \hat{r}_k^{m,p}(t+t_l) \Big/ N$ respectively. The latter are a function of forecast lead time. The rates of relaxation of $\sum_{p=0}^{N} r_k^{h,p}(t) \Big/ N$ and $\sum_{p=0}^{N} r_k^{m,p}(t) \Big/ N$ to their respective climatologies are determined by the measured auto-correlations of $\sum_{p=0}^{N} r_k^{h,p}(t) \Big/ N$ and $\sum_{p=0}^{N} r_k^{m,p}(t) \Big/ N$ over time.

Following equation (7), the blended forecast field is re-constituted using

$$\mu^p(t+t_l)=\frac{w_k^e(t+t_l)}{w_k^e(t+t_l)+w_k^{m,p}(t+t_l)+w_k^{h,p}(t+t_l)}\mu^e(t+t_l)+ \frac{w_k^{h,p}(t+t_l)}{w_k^e(t+t_l)+w_k^{m,p}(t+t_l)+w_k^{h,p}(t+t_l)}\mu^{h,p}(t+t_l)+\frac{w_k^{m,p}(t+t_l)}{w_k^e(t+t_l)+w_k^{m,p}(t+t_l)+w_k^{h,p}(t+t_l)}\mu^{m,p}(t+t_l) \quad (30).$$

Accounting for the covariances between the forecast components, the standard deviations of the blended cascade level fields are given by

$$\sigma_k^p(t+t_l)=a_k^p\cdot\sigma_k^{m,p}(t+t_l)+b_k^p\cdot\sigma_k^e(t+t_l)+c_k^p\cdot\sigma_k^{h,p}(t+t_l)- \sqrt{2\cdot a_k^p\cdot b_k^p\cdot \mathrm{cov}_k^{e/m,p}(t+t_l)}-\sqrt{2\cdot a_k^p\cdot c_k^p\cdot \mathrm{cov}_k^{h,p/m,p}(t+t_l)}-\sqrt{2\cdot b_k^p\cdot c_k^p\cdot \mathrm{cov}_k^{e/h,p}(t+t_l)} \quad (31),$$

where $\mathrm{cov}_k^{e/m,p}(t+t_l)$, $\mathrm{cov}_k^{h,p/m,p}(t+t_l)$ and $\mathrm{cov}_k^{e/h,p}(t+t_l)$ are the covariances and

$$a_k^p=\frac{w_k^{m,p}(t+t_l)}{w_k^e(t+t_l)+w_k^{m,p}(t+t_l)+w_k^{h,p}(t+t_l)},\ b_k^p=\frac{w_k^e(t+t_l)}{w_k^e(t+t_l)+w_k^{m,p}(t+t_l)+w_k^{h,p}(t+t_l)}\ \text{and}$$
$$c_k^p=\frac{w_k^{h,p}(t+t_l)}{w_k^e(t+t_l)+w_k^{m,p}(t+t_l)+w_k^{h,p}(t+t_l)} \quad (32).$$

Generation of control member blends

The various blending algorithm configurations described above focus on the generation of blended ensemble forecasts. However, there is also a requirement to generate seamless, high resolution control member forecasts with a similar forecast range.

This can readily be achieved in the short range by blending a deterministic extrapolation nowcast and UKV control member forecast. Since each of these components is generated on a 2 km resolution grid, there should be little need to perturb or downscale the blended cascade level fields with noise. Without a noise component, the weights described in (15) and (16) must be re-scaled to sum to unity to avoid any loss of variance in the blended forecasts.

© Crown copyright 2010

To produce a seamless forecast evolution beyond the range of the UKV control forecast, it will be necessary to downscale the 24 km grid length MOGREPS-R control forecast. The MOGREPS-R downscaler described in (9) can be adapted so that the injection of noise is restricted to unresolved scales (the bottom four cascade levels). This approach should be capable of adding plausible fine scale structures whilst leaving resolved scales unperturbed.

The above adaptations to the previously described ensemble blending algorithms should allow the construction of 2km resolution control member forecasts with a range 48 hours. The extent to which these forecasts will be seamless is questionable given the quite different characteristics of the high resolution (convective scale) structures produced by the UKV model and parametric noise generator. It maybe desirable to inject noise into the bottom few cascade levels of the blends of an extrapolation nowcast and UKV control forecast to smooth the handover from the UKV to MOGREPS-R.

4.2. The extrapolation nowcast

In STEPS, an extrapolation based precipitation nowcast is generated by advecting the most recent, radar based UKPP rain analysis (valid at time, *t*) in the direction of its apparent motion. The field of motion is derived by solving the optical flow constraint equation (Bowler and Pierce, 2002). This technique diagnoses a single, deterministic velocity field from a time sequential pair of UKPP rain analyses valid at t and t-Δt, where Δt=15 minutes. The resultant advection velocity field is perturbed using a statistical technique to produce an ensemble of extrapolated precipitation fields.

The formulation paper (Pierce, 2007) recommends that a single, deterministic extrapolation velocity field be employed in the blending algorithm. This can be combined with an ensemble of velocity fields inferred from an ensemble of UKV precipitation forecasts: in effect, the distinct evolution of each member of the UKV ensemble precipitation forecast serves to perturb the extrapolation velocity field. This is described in more detail in 4(iv) below.

In both STEPS and the proposed blending algorithm, it is the cascade level extrapolation nowcast fields that are advected. A hierarchy of second order Auto-Regressive (AR-2) models – one for each cascade level – is used to establish the time rate of evolution of these fields as function of scale

$$Y_k^e(t+t_l) = \phi_{k,1}(t)\cdot Y_k^e(t+t_l-\Delta t) + \phi_{k,2}(t)\cdot Y_k^e(t+t_l-2\Delta t) \qquad (33)$$

where $Y_k^e(t+t_l)$ is the predicted extrapolation cascade valid at lead time, t_l, based upon similar cascades valid at the two previous time steps. The AR-2 parameters, $\phi_{k,1}(t)$ and $\phi_{k,2}(t)$, control the rate of evolution at each scale, and are estimated (Box, 1970) from a temporal sequence of three rain analyses spanning a 30 minute time period.

$$\phi_{k,1}(t) = \frac{\gamma_{k,1}(t)(1-\gamma_{k,2}(t))}{1-(\gamma_{k,1}(t))^2} \qquad (34),$$

and

© Crown copyright 2010

$$\phi_{k,2}(t) = \frac{\gamma_{k,2}(t) - (\gamma_{k,1}(t))^2}{1 - (\gamma_{k,1}(t))^2} \quad (35),$$

where $\gamma_{k,1}(t)$ and $\gamma_{k,2}(t)$ are the lag 1 and lag 2 auto-correlation coefficients. The values of $\gamma_{k,1}(t)$ and $\gamma_{k,2}(t)$ are constrained to ensure that they are non-oscillatory (Bowler *et al*., ibid.). Current estimates of $\gamma_{k,1}(t)$ and $\gamma_{k,2}(t)$ are relaxed to climatologies derived by Bowler *et al*. (ibid.). The relaxation equations are exponential in form and are calibrated such that the rate of relaxation is consistent with the measured temporal auto-correlation of $\gamma_{k,1}(t)$ and $\gamma_{k,2}(t)$.

As a result of the dynamic scaling properties of precipitation fields (the rate of field evolution over time increases with decreasing scale), the auto-correlation coefficients, $\gamma_{k,1}(t)$ and $\gamma_{k,2}(t)$, decrease from the top of the cascade downwards. Consequently, the updated extrapolation cascade, $Y_k^e(t+t_l)$, becomes increasingly smooth from the smallest scale upwards with every, successive extrapolation step. The injection of noise serves to replace the lost variability on each cascade level.

4.3. Formulation of the noise

A parametric noise generator for downscaling and perturbing MOGREPS-R precipitation forecasts

Empirical evidence of the scaling (multi-fractal) properties of precipitation fields has been employed by numerous authors (e.g. Seed, 2003) to justify using a power law representation of the Power Spectral Density of precipitation fields

$$P(\omega) \propto \omega^{-\beta} \quad (36),$$

where $P(\omega)$ is the PSD of the field at frequency ω pixel^{-1} and the superscript β is known as the scaling exponent.

The parametric noise generator approximates the PSD of a target precipitation field using two power laws of the form

$$P(\omega) \propto \left(\frac{\omega}{\omega_0}\right)^{-\beta_0} \text{ when } \omega < \omega_b \quad (37)$$

and

$$P(\omega) \propto \left(\frac{\omega}{\omega_b}\right)^{-\beta_1} \text{ when } \omega > \omega_b \quad (38).$$

$\omega_0 = \frac{1}{L}$ where the target field has horizontal dimensions of *L* by *L* pixels. ω_b is the frequency at which the slope of the power law changes and is sometimes

© Crown copyright 2010

referred to as a *scaling break*. β_0 and β_1 are the slopes of the power spectrum at frequencies that are less than or greater than $\omega_b = \frac{1}{40}\,\mathrm{km}^{-1}$ respectively.

The power law filter is applied by multiplying each element in the FFT by

$$f_{x,y} = \left(\frac{\omega_{x,y}}{\omega_0} \right)^{\beta} \tag{39}$$

where $f_{x,y}$ is the power filter to be applied at wave number (x,y) in the FFT, $\omega_{x,y}$ is the frequency at wave number (*x,y*), ω_0 is the frequency of either the outer scale, *L*, of the cascade or the scale break, and β is the slope of the power spectrum at $\omega_{x,y}$.

A power law for the power spectrum implies that the ratio of the standard deviations for pairs of cascade levels, *k* and *k-1*, should be fixed for all levels in the cascade. Thus, the PSD of a field exhibiting these scaling properties can be represented by a straight line with a fixed slope when plotted in units of decibels. The parametric model described here represents the PSD by two such straight lines with different slopes and a break between them at the 40 km scale.

This form of parametric noise generator is used in STEPS to estimate the power spectra of precipitation fields when the raining fraction is <5%.

A non-parametric noise generator for perturbing extrapolation and UKV precipitation forecasts

An alternative to applying the power law filter is to renormalise the FFT of the target field and use it as a filter. In this case the field is normalised to have a mean of zero and a variance of 1 and the filter, $f_{x,y}$, is calculated as the modulus of the FFT at a particular (*x,y*). The advantage of this approach is that it is no longer necessary to fit a power law to the power spectrum and any anisotropy that may be present in the field is respected. This non-parametric noise generation technique is employed by the extrapolation and UKV based configuration of the blending algorithm to generate noise fields with the spatial statistical properties of a recent radar based UKPP rain analysis or a sequence of UKV precipitation forecasts.

Temporal updating of the non-parametric and parametric noise fields

A cascade of noise with the required spatial statistical properties is allowed to evolve in time using the same hierarchy of AR-2 models (one for each level of the cascade) employed to maintain the extrapolation nowcast cascade

$$Y_k^{n,p}(t+t_l) = \phi_{k,1}(t) \cdot Y_k^{n,p}(t+t_l-\Delta t) + \phi_{k,2}(t) \cdot Y_k^{n,p}(t+t_l-2\Delta t) + \phi_{k,0}(t) \cdot \varepsilon_k^{p}(t+t_l) \tag{40},$$

© Crown copyright 2010

where $Y_k^{n,p}(t+t_l)$ is the *p*'th realisation of the noise cascade valid at lead time, t_l, and $\varepsilon^{p}_{k,i,j}(t)$ is a cascade of temporally independent but spatially correlated noise generated at each forecast step for the *p*'th ensemble member.

4.4. Advection of the noise and extrapolation cascades

In the case of a blend incorporating an extrapolation nowcast, a UKV ensemble forecast and noise, the noise cascade, $Y_k^{n,p}(t+t_l)$, is advected using a blended velocity field which tends from the diagnosed, deterministic extrapolation velocity field to a velocity field inferred from the *p*'th member of the UKV precipitation forecast

$$\nu^{p}(t+t_l) = w_1^{e} \cdot \nu^{e}(t+t_l) + w_1^{h,p} \cdot \nu^{h,p}(t+t_l) \tag{41}$$

where $\nu^{p}(t+t_l)$, the blended velocity field, is a weighted combination of $\mathbf{v}^{e}(t+t_l)$, the deterministic extrapolation velocity field, and $\nu^{h,p}(t+t_l)$, the apparent field of motion inferred from the *p*'th member of a UKV ensemble precipitation forecast. The weights used to blend the velocities are those calculated on the second cascade level (numbered 1) using (25) and (26). This is because the temporal auto-correlation of the weights at this level, most closely matches the temporal auto-correlation of the velocity fields.

In the case of a MOGREPS-R downscale ensemble, the velocity field used to advect the noise cascade is that inferred from the *p*'th member of the UKV ensemble precipitation forecast since the MOGREPS-R precipitation forecast is of insufficient resolution to allow the diagnosis of a motion field using optical flow techniques.

$$\nu^{p}(t+t_l) = w_1^{h,p} \cdot \nu^{h,p}(t+t_l) \tag{42}.$$

Beyond the range of the UKV ensemble forecast (T+36h), the diagnosed ensemble of UKV velocity fields valid at T+36h are used. An alternative would be to make use of suitable MOGREPS-R horizontal wind fields as proxies for the movement of the MOGREPS-R forecast precipitation fields between T+36h and T+48h.

Once an operational, UKV ensemble forecast with its own initial condition perturbations is implemented, the proposed three way blend of extrapolation, UKV and MOGREPS-R forecasts will need to exploit a three way blended velocity field for advecting the noise cascades

$$\nu^{p}(t+t_l) = w_1^{e} \cdot \nu^{e}(t+t_l) + w_1^{h,p} \cdot \nu^{h,p}(t+t_l) + w_1^{m,p} \cdot \nu^{m,p}(t+t_l) \tag{43}.$$

This will tend from the diagnosed, deterministic extrapolation velocity field to a velocity field inferred from the *p*'th member of the UKV precipitation forecast (determined by optical flow methods), and ultimately, to the apparent velocity of the *p*'th member of the MOGREPS-R precipitation forecast, possibly inferred from a suitable wind field.

© Crown copyright 2010

4.5. Algorithm calibration

Overview

Calibration of the two configurations of the blending algorithm evaluated in this report has involved estimation of the following parameters:

1) cascade level adjustment factor climatologies, $\hat{f}_k^{h,p}$ and $\hat{f}_k^{m,p}$, for bias correcting the cascade level standard deviations of the UKV and MOGREPS-R ensembles precipitation forecasts, $\sigma_k^{h,p}$ $\sigma_k^{m,p}$;

2) cascade level model skill climatologies, $\hat{r}_k^h(t+t_l)$ and $\hat{r}_k^m(t+t_l)$, for the UKV and MOGREPS-R ensembles precipitation forecasts, computed as a function of forecast lead time.

Other parameter climatologies used (e.g. the AR-2 model auto-correlation coefficients) follow those derived by Bowler *et al*. (ibid.).

Estimation of $\hat{f}_k^{h,p}$ *and* $\hat{f}_k^{m,p}$

The precipitation forecast fields generated by the UKV and MOGREPS-R ensembles lack structure (variance) at scales close to model resolution. The standard deviations of the cascade level fields of precipitation rate derived from UKV and MOGREPS-R forecasts are biased relative to those inferred from quality controlled radar data. These biases can be corrected for by computing the cascade level climatologies, $\hat{f}_k^{h,p} = \left\langle \frac{\sigma_k^r}{\sigma_k^{h,p}} \right\rangle$ and $\hat{f}_k^{m,p} = \left\langle \frac{\sigma_k^r}{\sigma_k^{h,m}} \right\rangle$, where σ_k^r are the radar inferred cascade level standard deviations.

These expressions were evaluated using a month's worth of control member (member 0) UKV (May 2009) and MOGREPS-R (October 2008) forecasts of precipitation rate and equivalent, observed fields derived from time synchronous, quality controlled, radar data. The samples used were those for which at least 5% of the area of radar coverage was wet. Tables 1a-b below summarise the results.

Level	Range of spatial scales (km)	Climatological ratio $\hat{f}_k^{m,p} = \left\langle \frac{\sigma_k^r}{\sigma_k^{m,p=0}} \right\rangle$	σ
0	256-512-1024	0.903	0.323
1	128-256-512	0.914	0.205
2	64-128-256	0.944	0.162
3	32-64-128	1.057	0.207
4	16-32-64	1.208	0.258
5	8-16-32	1.725	0.135
6	4-8-16	1.92	0.195
7	Residual	2.013	0.196

Table 1a Estimates of $\hat{f}_k^{m,p}$ using MOGREPS-R control member forecasts for the month of October 2008.

© Crown copyright 2010

Level	Range of spatial scales (km)	Climatological ratio $\hat{f}_k^{h,p} = \left\langle \frac{\sigma_k^r}{\sigma_k^{h,p=0}} \right\rangle$	σ
0	256-512-1024	1.165	0.405
1	128-256-512	1.114	0.319
2	64-128-256	1.044	0.240
3	32-64-128	0.996	0.171
4	16-32-64	0.955	0.138
5	8-16-32	0.897	0.178
6	4-8-16	1.123	0.212
7	Residual	1.552	0.187

Table 1b Estimates of $\hat{f}_k^{h,p}$ using the UKV control member forecasts for the month of May 2009.

Figure 3 compares the two climatologies. The lack of variability in the 24 km resolution MOGREPS-R precipitation forecasts is confined to scales below 64 km (cascade level 3). On average, these forecasts exhibit only half the variability found in the 2 km resolution radar data at the bottom of the cascade (4 km scale). In the case of the UKV model, this deficiency is confined to the bottom two cascade levels (scales below 8 km) and is less pronounced. This finding is to be expected given the 1.5 km grid length of the UKV model over the composite area of radar coverage.

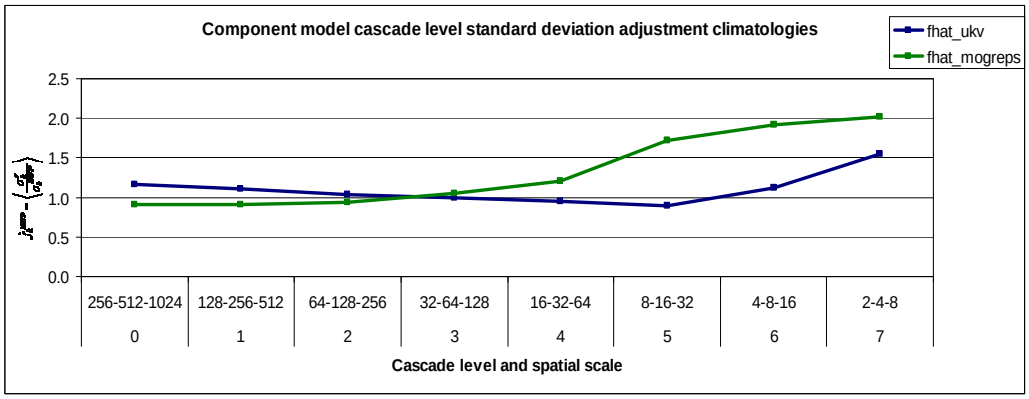

Figure 3 Comparison of climatologies of $\hat{f}_k^{h,p}$ and $\hat{f}_k^{m,p}$ derived using a month's worth of UKV and MOGREPS-R control member forecasts and quality controlled radar data.

The small deficiency in the variance of UKV precipitation forecasts at the top of the cascade (512 km scale) is likely to be a consequence of boundary effects and the limited domain size.

In both configurations of the blending algorithm evaluated in this report, current estimates of these adjustment factors, denoted by $f_k^{h,p}(t)$ and $f_k^{m,p}(t)$, are exponentially relaxed to their respective climatologies. This relaxation takes place over time periods consistent with the measured auto-correlations of $f_k^{h,p}(t)$ and $f_k^{m,p}(t)$ (Bowler *et al.*, ibid.).

© Crown copyright 2010

Estimation of $\hat{r}_k^m(t+t_l)$ ***and*** $\hat{r}_k^h(t+t_l)$

The weights assigned to the forecast components in the two configurations of blending algorithm evaluated in this report vary with cascade level and lead time. They are a function of forecast skill because, by design, their formulation makes the weight on a given cascade level for a given forecast lead time proportional to the fraction of the variance (in the radar observations) explained by the associated cascade level forecast field.

Estimates of the skill of the deterministic extrapolation nowcast, and the UKV and MOGREPS-R ensemble average forecast skill at time, *t* (the start time of a blended forecast), denoted by $r_k^e(t)$, $\sum_{p=0}^{N} r_k^{h,p}(t) \Big/ N$ and $\sum_{p=0}^{N} r_k^{m,p}(t) \Big/ N$ respectively, are relaxed to $\hat{r}_k^e$ (a single, lead time invariant climatology) and ensemble average, lead time dependent climatologies, $\hat{r}_k^h(t+t_l) = \sum_{p=0}^{N} \hat{r}_k^{h,p}(t+t_l) \Big/ N$ and $\hat{r}_k^m(t+t_l) = \sum_{p=0}^{N} \hat{r}_k^{m,p}(t+t_l) \Big/ N$ respectively.

In the case of the UKV and MOGREPS-R ensembles, the use of ensemble average estimates of forecast skill in the blending, rather than the skill of a given member, is necessary to avoid degrading the skill of the ensemble mean.

The UKV and MOGREPS-R forecast skill climatologies were calculated from a month's worth of UKV and MOGREPS-R ensemble precipitation forecasts and time synchronous UKPP rain analyses. The samples used were those for which at least 5% of the area of radar coverage was wet. Tables 2a-b below summarise the results.

Forecast lead time / T+h	Level	Range of spatial scales (km)	Climatology $\hat{r}_k^m(t+t_l) = \sum_{p=0}^{N} \hat{r}_k^{m,p}(t+t_l) \Big/ N$	Σ
T+3	0	256-512-1024	0.924	0.194
	1	128-256-512	0.763	0.132
	2	64-128-256	0.457	0.138
	3	32-64-128	0.132	0.089
	4	16-32-64	0.017	0.029
	5	8-16-32	0.008	0.016
	6	4-8-16	0.007	0.008
	7	Residual	0.005	0.007
T+6	0	256-512-1024	0.919	0.167
	1	128-256-512	0.727	0.150
	2	64-128-256	0.447	0.152
	3	32-64-128	0.131	0.086
	4	16-32-64	0.019	0.032
	5	8-16-32	0.009	0.014
	6	4-8-16	0.006	0.007
	7	Residual	0.005	0.007
T+9	0	256-512-1024	0.913	0.262
	1	128-256-512	0.695	0.235
	2	64-128-256	0.4	0.198
	3	32-64-128	0.116	0.103
	4	16-32-64	0.023	0.055
	5	8-16-32	0.011	0.017

© Crown copyright 2010

	6	4-8-16	0.006	0.007
	7	Residual	0.005	0.007
T+12	0	256-512-1024	0.882	0.281
	1	128-256-512	0.639	0.256
	2	64-128-256	0.331	0.191
	3	32-64-128	0.09	0.101
	4	16-32-64	0.019	0.048
	5	8-16-32	0.013	0.028
	6	4-8-16	0.007	0.008
	7	Residual	0.006	0.011
T+15	0	256-512-1024	0.862	0.306
	1	128-256-512	0.619	0.26
	2	64-128-256	0.294	0.168
	3	32-64-128	0.071	0.075
	4	16-32-64	0.013	0.03
	5	8-16-32	0.008	0.015
	6	4-8-16	0.006	0.008
	7	Residual	0.005	0.006
T+18	0	256-512-1024	0.865	0.212
	1	128-256-512	0.58	0.209
	2	64-128-256	0.279	0.173
	3	32-64-128	0.076	0.082
	4	16-32-64	0.012	0.03
	5	8-16-32	0.007	0.013
	6	4-8-16	0.006	0.007
	7	Residual	0.005	0.006
T+21	0	256-512-1024	0.833	0.285
	1	128-256-512	0.526	0.265
	2	64-128-256	0.24	0.189
	3	32-64-128	0.069	0.086
	4	16-32-64	0.016	0.043
	5	8-16-32	0.008	0.015
	6	4-8-16	0.006	0.007
	7	Residual	0.005	0.007
T+24	0	256-512-1024	0.823	0.296
	1	128-256-512	0.507	0.263
	2	64-128-256	0.21	0.181
	3	32-64-128	0.069	0.087
	4	16-32-64	0.017	0.046
	5	8-16-32	0.011	0.026
	6	4-8-16	0.007	0.008
	7	Residual	0.006	0.01
T+27	0	256-512-1024	0.794	0.307
	1	128-256-512	0.49	0.257
	2	64-128-256	0.201	0.17
	3	32-64-128	0.055	0.067
	4	16-32-64	0.011	0.029
	5	8-16-32	0.008	0.015
	6	4-8-16	0.006	0.008
	7	Residual	0.005	0.006
T+30	0	256-512-1024	0.817	0.276
	1	128-256-512	0.468	0.228
	2	64-128-256	0.2	0.169
	3	32-64-128	0.058	0.073
	4	16-32-64	0.01	0.027
	5	8-16-32	0.007	0.013
	6	4-8-16	0.006	0.008
	7	Residual	0.004	0.006
T+33	0	256-512-1024	0.799	0.302
	1	128-256-512	0.432	0.26
	2	64-128-256	0.189	0.187

© Crown copyright 2010

	3	32-64-128	0.063	0.088
	4	16-32-64	0.018	0.051
	5	8-16-32	0.009	0.016
	6	4-8-16	0.006	0.007
	7	Residual	0.005	0.006
T+36	0	256-512-1024	0.787	0.325
	1	128-256-512	0.432	0.274
	2	64-128-256	0.158	0.165
	3	32-64-128	0.056	0.087
	4	16-32-64	0.016	0.046
	5	8-16-32	0.01	0.024
	6	4-8-16	0.007	0.008
	7	Residual	0.005	0.01
T+39	0	256-512-1024	0.75	0.347
	1	128-256-512	0.412	0.272
	2	64-128-256	0.15	0.166
	3	32-64-128	0.043	0.065
	4	16-32-64	0.009	0.027
	5	8-16-32	0.006	0.014
	6	4-8-16	0.006	0.008
	7	Residual	0.004	0.006
T+42	0	256-512-1024	0.755	0.345
	1	128-256-512	0.378	0.26
	2	64-128-256	0.15	0.168
	3	32-64-128	0.049	0.074
	4	16-32-64	0.007	0.027
	5	8-16-32	0.005	0.012
	6	4-8-16	0.006	0.007
	7	Residual	0.004	0.006
T+45	0	256-512-1024	0.721	0.37
	1	128-256-512	0.347	0.28
	2	64-128-256	0.154	0.18
	3	32-64-128	0.052	0.082
	4	16-32-64	0.015	0.048
	5	8-16-32	0.008	0.015
	6	4-8-16	0.006	0.007
	7	Residual	0.005	0.006
T+48	0	256-512-1024	0.722	0.389
	1	128-256-512	0.333	0.281
	2	64-128-256	0.133	0.165
	3	32-64-128	0.052	0.082
	4	16-32-64	0.016	0.046
	5	8-16-32	0.01	0.026
	6	4-8-16	0.007	0.008
	7	Residual	0.005	0.009

Table 2a Estimates of $\hat{r}_k^m(t+t_l)$ from MOGREPS-R ensemble forecasts for the month of October 2008

© Crown copyright 2010

Forecast lead time / T+h	Level	Range of spatial scales (km)	Climatology $\hat{r}_k^h(t+t_l) = \sum_{p=0}^{N} \hat{r}_k^{h,p}(t+t_l) \Big/ N$	Σ
T+3	0	256-512-1024	0.966	0.21
	1	128-256-512	0.885	0.2
	2	64-128-256	0.660	0.207
	3	32-64-128	0.304	0.186
	4	16-32-64	0.112	0.158
	5	8-16-32	0.038	0.144
	6	4-8-16	0.007	0.089
	7	Residual	0.005	0.113
T+6	0	256-512-1024	0.961	0.272
	1	128-256-512	0.874	0.23
	2	64-128-256	0.642	0.196
	3	32-64-128	0.289	0.158
	4	16-32-64	0.096	0.142
	5	8-16-32	0.023	0.128
	6	4-8-16	0.006	0.071
	7	Residual	0.005	0.089
T+9	0	256-512-1024	0.940	0.258
	1	128-256-512	0.809	0.226
	2	64-128-256	0.513	0.211
	3	32-64-128	0.194	0.109
	4	16-32-64	0.055	0.079
	5	8-16-32	0.020	0.08
	6	4-8-16	0.006	0.057
	7	Residual	0.006	0.062
T+12	0	256-512-1024	0.94	0.35
	1	128-256-512	0.814	0.283
	2	64-128-256	0.548	0.195
	3	32-64-128	0.205	0.097
	4	16-32-64	0.035	0.051
	5	8-16-32	0.016	0.045
	6	4-8-16	0.005	0.042
	7	Residual	0.005	0.042
T+15	0	256-512-1024	0.918	0.327
	1	128-256-512	0.768	0.275
	2	64-128-256	0.468	0.215
	3	32-64-128	0.183	0.097
	4	16-32-64	0.055	0.05
	5	8-16-32	0.021	0.045
	6	4-8-16	0.007	0.042
	7	Residual	0.005	0.042
T+18	0	256-512-1024	0.905	0.368
	1	128-256-512	0.72	0.305
	2	64-128-256	0.379	0.186
	3	32-64-128	0.128	0.085
	4	16-32-64	0.043	0.049
	5	8-16-32	0.02	0.042
	6	4-8-16	0.006	0.042
	7	Residual	0.006	0.042
T+21	0	256-512-1024	0.886	0.362
	1	128-256-512	0.656	0.289
	2	64-128-256	0.345	0.185
	3	32-64-128	0.131	0.091
	4	16-32-64	0.051	0.053
	5	8-16-32	0.018	0.045
	6	4-8-16	0.005	0.042

© Crown copyright 2010

	7	Residual	0.007	0.042
T+24	0	256-512-1024	0.912	0.366
	1	128-256-512	0.689	0.302
	2	64-128-256	0.334	0.201
	3	32-64-128	0.079	0.086
	4	16-32-64	0.04	0.052
	5	8-16-32	0.018	0.043
	6	4-8-16	0.006	0.042
	7	Residual	0.005	0.042
T+27	0	256-512-1024	0.896	0.378
	1	128-256-512	0.687	0.273
	2	64-128-256	0.322	0.176
	3	32-64-128	0.138	0.097
	4	16-32-64	0.048	0.054
	5	8-16-32	0.017	0.045
	6	4-8-16	0.005	0.042
	7	Residual	0.006	0.042
T+30	0	256-512-1024	0.876	0.404
	1	128-256-512	0.711	0.272
	2	64-128-256	0.279	0.15
	3	32-64-128	0.131	0.079
	4	16-32-64	0.047	0.051
	5	8-16-32	0.016	0.044
	6	4-8-16	0.005	0.042
	7	Residual	0.004	0.042
T+33	0	256-512-1024	0.837	0.403
	1	128-256-512	0.638	0.282
	2	64-128-256	0.309	0.136
	3	32-64-128	0.123	0.079
	4	16-32-64	0.042	0.054
	5	8-16-32	0.014	0.045
	6	4-8-16	0.007	0.042
	7	Residual	0.006	0.042
T+36	0	256-512-1024	0.966	0.415
	1	128-256-512	0.885	0.308
	2	64-128-256	0.660	0.169
	3	32-64-128	0.304	0.066
	4	16-32-64	0.112	0.046
	5	8-16-32	0.038	0.043
	6	4-8-16	0.007	0.042
	7	Residual	0.005	0.042

Table 2b Estimates of $\hat{r}_k^h(t+t_l)$ from UKV ensemble precipitation forecasts for the month of May 2009.

Figure 4 compares the two ensemble forecast skill climatologies. It is clear that forecast skill declines on all cascade levels with increasing forecast lead time. This decline is not a steady one below cascade level 1 due to under sampling. The skill climatologies used in the blending algorithm case study evaluations are the dotted, least squares fitted trend lines shown in Figure 4.

© Crown copyright 2010

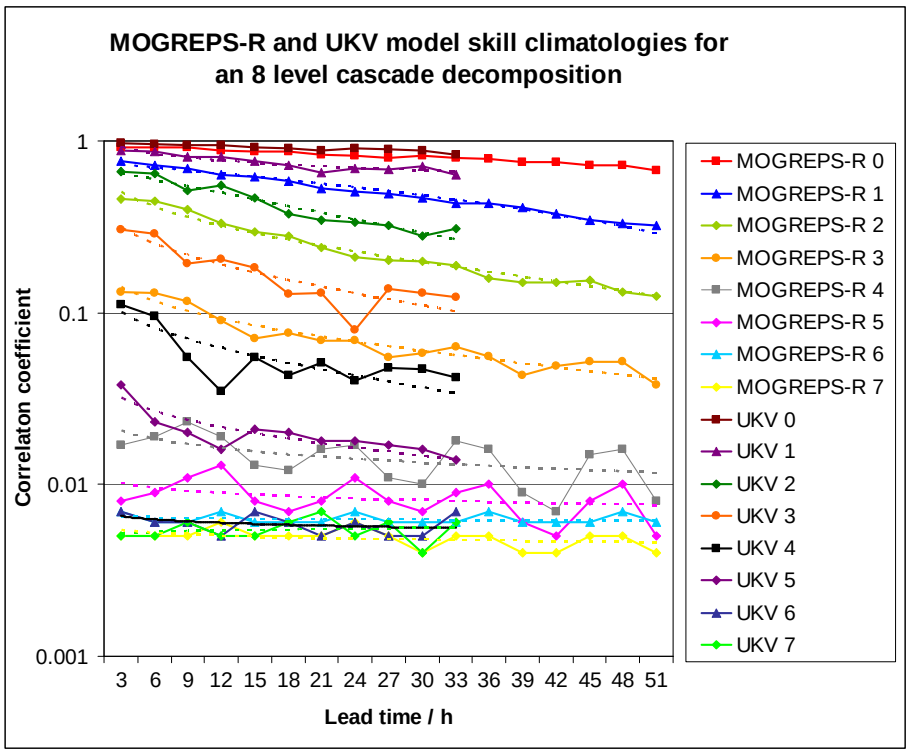

Figure 4 MOGREPS-R and UKV ensemble mean skill climatologies as a function of cascade level and forecast lead time.

In the case of the extrapolation nowcast, lead time invariant cascade level skill climatologies, $\hat{r}_k^e$, are derived from climatologies of the lag 1 and lag 2 auto-correlation coefficients, $\gamma_{k,1}(t)$ and $\gamma_{k,2}(t)$ (see Table 3). These are employed by a hierarchy of AR-2 models to predict the Lagrangian evolution of the nowcast precipitation field. Figure 5 shows plots of the climatological values of $\gamma_{k,1}(t)$ and $\gamma_{k,2}(t)$ as a function of cascade level. It is apparent that the skill of an extrapolation nowcast declines rapidly at scales below ~128 km. In the configuration of the blending algorithm combining an extrapolation precipitation nowcast with a UKV ensemble precipitation forecast (see equation 14), the extrapolation nowcast is rapidly replaced by noise at the bottom of the cascade and more slowly by the UKV forecast higher up the cascade at larger scales.

© Crown copyright 2010

Level	Range of spatial scales (km)	Climatology $\gamma_{k,1}(t)$	+/-	Climatology $\gamma_{k,2}(t)$	+/-
0	256-512-1024	0.99805	0.00007	0.9933	0.0002
1	128-256-512	0.9925	0.0002	0.9752	0.0005
2	64-128-256	0.9776	0.0004	0.923	0.001
3	32-64-128	0.9297	0.0009	0.75	0.003
4	16-32-64	0.796	0.002	0.367	0.005
5	8-16-32	0.482	0.005	0.005	0.003
6	4-8-16	0.079	0.004	0.0018	0.0009
7	Residual	0.0006	0.0008	0.0008	0.0006

Table 3 The climatological values of the lag 1 and lag 2 auto-correlation coefficients for Δt=15 minutes (after Bowler *et al*., 2006).

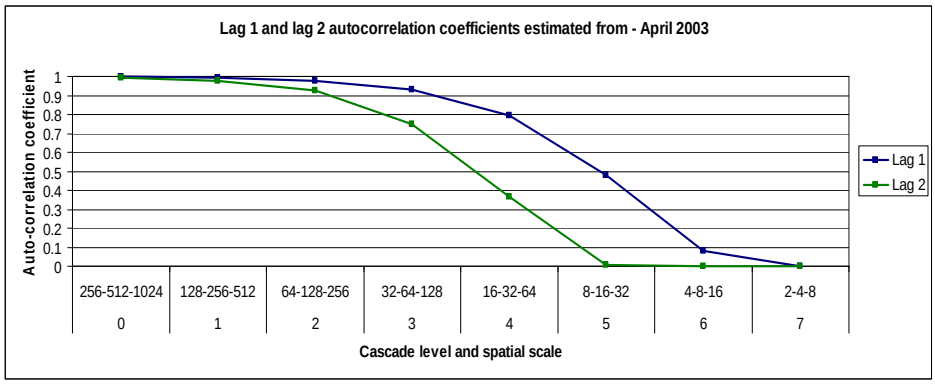

Figure 5 Climatologies of $\gamma_{k,1}(t)$ and $\gamma_{k,2}(t)$ as a function of cascade level for Δt=15 minutes (after Bowler *et al*., 2006).

4.6. Configurations of the blending algorithms evaluated in this report

Use of spatially varying target means and variances

To improve the representation of any spatial heterogeneities present in one or more of the blended forecast components, the target means and variances used to collapse the blended cascades will be computed on grid squares with dimensions of approximately 250 km by 250 km. This enhancement to the formulations described earlier is intended to ensure that any regional variations in the character of the forecast precipitation fields are preserved in the blended forecasts, even if the noise used to perturb the forecast precipitation is spatially homogeneous in character.

Control member forecast configurations

Two configurations of blended control member forecasts will be evaluated:

1) blends of a deterministic extrapolation nowcast and UKV control member forecast with non-parametric noise confined to the bottom two cascade levels (scales ≤ 8 km);

© Crown copyright 2010

2) downscaled MOGREPS-R control member forecasts in which parametric noise is restricted to the bottom 4 cascade levels (scales ≤ 32 km) and the top four cascade levels are the control member forecast only.

Ensemble members forecast configurations

In a similar vein, two configurations of blended ensemble forecasts will be assessed:

1) blends of an extrapolation nowcast and UKV control member forecast with non-parametric noise, where the weights are a function of the skill of the nowcast and UKV forecast components on each cascade level;

2) downscaled MOGREPS-R control member forecasts in which the weights assigned to the MOGREPS-R forecast on each cascade level are a function of its skill and the parametric noise preserves the variance on each level.

Blended ensembles of 23 members will be generated by perturbing UKV and MOGREPS-R control forecasts with 23 noise realisations. These will be evaluated against their associated blended control member forecasts, 23 member operational MOGREPS-R ensembles and some experimental 23 member UKV ensembles generated by the Convective-scale Ensembles Project.

The evaluation of blended ensemble forecasts incorporating UKV and MOGREPS-R ensembles will not be considered in this report owing to resource constraints. Here, the emphasis is placed on demonstrating the capability to produce plausible, seamless, blended ensemble forecasts by perturbing a control forecast with non-parametric or parametric noise. If the blending algorithms are well calibrated, these ensemble forecasts should exhibit skill relative to the control.

4.7. Software design

The benefits of object-oriented programming

The software design employed for the various configurations of the blending algorithm described in section 4.1 is based upon that of STEPS. In common with STEPS, the blending algorithms are written in the C++ language. This supports object-oriented programming (OOP). The main benefits of an OOP language are:

- abstraction of code;
- re-use of code through inheritance of complex data types;
- polymorphism.

Classes are a form of user-defined complex data type, which can contain variables and functions which operate on those variables. A variable of a class type (also known as an instance) can be used in a way that does not require a knowledge of the internal workings of the class, because it provides an interface through which one interacts with the variable's data and the functions which manipulate that data. In this way the complex inner workings of the class are abstracted away from the user.

© Crown copyright 2010

Effective re-use of code is achieved by defining a class type (known as the parent or base class), then defining another class (known as the child or derived class) which inherits (that is to say, contains) all the functionality and variables of the parent class, without the need to re-define them. The child class can implement extra functionality over and above the parent functionality. Theoretically, there is no limit to how many inheritance generations can be created in this way. Instances of the parent or the child class can be created as for any other data type.

Design of the STEPS source code

STEPS uses these ideas to define three classes (see Figure 6):

- *BCascade* contains all functionality to decompose and process input fields for one forecast component. Instances of BCascade are created for both extrapolation and UM components;

- *Merged_Cascade* is defined for managing blended forecasts and is derived from BCascade, inheriting all functionality from the latter; this class contains specific algorithms to create a blended forecast;

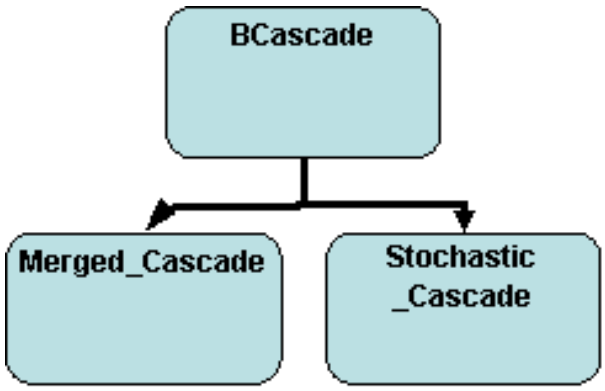

Figure 6 The classes employed by the STEPS object-oriented C++ source code.

Design of source code for blending a nowcast with multiple forecast components and noise

This project has provided a good opportunity to re-design the STEPS software in order to incorporate new ideas and to improve the flexibility of the code design. In particular, the capability to allow the number of components in the blended forecast to depend on lead time was considered useful; for instance, blending an extrapolation nowcast, UKV forecast and noise between T+15 minutes and T+36 hours, and blending a MOGREPS-R forecast with noise alone between T+36 hours and T+48 hours. It was also considered necessary to structure the software is a way that facilitates parallel processing on multiple CPUs, a capability that would enable full utilization of the resources provided by the Met Office's IBM supercomputer.

The software design thus envisaged, contains the following classes (see Figure 7):

© Crown copyright 2010

- *baseCascade* contains generic functionality to decompose and process input fields; an instance of this class type is created for each model input (e.g. a UKV or MOGREPS-R forecast) depending on the configuration of the blended forecast;

- *extrapCascade* inherits all functionality from *baseCascade* and adds capabilities to generate the extrapolation component of the blended forecast and calculate AR(2) parameters; inheritance of the *baseCascade* algorithms prevents re-writing of code to decompose and process UKPP rain analyses;

- *noiseCascade* contains functionality to create and update a noise cascade; this class does not inherit from any other classes.

Additionally, there are several support functions which reside outside any class. These include an algorithm to produce the blended forecast given an instance of each relevant input class, algorithms to find, ingest and re-grid required input fields to a common domain before passing them to the relevant class instance, functions to calculate weights and target parameters for each forecast lead time of the blended forecast, and functions to write output products to disc.

A consistent convention has been used for the naming of variables and functions. The code structure and in-line documentation meet UM programming standards. Strict code review practices and unit testing have been adhered to throughout the project. This has facilitated the development of a reliable body of code that can easily be maintained and upgraded once in operational use.

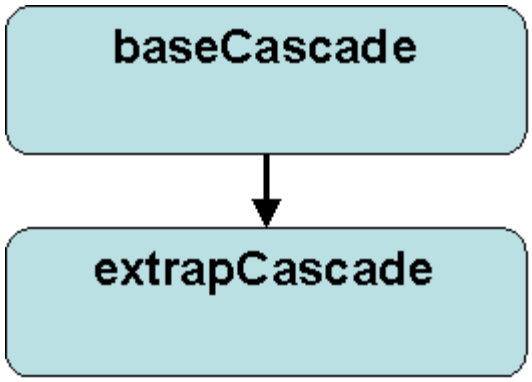

Figure 7 Inheritance of classes employed by the source code written for the blending algorithm.

Unit testing

A large and complex piece of software such as that developed for this project requires a methodical and rigorous approach to testing to ensure a bug-free code base. A method of testing each section (or unit) of code has been employed to debug the software. The following key principles have been followed:

- isolate the section of code of interest from any other non-tested code;

© Crown copyright 2010

- create a test routine to execute the isolated code with a range of test data;

- write out the contents of arrays in a manner which clearly shows the contents of each dimension before and after array use;

- examine outputs and correct bugs if necessary, ensuring unexpected inputs are correctly handled.

Checks have been performed on each section of the code base to ensure that:

- coded algorithms correspond with formulae in technical documentation;
- values denoting missing data are handled correctly;

- functions are called with correct arguments;

- loops are executed over the correct data ranges and use the correct iterator variables;

- returned values from functions are stored in a variable of the correct type and checked for error conditions.

A memory checking utility has also used to ensure that all variables are initialized before use, array indices are correct and within range, and dynamic arrays are allocated with the correct size and de-allocated properly, even when the code unexpectedly fails.

Functions contained in classes usually operate using class variables. These have been tested within a simplified class containing only essential components (already unit tested) required for the functioning of the code. In this way the class functions have been debugged fully in their proper environment.

Several components of the software are very similar to STEPS components and in these cases the test results have been compared to those produced by STEPS. In some cases, components of STEPS (for instance the optical flow advection scheme) used within the blending software are known to have been working well over several years and have been fully tested in the past. In these cases, additional testing has been limited to scrutinizing their performance within the new code base.

© Crown copyright 2010

5. Evaluation of two configurations of blending algorithm

5.1. Approach

The approach adopted for evaluating the blending algorithm has been shaped by several factors, most notably the formulation of the noise and the availability of model forecast data.

The proposal to use two alternative noise generation methods, according to whether the target distribution for the noise has the required horizontal resolution (non-parametric) or not (parametric), has favoured the evaluation of several blended forecasts, one incorporating an extrapolation nowcast, a UKV forecast and non-parametric noise, the other incorporating a MOGREPS-R forecast and parametric noise.

The limited availability of UKV ensemble forecasts generated by the *Convective-scale Ensembles Project* has meant that the case study oriented evaluation of the blending algorithm has been based, in part, on several extreme precipitation events (5 September 2008 and 29 October 2008) under investigation by the CEP, but also on a selection of more recent precipitation events for which archives of operational forecast data including control runs of the UKV and MOGREPS-R ensembles are available. The number of case studies has been restricted to 5 chiefly because of constraints on computer resources and time.

Preceding discussions on the key challenges faced by the project have been consolidated into the following questions which are the focus of the remainder of this report.

1) *Can time series of ensembles of synthetic, 2 km precipitation fields be generated whose spatial statistical properties reliably evolve from a target distribution based on quality controlled radar to spectra based on a UKV forecast sequence?*

These noise fields will be required to produce extrapolation and UKV based blended ensemble forecasts with a range of 36 hours.

2) *Can plausible, synthetic, 2km precipitation fields be generated using power spectra inferred from 24 km resolution MOGREPS-R forecasts. If not, are there suitable alternative target distributions which can be used instead?*

It is unclear whether or not a parametric technique for generating high resolution synthetic precipitation fields with power spectra inferred from 24 km resolution MOGREPS–R precipitation forecasts will be adequate for downscaling MOGREPS-R ensembles.

3) Can plausible, seamless, 2km resolution precipitation forecasts with a range of 48 hours be generated from the two configurations of blending algorithm under investigation?

The term *seamless* implies a smooth evolution of the blended field mean, variance, raining fraction, cumulative frequency distribution and power spectrum. The blended forecasts must be at least as skilful as their

© Crown copyright 2010

constituent forecast components measured on the hierarchy of scales represented by the cascade.

4) Can skilful, well calibrated ensembles of blended precipitation forecasts with useful resolution be generated using multiple realisations of noise to perturb and downscale the forecast components?

The ability of the blending algorithm to generate ensembles with useful levels of skill will depend on two main factors. Firstly, the space-time statistical properties of blends of model forecast precipitation and noise must be similar to those of the model forecast precipitation and noise alone. Secondly, the true skill of the component forecasts on each scale represented by the cascade model, must not deviate substantially from the field wide estimates used to compute the weights assigned to the noise and model forecasts components. Both these conditions must be met if skilful blended ensemble precipitation forecasts are to be produced.

5.2. Descriptions of the case study events

5.2.1. Case study selection

Two of the five case studies chosen for evaluating the blending algorithm (5 September 2008, 29 October 2008) were selected by the *Convective-scale Ensembles Project* as suitable candidates for assessing the performance of ensembles of UKV (1.5 km resolution) forecasts. From a CEP perspective, the primary focus of interest in both these cases is the localised, extreme precipitation which affected parts of north-east England and Devon; this aspect of the two cases studies is also relevant in the context of blending algorithm performance. However, the verification techniques employed here consider average performance over the wider area of the UK radar composite.

The remaining three case studies have been selected from archives of operational forecasts. The precipitation event spanning the period from 18/11/2009 to 20/11/2009 was associated with a moist, sub-tropical maritime airmass and accompanying quasi-stationary frontal zone. This produced rainfall accumulations in excess of 300 mm in parts of the English Lake District. The remaining two case studies are not associated with extreme rainfall, but are representative of late winter and early spring time precipitation events including frontal precipitation and organised areas of shower activity.

5.2.2. Case study 1 – 5–6 September 2008

Synopsis

The synoptic chart for 1200 GMT on 05/09/2008 (Figure 8a) shows the United Kingdom to have been under the influence of a complex area of low pressure centred over sea area Lundy, west of the Bristol Channel. A deep, moist sub-tropical maritime airmass (Figure 8b) entrained in the cyclonic circulation on the eastern flank of the low was lifted along the line of an occluding, quasi-stationary frontal zone over northern England. Forced ascent of the lower tropospheric easterly

© Crown copyright 2010

flow over the Cheviots led to seeder-feeder enhancement of the frontal precipitation.

A 6 hourly sequence of four, UKPP analyses of surface rain rate starting from 1200 GMT on 05/09/2008 (Figure 9) shows a broad band of frontal precipitation wrapped around the low centres. To the south are areas of organised, intense shower activity. Over the 18 hour period spanned by the analysis sequence in Figure 9, the orientation of the frontal zone gradually changed as the centre of the depression drifted slowly across Wales and central England. Orographically enhanced frontal precipitation persisted over north-east England. This can be seen in the analyses for 0000 GMT and 0600 GMT on 06/09/2008, despite the known under estimation of surface rain rate by the radar.

Features of relevance to the blending algorithms

The two blending algorithm configurations evaluated in this report rely on radar or model based downscaling to represent the fine scale structure of the blended forecast precipitation fields. In this case, it is known that radar estimates of surface rain rate in the frontal zone over north-east England were too low (this is less likely to be the case in other areas) chiefly because seeder-feeder orographic enhancement occurred below the height of the lowest elevation scan of the nearest radar. In these circumstances use of the radar for downscaling may produce low biased precipitation forecasts. However, UKV forecasts of surface precipitation rate are not subject to these deficiencies, so the use of UKV based noise for perturbing the blended ensembles beyond T+6h should remedy any low bias.

The value of the parametric, downscaling technique applied to MOGREPS-R precipitation forecasts remains to be demonstrated. The power spectra of precipitations fields do not always follow a power law. If this approximation is poor then the downscaled MOGREPS-R forecasts may lack structure (variance) at scales below ~32 km.

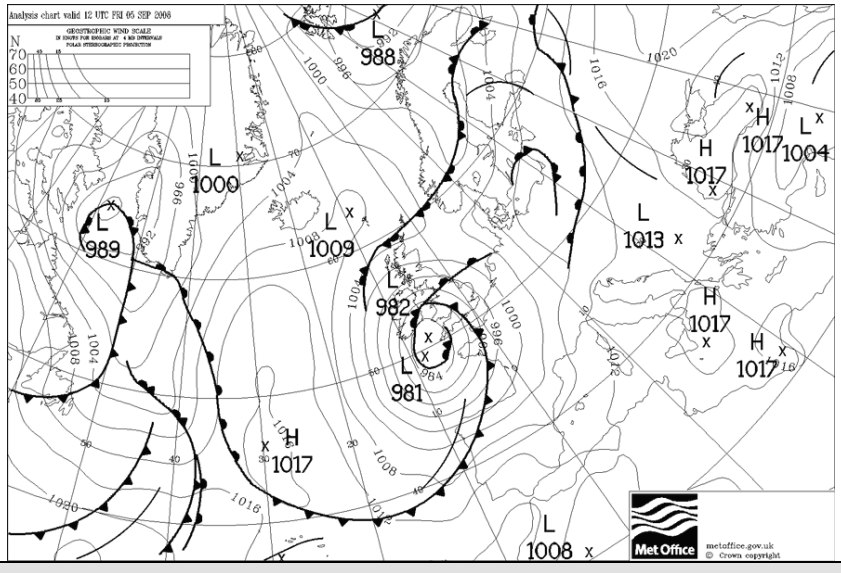

a) Surface analysis valid at 1200 GMT on 05/09/2008

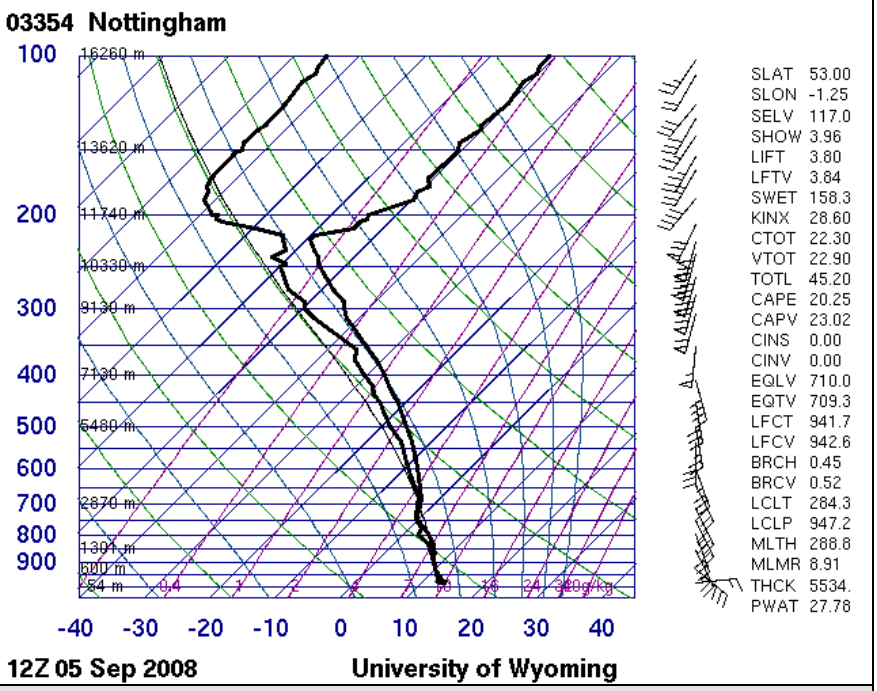

b) Upper air sounding from Nottingham valid at 1200 GMT on 05/09/2008

Figure 8 Surface and upper air charts for 1200 GMT on 05/09/2008

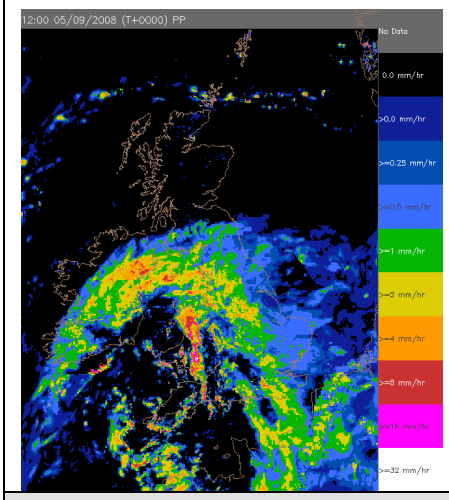

a) UKPP analysis of surface rain rate valid at 1200 GMT on 05/09/2008

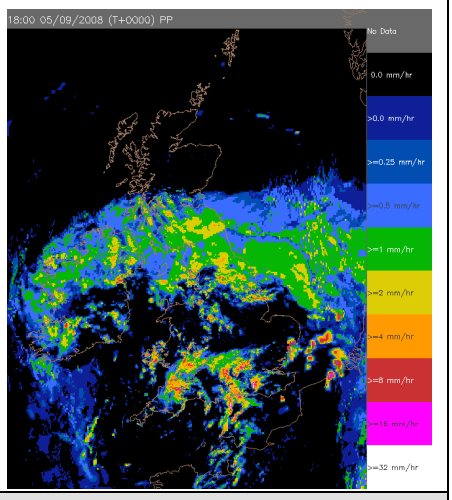

b) UKPP analysis of surface rain rate valid at 1800 GMT on 05/09/2008

© Crown copyright 2010

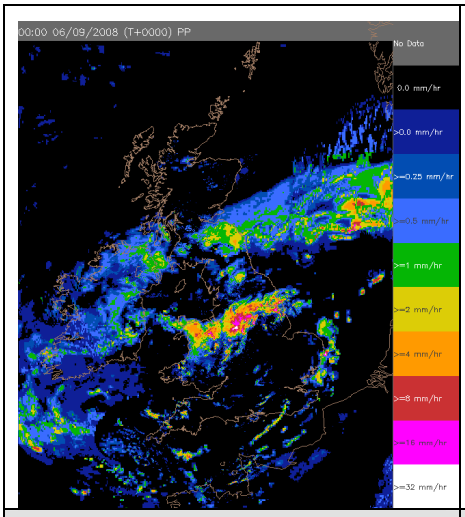

c) UKPP analysis of surface rain rate valid at 0000 GMT on 06/09/2008

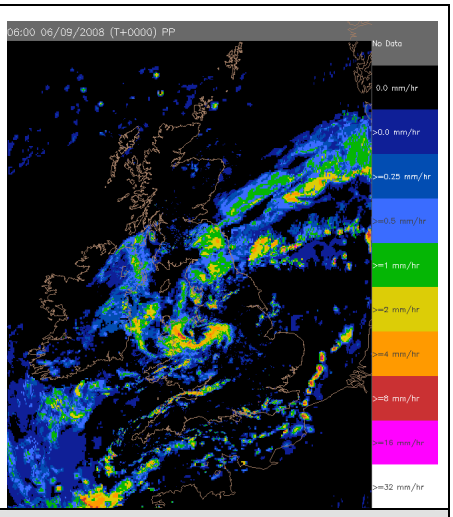

d) UKPP analysis of surface rain rate valid at 0600 GMT on 06/09/2008

Figure 9 A sequence of UKPP surface analyses of rain rate for the period from 1200 GMT on 05/09/2008 to 0600 GMT on 06/09/2008.

5.2.3. Case study 2 – 29 October 2008

Synopsis

On 29/10/2008, a deepening low pressure system, originating over Iceland, moved steadily south-south-eastwards across Northern Ireland and over the Irish Sea (see Figure 10a). An unusually cold, polar-maritime airmass spread its influence down the western side of the UK in its wake. Ahead of the advancing low, to the south and east, a relatively warm, moist, sub-tropical maritime airmass was drawn northwards from the English Channel and Bay of Biscay. An occluding frontal zone. oriented north-south across south-west England and marking the dividing line between the two airmasses, remained quasi-stationary into daylight hours on 30/10/2008.

The upper air sounding from Camborne valid at 0000 GMT on 30/10/2008 (Figure 10b) shows a convectively unstable profile characterised by a comparatively warm, moist near surface layer (moderately high wet-bulb potential temperature) beneath a ‘cold pool’ of mid-tropospheric air originating from polar latitudes (lower wet-bulb potential temperature).

The 6 hourly sequence of UKPP analyses of surface rain rate valid between 1800 GMT on 29/10/2008 and 1200 GMT on 30/10/2008 (Figure 11) shows a broad belt of precipitation lying across Wales and the south-west. This contains some intense precipitation areas associated with embedded convection. Areas of shower activity are also apparent in the English channel, and around the coasts of Scotland and eastern England. By 0000 GMT on 30/10/2008 the heaviest precipitation over south-west England coincides with the surface position of the occlusion. The extreme precipitation which fell

© Crown copyright 2010

over Ottery St. Mary in the early hours of the 30/10/2008 is not visible in Figure 11.

Features of relevance to the blending algorithms

By design, the noise fields used to perturb and downscale the blended forecasts exhibit spatially homogeneous statistical properties. Thus, they represent the domain average power spectra of the radar or model forecast precipitation fields. In cases involving both widespread (frontal) precipitation and showers, this implies that the noise will contain features which are neither solely frontal, nor entirely showery in nature, but are a composite of these two distributions. Such behaviour might result in unrealistic blends of noise and one or more forecast components, for example, introducing inappropriate structures into frontal precipitation or weakening areas of showers.

Given that the noise fields are spatially homogeneous in character, they cannot generate localised, extreme features such as the Ottery St. Mary thunderstorms. Nonetheless, it should be possible for the blended forecasts to represent, at least in part, regional variations in the character of precipitation fields. This can be achieved through the use of spatially varying target means and variances when blending forecast components (for example, an extrapolation nowcast and UKV forecast). To this end, the blended ensemble forecasts evaluated in this report have been generating using blended target means and variances, calculated on grid boxes of ~250 km by ~250 km.

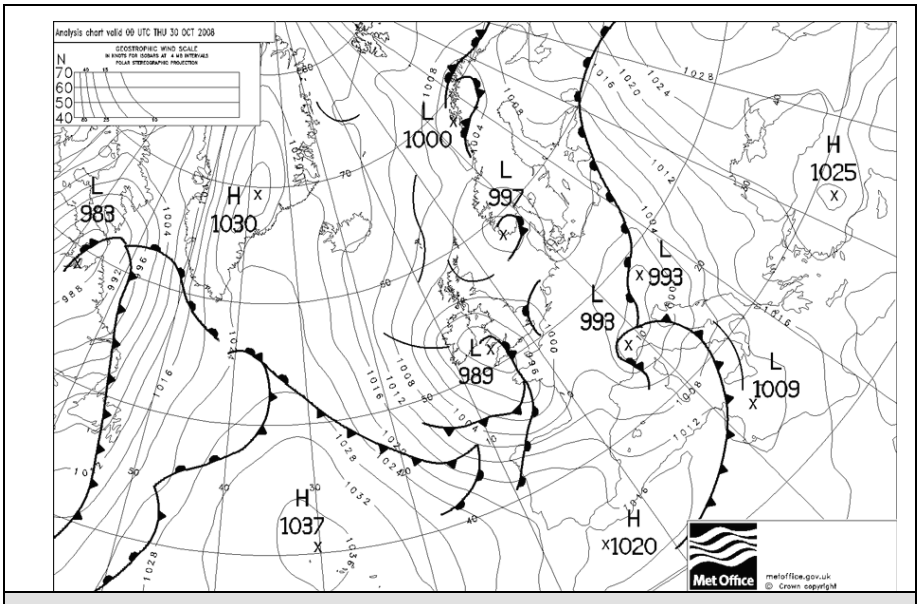

a) Surface analysis valid at 0000 GMT on 30/10/2008

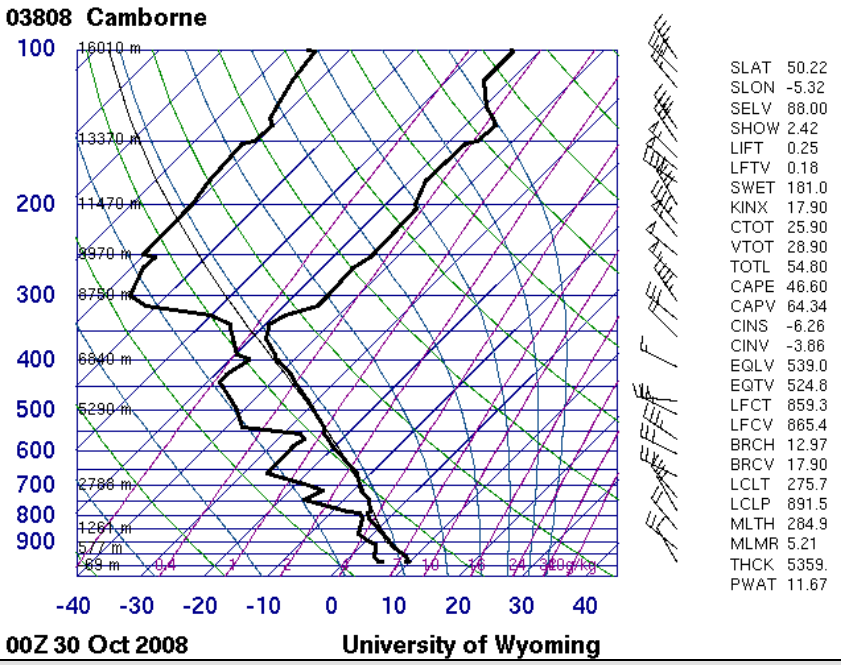

b) Upper air sounding from Camborne valid at 0000 GMT on 30/10/2008

Figure 10 Surface and upper air charts for 0000 GMT on 30/10/2008.

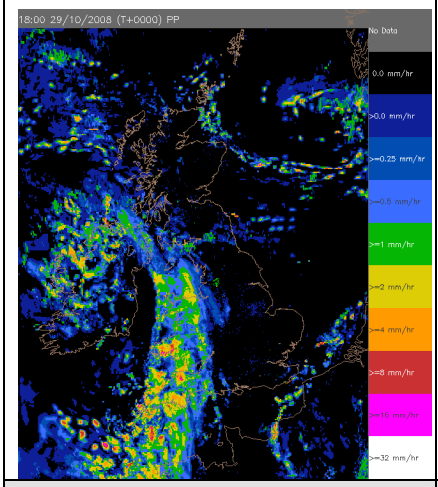

a) UKPP analysis of surface rain rate valid at 1800 GMT on 29/10/2008

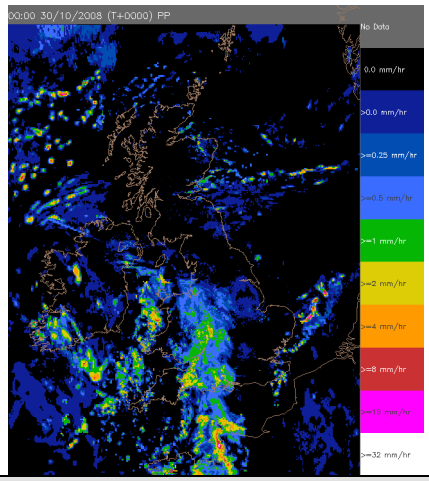

b) UKPP analysis of surface rain rate valid at 0000 GMT on 30/10/2008

© Crown copyright 2010

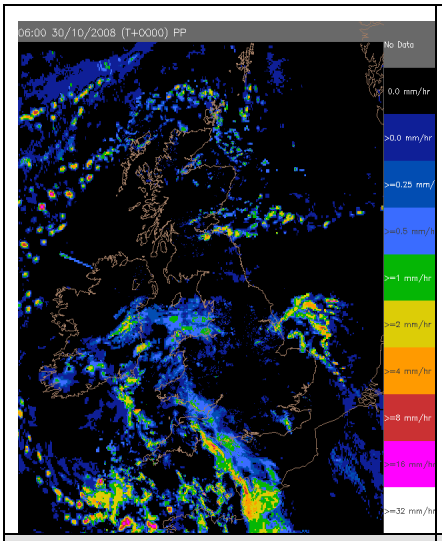

c) UKPP analysis of surface rain rate valid at 0600 GMT on 30/10/2008

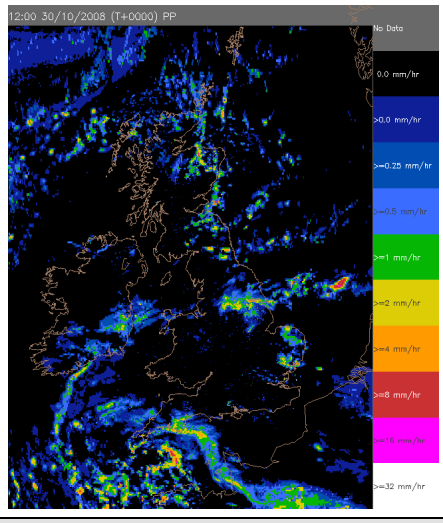

d) UKPP analysis of surface rain rate valid at 1200 GMT on 30/10/2008

Figure 11 A sequence of UKPP surface analyses of rain rate for the period from 1800 GMT on 29/10/2008 to 1200 GMT on 30/10/2008.

5.2.4. Case study 3– 18-19 November 2009

Synopsis

A developing depression in mid-Atlantic moved north-eastwards to a position south of Iceland by 1200 GMT on 19/11/2009 (Figure 12a). An associated polar front extending from Scandinavia to the Azores lay across Scotland. To the south of this frontal zone, an unusually warm, moist sub-tropical maritime airmass moved north-eastwards across England and Wales. A broad band of precipitation, orientated from south-west to north-east across Ireland, north-west England and Scotland at 1200 GMT on 19/11/2009 moved very slowly south-eastwards over the following 24 hours. Strong south-westerly winds led to dramatic orographic enhancement of the precipitation over the mountains of Ireland, the English Lake District and Scotland.

The upper air sounding from Valentia Observatory at 1200 GMT (Nottingham not available) on 19/11/2009 (Figure 12b) shows a remarkably warm, saturated vertical profile characteristic of a sub-tropical airmass originating from the Azores. The bulge in the profile in the mid-troposphere and the height of the upper tropospheric temperature inversion (above 200 hPa) are indicators that the airmass extends through the full depth of the troposphere. The lowest ~3 km of the atmosphere are neutrally stable with respect to a saturated air parcel (the profile follows a saturated adiabat). The potential for extreme rainfall is clear, particularly, where dynamically driven ascent is enhanced by forced ascent over orography.

The sequence of 6 hourly UKPP analyses of surface rain rate valid between 1200 GMT on 19/11/2009 and 0600 GMT on 20/11/2009

© Crown copyright 2010

shows a broad belt of precipitation, initially lying across Wales, north-west England and western Scotland. Areas of enhancement are apparent over the mountains in southern Ireland, western Scotland and north-west England. On the 20/11/2009, the precipitation band narrowed and weakened as it moved into England and Wales, leaving scattered showers over Ireland and western parts of England and Scotland. The heaviest precipitation fell over the Lake District: over the 34 hour period ending at 0600 GMT on 20/11/2009, rain gauges at Seathwaite and Honister Pass recorded 377.8mm and 368.2 mm respectively.

Features of relevance to the blending algorithms

In precipitation events involving seeder-feeder orographic enhancement it is known that radar based estimates of surface rain rate tend to be too low because the lowest elevation radar scan often overshoots the enhancement zone. Here, the vertical profile correction applied in the radar processing cannot replicate the precise structure or magnitude of the enhancement and significant underestimation of surface rain rate in hilly or mountainous areas is to be expected.

As previously explained, UKV forecasts of surface precipitation rate are not subject to these deficiencies. However, because UKV based noise fields are statistically homogeneous in space, geographical variations in the character of the precipitation cannot be replicated in the noise. As a result, noise injected into the bottom of a cascade of blended forecasts may act to reduce local extremes predicted by the UKV model. The use of spatially varying means and variances in the blending should tend to counter such problems, although, in the case of very localised extreme precipitation, this cannot entirely compensate for the lack of spatial heterogeneity in the noise.

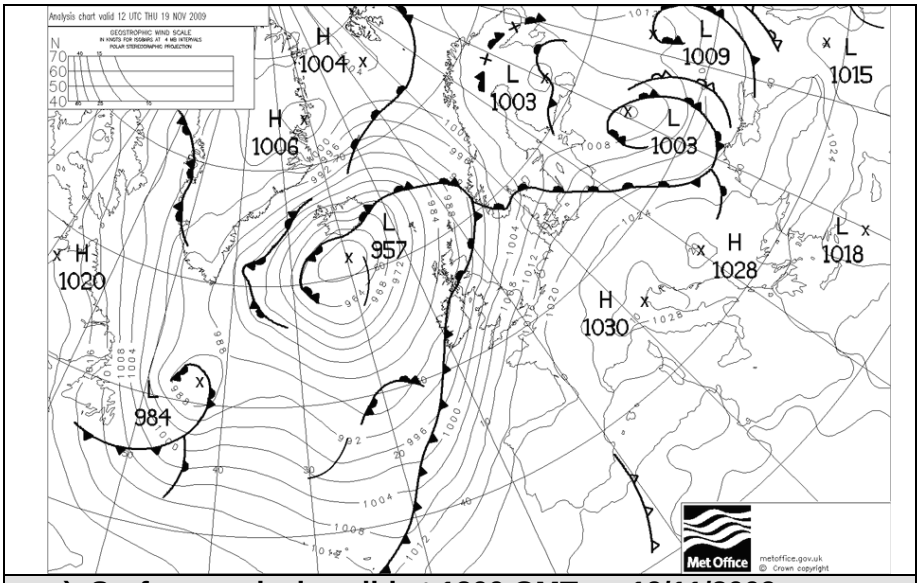

a) Surface analysis valid at 1200 GMT on 19/11/2009

© Crown copyright 2010

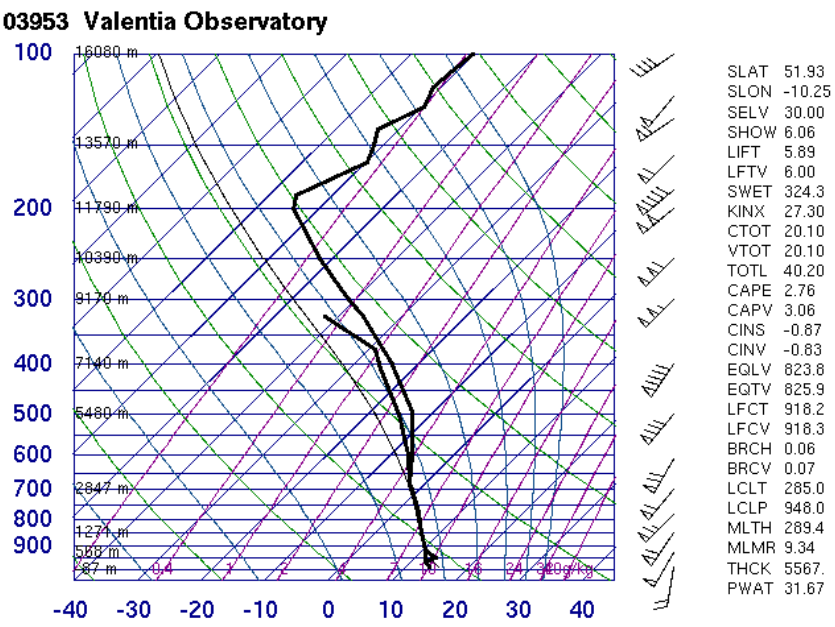

b) Upper air sounding from Camborne valid at 1200 GMT on 19/11/2009

Figure 12 Surface and upper air charts for 1200 GMT on 19/11/2009

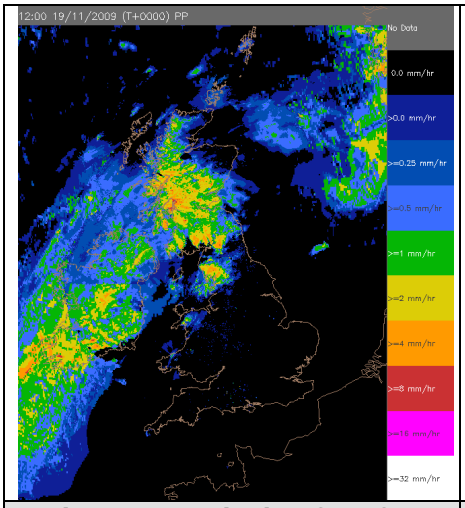

a) UKPP analysis of surface rain rate valid at 1200 GMT on 19/11/2009

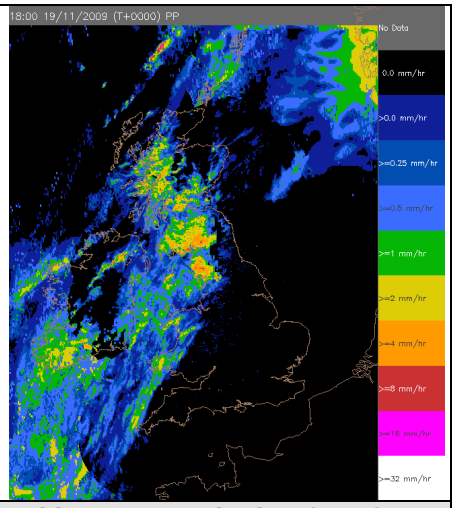

b) UKPP analysis of surface rain rate valid at 1800 GMT on 19/11/2009

© Crown copyright 2010

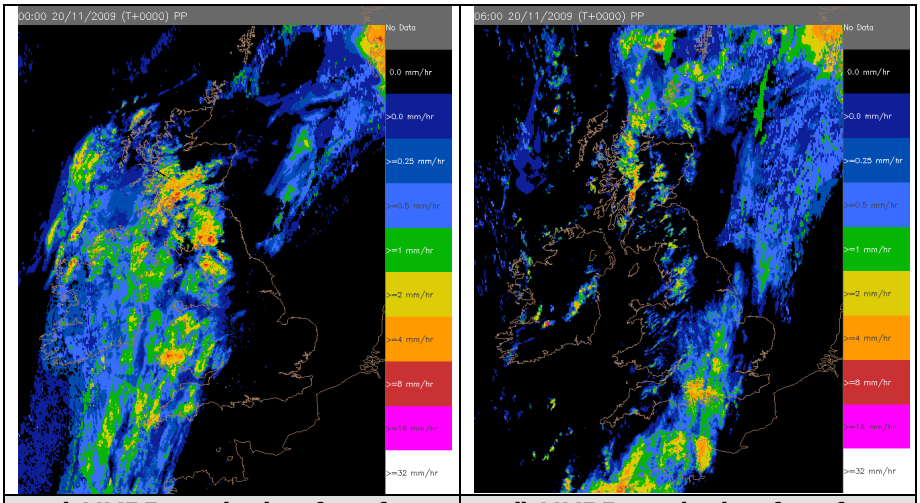

c) UKPP analysis of surface rain rate valid at 0000 GMT on 20/11/2009	d) UKPP analysis of surface rain rate valid at 0600 GMT on 20/11/2009

Figure 13 A sequence of UKPP surface analyses of rain rate for the period from 1200 GMT on 19/11/2009 to 0600 GMT on 20/11/2009.

5.2.5. Case study 4– 17 February 2010

Synopsis

On the 17/02/2010, an extensive, complex area of low pressure dominated the synoptic situation over western Europe. One of the low centres lay over northern Scotland at 1200 GMT on 17/02/2010 with an associated occluded front and precipitation extended across the UK from north-east Scotland to south-west England. Several troughs, one wrapped around a second low centre to south of Ireland, were responsible for organised shower activity to west of Scotland and over the south-west approaches.

The upper air sounding from Nottingham at 1200 GMT on 17/02/2010 shows a statically stable profile with a saturated boundary layer and several moist layers aloft separated by a drier region between 800 hPa and 700 hPa. The weak inversion at ~925 hPa marks the boundary between the surface airmass of polar origin and the occluded warm sector airmass above, probably of returning polar maritime origin.

The sequence of 6 hourly UKPP analyses of surface rain rate valid between 1200 GMT on 17/02/2010 and 0600 GMT on 18/02/2010 shows a weakening band of frontal precipitation over England associated with the occlusion. This is more active east of the low centre over Scotland. Several areas of organised shower activity are apparent to the west of Scotland and over the south-west approaches. The latter region contains some intense showers or thunderstorms.

© Crown copyright 2010

Features of relevance to the blending algorithms

In this case study, the character of the precipitation in the UKPP rain analyses varies significantly from region to region. The two areas of shower activity to the west of Scotland and in the south-west approaches are quite different in character to the broad area of frontal precipitation over the North Sea and the dissipating frontal precipitation over England. Here, the principle challenge for the blending algorithm lies in the maintenance of these different distributions when the forecast blends incorporate noise which has spatially homogenous statistical properties.

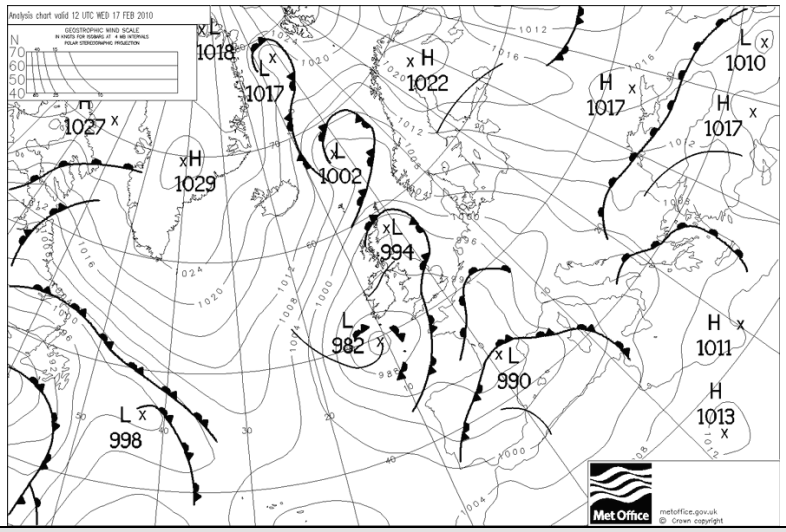

a) Surface analysis valid at 1200 GMT on 17/02/2010

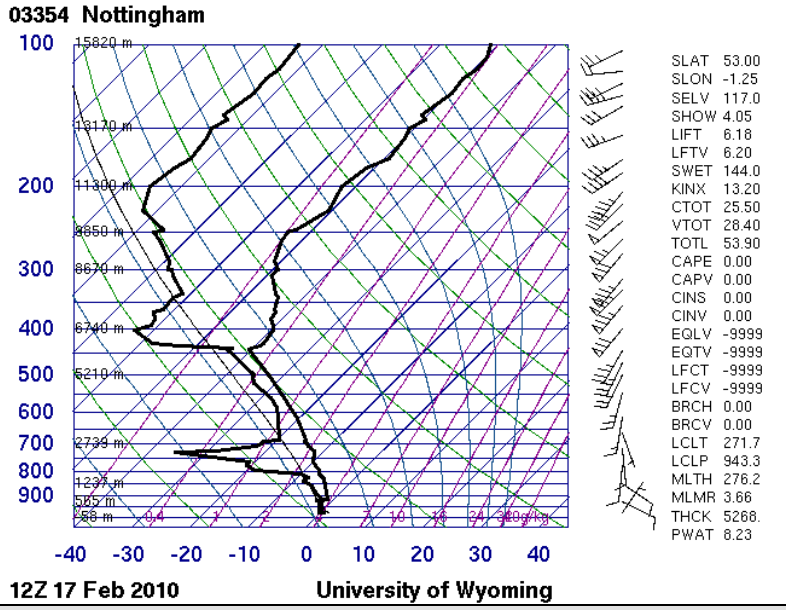

b) Upper air sounding from Camborne valid at 1200 GMT on 17/02/2010

Figure 14 Surface and upper air charts for 1200 GMT on 17/02/2010.

© Crown copyright 2010

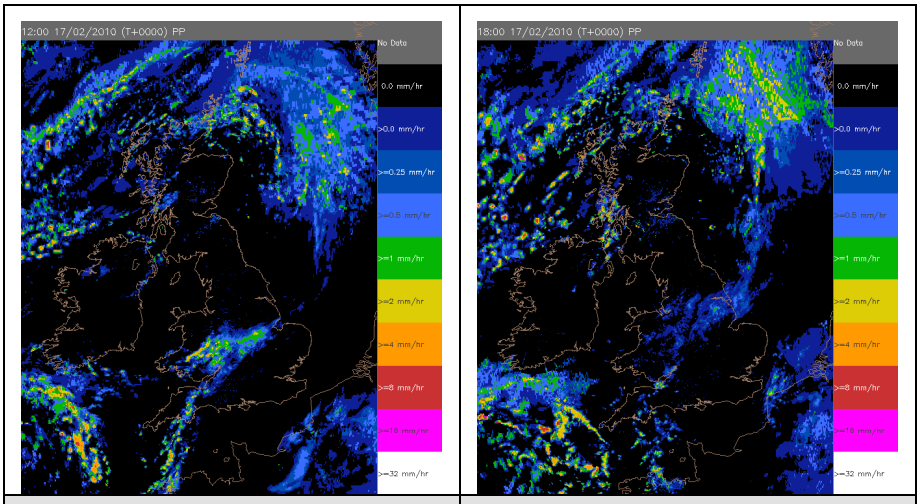

a) UKPP analysis of surface rain rate valid at 1200 GMT on 17/02/2010

b) UKPP analysis of surface rain rate valid at 1800 GMT on 17/02/2010

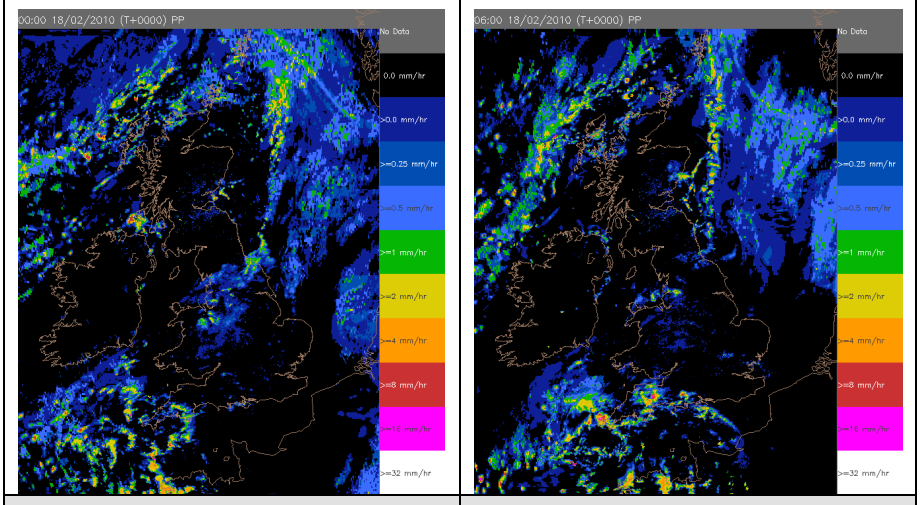

c) UKPP analysis of surface rain rate valid at 0000 GMT on 18/02/2010

d) UKPP analysis of surface rain rate valid at 0600 GMT on 18/02/2010

Figure 15 A sequence of UKPP surface analyses of rain rate for the period from 1200 GMT on 17/02/2010 to 0600 GMT on 18/02/2010.

5.2.6. Case study 5– 25 March 2010

Synopsis

In common with the previous case study, an extensive, complex area of low pressure dominated the synoptic situation over western Europe on 25/03/2010. A developing frontal wave in the English Channel, accompanied by spiralling bands of precipitation, moved northwards across England and Wales in a moist, southerly flow of polar maritime returning origin. At the same time, another band of precipitation,

© Crown copyright 2010

associated with an occluding frontal system over Scotland, moved north and eastwards.

The upper air sounding from Nottingham at 1200 GMT on 25/03/2010 shows a statically stable profile with a strong temperature inversion and dry air above the boundary layer up to a height of about 5 km. This is associated with a region of mid-tropospheric subsidence ahead of the developing frontal wave moving up from the south.

The sequence of 6 hourly UKPP analyses of surface rain rate valid between 1200 GMT on 25/03/2010 and 0600 GMT on 26/03/2010 shows several spiralling bands of precipitation moving northwards across England and Wales. Initially, this is locally intense close to the low centre but the precipitation area weakens as it drifts northwards. The area of precipitation in the north-east corner of the domain persists throughout the period, though it remains mostly light or moderate in intensity.

Features of relevance to the blending algorithms

This type of event is one that should be handled well by the two blending algorithm configurations under investigation. The character of the precipitation is more or less uniform over the UKPP domain. Consequently, the use of spatially homogenous noise fields for downscaling and perturbing the forecast components should be adequate. Also, the use of a power law based scaling model for parametric noise generation might be expected to be successful since widespread precipitation fields often exhibit power spectra of a similar form.

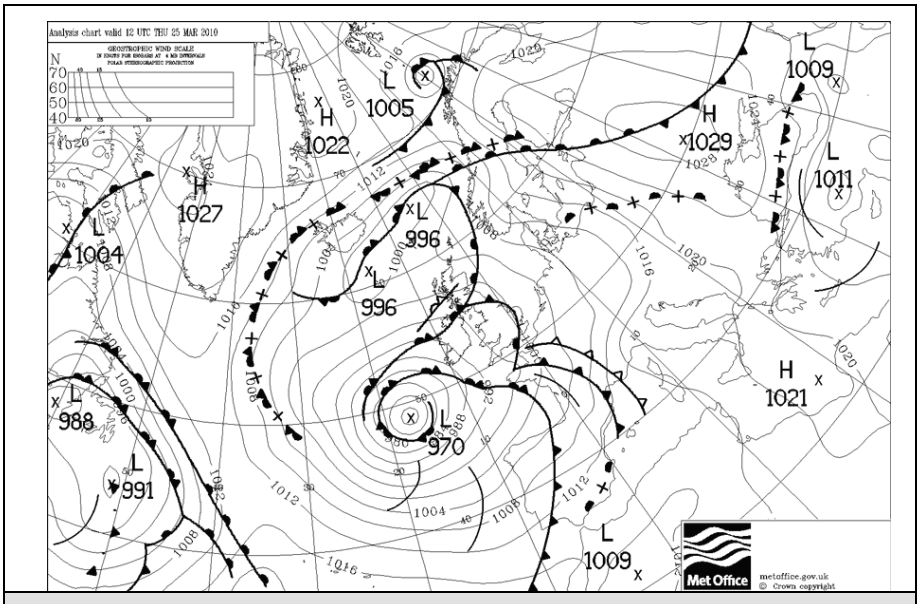

a) Surface analysis valid at 1200 GMT on 25/03/2010

© Crown copyright 2010

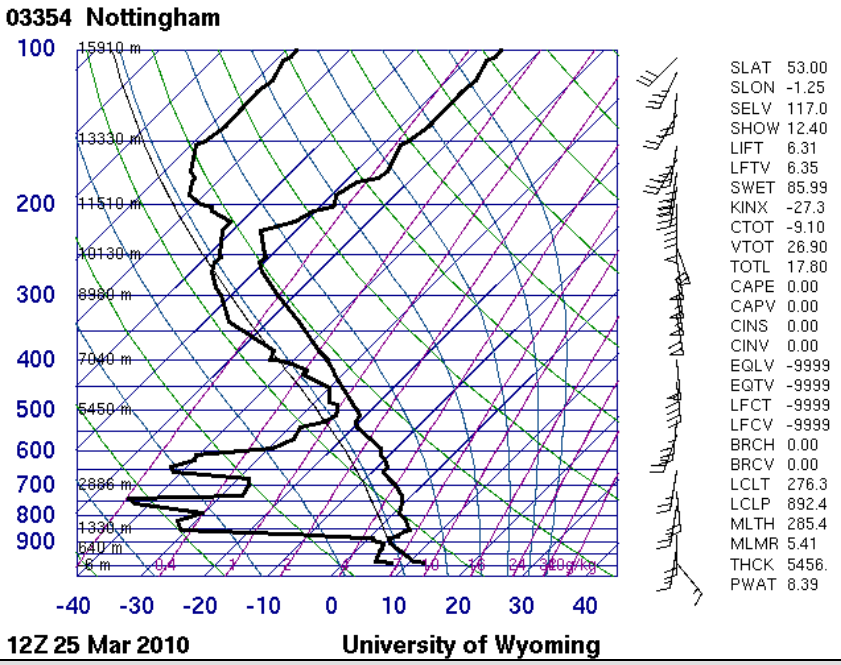

b) Upper air sounding from Camborne valid at 1200 GMT on 25/03/2010

Figure 16 Surface and upper air charts for 1200 GMT on 17/02/2010.

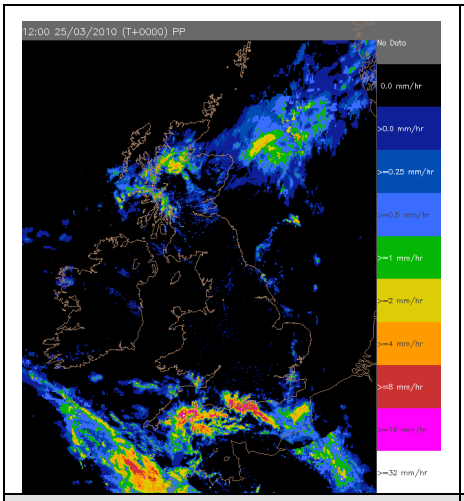

a) UKPP analysis of surface rain rate valid at 1200 GMT on 25/03/2010

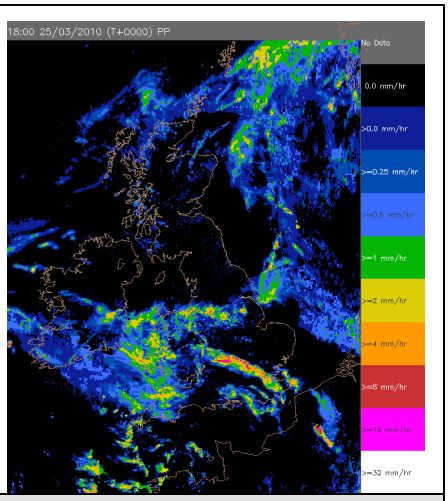

b) UKPP analysis of surface rain rate valid at 1800 GMT on 25/03/2010

© Crown copyright 2010

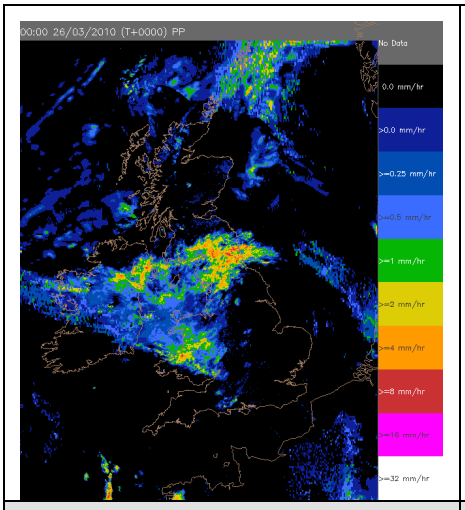

c) UKPP analysis of surface rain rate valid at 0000 GMT on 26/03/2010

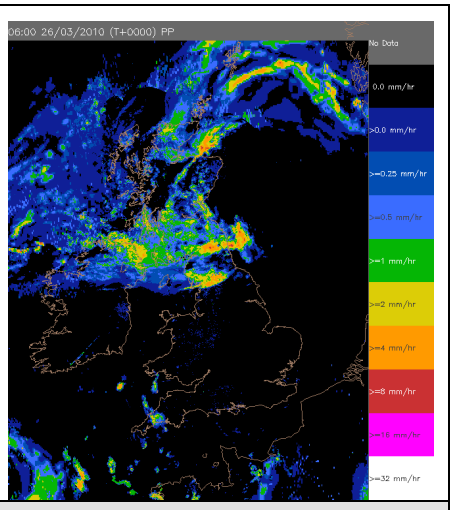

d) UKPP analysis of surface rain rate valid at 0600 GMT on 26/03/2010

Figure 17 A sequence of UKPP surface analyses of rain rate for the period from 1200 GMT on 25/03/2010 to 0600 GMT on 26/03/2010.

5.3. Performance of the noise generation algorithms

5.3.1. Overview

Several noise generation algorithms have been developed and tested for perturbing and downscaling blended forecasts in two, alternative forecast configurations. This requirement has arisen because there is no obvious 2km resolution target distribution of rain rate for noise generation beyond the forecast range of the UKV model (T+36h), whereas, at shorter lead times, either the 2km resolution, radar based UKPP rain analyses or 2 km interpolated UKV forecasts can be employed as the target. Thus, the noise generation method proposed for downscaling and perturbing MOGREPS-R ensemble precipitation forecasts beyond T+36h (the *parametric* method) is distinct from that recommended for a similar treatment of extrapolation nowcasts and ensemble UKV forecasts at shorter lead times (the *non-parametric* method).

The *non-parametric* noise generation method uses the FFT of the target distribution as a filter to replicate its precise Power Spectral Density and any anisotropy in the target field. This is intended for use in generating blends of an extrapolation nowcast and a UKV ensemble precipitation forecast in which the spatial statistical properties of the noise evolve from those inferred from a radar based UKPP rain analysis to those determined from a time series of UKV precipitation forecasts. To achieve this goal, it must be demonstrated that a time series of non-parametric noise fields can be generated whose spatial statistical properties tend seamlessly from a radar based target distribution to a UKV based distribution. Furthermore, it is desirable to demonstrate that the anisotropy present in a target field can be replicated in the noise.

© Crown copyright 2010

The parametric technique, assumes that the PSD of the target precipitation field can be approximated by a power law relationship between frequency and PSD. This approach has the advantage that the variance (variability) at any given spatial scale can be inferred even if there is insufficient information in the target field at this scale. However, the power law assumption provides only an approximation of the PSD of the target field. Furthermore, it can only represent the average spatial statistical properties of the field (in common with the non-parametric method), not distinguish between frontal precipitation and showers. Therefore, it is unclear to what extent this parametric noise generation technique can be used effectively to downscale 24 km resolution MOGREPS-R ensemble forecasts. A comparison of these downscaled forecasts with radar based UKPP rain analyses should provide some indication of value.

In summary, the aim of this section is to answer the following questions.

1) *Can time series of ensembles of synthetic, 2 km precipitation fields be generated whose spatial statistical properties reliably evolve from a target distribution based upon quality controlled radar to spectra based upon a UKV forecast sequence?*

2) *Can plausible, synthetic, 2 km precipitation fields be generated using power spectra inferred from 24 km resolution MOGREPS-R forecasts. If not, are there suitable alternative target distributions which can be used instead?*

5.3.2. Verification criteria

Since the aim is to generate noise fields which are indistinguishable in character from a given target field, the verification presented below is based upon two sources of evidence: a visual comparison of the target and noise fields and a comparison of field statistics including field mean, variance, raining fraction and PSD.

5.3.3. Performance of the non-parametric noise generator

Generation of noise fields that evolve seamlessly from one target distribution to another

The purpose of this experiment is to demonstrate that it is possible to generate synthetic precipitation fields which reliably and seamlessly evolve from a target distribution based upon a UKPP rain analysis to one based upon a high resolution NWP forecast field. This functionality will be exploited to generate blends of an extrapolation nowcast and ensembles of UKV precipitation forecasts.

The target fields used in this demonstration (see Figure 18) have deliberately been chosen to be of very different character (they are taken from different events) so that the evolution of the noise from one target distribution to the other is emphasised. The temporal updating of the noise cascade follows (40), although the advection of the noise

© Crown copyright 2010

cascades is disabled. The power spectral densities of the two target fields as a function of wave number and orientation (the non-parametric noise is anisotropic) would normally be blended using weights that are a function of scale and the measured skill of the target fields. However, in this demonstration, the weights have been artificially defined (see Figure 19) to simplify the blending of the PSDs and facilitate interpretation of the resulting noise fields.

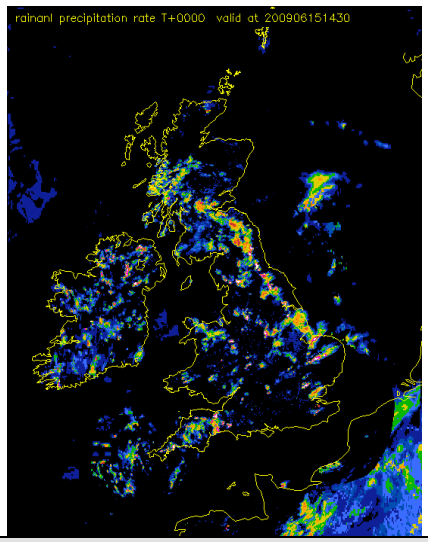

a) Target field based upon a 2 km resolution UKPP rain analysis

b) Target field based upon a 2 km resolution UM precipitation forecast

Figure 18 The target fields used to demonstrate the performance of the non-parametric noise generator.

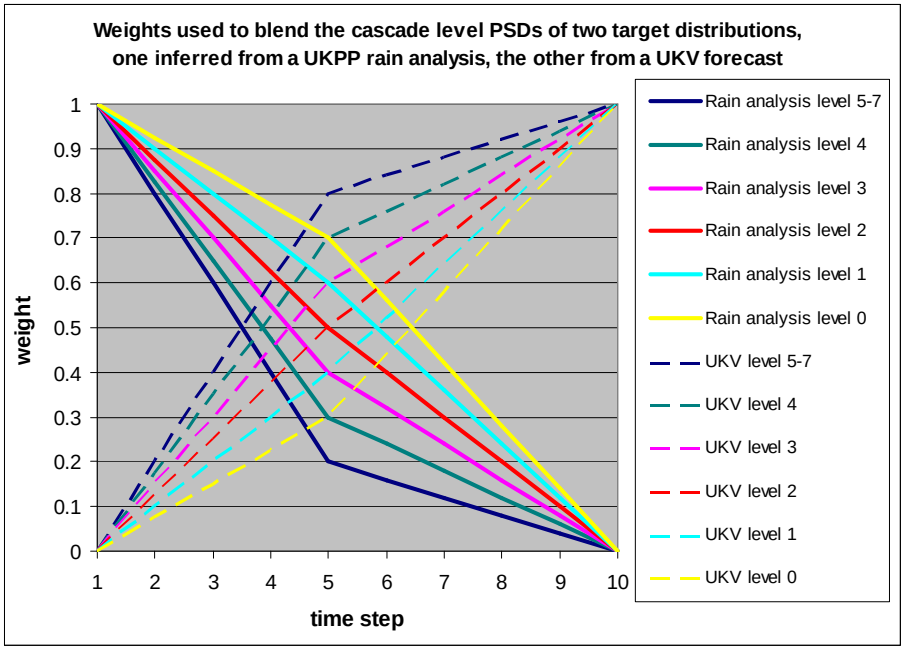

Figure 19 The weights applied to the PSDs of the two target fields shown in Figure 18. These are a function of cascade level and time step.

© Crown copyright 2010

Figure 20 shows a 10 step time series of noise fields that evolve from a target distribution based upon the UKPP rain analysis shown in Figure 18a to a target distribution based upon the UKV forecast shown in 18b.

The first noise field in the sequence in Figure 20 (top-left) replicates the showery nature of the precipitation in Figure 18a. In common with the target field, some of the showers in the synthetic field are clustered into more organised areas of precipitation. The diagonal alignment of the showers in the UKPP rain analysis, from north-west to south-east through southern Scotland and the northern half of England, is also represented. However, the area of frontal precipitation in the bottom right-hand corner of Figure 18a is not replicated. It must be remembered that each noise field is a random realisation of the average, spatial statistical properties of the target and cannot reproduce specific features.

Subsequent fields in the time series in Figure 20 demonstrate a tendency towards larger scale precipitation areas with reduced fine scale structure and intensity. The orientation of features is also seen to change so that features with an alignment from south-south-west to north-north-east dominate in the last few time steps. This evolution is visually consistent with a transition towards the target properties of the UKV forecast in Figure 18b.

Figures 21 and 22 demonstrate that the statistical properties of the noise fields in Figure 20 evolve from those of the UKPP rain analysis in Figure 18a to those of the UKV forecast in Figure 18b. The evolution of the variance of the synthetic fields is not smooth but does show the correct tendency. Field variance is sensitive to the tail of the distribution of rain rate and small errors in the representation of frequencies of high precipitation rates are responsible for this behaviour. Nonetheless, the frequency distributions of the noise fields in Figure 22 show a plausible development and close correspondence with the relevant target distributions at either end of the sequence.

The power spectra plots in Figure 23 provide further evidence of the skill of the non-parametric noise generator. The PSD of a field as a function of wave length elucidates how the variance of the field varies with spatial scale. In the case of precipitation, the power in units of dB (Y axis) always decreases with decreasing scale (from left to right on the X axis), but the rate of decrease varies depending on whether the precipitation is predominantly showery or frontal in nature. For a given raining fraction, showery precipitation fields exhibit more (less) power at the small (large) scales than frontal precipitation fields.

The thick dark blue line in Figure 23 is the PSD of the UKPP rain analysis shown in Figure 18a. The thick red line in the same Figure is the PSD of the UKV forecast in Figure 18b. One would expect the PSDs of the time series of noise fields to tend from the former to the latter. Scrutiny of Figure 23 largely confirms this behaviour. The noise power spectra tend to lose power relative the rain analysis (Figure 18a) at scales below about 150 km and gain power at scales above

© Crown copyright 2010

this. These trends are consistent with an evolution towards the PSD of the UKV forecast in Figure 18b.

Nonetheless, there are some imperfections in the PSDs of the noise fields. For example, the first noise field in the sequence in Figure 20 (the pink line) exhibits an excess of power relative to the UKPP rain analysis at scales above ~40 km. This is most prominent at around 100 km and implies that the noise has more variability (structure) at this scale than the rain analysis. Such discrepancies arise from the way the noise fields are constructed from the PSDs of the two target fields.

Each synthetic precipitation field is constructed from 8 cascade level fields. These component fields represent the average variability in the target field(s) over a discrete range of scales, as explained in section 2(iii). Consequently, they cannot replicate the target power spectrum accurately over all scales: errors should be largest at scales which fall mid-way between cascade levels.

Despite this limitation, the results in Figures 20 to 23 demonstrate that the non-parametric noise generator can usefully be employed to generate believable, synthetic precipitation fields with the attributes which closely follow those of a specified target distribution.

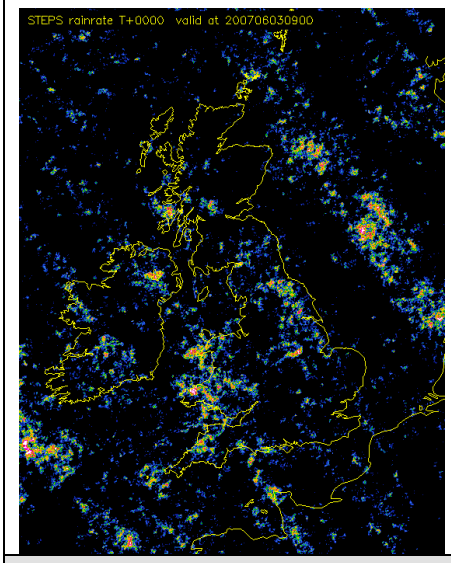

a) Noise field valid at time first target field (a UKPP rain analysis) denoted T+Δt

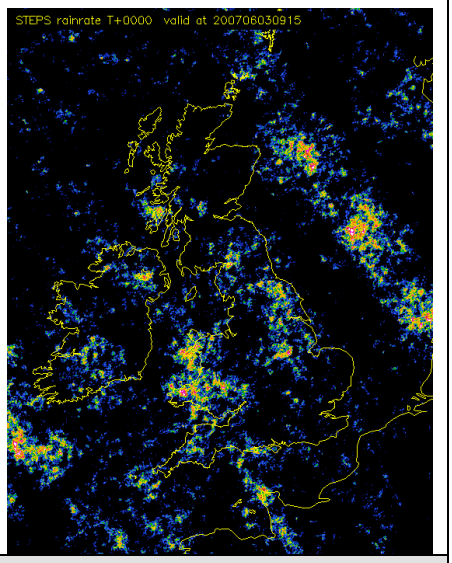

b) Noise field valid at T+2Δt

© Crown copyright 2010

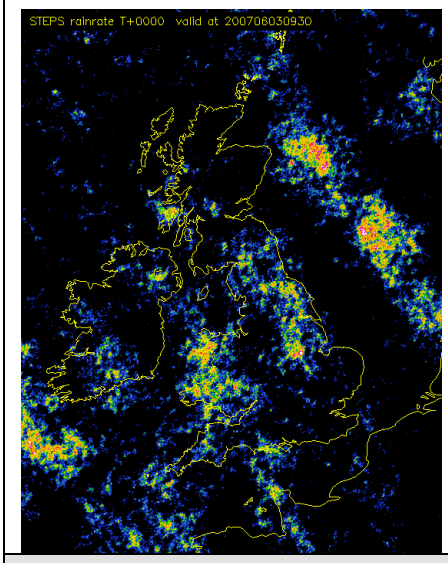

c) Noise field valid at T+3Δt

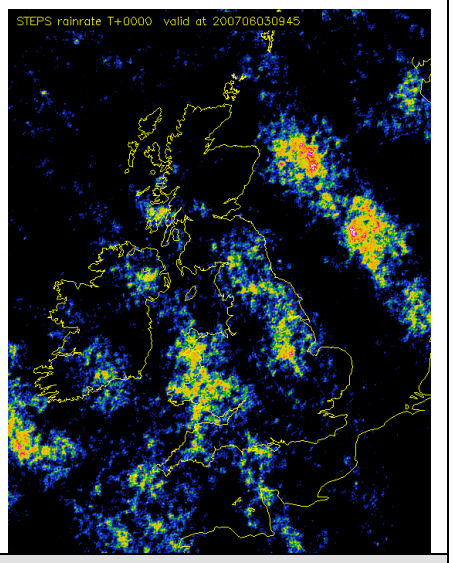

d) Noise field valid at T+4Δt

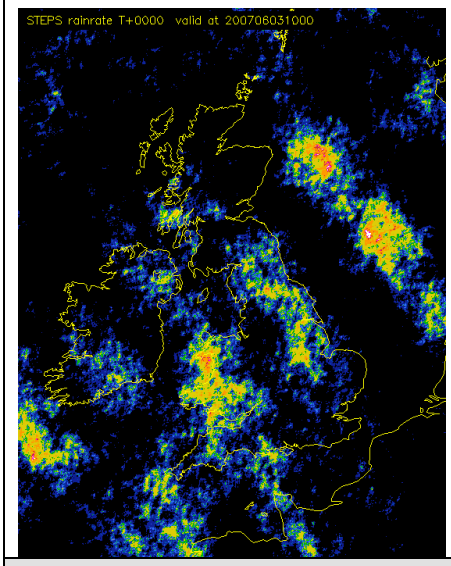

e) Noise field valid at T+5Δt

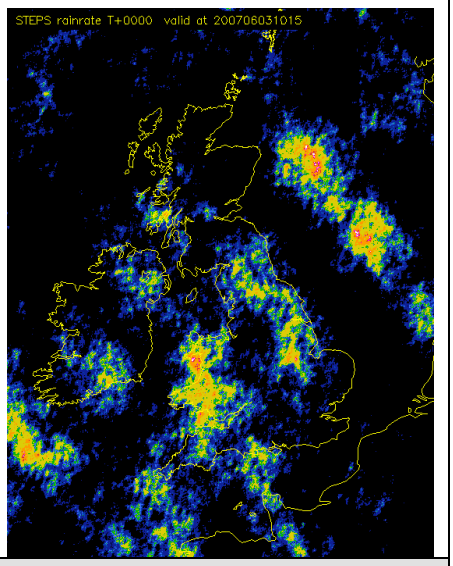

f) Noise field valid at T+6Δt

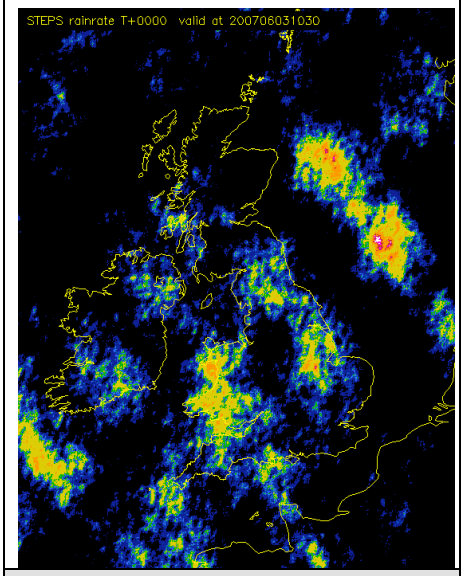

g) Noise field valid at T+7Δt

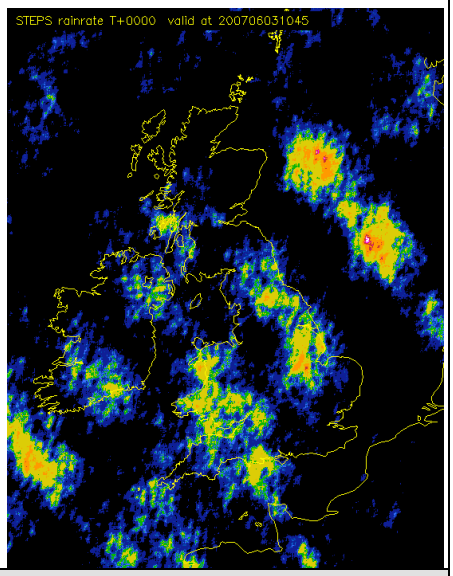

h) Noise field valid at T+8Δt

© Crown copyright 2010

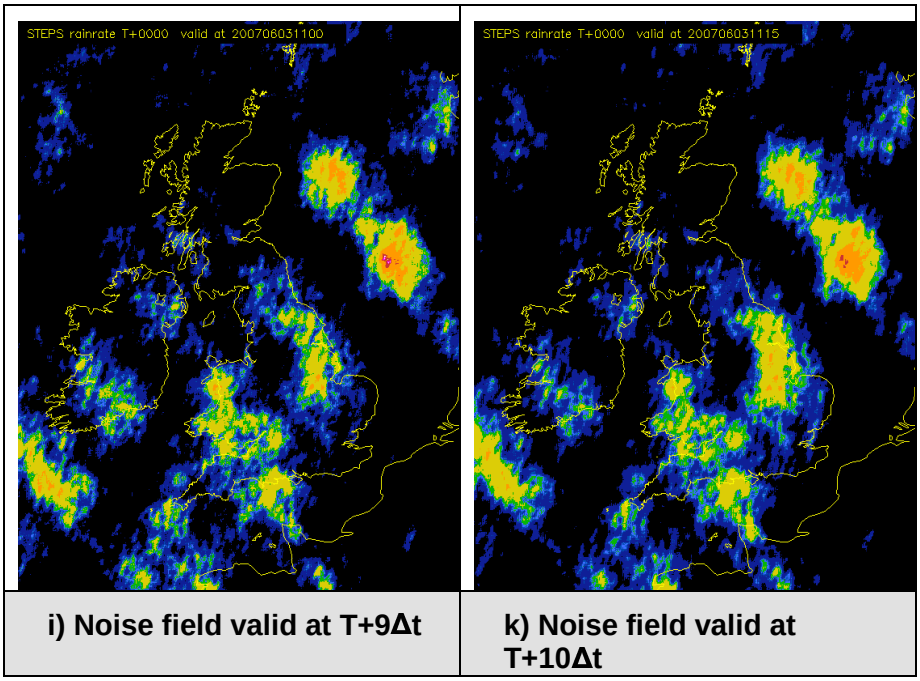

i) Noise field valid at T+9Δt	k) Noise field valid at T+10Δt

Figure 20 Temporal evolution of non-parametric noise fields from a target distribution based upon a UKPP rain analysis towards one based upon a high resolution UKV precipitation forecast.

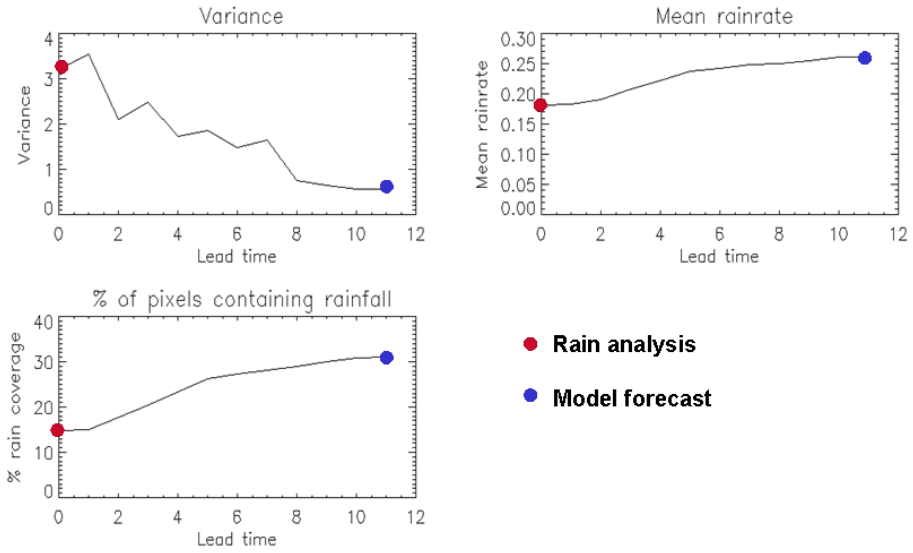

Figure 21 Temporal evolution of the field variance, mean rain rate and raining fraction in the non-parametric noise fields shown in Figure 19. The points labelled with the red and blue dots are the statistics for the UKPP analysis of rain rate (Figure 18a) and UKV forecast (Figure 18b) respectively. The lines joining the dots show the evolution of the field statistics of the noise fields displayed in Figure 20.

© Crown copyright 2010

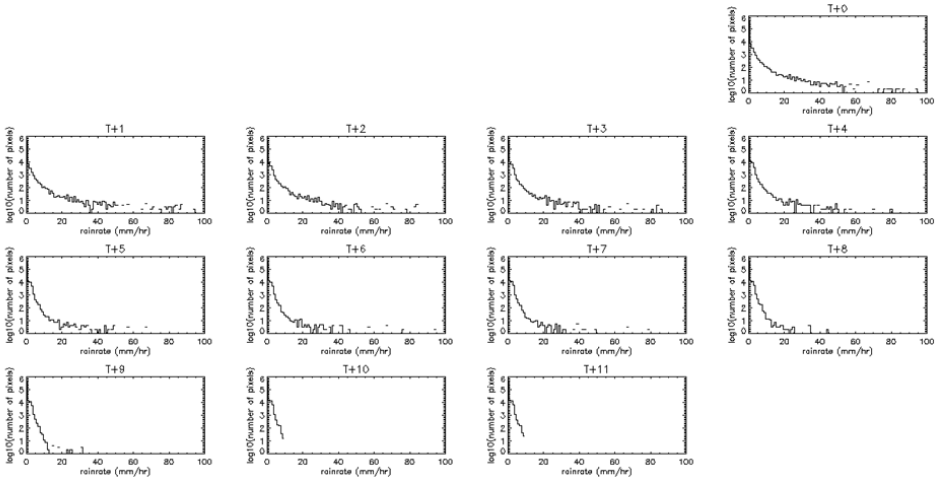

Figure 22 Temporal evolution of the frequency distribution of rain rate in the non-parametric noise fields shown in Figure 19. The graph labelled T+0 shows the distribution of rain rate in the UKPP analysis of rain rate (Figure 18a). The graph labelled T+11 shows the distribution of rain rate in the high resolution UM precipitation forecast (Figure 18b). The remaining graphs show the distributions in the noise fields displayed in Figure 19.

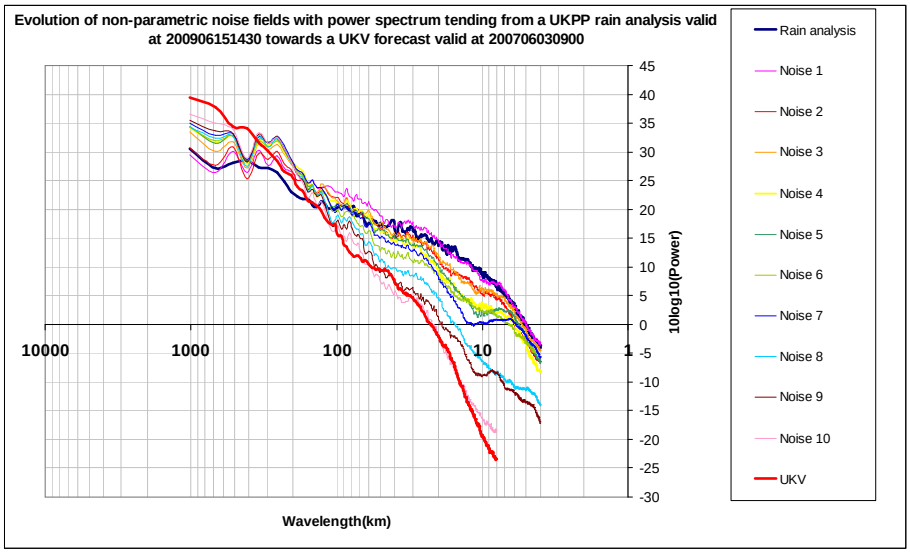

Figure 23 Evolution of the PSD of the synthetic precipitation fields shown in Figure 19. The thick power spectrum line plotted in dark blue belongs to the UKPP analysis of rain rate (Figure 18a). The thick power spectrum line plotted in red belongs to the high resolution UM precipitation forecast (Figure 18b). The lines lying largely between these are the power spectra of the time series of noise fields displayed in Figure 19.

© Crown copyright 2010

5.3.4. Performance of the parametric noise generator

In a similar vein to the investigation for the non-parametric noise generator, the performance of the parametric scheme has been investigated using a range of case study data sets. A selection of representative findings is presented below.

The parametric noise generator is designed to model the power spectrum of a given precipitation field using two power law relationships between PSD and frequency: one for scales above 40 km (the so called scale break), the other for scales below this. Precipitation fields often have power spectra which closely approximate this type of model over a wide range of scales. Such an approach has the advantage that it can be employed to infer PSD over a range of scales not adequately represented by the precipitation field.

When plotted in dB, a power spectrum modelled with two power law relationships and a scale break is composed of two straight lines with negative slopes. By design, the slope of the model fitted to scales below the scale break cannot be less negative than the slope of the line above. This technique is employed in STEPS to derive a power spectrum from a UKPP rain analysis when the raining fraction is < 5%. Here, is it used to infer the slopes of power spectra of a 24 km resolution MOGREPS-R precipitation forecasts with the aim of downscaling the forecasts to the 2 km scale.

The purpose of the selected case study results presented below is to demonstrate that the fitted power law models closely approximate the true power spectrum of MOGREPS-R precipitation forecasts at resolved scales. Since there is no information on the slope of the MOGREPS-R spectrum below 40 km (the scale corresponding to the Nyquist frequency is 48 km), the power law model fitted below the scale break will have a similar slope to that above (this a design feature of the scheme). No direct comparison is made between the modelled power spectra and those of corresponding UKPP rain analyses. The aim of this exercise is to demonstrate the goodness of fit of the model to the target field.

Figure 24 compares a control member MOGREPS-R precipitation forecast valid at 1400 GMT on 05/09/2008 with a UKPP rain analysis for the same time and two synthetic precipitation fields generated using the parametric noise generation algorithm. Scrutiny of the MOGREPS-R precipitation forecast and UKPP rain analysis demonstrates that the broad arc of precipitation extending over Ireland and northern and eastern England is quite different in character to the heavy showers to the south.

The two noise fields capture some of the large scale coherence in the MOGREPS-R forecast, and also add fine scale structure consistent with that visible in the showers over south-west and central southern England in the rain analysis. As explained previously, both parametric and non-parametric noise generators produce synthetic precipitation fields with power spectra that represent the domain average spatial statistics of the target field. In this case the resulting noise fields are a

© Crown copyright 2010

composite of the characteristics of showers and frontal precipitation and, therefore, are not a precise representation of either.

Figure 25 compares the power spectra of an ensemble of 23 noise fields, including the two shown in Figures 24c-d (members 1 and 2), with the MOGREPS-R forecast precipitation field in Figure 24a. It is apparent that the slope of the power spectrum of the MOGREPS-R forecast is a little steeper than those of the noise fields. Nonetheless, the power law model fit to the slope of the spectrum is a reasonable approximation. Furthermore, the slopes of the spectra of all 23 realisations of noise are consistent and exhibit the expected scaling properties (a straight line relationship between power in dB and scale).

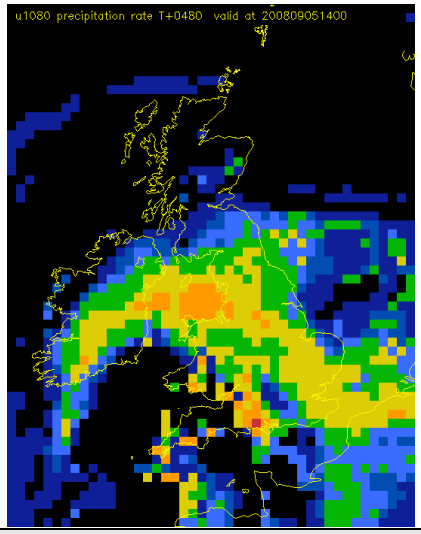

a) MOGREPS-R control forecast valid at 1400 GMT on 05/09/2008

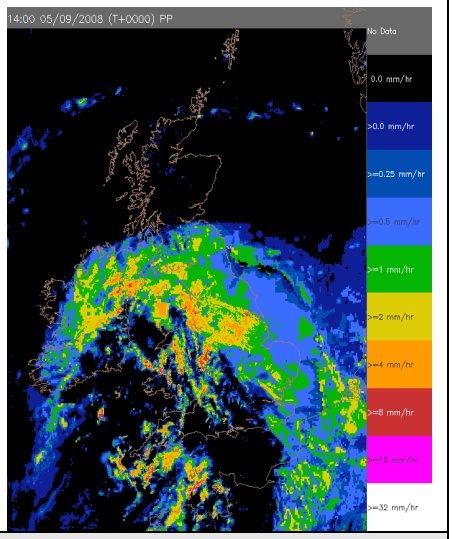

b) UKPP rain analysis valid at 1400 GMT on 05/09/2008

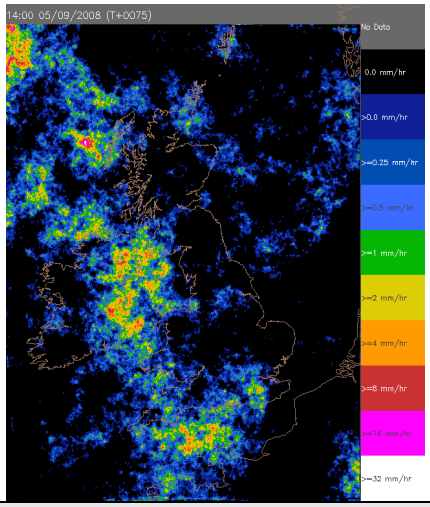

c) Noise field from ensemble member 10 valid at 1400 GMT on 05/09/2008

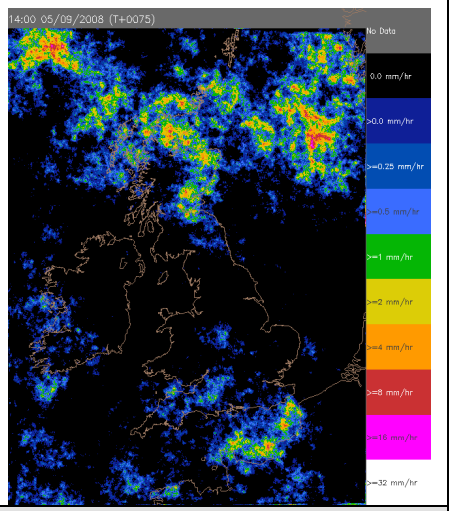

d) Noise field from ensemble member 13 valid at 1400 GMT on 05/09/2008

Figure 24 Comparison of a MOGREPS-R precipitation forecast field valid at 1400 GMT on 05/09/2008 with a corresponding UKPP rain analysis and two synthetic precipitation fields generated using the parametric noise generator.

© Crown copyright 2010

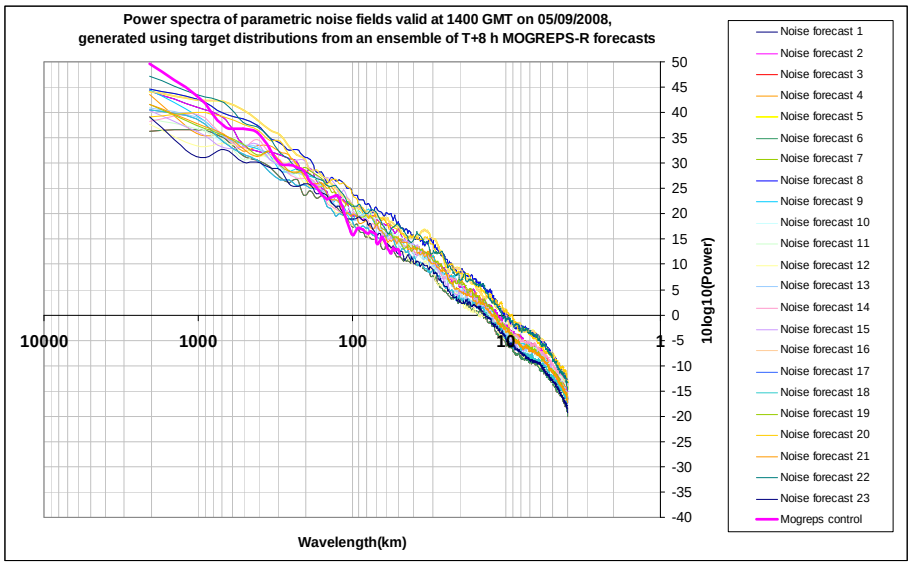

Figure 25 Comparison of the power spectrum of a MOGREPS-R precipitation forecast field valid at 1400 GMT on 05/09/2008 with the power spectra of 23 synthetic precipitation fields generated using a parametric model fit to the MOGREPS-R spectrum.

Figures 26 and 27 present a similar selection of case study data for a widespread precipitation event on 19/11/2009. On this occasion, convection is almost entirely absent from the MOGREPS-R forecast of precipitation rate and UKPP rain analysis valid at 1100 GMT on 19/11/2009. However, the broad belt of mostly light or moderate rain does contain some locally, more intense features associated with orographic enhancement. These can be seen over the hills and mountains of Ireland, north-west England and Scotland in Figure 26b. The two noise fields shown in the same Figure exhibit similar distributions of precipitation rate. However, there is a noticeable lack of coherence in the features at the synoptic scale.

This observation is consistent with the power spectra of the two noise fields (member1 and 2) shown in Figure 27. A comparison of the power spectra of a 23 member ensemble of noise fields with the spectrum of the MOGREPS-R forecast reveals that the majority of the 23 noise realisations lack power at the largest scales and have a little too much power below ~100 km. Thus, the power law model fit to the slope of the MOGREPS-R spectrum is rather poor, although the slopes of the spectra of all 23 realisations of noise are consistent. In this case, the error in the modelled slope of the MOGREPS-R power spectrum has produced synthetic precipitation fields which lack the coherence typical of frontal precipitation.

© Crown copyright 2010

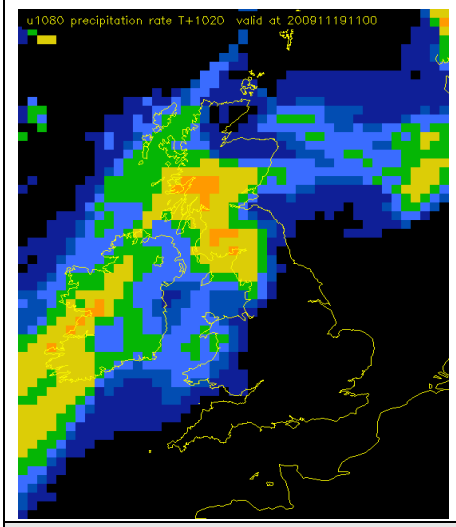

a) T+17 h MOGREPS-R control forecast valid at 1100 GMT on 19/11/2009

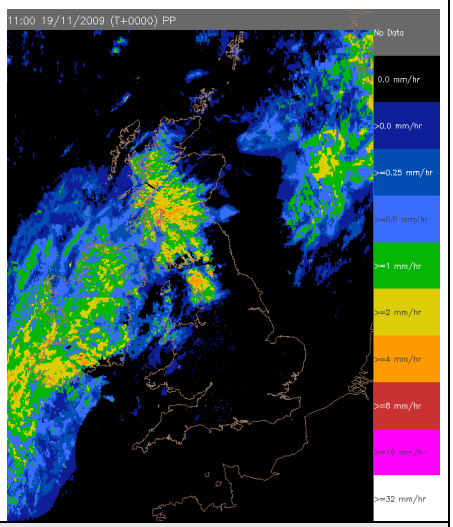

b) UKPP rain analysis valid at 1100 GMT on 19/11/2009

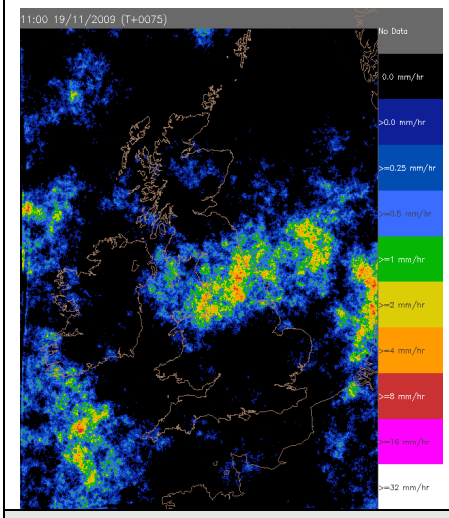

c) Noise field from ensemble member 01 valid at 1100 GMT on 19/11/2009

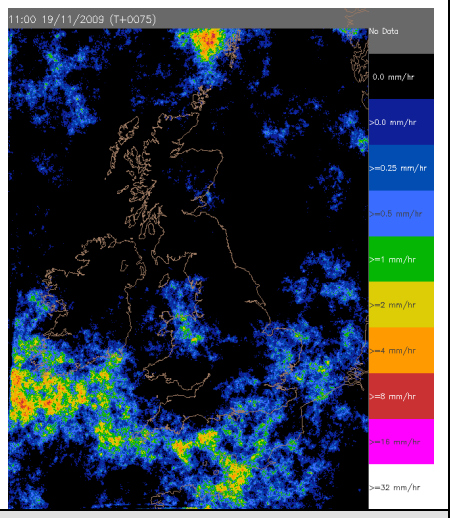

d) Noise field from ensemble member 11 valid at 1100 GMT on 19/11/2009

Figure 26 Comparison of a MOGREPS-R precipitation forecast field valid at 1100 GMT on 19/11/2009 with a corresponding UKPP rain analysis and two synthetic precipitation fields generated using the parametric noise generator.

© Crown copyright 2010

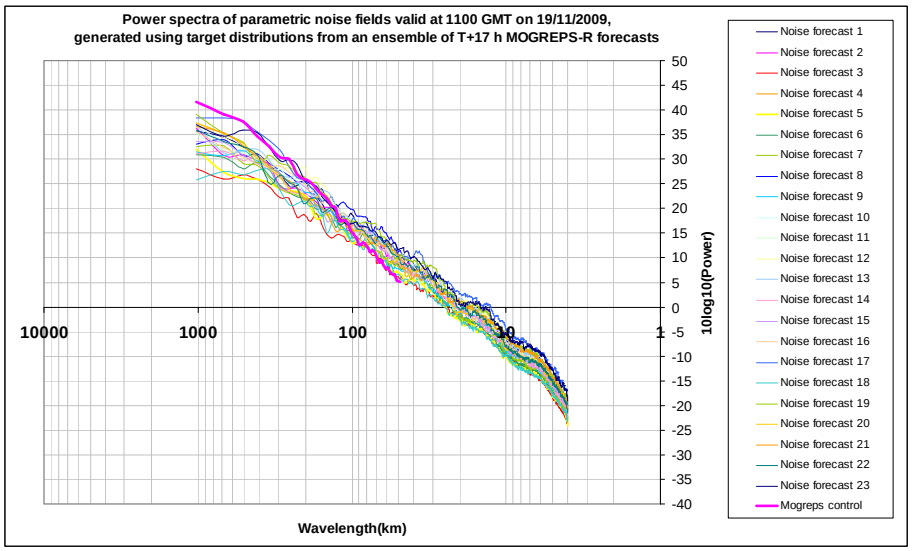

Figure 27 Comparison of the power spectrum of a MOGREPS-R precipitation forecast field valid at 1100 GMT on 19/11/2009 with the power spectra of 23 synthetic precipitation fields generated using a parametric model fit to the MOGREPS-R spectrum.

5.4. Performance of the blending algorithms

5.4.1. Configurations of blended forecasts evaluated

As summarised in section 4.6, the performances of the following configurations of blended forecasts will be assessed using data from the five case study events described in section 5.2:

Control member forecast configurations

1) a blend of a deterministic extrapolation nowcast and UKV control member forecast with non-parametric noise confined to the bottom two cascade levels (scales ≤ 8 km);

2) a downscaled MOGREPS-R control member forecast in which parametric noise is restricted to the bottom 4 cascade levels (scales ≤ 32 km) and the top four cascade levels are the control member forecast only;

Ensemble member forecast configurations

3) blends of an extrapolation nowcast and UKV control member forecast perturbed with 23 realisations (time series) of non-parametric noise, where the weights are a function of the skill of the nowcast and UKV forecast components on each cascade level;

4) downscaled MOGREPS-R control member forecasts perturbed with 23 realisations (time series) of parametric noise where the weights assigned to the MOGREPS-R forecast on each cascade level are a function of its skill.

© Crown copyright 2010

Note that blended forecasts incorporating ensembles of UKV or MOGREPS-R precipitation forecasts have not been run owing to resource constraints. In an operational context, multiple forecast realisations would be generated from selected UKV or MOGREPS-R ensemble members using multiple realisations of non-parametric or parametric noise.

The restriction of this performance evaluation to the verification of blended forecasts incorporating control runs of the UKV and MOGREPS-R is justified because an ensemble of blended forecasts generated from any given UKV or MOGREPS-R forecast member (whether it be a control run or perturbed member) can be used to demonstrate whether or not the blending algorithms are well calibrated.

Nonetheless, further verification is required to demonstrate the impact of using MOGREPS-R and UKV ensembles in the blended forecasts. Since, by design, the nowcast advection scheme implemented in the various blending algorithm configurations omits advection perturbations of the form employed by STEPS (Bowler *et al*., 2006), one would expect the inclusion of synoptic and mesoscale perturbations originating from the MOGREPS-R and/or UKV ensemble forecasts to improve the spread and skill of the ensembles of blended forecasts.

5.4.2. Scope of the performance assessment

Verification of the various configurations of blended precipitation forecasts described in section 5.4.1 above will be focused on two key aspects of performance.

Firstly, it must be demonstrated that the blended forecasts evolve smoothly from extrapolation nowcast to UKV forecast to MOGREPS-R forecast. This is best achieved using a combination of approaches similar to those adopted for appraisal of the noise generators: a case study oriented comparison of the blended forecasts and their components, and a comparison of field statistics including field mean, variance, raining fraction and frequency distribution.

A seamless handover from the UKV to MOGREPS-R will be difficult to achieve given the generation of two distinct blended forecast configurations exploiting different noise generation techniques. This is especially pertinent in relation to the blending of control member forecasts. In this case, the requirement to downscale MOGREPS-R control forecasts to 2 km implies a transition from UKV resolved high resolution precipitation features to parametric noise at scales below 32 km (cascade level 4). Unlike the UKV resolved precipitation, the latter is composed of isotropic features.

Secondly, it must be demonstrated that the blended forecasts are at least as skilful as their component forecasts. Since the blending is performed on a hierarchy of scales, it is appropriate to evaluate the skill of the blends on the same hierarchy of scales. The Fractions Skill Score is a suitable statistic to use in this context. The skill of the

© Crown copyright 2010

blended forecasts and components can be measured at the scales represented by the 8 level cascade decomposition and assessed independently of any forecast bias.

In addition, it must be shown that the blended ensemble forecasts exhibit skill relative to the blended control member forecasts. This entails demonstrating that the blended ensembles are: 1) reliable (the forecast probabilities of events are similar to the observed frequencies of those same events); 2) have resolution or sharpness (forecast probabilities exhibit a range of values other than climatology); 3) exhibit an increase (decrease) in spread about the ensemble mean with increasing (decreasing) error in the ensemble mean. A fuller explanation of these aspects of ensemble performance is provided below.

5.4.3. Verification criteria and their application

Tests to demonstrate the generation of plausible, seamless blended forecasts

The behaviours of the blended, control member forecasts are considered separately from those of the blended ensemble forecasts because, in the former case, the use of noise is constrained to the poorly resolved scales and this leads to rather different performance characteristics. The verification statistics presented include the field mean, variance, raining fraction, frequency distribution and power spectrum.

Tests to demonstrate the generation of skilful, blended control member and ensemble forecasts

The Fractions Skill Score

The Fractions Skill Score is employed to assess the skill of the blended forecasts and their associated UKV or MOGREPS-R precipitation forecasts on the hierarchy of scales represented by the cascade model. Since the FSS is a spatial statistic, performance must be measured relative to an observed field of precipitation rate or accumulation. Quality controlled radar estimates of surface precipitation rate and accumulation are used. Despite its many limitations, radar is the only observation source providing contiguous estimates of the distributions of precipitation rate and accumulation.

The FSS is derived as follows. For each grid point in a given forecast and corresponding UKPP rain analysis, the fraction of surrounding grid points that exceed a specified threshold (e.g. 1 mm/h) within a specified neighbourhood is calculated. The neighbourhood size is defined according the scale of interest and the methodology repeated for all relevant thresholds and scales. To avoid the effects of any residual bias in the radar observations, the FSS can be computed on thresholds that are fixed percentiles of the forecast and observed distributions.

The FSS is a variation on the Brier Skill Score:

© Crown copyright 2010

$$FSS = 1 - \frac{FBS}{FBS_{worst}} \quad (44),$$

where *FBS* is the Fractions Brier Score: a variation on the Brier Score (Brier, 1950) in which the forecast and observed (radar) fractions can have any value between 0 and 1. The FBS is given by

$$FBS = \frac{1}{N}\sum_{s=1}^{N}(O_s - M_s)^2 \quad (45),$$

where O_s and M_s are the forecast and observed fractions at each grid point, *s*. FBS_{worst} is the worst possible FBS, obtained if there is no collocation of non-zero forecast and observed fractions:

$$FBS_{worst} = \frac{1}{N}\left[\sum_{s=1}^{N}O_s^{\,2} + \sum_{s=1}^{N}M_s^2\right] \quad (46).$$

In this work, the FSS has been evaluated for the 75th, 90th, 95th and 99th percentiles of the forecast and radar distributions of instantaneous precipitation rate or 1 h accumulation, on neighbourhood sizes of 8 km, 16 km, 32 km, 64 km, 128 km, 256 km and 512 km.

An example of a FSS plot for a control member forecast blending an extrapolation nowcast and UKV control forecast is shown in Figure 28. The 8 curves represent the performance of the forecast measured at neighbourhood sizes equivalent to the scales represented by the 8 levels of the cascade model. The horizontal orange line is a target skill level defined as

$$FSS_{target} = 0.5 + \frac{clim}{2} \quad (47),$$

where *clim* refers to the base rate or climatological frequency of the event under evaluation (*clim*=0.25 for the 75th percentile of 1h accumulation). This target skill is equivalent to the no-skill line on a *reliability* or *attributes diagram* and the diagonal, no-skill line on a Relative Operating Characteristic plot (see below for further explanation).

The horizontal pink line towards the bottom of the FSS plot in Figure 28 represents the FSS of a random forecast with the same raining fraction as the UKV control member forecast (FSS_{random} = *clim*).

© Crown copyright 2010

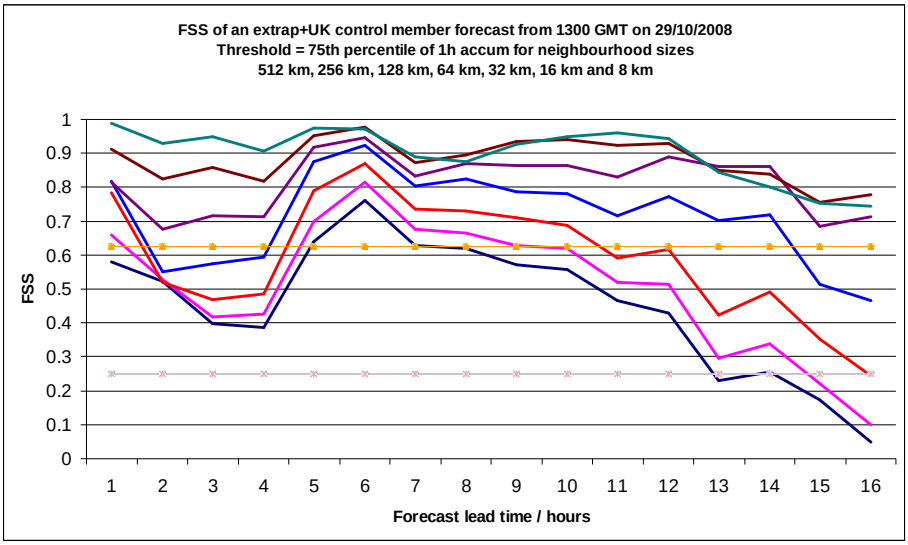

Figure 28 A FSS plot for a blended control member precipitation forecast comprising an extrapolation nowcast and a UKV control forecast. The FSS has been computed for the 75th percentile of 1 h accumulation for 8 neighbourhood sizes corresponding to the 8 scales represented by the cascade model. Here FSS_{target} = 0.6125 and FSS_{random}=0.25.

Measures of ensemble forecast skill

A range of verification scores are routinely used to evaluate the performance of ensemble forecasts and the event probabilities that can be derived from them. Here, the use of the term, event, refers to a threshold exceedence, for example, a grid point precipitation rate exceeding 4 mm /h or an accumulation exceeding 10 mm over a defined area and time period.

Ensemble forecasting systems are formulated in such a way that the forecast evolution predicted by each member should be equally likely to occur. Therefore, in principle, the likelihood of an event happening is simply the fraction of ensemble members exceeding the defined event threshold. However, this assumes that the ensemble forecast is perfectly calibrated; in other words, the observed frequency of a given event is always perfectly predicted by the ensemble. In reality, this level of skill is unattainable, because, *a priori*, it is not possible to model all sources of forecast error precisely.

Ensemble reliability is just one of a number of important attributes of ensemble forecasts which must be evaluated in any comprehensive appraisal of ensemble forecast skill. Others include resolution or sharpness (the ability to forecast event probabilities different from climatology) and spread-skill (the spread about the ensemble mean should follow the error in the ensemble mean). Verification scores for measuring these attributes are described in the following sub-sections and are used as the basis for assessing the performance of the blended ensemble forecasts.

© Crown copyright 2010

Brier Skill Score, resolution score and reliability score

The Brier Skill Score, reliability score and resolution score are derived from a decomposition of the Brier Score:

$$BS = \frac{1}{N}\sum_{c=1}^{I} N_c (p_c - \overline{o}_c)^2 - \frac{1}{N}\sum_{c=1}^{I} N_c (\overline{o}_c - \overline{o}_c)^2 + \overline{o}(1-\overline{o}) \quad (48),$$

where N is the total number of forecasts, $\overline{o}$ is the climatological frequency of an event within the sample of observations (the sample climatology),

$$\overline{o} = \frac{1}{N}\sum_{c=1}^{I} o_c \quad (49),$$

$\overline{o}_c$ is the frequency of the same event in a subset of samples of size, N_c, for which the forecast probability of the event, p_c, lies in the category, c.

The BSS is defined as

$$BSS = 1 - \frac{BS}{BS_{ref}} \quad (50).$$

The sample climatology is usually chosen as the reference forecast. This allows the BSS to be defined in terms of a *resolution score* and *reliability score*

$$BSS = B_{resolution} + B_{reliability} \quad (51),$$

where

$$B_{resolution} = \frac{1}{\overline{o}(1-\overline{o})N}\sum_{c=1}^{I} N_c (\overline{o}_c - \overline{o})^2 \quad (52),$$

and

$$B_{reliability} = \frac{1}{\overline{o}(1-\overline{o})N}\sum_{c=1}^{I} N_c (p_c - \overline{o})^2 \quad (53).$$

The resolution score, $B_{resolution}$, measures the propensity of an ensemble forecast to predict event probabilities that are higher or lower than the sample climatological probability. This attribute of an ensemble forecast is some times referred to as *sharpness*.

The reliability score, $B_{reliability}$, is a penalty function measuring the departure of ensemble forecast probabilities from perfect reliability.

© Crown copyright 2010

Reliability (Attributes) diagram

The *reliability* or *attributes diagram* is a plot of the observed frequency of an event (Y axis) versus its forecast probability (X axis) and includes several reference lines relating to the algebraic decomposition of the BSS. An example is shown in Figure 28 below. The reliability curve for a perfectly reliable ensemble forecasting system will lie on the diagonal line with gradient 1:1. The inset histogram, known as the *sharpness* or *refinement distribution,* demonstrates the frequency of use of each probability category (i.e. the forecast sample size in each category).

The horizontal dashed lines labelled 'no resolution', represent the climatological frequency of the event in the data sample at each forecast lead time. Note that this climatological frequency is some times referred to as the *base rate*. Points on a reliability curve falling on the pertinent 'no resolution' line indicate that the ensemble forecasting system is unable to resolve occasions where the event is more or less likely to happen than the climatological probability. The bigger the distance between a reliability curve and the no resolution line, the greater the resolution of the ensemble forecasts.

The dashed diagonal lines labelled 'no skill' represent points where the resolution score is equal to the reliability score. A reliability curve lying on or beneath such a line implies that the proportion of events successfully forecast (the *hit rate*) is similar or worse than proportion of non-events incorrectly forecast (the *false alarm rate*). These no-skill lines are equivalent to the diagonal, no-skill line plotted on Relative Operating Charateristic diagrams (see Figures 29 and 30 below).

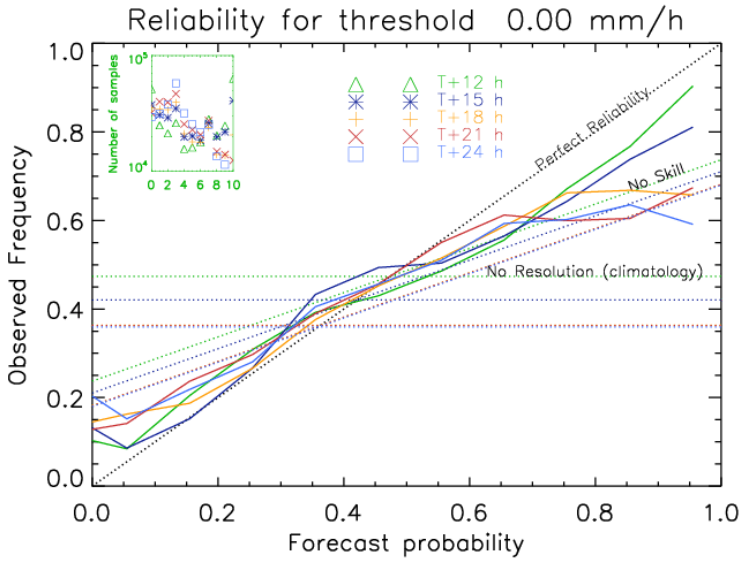

Figure 29 A reliability or attributes diagram for a 23 member UKV ensemble precipitation forecast. The reliability curves show the relationship between forecast probability and radar observed frequency as a function of forecast lead time for precipitation rate > 0.0 mm/h. Statistics are based upon data from 05/09/2008 and 29/10/2008.

© Crown copyright 2010

Relative Operating Characteristic

Plots of the ROC (Mason, 1999) show the *Hit Rate* versus the *False Alarm Rate* for a range of confidence levels or probability bins where

$$HR = a/(a+c) \quad (54),$$

$$FAR = b/(b+d) \quad (55).$$

The event contingencies, a, b, c and d are defined in Table 4 below.

The plotted point values of HR versus FAR for different confidence levels can be joined by straight lines. The area under the resulting ROC curve provides a measure of forecast skill. Examples of ROC plots for a UKV ensemble and control member forecast sequence are shown in Figure 30.

Forecast	Observed	
	Yes	No
Yes	Hit a	False alarm b
No	Miss c	Correct rejection d

Table 4 Event contingency table used to define the categorical scores, Hit Rate and False Alarm Rate, used in ROC plots.

If the proportion of events successfully predicted (the *hit rate*) is similar to the proportion of non-events incorrectly predicted (the *false alarm rate*) then the forecast is not considered skilful. This level of performance is represented by the diagonal, dashed line in Figure 30. The series of coloured lines in the same Figure represent the skill of the UKV ensemble forecast at 6 hourly forecast steps. The coloured symbols denote the skill of the control member (deterministic) forecast. For an ensemble with useful levels of skill, the area under the associated ROC curves should encompass the points representing the skill of the control member. The more skilful the ensemble forecast, the larger will be the area between the ROC curves and the no-skill line.

© Crown copyright 2010

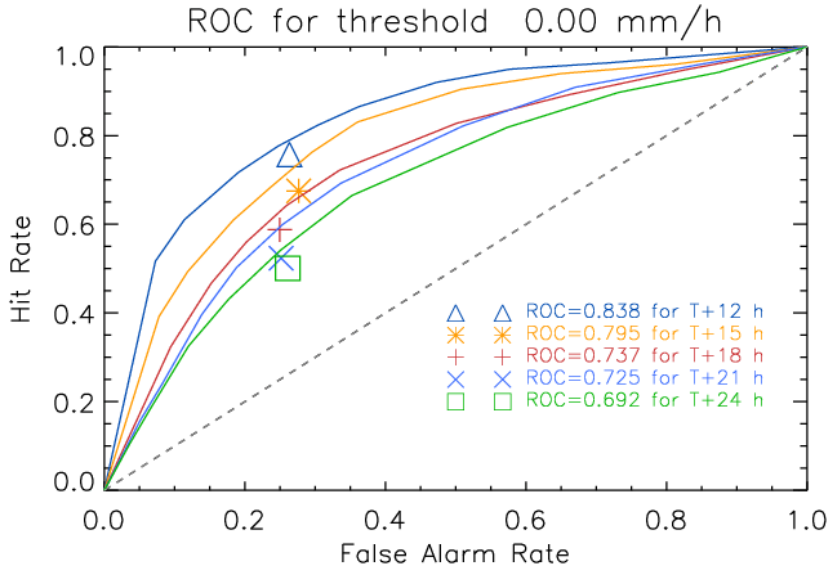

Figure 30 A ROC plot for a 23 member UKV ensemble forecast of precipitation rate and an associated control member forecast. The coloured lines are the ROC curves for ensemble forecasts valid at 3 hourly forecast steps between T+12h and T+24h. The symbols represent the skill of the control member forecast at the same forecast steps. The event threshold is 0.0 mm/h. Statistics are based upon data from 05/09/2008 and 29/10/2008.

Spread-Skill

One of the aims of ensemble forecasting is to predict the skill of the control (deterministic) forecast. Ideally, when the spread of an ensemble forecast is small then the control member forecast should be more trustworthy than when the spread is large.

Two aspects of ensemble spread-skill are of interest. Firstly, on average, the spread of the ensemble about the ensemble mean should match the error in the ensemble mean forecast. This can be assessed by comparing average ensemble spread and error for a particular lead time. A second aspect concerns the relationship between ensemble spread and error in the ensemble mean at any given instant. This is normally established by examining the correlation between spread and error.

In this report, the focus of the spread-skill verification is a case study oriented comparison of average ensemble spread and skill as a function of forecast lead time (measured using radar data as the reference). Figure 31 shows an example of a spread-skill plot produced from a single, 23 member UKV ensemble forecast of precipitation rate with a data time of 0600 GMT on 05/09/2008. The RMS error and bias are calculated relative to a quality controlled, radar composite field of surface rain rate.

The spread about the ensemble mean and RMS error in the ensemble mean are compared with spread about the control member and RMS

© Crown copyright 2010

error of the control member. For a skilful ensemble, the spread about the ensemble mean should be less than the spread about the control. Similarly, the error in the ensemble mean (in this case, measured relative to radar estimates of surface rain rate and accumulation) should be less than the error in the control forecast. In these respects, one can conclude that the UKV ensemble forecast assessed in Figure 31 is skilful, although it is also apparent that the ensemble is over spread.

In comparing ensemble spread and ensemble mean error it is important to consider the effects of observation error on the verification results. The root mean squared error of an ensemble forecast against the truth can be approximated by

$$rmse_{truth} = \sqrt{rmse_{forecast}^{2} - rmse_{obs}^{2}} \qquad (56).$$

Thus, accounting for observation error should tend to reduce the estimated forecast error. Radar errors vary significantly in both space and time and are therefore difficult to quantify. Consequently, their effects have not been accounted for in the radar based spread-skill verification presented in later sections of this report. However, since radar errors are likely to be significant over a large fraction of the UK radar composite area, the statistics for RMS error in the ensemble mean shown in Figure 31 will be over estimates of the true error. The implication here is that the UKV ensemble forecast is more over spread than the results in Figure 31 indicate.

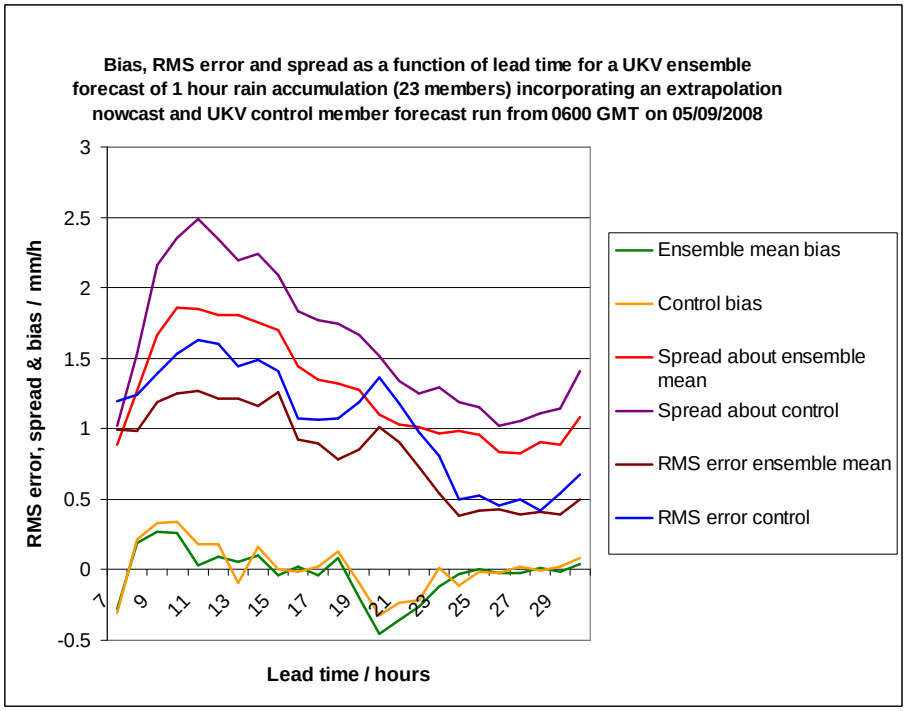

Figure 31 Spread-skill statistics for a 23 member UKV ensemble forecast of precipitation rate, run from 0600 GMT on 05/09/2008 and evaluated using quality controlled radar estimates of surface rain rate as the reference.

© Crown copyright 2010

5.4.4. Can the blending algorithms generate plausible, seamless blended forecasts?

A case study based evaluation of control member blends

The performances of the two configurations of blended control forecasts described in 5.4.1 have been examined on a case by case basis. Results from several cases are presented below. These have been selected to demonstrate the strengths and weaknesses of the two configurations of blended control forecast. A selection of forecast images and verification statistics for the remaining case studies can be found in Appendix A.1.

Case study 5 – 25/03/2010

This case study has been selected to demonstrate some of the strengths of the blended control member forecasts.

Figure 32a shows a sequence of blended forecasts commencing at 1300 GMT on 25/03/2010 and incorporating an extrapolation nowcast, UKV control member precipitation forecast and non-parametric noise. In this control member blend, the noise is confined to the bottom two levels of the cascade (scales ≤ 8 km), its purpose being to add structure (variance) close to the grid scale and make the transition to a downscaled MOGREPS-R forecast more seamless beyond the forecast range of the UKV model.

Figure 33 is a plot of the weights assigned to the forecast components (including the noise) as a function of forecast lead time. These relate an ensemble blend. In the control member, the weight on the noise component is zero on the top six cascade levels and one on the bottom two levels; the weights on the two model forecast components are re-scaled so that they sum to unity.

Comparison of the blended forecast sequence in Figure 32a with the associated UKV forecast sequence and UKPP rain analysis (top-left) demonstrates that the blended forecast evolves smoothly from the rain analysis to the UKV forecast over a 6 hour period. This observation is consistent with the smooth evolution of the weights shown in Figure 33.

The influence of the noise is seen in the fine scale structure of the blended forecasts. These fine scale perturbations appear rather uniform in character owing, in part, to the spatial homogeneity of the noise. Since the noise is confined to the bottom two cascade levels, the speckled appearance of the blended forecast and noise may be due to the fact that the latter is uncorrelated with the extrapolation and UKV model forecast features above. The realism of the perturbations might be improved by allowing the weights on the noise to decline exponentially up the cascade.

There is a noticeable deficit of very light rain in the blended forecast (the dark blue areas) when compared to the UKV forecast. These light rain areas have intensities < 0.1 mm/h. Small biases in the blended

© Crown copyright 2010

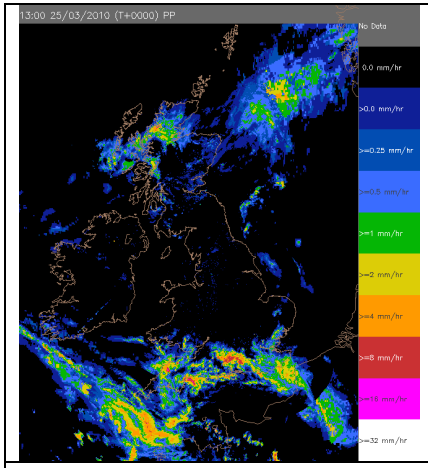	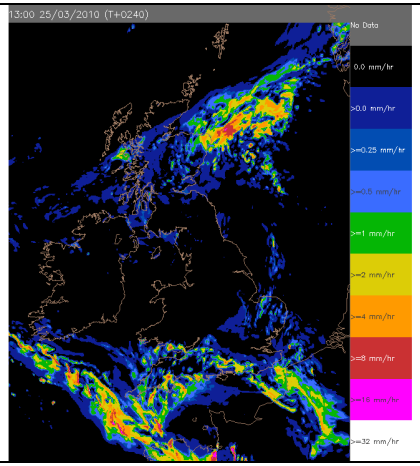	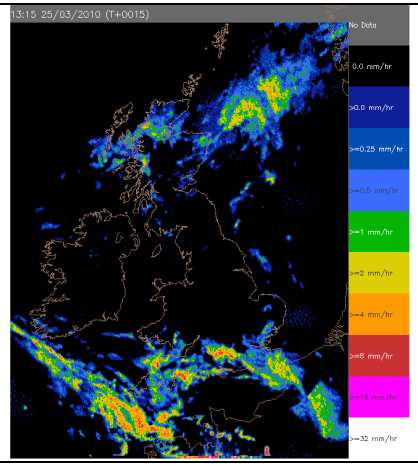	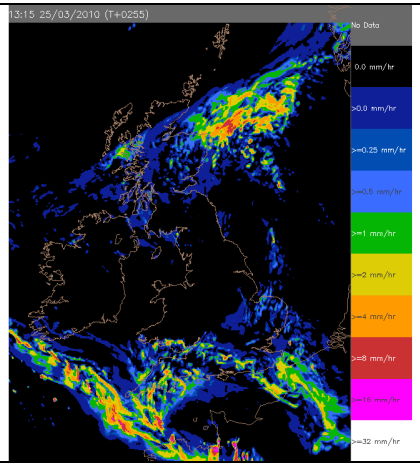
UKPP rain analysis valid at 1300 GMT on 25/03/2010	**T+7h UKV forecast valid at 1300 GMT on 25/03/2010**	**T+15 min blend of an extrapolation nowcast, a UKV control forecast and non-parametric noise valid at 1315 GMT on 25/03/2010**	**T+7h 15 min UKV forecast valid at 1315 GMT on 25/03/2010**
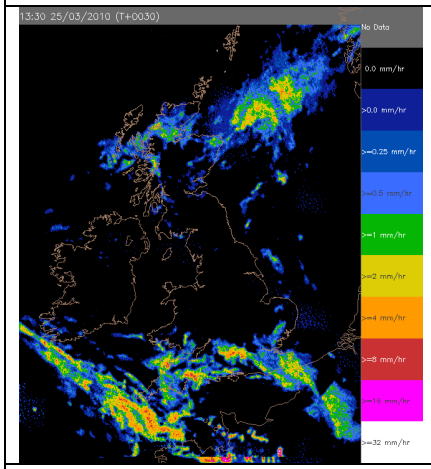	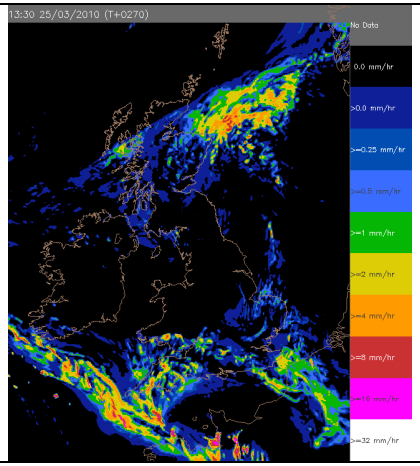	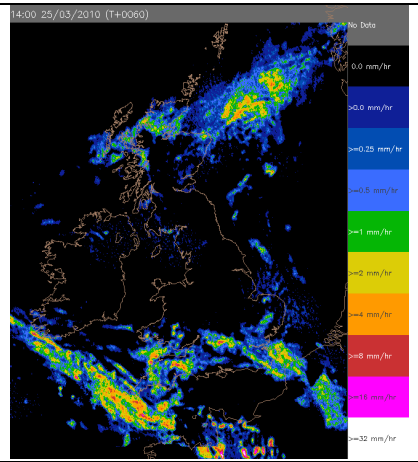	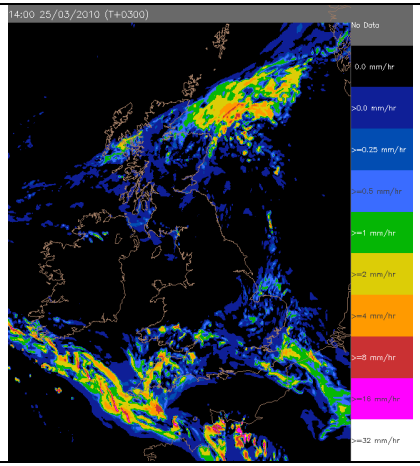
T+30 min blend of an extrapolation nowcast, a UKV control forecast and non-parametric noise valid at 1400 GMT on 25/03/2010	**T+7h 30 min UKV forecast valid at 1330 GMT on 25/03/2010**	**T+1 h blend of an extrapolation nowcast, a UKV control forecast and non-parametric noise valid at 1400 GMT on 25/03/2010**	**T+8 UKV h forecast valid at 1400 GMT on 25/03/2010**

© Crown copyright 2010

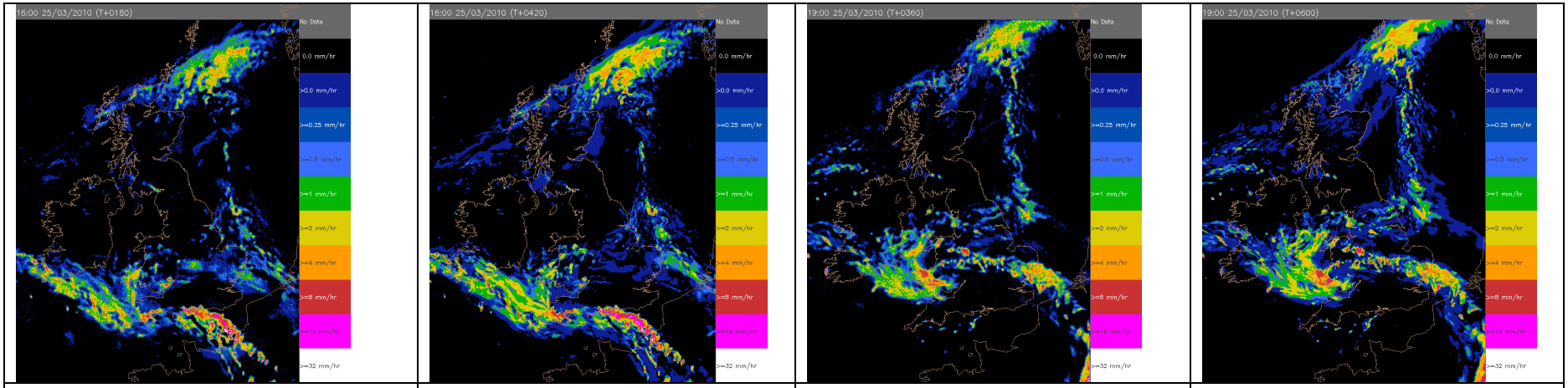

T+3 h blend of an extrapolation nowcast, a UKV control forecast and non-parametric noise valid at 1600 GMT on 25/03/2010	**T+10 h UKV forecast valid at 1600 GMT on 25/03/2010**	**T+6 h blend of an extrapolation nowcast, a UKV control forecast and non-parametric noise valid at 1800 GMT on 25/03/2010**	**T+13 h UKV forecast valid at 1800 GMT on 25/03/2010**

Figure 32a Selected steps in a blended, control member forecast of precipitation rate, comprising an extrapolation nowcast, UKV control forecast and non-parametric noise (confined to scales ≤ 8 km), run from 1300 GMT on 25/03/2010. The UKPP rain analysis used as the starting point for the extrapolation nowcast is also shown, as well corresponding forecast steps from the associated UKV control member forecast (data time 0600 GMT, 25/03/2010).

© Crown copyright 2010

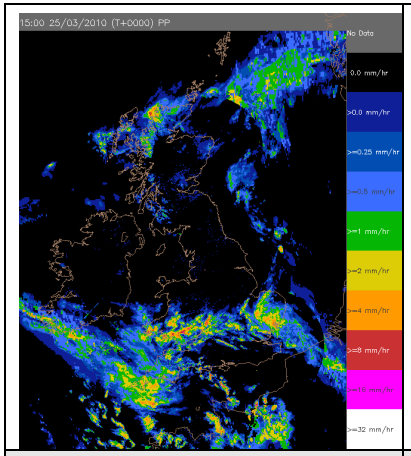	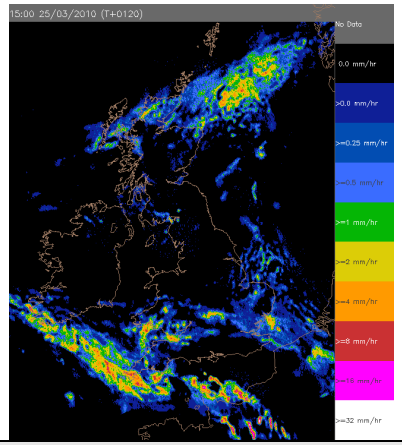	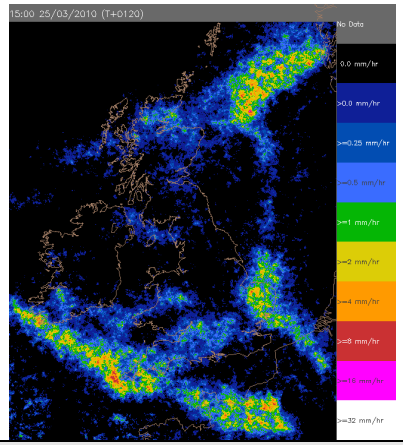	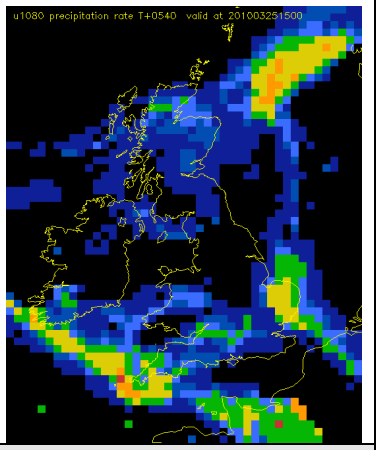
UKPP rain analysis valid at 1500 GMT on 25/03/2010	**T+2 h blend of an extrapolation nowcast, a UKV control forecast and non-parametric noise valid at 1500 GMT on 25/03/2010**	**T+9 h MOGREPS-R downscale forecast valid at 1500 GMT on 25/03/2010**	**T+9 h MOGREPS-R forecast valid at 1500 GMT on 25/03/2010**
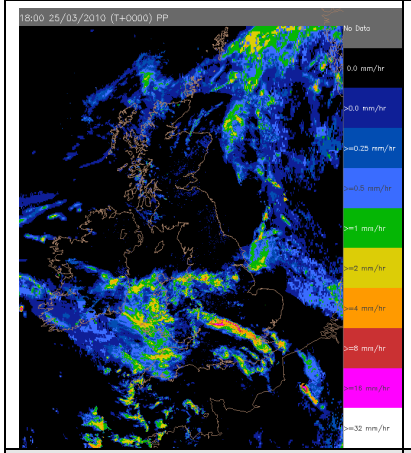	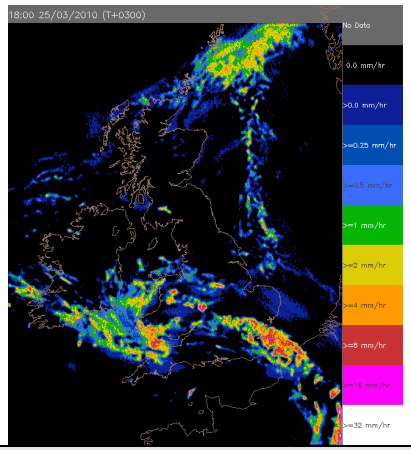	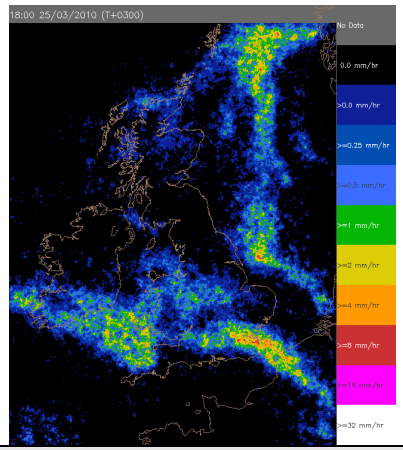	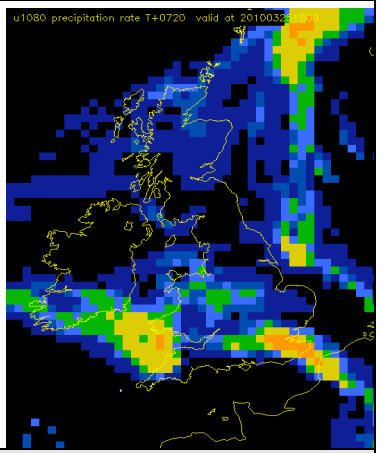
UKPP rain analysis valid at 1800 GMT on 25/03/2010	**T+5 h blend of an extrapolation nowcast, a UKV control forecast and non-parametric noise valid at 1800 GMT on 25/03/2010**	**T+12 h MOGREPS-R downscale forecast valid at 1800 GMT on 25/03/2010**	**T+12 h MOGREPS-R forecast valid at 1800 GMT on 25/03/2010**

© Crown copyright 2010

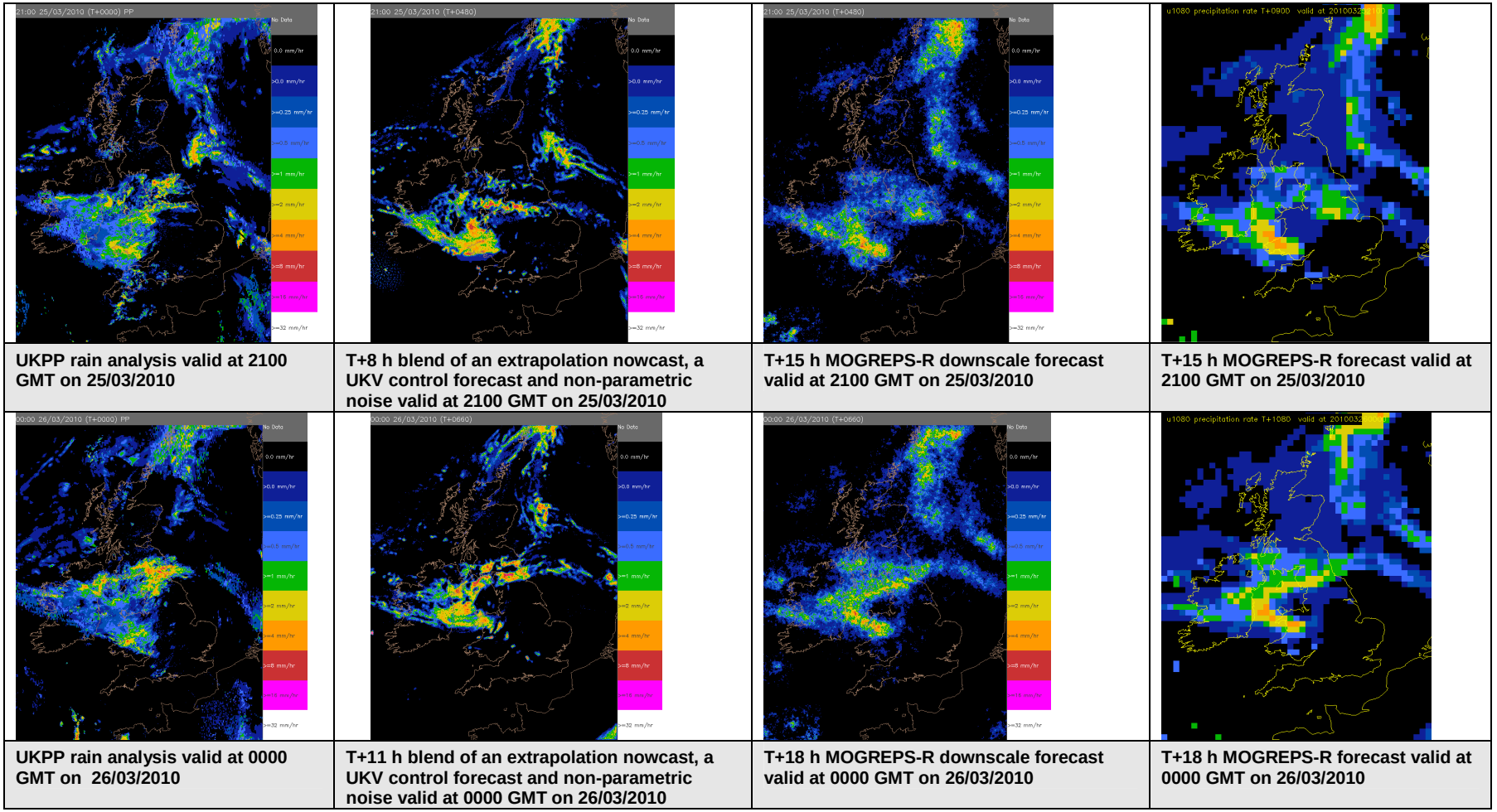

UKPP rain analysis valid at 2100 GMT on 25/03/2010	**T+8 h blend of an extrapolation nowcast, a UKV control forecast and non-parametric noise valid at 2100 GMT on 25/03/2010**	**T+15 h MOGREPS-R downscale forecast valid at 2100 GMT on 25/03/2010**	**T+15 h MOGREPS-R forecast valid at 2100 GMT on 25/03/2010**
UKPP rain analysis valid at 0000 GMT on 26/03/2010	**T+11 h blend of an extrapolation nowcast, a UKV control forecast and non-parametric noise valid at 0000 GMT on 26/03/2010**	**T+18 h MOGREPS-R downscale forecast valid at 0000 GMT on 26/03/2010**	**T+18 h MOGREPS-R forecast valid at 0000 GMT on 26/03/2010**

Figure 32b Selected forecast steps in a blended, control member forecast of precipitation rate, comprising a MOGREPS-R control forecast and parametric noise (confined to scales ≤ 64 km), run from 0600 GMT on 25/03/2010 (3rd column from left). A corresponding sequence of UKPP rain analyses and forecasts steps from the associated MOGREPS-R control forecast (data time 0600 GMT, 25/03/2010) and UKV based blended forecast (extracts of which appear in Figure 32a) are also shown for comparison.

© Crown copyright 2010

forecasts have led to a reduction in the size of these areas and a consequent negative bias in raining fraction relative the UKV model.

Figure 32b displays a sequence of downscaled (2 km) MOGREPS-R control member forecasts constructed from a MOGREPS-R run for 0600 GMT on 25/03/2010 (3rd column from left). This is compared with similar forecast sequences from the 24 km resolution MOGREPS-R control member forecast (right-most column), and the UKV based blended forecast (excerpts of which are shown in Figure 32a). The far left-hand column in the Figure contains a corresponding time series of UKPP rain analyses.

A comparison of the original MOGREPS-R control member forecast with its downscaled (2 km) counterpart (Figure 32b) reveals that the injected parametric noise has added some structure (variance) to the 24 km resolution forecast fields at scales below several grid lengths. However, the added features also seem rather uniform in character. This is largely due to the isotropic properties and spatial homogeneity of the parametric noise. A downscaled product based upon anisotropic (non-parametric) noise would look more plausible, but this can only be achieved if a suitable, high resolution target distribution exists for the noise generation.

To further investigate the performance of these two configurations of blended forecasts, a selection of field statistics has been compiled. These include the field mean, variance, raining fraction, frequency distribution and power spectrum.

Figures 33 to 35 are plots of field mean, variance and raining fraction for the blended control member forecasts and associated model forecast components (UKV and MOGREPS-R forecasts) as a function of forecast lead time. These are compared to the equivalent statistics for a time series of UKPP rain analyses. The lead time labels on the X axes of the plots relate to the data time of the extrapolation nowcast (1300 GMT on 25/03/2010) and not to the run times of the UKV and MOGREPS-R model forecasts. Note that operational MOGREPS-R forecasts of precipitation rate are only available at three hourly intervals. This explains the step changes seen in the field mean, variance and raining fraction of the control forecast (pink line) and downscaled control forecast (red line) in the plots.

A number of distinguishing, characteristic features of the MOGREPS-R and UKV model forecasts are revealed in the time series of field mean, variance and raining fraction. As expected, the coarse resolution MOGREPS-R forecast exhibits a smaller field variance and larger raining fraction than the high resolution UKV forecast. Relative to the radar, the UKV forecast also has a significantly higher variance during episodes of convection (see T+4h in Figure 34) and this coincides with an apparent positive bias in the field mean. Despite the known limitations of radar, this discrepancy is not thought to be the result of under estimates of mean and variance by the radar network; rather, it is seems likely to be a consequence of the UKV's tendency to produce small, intense showers.

© Crown copyright 2010

In agreement with expectation, the field mean and variance of the blended control forecast incorporating an extrapolation nowcast, a UKV control forecast and non-parametric noise generally lie between those of the radar based UKPP rain analysis valid at T+0 (the starting point for the extrapolation nowcast) and those of the UKV model at short lead times. Beyond this, the statistics of the blended forecast tend to follow those of the UKV more closely. Similar behaviour and encouraging performance characteristics have been demonstrated in other case studies, notably the 17/02/2010 and 19/11/2009. Forecast examples and images can be seen in Appendix A.1.The smaller raining fraction is attributed to small biases in the blended forecasts which result in the removal of the areas of very light rain (< 0.1 mm/h) seen in the UKV forecasts.

A comparison of the statistics for the downscaled MOGREPS-R control forecast with those of the original product suggests that the downscaling methodology has corrected a small positive bias in the field mean and a larger positive bias in the raining fraction. However, the field variance has also been reduced slightly and this has resulted in forecasts which seem to be lacking in intensity in some areas. This latter characteristic is probably due to a combination of factors, namely, small errors in the estimated slope of the MOGREPS-R power spectrum, the use of spatially homogeneous parametric noise, and the way in which this noise has been added: it is confined the bottom four cascade levels only.

In other cases, for example 19/11/2009, the MOGREPS-R downscaler demonstrated some capability to correct a negative bias in field variance relative to the radar. However, on this occasion, the noise perturbations were unrealistic, largely as a result of using spatially homogenous noise to represent a distribution of rain rate comprising both showers and widespread precipitation (see Appendix A.1).

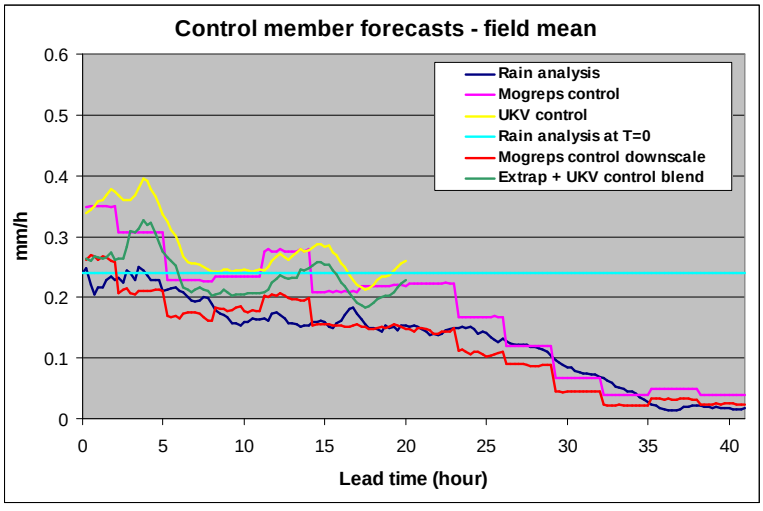

Figure 33 Time evolution of the field mean of UKPP rain analyses, MOGREPS-R and UKV control member forecasts and the two configurations of blended forecast for 25/03/2010. The forecast lead times on the X axis are those of the blended forecasts (run from 1300 GMT on 25/03/2010). The UKV and MOGREPS-R forecasts were run from 0600 GMT on 25/03/2010.

© Crown copyright 2010

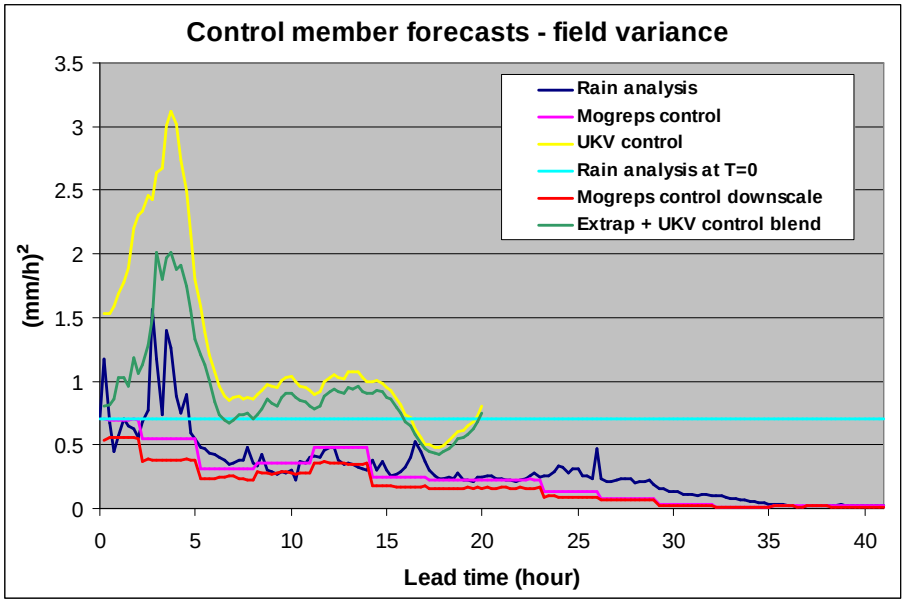

Figure 34 Time evolution of the field variance of UKPP rain analyses, MOGREPS-R and UKV control member forecasts and the two configurations of blended forecast for 25/03/2010. The forecast lead times on the X axis are those of the blended forecasts (run from 1300 GMT on 25/03/2010).

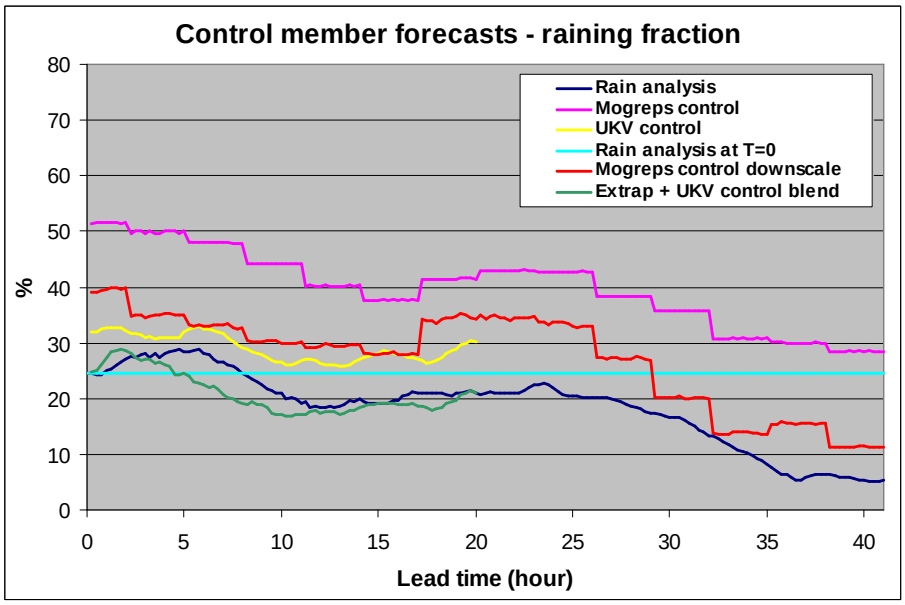

Figure 35 Time evolution of the raining fraction of UKPP rain analyses, MOGREPS-R and UKV control member forecasts and the two configurations of blended forecast for 25/03/2010. The forecast lead times on the X axis are those of the blended forecasts (run from 1300 GMT on 25/03/2010).

The frequency distribution plots shown in Figures 36a-b confirm some of the earlier observations made in relation to the performance of the blended forecasts. Figure 36a demonstrates that the distribution of rain rate in the UKV based T+8h blended control forecast is very

© Crown copyright 2010

similar to that of the UKV itself. The one exception is the amount of precipitation with rates < 1/16 mm/h. For these very light precipitation rates, the blended control forecast is more like the UKPP rain analysis.

Figure 36b shows that the parametric downscaling of the MOGREPS-R forecast has been partly successful in injecting some more intense features into the T+15 h MOGREPS-R forecast. However, the tail of the distribution is still too small: the UKPP rain analysis contains a handful of pixels which exceed precipitation rates of 32 mm/h. Similar levels of performance were observed in other case studies, for example, 17/02/2010 and 19/11/2009.

The power spectrum plots in Figure 37 support earlier conclusions regarding the behaviour of the blended forecasts. As expected, the T+8h blended control member forecast combining the extrapolation nowcast and UKV forecast has a similar power spectrum to the UKV model. Similarly, the power spectrum of the downscaled MOGREPS-R forecast follows that of the raw model at resolved scales and extends linearly beyond this to the Nyquist interval.

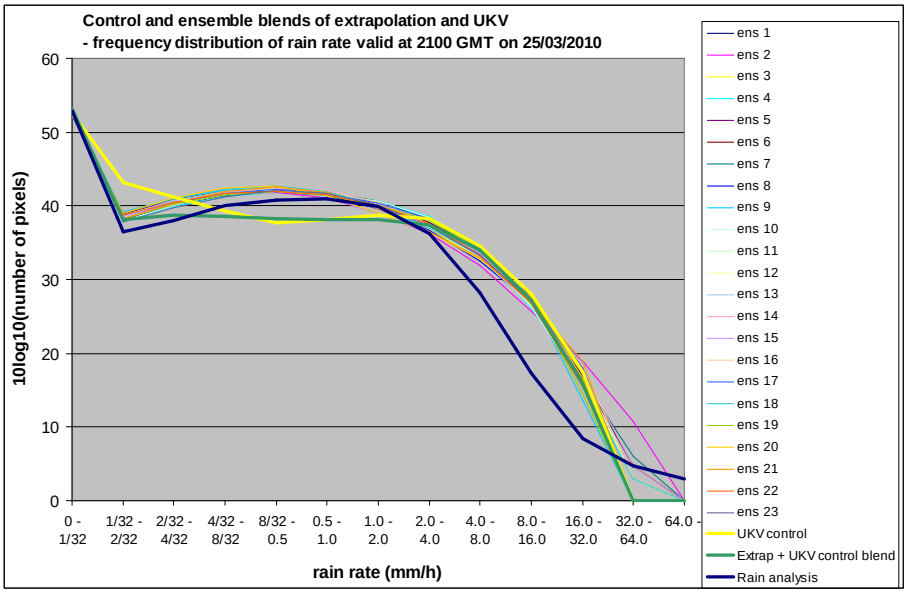

Figure 36a Frequency distributions of precipitation rate for a UKPP rain analysis, a 2 km resolution UKV control member forecast, and a blended control forecast and 23 member ensemble forecast incorporating an extrapolation nowcast and UKV control forecast, all valid at 2100 GMT on 25/03/2010. The blended forecasts were run from 1300 GMT on 25/03/2010 and the UKV control forecast from 0600 GMT on the same day. The validation area is the UK radar composite.

© Crown copyright 2010

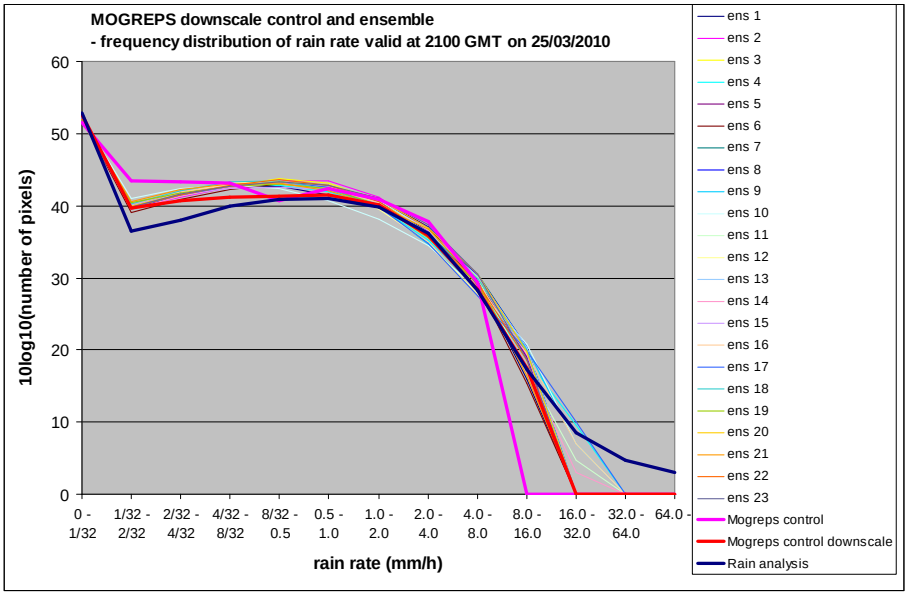

Figure 36b Frequency distributions of precipitation rate for a UKPP rain analyses, a 24 km resolution MOGREPS-R control member and its downscaled counterpart, and 23 members of a downscaled MOGREPS-R control forecast, all valid at 2100 GMT on 25/03/2010. The MOGREPS-R control forecast was run from 0600 GMT on 25/03/2010. The validation area is the UK radar composite.

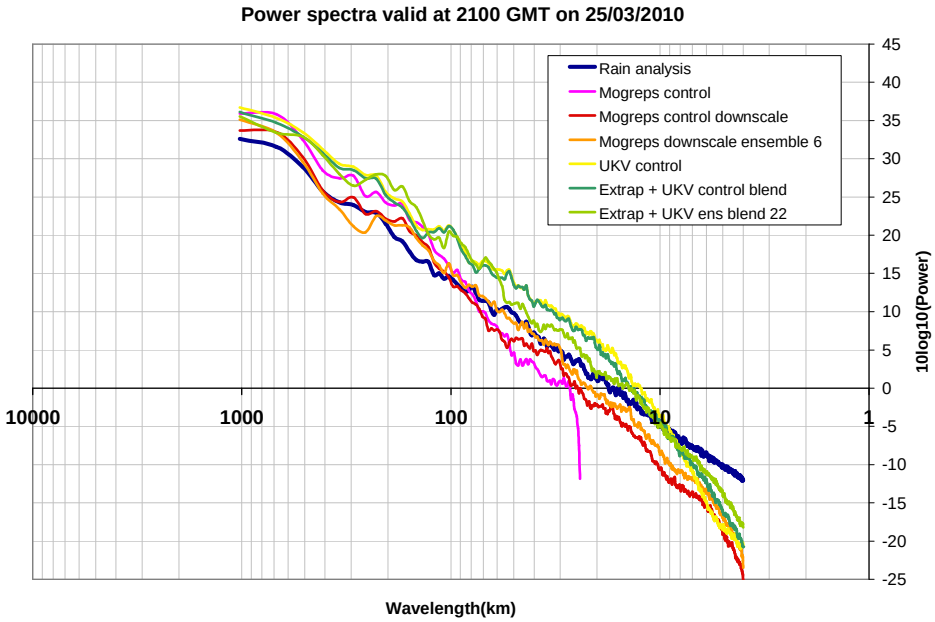

Figure 37 Power spectra for a UKPP rain analysis, MOGREPS-R (T+15 h) and UKV (T+12h) control member forecasts and the two configurations of blended forecasts (T+8 h) all valid at 2100 GMT on 25/03/2010.

© Crown copyright 2010

Case study 2 – 29/10/2008

This case study has been selected to demonstrate some of the weaknesses of the blended control member forecasts.

The MOGREPS-R and UKV precipitation forecast data used for this case study and for that of 05/09/2008 (see Appendix A-1) were supplied by the *Convective-scale Ensembles Project*. The UKV data cover only that fraction of the UKV model domain where the grid length is 1.5 km; the data in the variable resolution border around the edges of the model domain were omitted.

This has constrained the use of the UKV model precipitation forecasts in the blending algorithms. Most importantly, it has prevented the generation of UKV based non-parametric noise. This is because the power spectrum of the noise must be derived from data on the UKPP domain; it cannot be estimated sensibly when data are missing around the edges. As a result, the control member blend incorporating a UKV forecast was generated using non-parametric noise with a distribution inferred from the UKPP rain analysis valid at T+0 h (the start of the extrapolation nowcast). Thus, the noise distribution does *not* tend towards that of the UKV forecasts with advancing lead time.

In the following case study examples, the blended forecasts shown are displayed on a reduced area to avoid boundary effects arising from the missing UKV model data. The weaknesses of the control member blending algorithms identified in this section cannot be attributed to this limitation of the data, but the use of a fixed distribution for the noise does have some bearing on performance, as discussed below.

Figure 38a shows a sequence of blended forecasts commencing at 1300 GMT on 29/10/2008. These incorporate an extrapolation nowcast, UKV control member precipitation forecast and non-parametric noise (bottom two cascade levels only). Although the blended forecast evolution is smooth, the solution at T+6h does not correspond as closely as it should with the equivalent UKV control forecast: there is a noticeable loss of intensity in the frontal zone. This is attributed to the use of a single, radar inferred target distribution for the non-parametric noise and the spatial homogeneity of this noise.

Although the band of frontal precipitation seen in the top-left image in Figure 38a (the UKPP rain analysis) dominates the precipitation field, there are discernable, spatial variations in the coherence and variability of the field. For example, the southern portion of the precipitation band, to the west of Cornwall, is noticeably smoother than the showery structures behind (to the left of) it and those in the top right-hand corner of the UKPP domain. The non-parametric noise generator models the entire precipitation field as a single distribution. Consequently, spatial variations in the statistical properties of this distribution cannot be preserved. In principle, it should be possible to remedy this behaviour by maintaining separate noise distributions for showers and frontal (widespread) precipitation.

© Crown copyright 2010

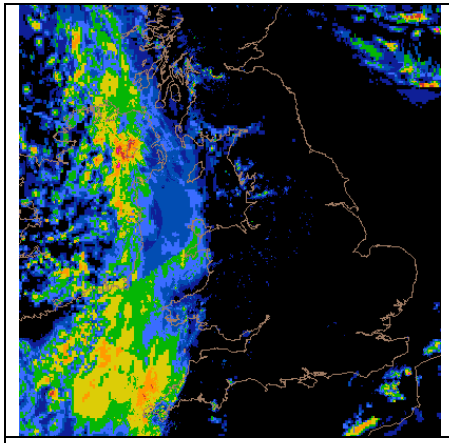	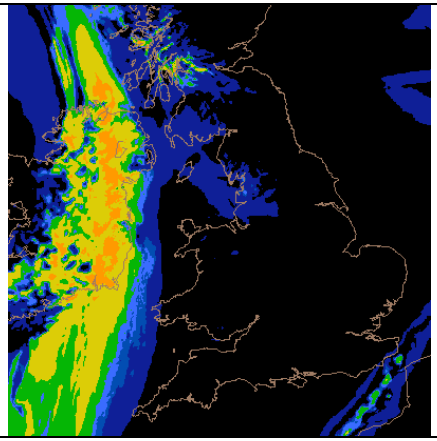	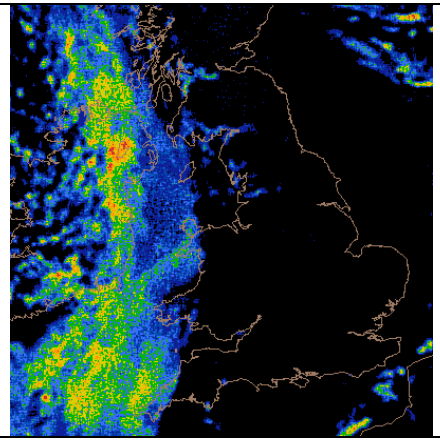	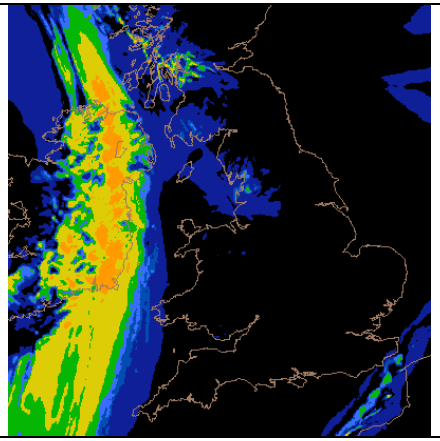
UKPP rain analysis valid at 1300 GMT on 29/10/2008	**UKV T+7h forecast valid at 1300 GMT on 29/10/2008**	**T+15 min blend of an extrapolation nowcast, a UKV control forecast and non-parametric noise valid at 1315 GMT on 29/10/2008**	**UKV T+7h 15 min forecast valid at valid at 1315 GMT on 29/10/2008**
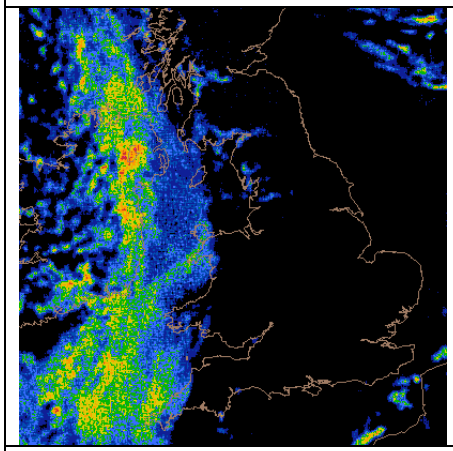	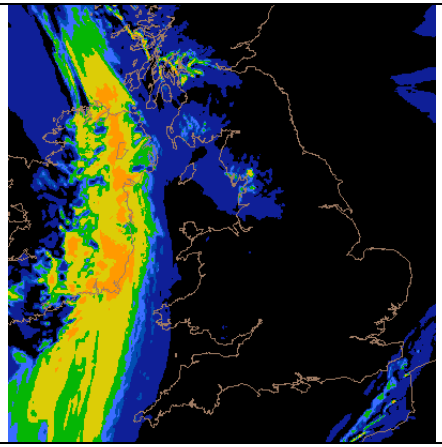	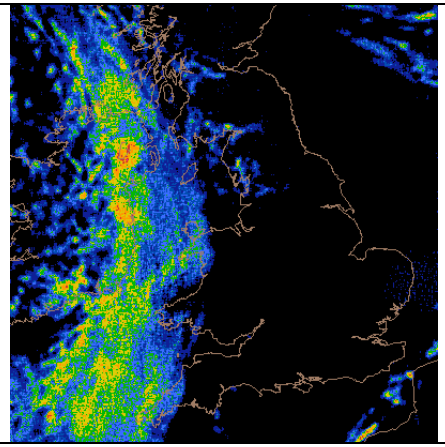	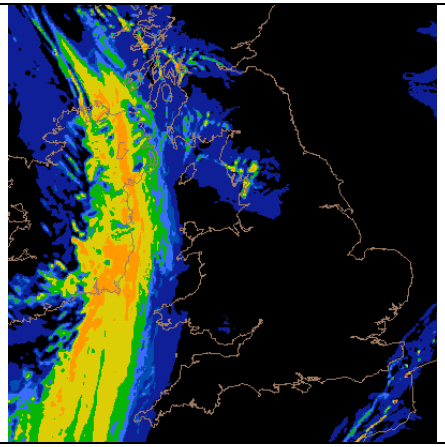
T+30 min blend of an extrapolation nowcast, a UKV control forecast and non-parametric noise valid at 1330 GMT on 29/10/2008	**T+7h 30 min UKV forecast valid at valid at 1330 GMT on 29/10/2008**	**T+1 h blend of an extrapolation nowcast, a UKV control forecast and non-parametric noise valid at 1400 GMT on 29/10/2008**	**T+8 h UKV forecast valid at 1400 GMT on 29/10/2008**

© Crown copyright 2010

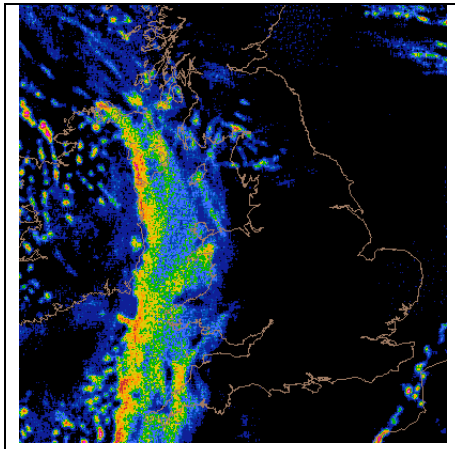

T+3 h blend of an extrapolation nowcast, a UKV control forecast and non-parametric noise valid at 1600 GMT on 29/10/2008

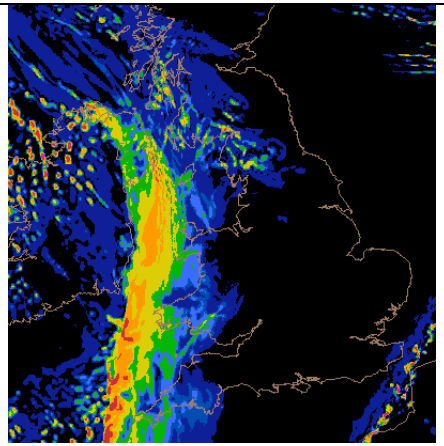

T+10 h UKV forecast valid at 1600 GMT on 29/10/2008

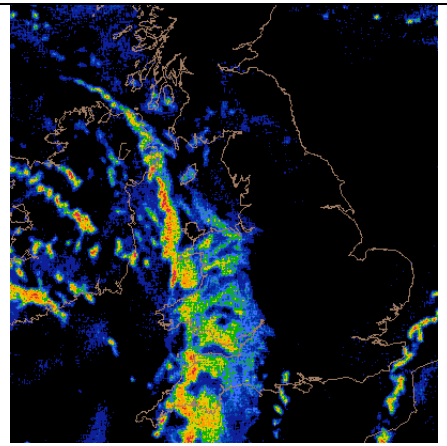

T+6 h blend of an extrapolation nowcast, a UKV control forecast and non-parametric noise valid at 1900 GMT on 29/10/2008

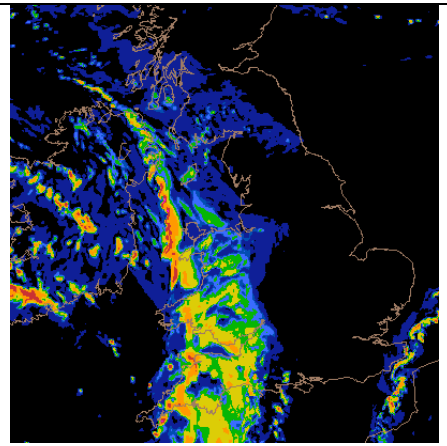

T+13 h UKV forecast valid at 1900 GMT on 29/10/2008

Figure 38a Selected steps in a blended, control member forecast of precipitation rate, comprising an extrapolation nowcast, UKV control forecast and non-parametric noise (confined to scales ≤ 8 km), run from 1300 GMT on 2910/2008. The UKPP rain analysis used as the starting point for the extrapolation nowcast is also shown, as well corresponding forecast steps from the associated UKV control member forecast (data time 0600 GMT, 29/10/2008).

© Crown copyright 2010

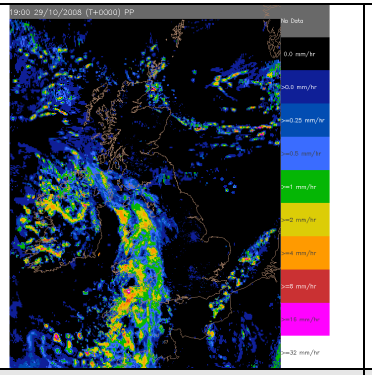	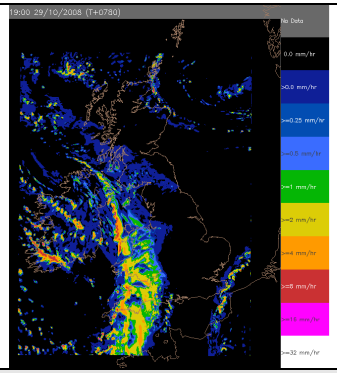	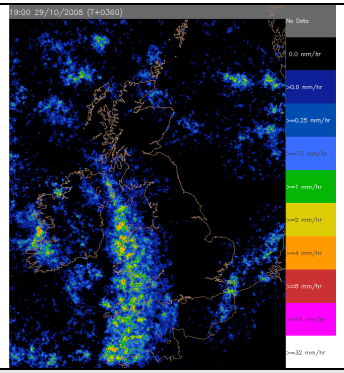	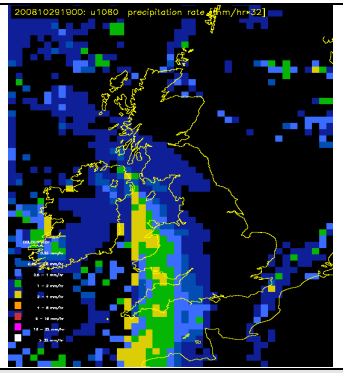
UKPP rain analysis valid at 1900 GMT on 29/10/2008	**UKV T+13 h control forecast and non-parametric noise valid at 1900 GMT on 29/10/2008**	**MOGREPS-R T+13 h downscale forecast valid at 1900 GMT on 29/10/2008**	**MOGREPS-R T+13 h forecast valid at 1900 GMT on 29/10/2008**
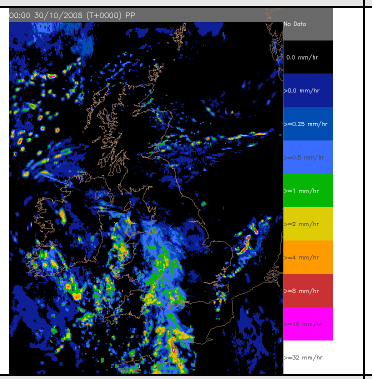	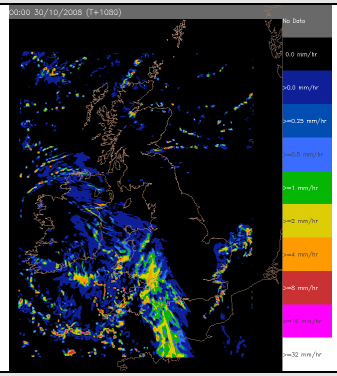	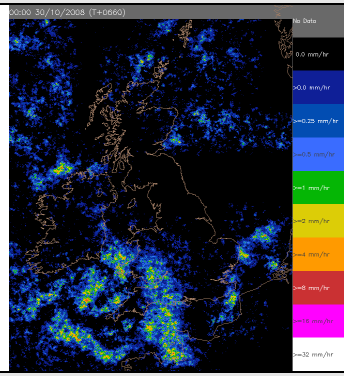	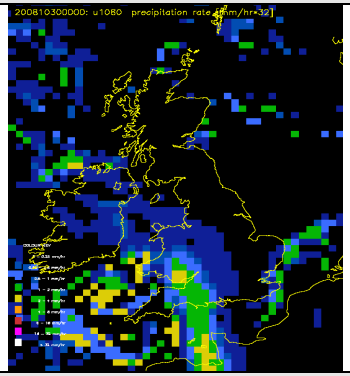
UKPP rain analysis valid at 0000 GMT on 30/10/2008	**UKV T+18 h control forecast and non-parametric noise valid at 0000 GMT on 30/10/2008**	**MOGREPS-R T+18 h downscale forecast valid at 0000 GMT on 30/10/2008**	**MOGREPS-R T+18 h forecast valid at 0000 GMT on 30/10/2008**

Figure 38b Selected forecast steps in a blended, control member forecast of precipitation rate, comprising a MOGREPS-R control forecast and parametric noise (confined to scales ≤ 64 km), run from 1300 GMT on 29/10/2008 (3rd column from left). A corresponding sequence of UKPP rain analyses and forecasts steps from the associated MOGREPS-R control forecast (data time 0600 GMT, 29/10/2008) and UKV control forecast (data time 0600 GMT, 29/10/2008) are also shown for comparison.

© Crown copyright 2010

As previously discussed, the speckling introduced by the injection of non-parametric noise into the bottom two cascade levels only should be preventable by allowing the weight on the noise component to decay exponentially up the cascade.

Despite the obvious, negative impact of spatially homogenous noise on the appearance of the blended forecasts, it is noteworthy that time evolutions of the field mean, variance and raining fraction (Figures 39 to 41 respectively) of the extrapolation and UKV blended control forecasts remain plausible. This finding is consistent with the close correspondence between the radar and blended forecast distributions of rain rate shown in Figure 42a and the similarity between the power spectra of the radar and blended forecasts seen in Figure 43. It is evident that the bulk statistical properties of the blended forecast fields remain sensible because the bulk statistical properties of the noise are good approximations to those of the radar.

Figure 38b shows a time series of downscaled MOGREPS-R control member precipitation forecasts for 29/10/2008. In common with the corresponding extrapolation and UKV blended control forecasts, these lack intensity relative to their equivalent radar based UKPP rain analyses. This is confirmed by the negative bias in forecast field mean and variance relative to radar seen in Figures 39 and 40 (although the raining fraction in Figure 41 is improved). Figure 42b demonstrates that the distribution of precipitation rate in the downscaled forecast valid at 1400 GMT on 29/10/2008 is deficient in the representation of rates above about 1 mm/h. This finding is consistent with the power spectra plots in Figure 43. These show that the downscaled MOGREPS-R control precipitation forecast lacks variance relative to radar at all scales.

It is evident that that the poor performance of the MOGREPS-R downscaler is largely a consequence of the limitations of the parametric noise generator. Firstly, the application of a power law fit to the MOGREPS-R power spectrum is inadequate, even if the former follows a power law, because the slope of the MOGREPS-R power spectrum is invariably steeper than the equivalent radar power spectrum. Secondly, downscaling with spatially homogenous noise when the target field contains both widespread precipitation and showers can degrade the power spectrum of the forecasts further by adding too much variance in some areas and too little in others.

© Crown copyright 2010

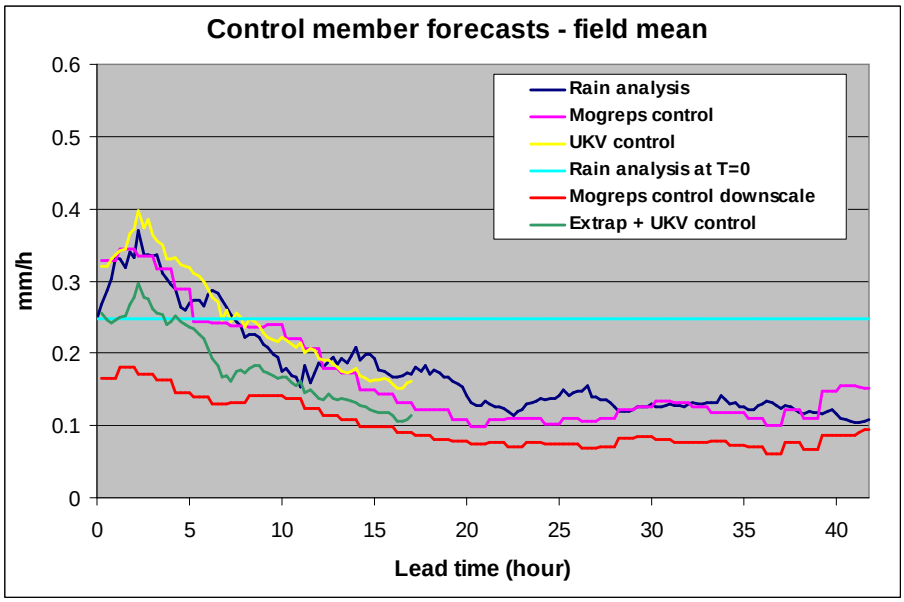

Figure 39 Time evolution of the field mean of UKPP rain analyses, MOGREPS-R and UKV control member forecasts and the two configurations of blended forecast for 29/10/2008. The forecast lead times on the X axis are those of the blended forecasts (run from 1300 GMT on 29/10/2008). The UKV and MOGREPS-R forecasts were run from 0600 GMT on 29/10/2008.

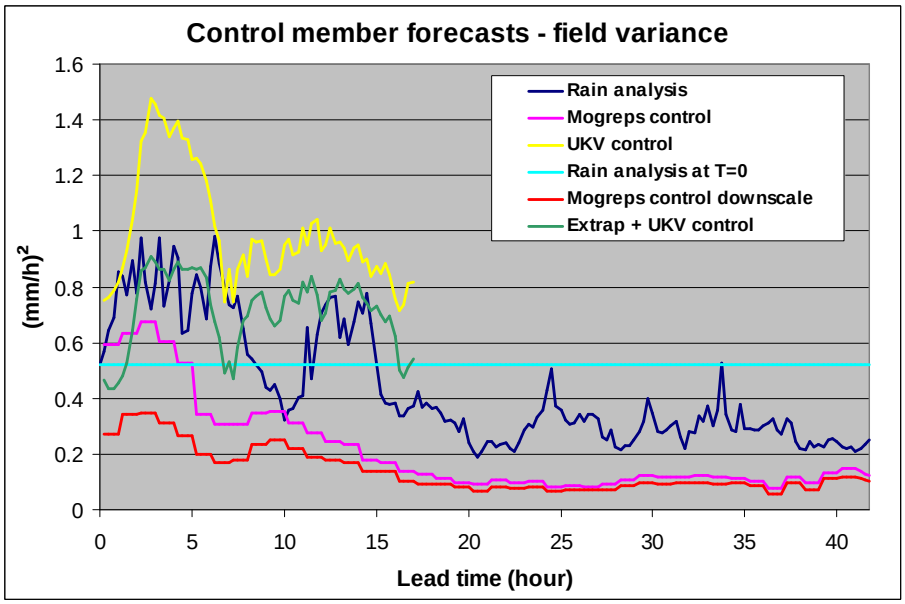

Figure 40 Time evolution of the field variance of UKPP rain analyses, MOGREPS-R and UKV control member forecasts and the two configurations of blended forecast for 29/10/2008. The forecast lead times on the X axis are those of the blended forecasts (run from 1300 GMT on 29/10/2008).

© Crown copyright 2010

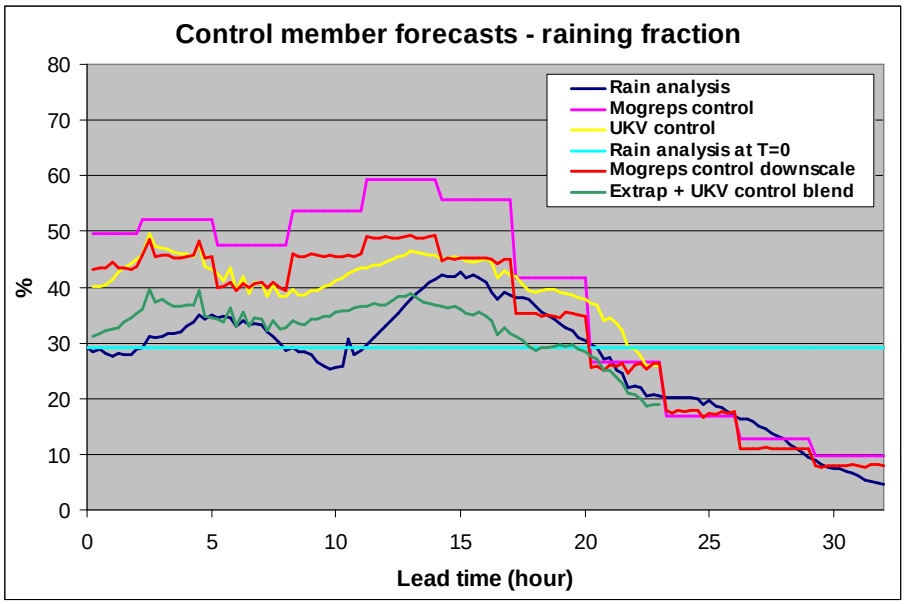

Figure 41 Time evolution of the raining fraction of UKPP rain analyses, MOGREPS-R and UKV control member forecasts and the two configurations of blended forecast for 29/10/2008. The forecast lead times on the X axis are those of the blended forecasts (run from 1300 GMT on 29/10/2008).

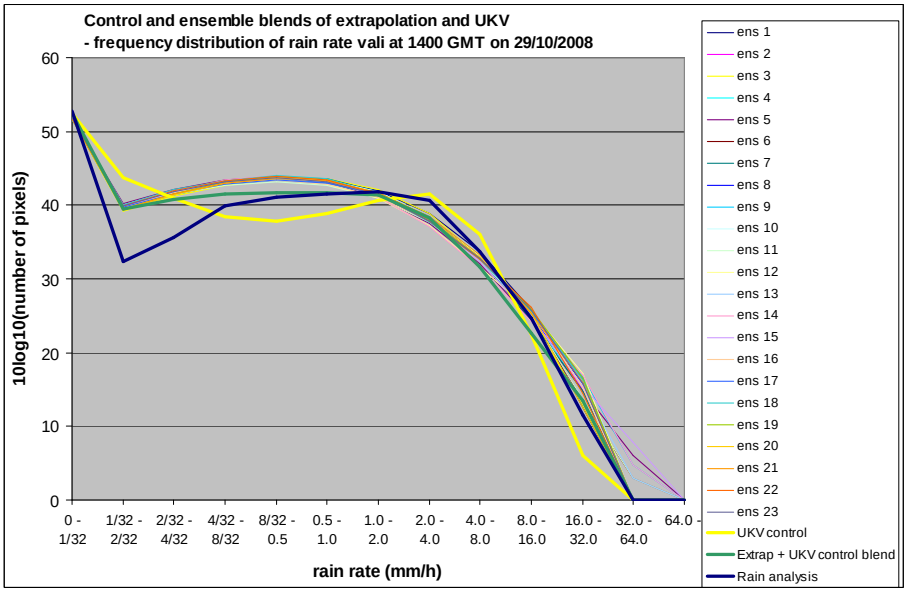

Figure 42a Frequency distributions of precipitation rate for a UKPP rain analysis, a 2 km resolution UKV control member forecast, and a blended control forecast and 23 member ensemble forecast incorporating an extrapolation nowcast and UKV control forecast, all valid at 1400 GMT on 29/10/2008. The blended forecasts were run from 1300 GMT on 29/10/2008 and the UKV control forecast from 0600 GMT on the same day. The validation area is the UK radar composite.

© Crown copyright 2010

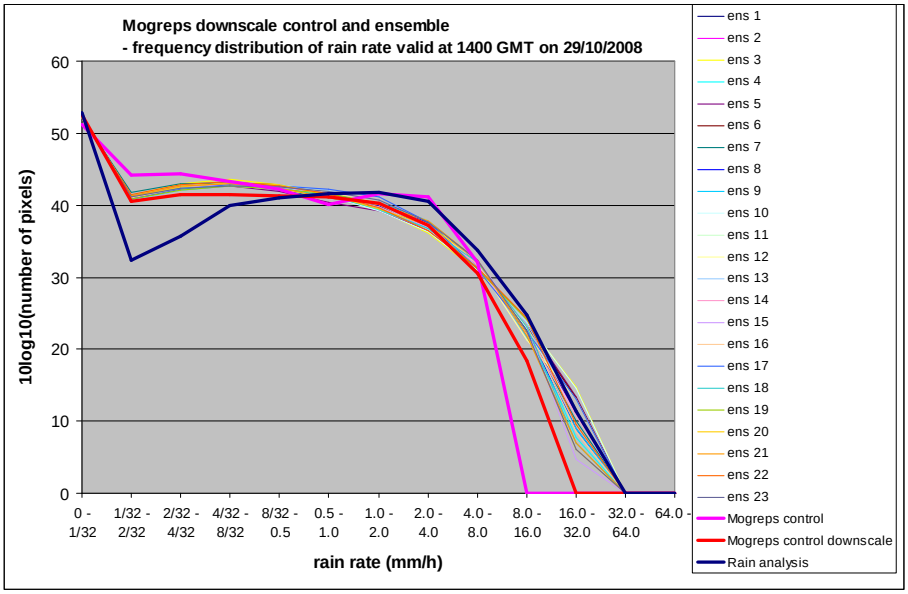

Figure 42b Frequency distributions of precipitation rate for a UKPP rain analyses, a 24 km resolution MOGREPS-R control member and its downscaled counterpart, and 23 members of a downscaled MOGREPS-R control forecast, all valid at 1400 GMT on 29/10/2008. The MOGREPS-R control forecast was run from 0600 GMT on 29/10/2008. The validation area is the UK radar composite.

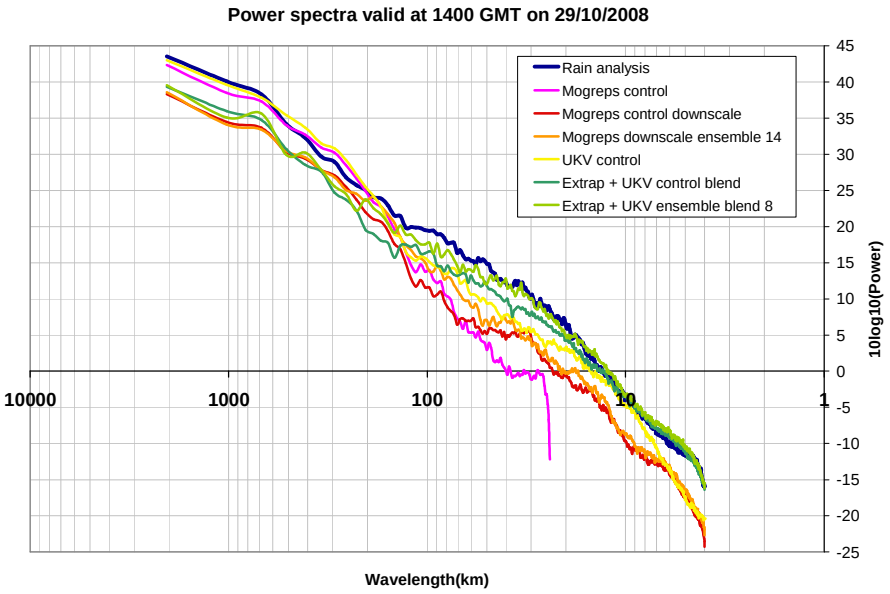

Figure 43 Power spectra for a UKPP rain analysis, MOGREPS-R (T+8 h) and UKV (T+8h) control member forecasts and the two configurations of blended forecasts (T+1 h) all valid at 1400 GMT on 29/10/2008.

© Crown copyright 2010

Case study based evaluation of ensemble member blends

The performances of the two ensemble configurations of blended forecasts described in section 5.4.1 have also been examined on a case by case basis. Results from the two case studies considered in the previous section are presented to illustrate their strengths and weaknesses. A selection of forecast images and verification statistics for the remaining case studies can be found in Appendix A.2.

Case study 5 – 25/03/2010

Figure 44a shows the time evolution of two members of a 23 member ensemble of blended forecasts incorporating an extrapolation nowcast, UKV control member precipitation forecast and non-parametric noise. The noise injected into each level of the cascade is constrained by the skill of the extrapolation nowcast and UKV forecast. This was not the case in the control member blended forecast where the addition of noise was restricted to the bottom 2 cascade levels. The weights assigned to the noise and forecast components in each ensemble member are shown in Figure 45.

Comparison of two members of an ensemble of blended forecasts with the equivalent UKV control forecast and a time series of UKPP rain analyses (see Figure 44a) demonstrates that the former evolve smoothly over time towards the UKV model. The influence of the noise is first seen in the divergent evolution of the fine scale structures in the two blended forecast members. The scale of these perturbations grows with forecast lead time. The anisotropic properties of the noise are most apparent at T+3h, replicating the linear organisation of the precipitation over the English Channel.

It is reasonable to conclude that the overall appearance and behaviour of these ensembles of blended forecasts is plausible: they seem to capture the key features visible in the radar data at T+0h and in the UKV control forecast. The effects of using spatially varying target means and variances are illustrated by the two, T+3h blended forecasts. In common with the UKV control forecast, these both reproduce the area of intense precipitation over the English Channel.

Figure 44b shows the time evolution of two members of a 23 member ensemble of downscaled MOGREPS-R control member precipitation forecasts. Here, the parametric noise injected into each level of the cascade is constrained by the skill of the MOGREPS-R control forecast. The skill climatology shown in Table 2a (pages 31-33) determines the weight assigned to the MOGREPS-R forecast and noise on each cascade level. The character of these blended ensemble forecasts is similar to that of the extrapolation and UKV based ensembles, although the isotropic nature of the parametric noise is a distinguishing feature.

© Crown copyright 2010

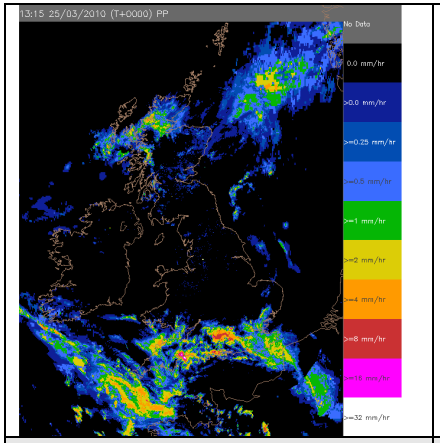	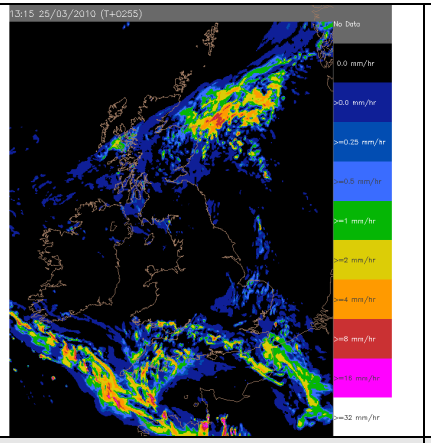	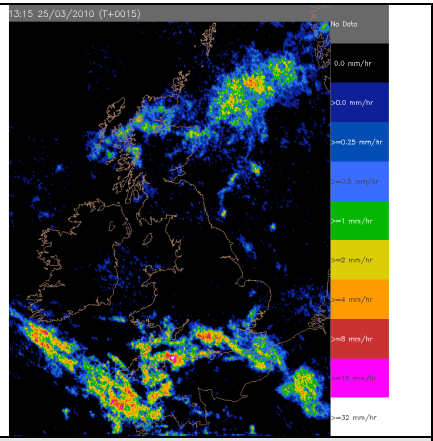	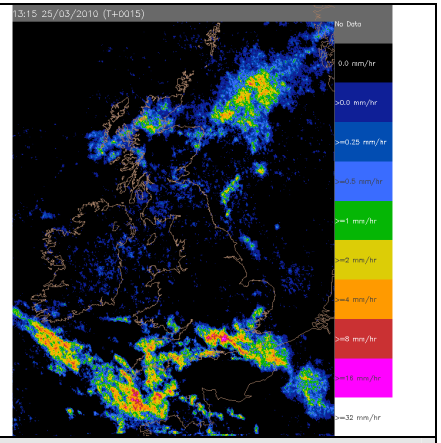
UKPP rain analysis valid at 1315 GMT on 25/03/2010	**T+4 h 15 min UKV control forecast valid at 1315 GMT on 25/03/2010**	**Member 1 of a T+15 min blend of an extrapolation nowcast, a UKV control forecast and non-parametric noise valid at 1315 GMT on 25/03/2010**	**Member 2 of a T+15 min blend of an extrapolation nowcast, a UKV control forecast and non-parametric noise valid at 1315 GMT on 25/03/2010**
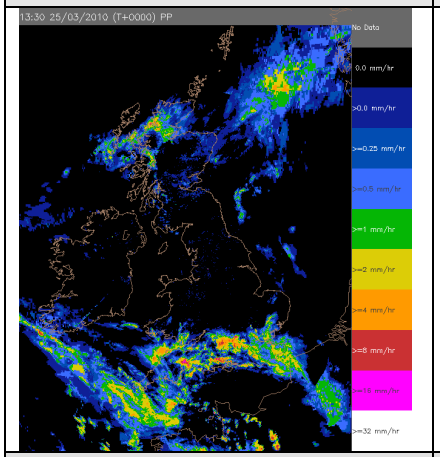	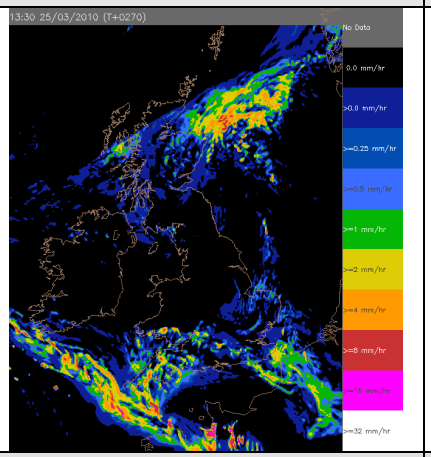	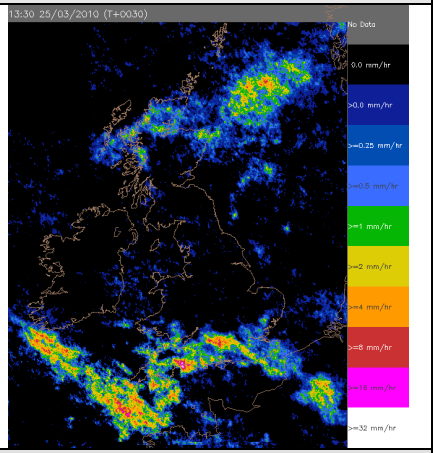	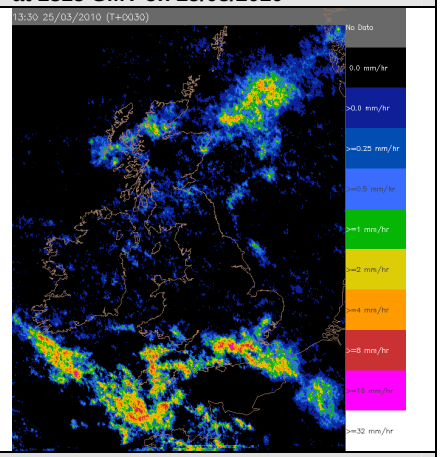
UKPP rain analysis valid at 1330 GMT on 25/03/2010	**T+4 h 30 min UKV control forecast valid at 1330 GMT on 25/03/2010**	**Member 1 of a T+30 min blend of an extrapolation nowcast, a UKV control forecast and non-parametric noise valid at 1330 GMT on 25/03/2010**	**Member 2 of a T+30 min blend of an extrapolation nowcast, a UKV control forecast and non-parametric noise valid at 1330 GMT on 25/03/2010**

© Crown copyright 2010

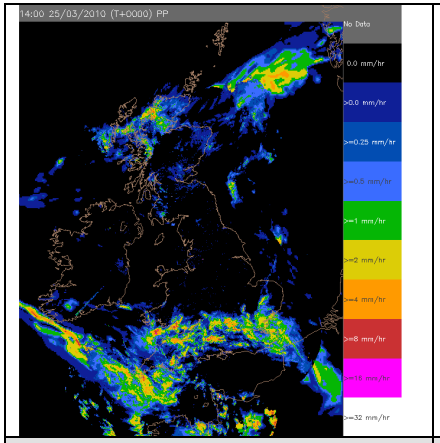	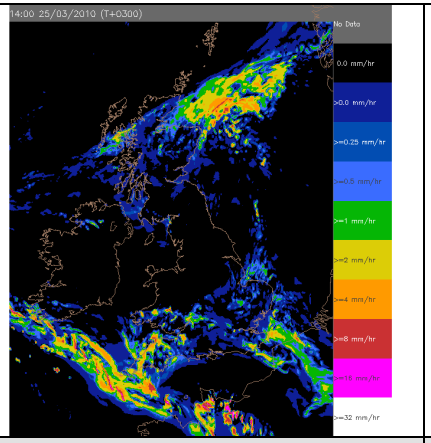	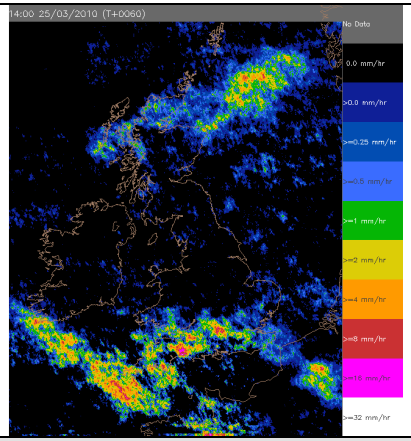	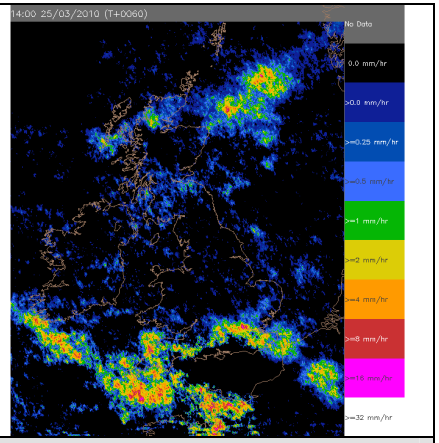
UKPP rain analysis valid at 1400 GMT on 25/03/2010	**T+5 h UKV control forecast valid at 1400 GMT on 25/03/2010**	**Member 1 of a T+1 h blend of an extrapolation nowcast, a UKV control forecast and non-parametric noise valid at 1400 GMT on 25/03/2010**	**Member 2 of a T+1 h blend of an extrapolation nowcast, a UKV control forecast and non-parametric noise valid at 1400 GMT on 25/03/2010**
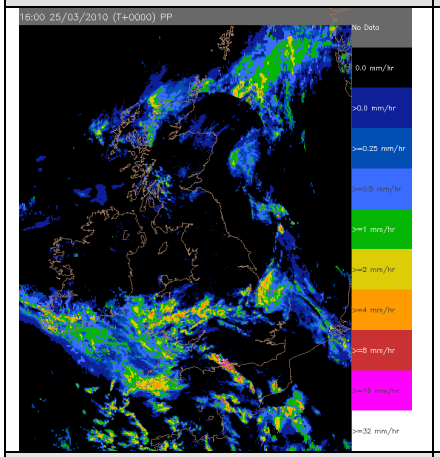	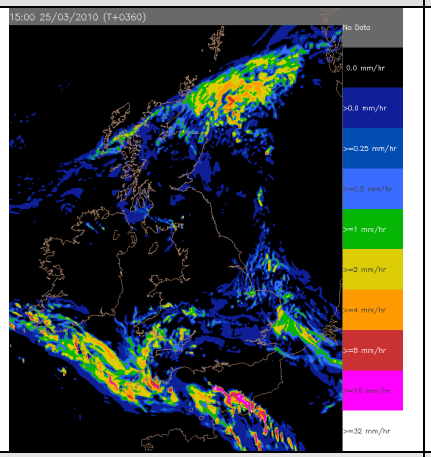	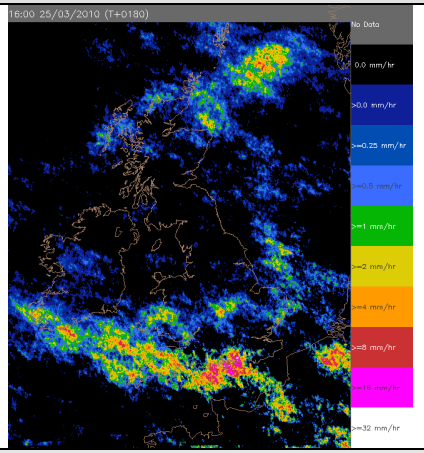	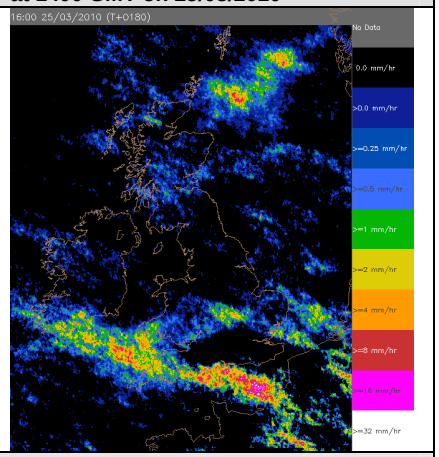
UKPP rain analysis valid at 1600 GMT on 25/03/2010	**T+7 h UKV control forecast valid at 1600 GMT on 25/03/2010**	**Member 1 of a T+3 h blend of an extrapolation nowcast, a UKV control forecast and non-parametric noise valid at 1600 GMT on 25/03/2010**	**Member 2 of a T+3 h blend of an extrapolation nowcast, a UKV control forecast and non-parametric noise valid at 1600 GMT on 25/03/2010**

© Crown copyright 2010

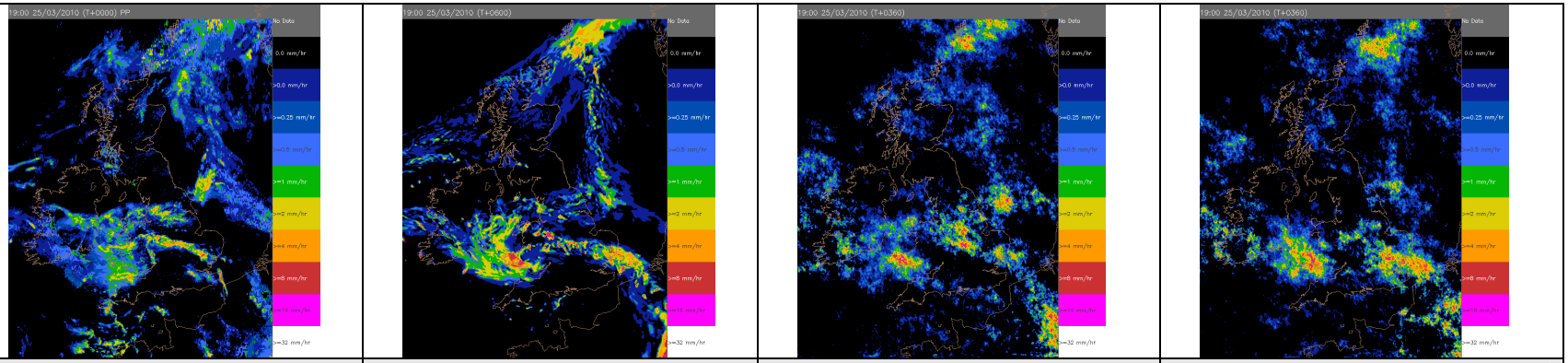

UKPP rain analysis valid at 1900 GMT on 25/03/2010	**T+10 h UKV control forecast valid at 1900 GMT on 25/03/2010**	**Member 1 of a T+6 h blend of an extrapolation nowcast, a UKV control forecast and non-parametric noise valid at 1900 GMT on 25/03/2010**	**Member 2 of a T+6 h blend of an extrapolation nowcast, a UKV control forecast and non-parametric noise valid at 1900 GMT on 25/03/2010**
UKPP rain analysis valid at 0100 GMT on 26/03/2010	**T+16 h UKV control forecast valid at 0100 GMT on 26/03/2010**	**Member 1 of a T+12 h blend of an extrapolation nowcast, a UKV control forecast and non-parametric noise valid at 0100 GMT on 26/03/2010**	**Member 2 of a T+12 h blend of an extrapolation nowcast, a UKV control forecast and non-parametric noise valid at 0100 GMT on 26/03/2010**

Figure 44a Selected steps in two members of a blended ensemble forecast of precipitation rate, comprising an extrapolation nowcast, UKV control forecast and non-parametric noise, run from 1300 GMT on 25/03/2010. The UKPP rain analysis used as the starting point for the extrapolation nowcast is also shown, as well corresponding forecast steps from the associated UKV control member forecast (data time 0900 GMT, 25/03/2010).

© Crown copyright 2010

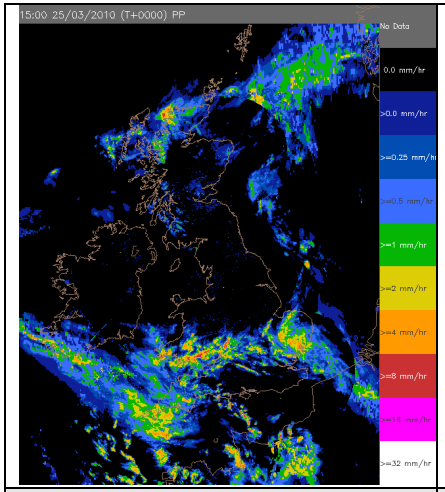

UKPP rain analysis valid at 1500 GMT on 25/03/2010

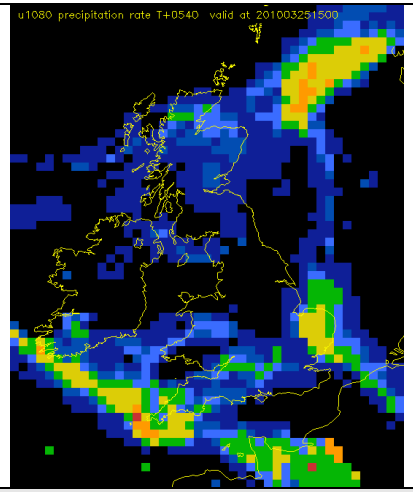

MOGREPS-R T+9 h forecast valid at 1500 GMT on 25/03/2010

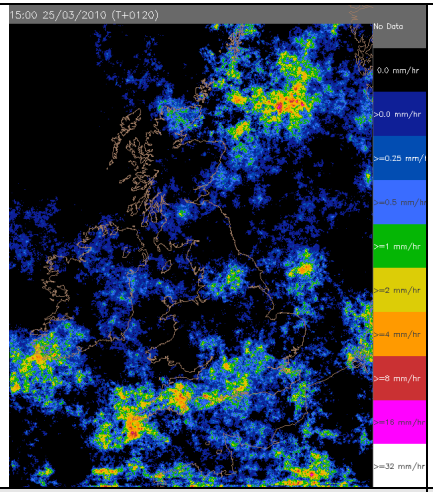

Member 1 of a T+9 h MOGREPS-R downscale ensemble forecast valid at 1500 GMT on 25/03/2010

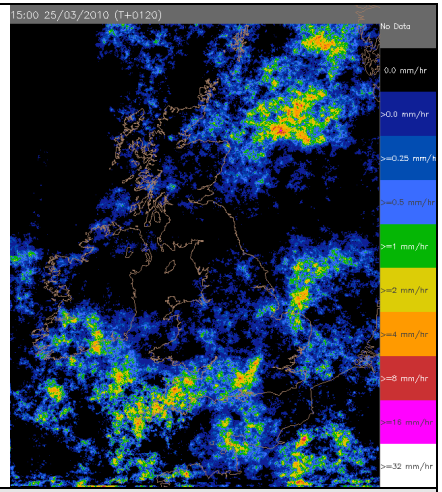

Member 2 of a T+9 h MOGREPS-R downscale ensemble forecast valid at 1500 GMT on 25/03/2010

© Crown copyright 2010

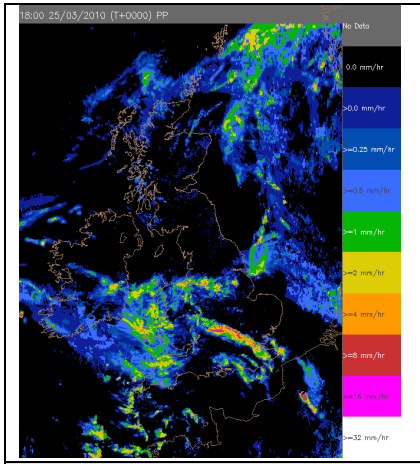	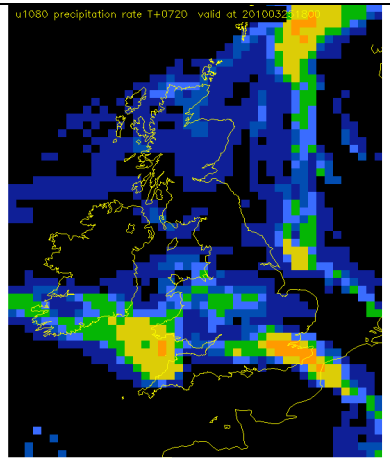	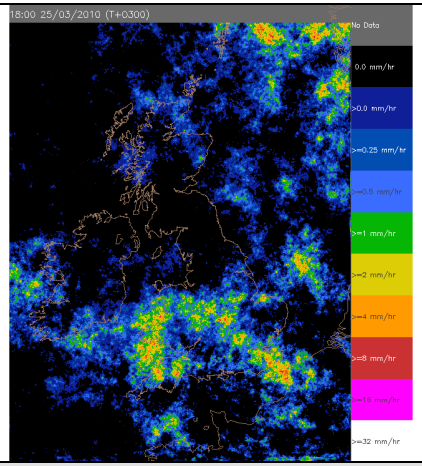	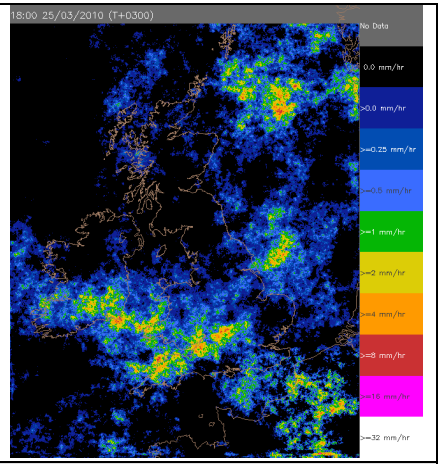
UKPP rain analysis valid at 1800 GMT on 25/03/2010	**MOGREPS-R T+12 h forecast valid at 1800 GMT on 25/03/2010**	**Member 1 of a T+12 h MOGREPS-R downscale ensemble forecast valid at 1800 GMT on 25/03/2010**	**Member 2 of a T+12 h MOGREPS-R downscale ensemble forecast valid at 1800 GMT on 25/03/2010**
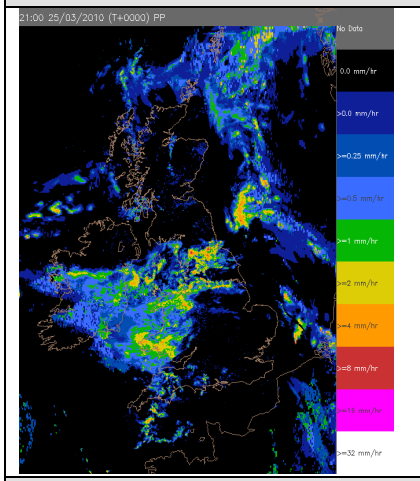	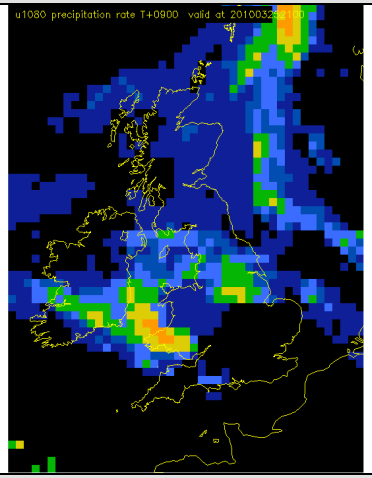	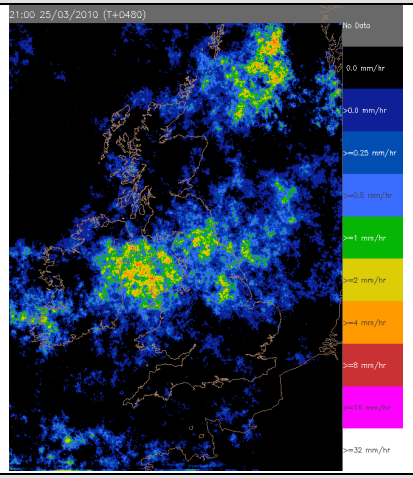	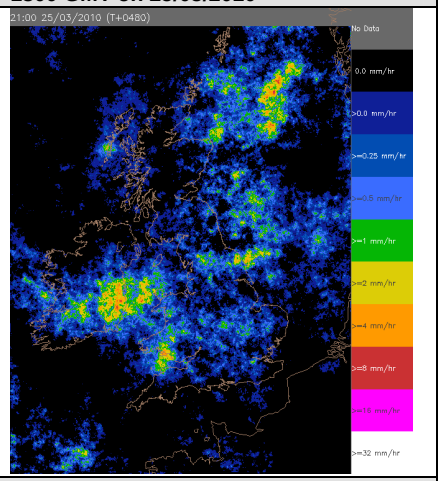
UKPP rain analysis valid at 2100 GMT on 25/03/2010	**MOGREPS-R T+15 h forecast valid at 2100 GMT on 25/03/2010**	**Member 1 of a T+15 h MOGREPS-R downscale ensemble forecast valid at 2100 GMT on 25/03/2010**	**Member 2 of a T+15 h MOGREPS-R downscale ensemble forecast valid at 2100 GMT on 25/03/2010**

© Crown copyright 2010

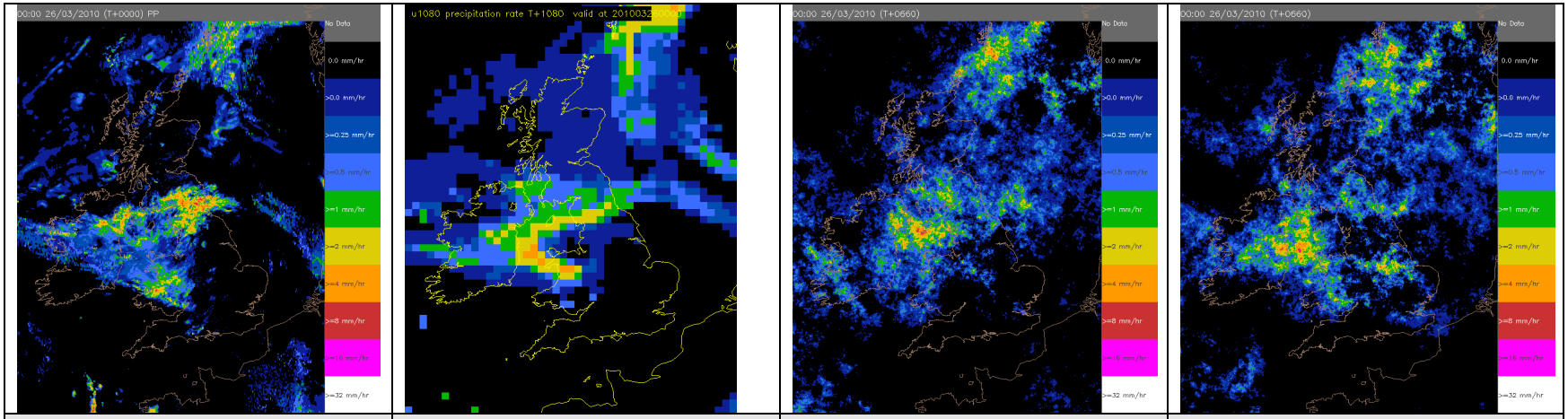

UKPP rain analysis valid at 0000 GMT on 26/03/2009	**MOGREPS-R T+18 h forecast valid at 0000 GMT on 26/03/2009**	**Member 1 of a T+18 h MOGREPS-R downscale ensemble forecast valid at 0000 GMT on 26/03/2010**	**Member 2 of a T+18 h MOGREPS-R downscale ensemble forecast valid at 0000 GMT on 26/03/2010**

Figure 44b Selected forecast steps in two members of a blended ensemble forecast of precipitation rate, comprising a MOGREPS-R control forecast and parametric noise, run from 1300 GMT on 25/03/2010 (3rd column from left). A corresponding sequence of UKPP rain analyses and forecasts steps from the associated MOGREPS-R control forecast (data time 0600 GMT, 25/03/2010) are also shown for comparison.

© Crown copyright 2010

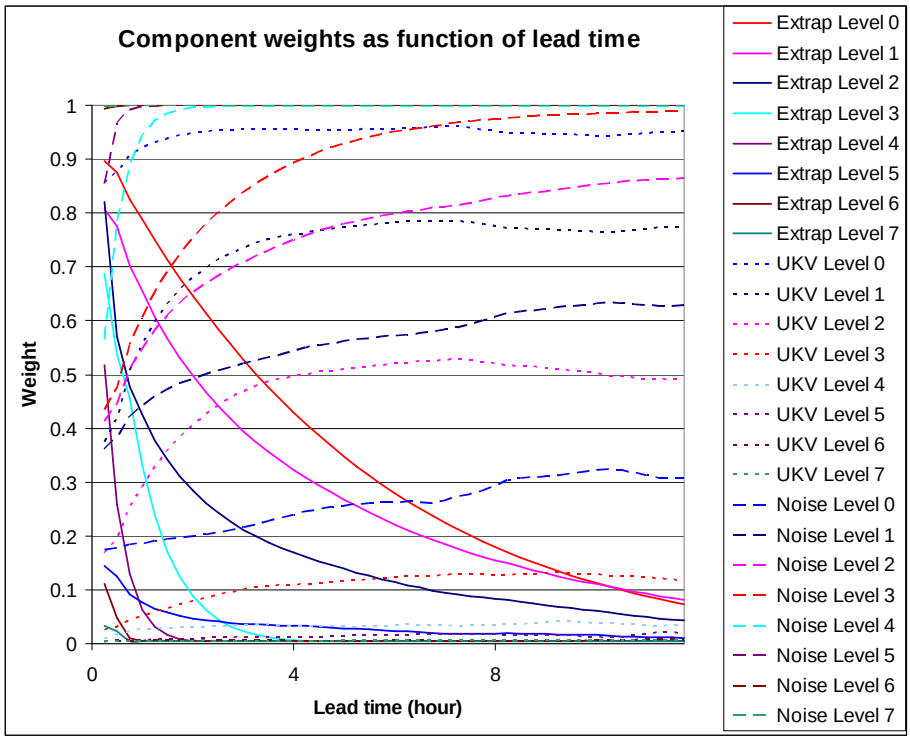

Figure 45 A plot of the weights assigned to the extrapolation and UKV forecast components and noise as a function of lead time in the blended ensemble forecast, excerpts of which are shown in Figure 44a.

The performances of the two ensemble configurations of blended forecasts can be clarified using the field oriented statistics shown in Figures 46 to 51. The frequency distribution plots and power spectra shown in Figures 36a-b and 37 are also relevant to the discussion.

Figures 46 to 48 are plots of the time evolution of the field mean, variance and raining fraction for the control member and a 23 member ensemble of blended forecasts comprising an extrapolation nowcast, UKV control member forecast and non-parametric noise. These are compared to equivalent statistics derived from a time series of UKPP rain analyses.

As expected, the mean, variance and raining fraction of the control member and ensemble of blended forecasts tend from those of the radar towards those of the UKV model in the first few hours. However, the statistics for the control member blend show small discrepancies in the mean and larger discrepancies in the raining fraction. These are the result of small biases introduced when collapsing the blended cascades and can lead to the removal of precipitation areas with rates < 0.1 mm/h. This may have a significant impact on the raining fraction because UKV model forecasts often contain substantial areas of very light precipitation. By contrast, there is a tendency to produce too much precipitation in the ensemble of blended forecasts. This behaviour is caused by small biases in the noise.

© Crown copyright 2010

Figure 36a compares the frequency distributions of the control member and ensemble, blended forecasts of precipitation rate, derived by combining an extrapolation nowcast, UKV control member forecast and non-parametric noise. It can be seen that the former tend to be a better representation of the radar inferred distribution of precipitation rate than the raw model at rates below about 1 mm/h. However, at rates above 2 mm/h, the blended forecasts look more like the UKV control member forecast. This amalgam of the characteristics of the radar and UKV control forecast is confirmed by the power spectrum plots in Figure 37.

Figures 49 to 51 are plots of the time evolution of the field mean, variance and raining fraction for the MOGREPS-R control member precipitation forecast and an ensemble of downscale forecasts generated by injecting multiple realisations of parametric noise into the cascade. Note that operational MOGREPS-R forecasts of precipitation rate are only available at three hourly intervals. This explains the step changes seen in the field mean, variance and raining fraction of the MOGREPS-R control forecast (pink line) and associated downscale forecasts (points between the three hourly steps are multiple realisations of the three hourly forecasts).

The field means and variances of the ensemble of MOGREPS-R downscale precipitation forecasts closely follow those of the raw model. However, for reasons explained earlier, the downscaled control member, generated by injecting noise into the bottom four cascade levels only (scales ≤ 32 km), has a reduced raining fraction relative to the raw model. This effect is less apparent in the downscale ensemble: here, the addition of parametric noise to the cascade is constrained by the skill of the MOGREPS-R control member forecast. Early on in the forecast sequence, the deficit of variance in the downscale forecasts relative to the radar is noteworthy. This is probably due to previously described limitations of the parametric noise generation method.

Figure 36b compares the frequency distributions of the downscale ensemble forecasts of precipitation rate with the equivalent radar and MOGREPS-R control forecast distributions. It can be seen that the former are a better representation of the radar than the raw model. This is confirmed by the power spectrum plots in Figure 37.

© Crown copyright 2010

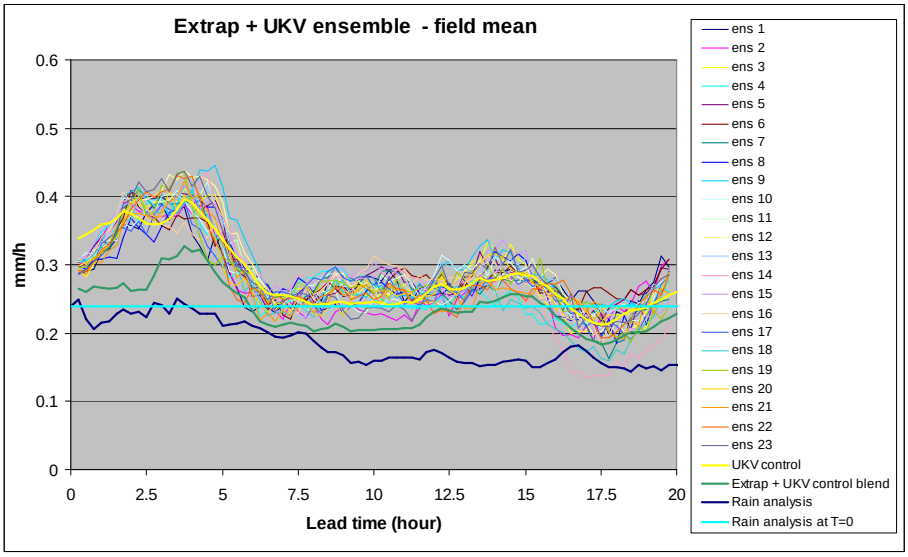

Figure 46 Time evolution of the field mean of UKPP rain analyses, a UKV control member forecast (data time 0900 GMT on 25/03/2010), and control and ensemble blended forecasts (data time 1300 GMT on 25/03/2010) comprising extrapolation, UKV and non-parametric noise. The forecast lead times on the X axis are those of the blended forecasts (run from 1300 GMT).

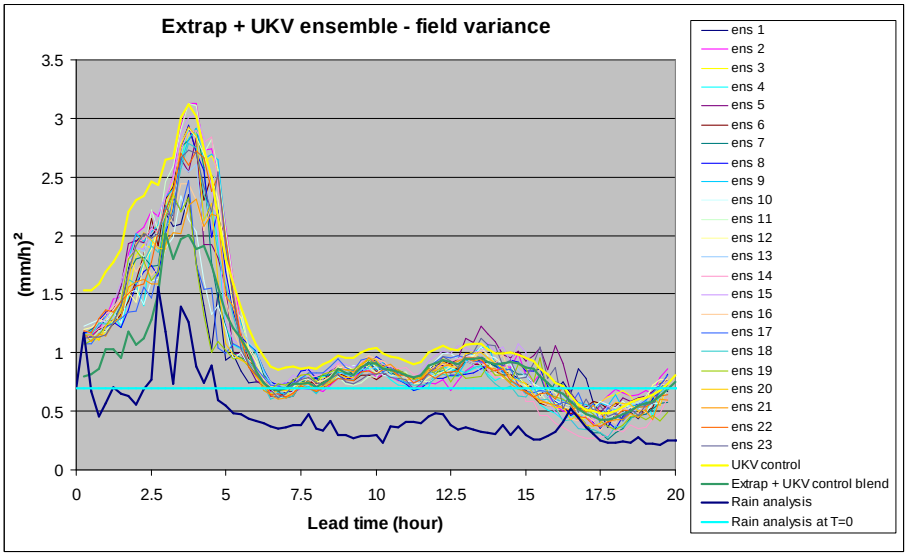

Figure 47 Time evolution of the field variance of UKPP rain analyses, a UKV control member forecast (data time 0900 GMT on 25/03/2010), and control and ensemble blended forecasts (data time 1300 GMT on 25/03/2010) comprising extrapolation, UKV and non-parametric noise. The forecast lead times on the X axis are those of the blended forecasts (run from 1300 GMT).

© Crown copyright 2010

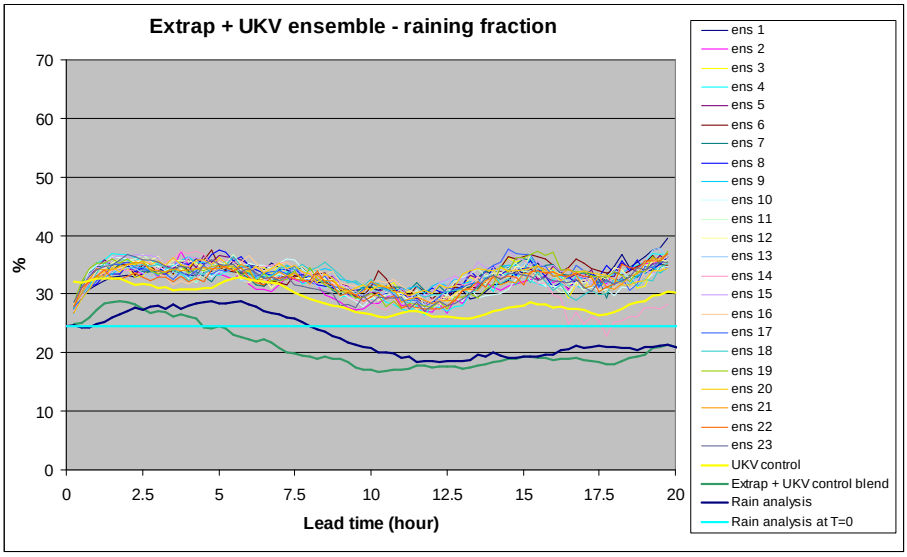

Figure 48 Time evolution of the field raining fraction of UKPP rain analyses, a UKV control member forecast (data time 0900 GMT on 25/03/2010), and control and ensemble blended forecasts (data time 1300 GMT on 25/03/2010) comprising extrapolation, UKV and non-parametric noise. The forecast lead times on the X axis are those of the blended forecasts (run from 1300 GMT).

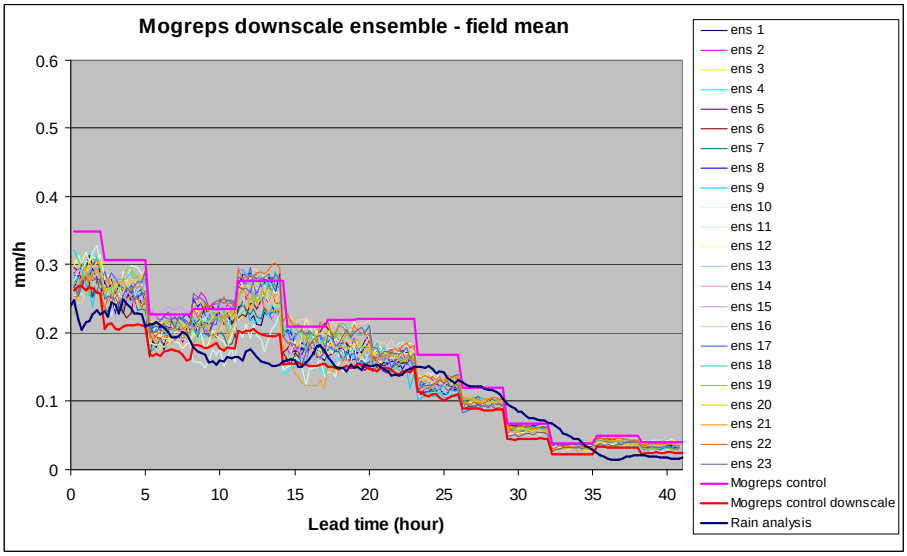

Figure 49 Time evolution of the field mean of UKPP rain analyses, a MOGREPS-R control member forecast (data time 0600 GMT on 25/03/2010), and control and ensemble blended forecasts (data time 1300 GMT on 25/03/2010) comprising MOGREPS-R and parametric noise. The forecast lead times on the X axis are those of the blended forecasts (run from 1300 GMT).

© Crown copyright 2010

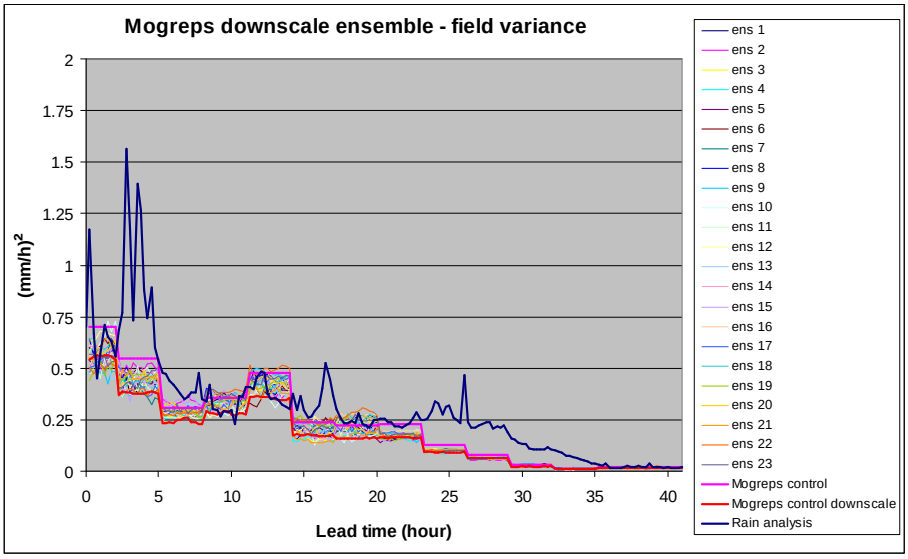

Figure 50 Time evolution of the field variance of UKPP rain analyses, a MOGREPS-R control member forecast (data time 0600 GMT on 25/03/2010), and control and ensemble blended forecasts (data time 1300 GMT on 25/03/2010) comprising MOGREPS-R and parametric noise. The forecast lead times on the X axis are those of the blended forecasts (run from 1300 GMT).

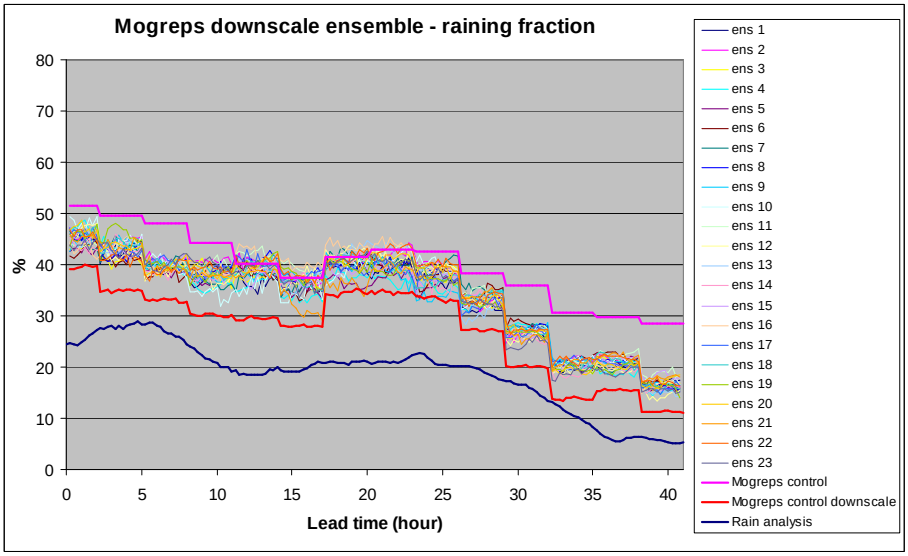

Figure 51 Time evolution of the field raining fraction of UKPP rain analyses, a MOGREPS-R control member forecast (data time 0600 GMT on 25/03/2010), and control and ensemble blended forecasts (data time 1300 GMT on 25/03/2010) comprising MOGREPS-R and parametric noise. The forecast lead times on the X axis are those of the blended forecasts (run from 1300 GMT).

© Crown copyright 2010

Case study 2 – 29/10/2008

The UKV precipitation forecast data employed in this case study were supplied by the *Convective-scale Ensembles Project*. These data cover only that fraction of the UKV model domain where the grid length is 1.5 km. For this reason, the case study examples presented here are for a reduced domain size to avoid boundary effects caused by the missing data in the variable resolution border around the edges of the UKV model domain. In addition, the non-parametric noise employed in the blending of extrapolation and UKV model forecasts is based upon the T+0 h UKPP rain analyses (the start of blended forecasts) for the full duration of the blended forecasts, for reasons explained earlier.

Figure 52a shows two members of an ensemble of blended forecasts generated from 1300 GMT on 29/10/2008. These incorporate an extrapolation nowcast, UKV control member precipitation forecast and non-parametric noise. The weights assigned to these components are plotted in Figure 53. In common with the performance of the control member blend described earlier, the area of frontal precipitation lacks intensity and exhibits too much variability. This is largely a consequence of the spatial homogeneity of the non-parametric noise and the mixed character of the precipitation in the UKPP rain analyses. A comparison of results from this and other case studies involving co-existing areas of frontal precipitation and showers (e.g. 05/09/2008, 17/02/2010, 19/11/2009 – see Appendix A.2) with evidence from cases associated with a single precipitation regime (25/03/2010) confirms this explanation.

Scrutiny of Figures 54 and 55 reveals that the field mean and variance of all members of the ensemble of blended forecasts follow those of the UKPP rain analyses quite closely. Furthermore, the power spectrum of a randomly selected member (member 8) in Figure 43 is close to that of the radar and UKV forecast. It can be concluded that the average spatial statistical properties of the blended forecasts are reasonably good approximations of the analysed fields. Thus, the deficiencies describe above must arise from local differences in the character of the noise and the forecast components. This finding lends support to the idea of maintaining two noise cascades, one for frontal precipitation the other for showers.

Similar performance issues are apparent in the downscaled MOGREPS-R forecasts shown in Figure 52b. Here the problems arising from the use of a single noise distribution to represent fronts and showers are probably exacerbated by errors in the parametric model fit to the MOGREPS-R power spectrum (see Figure 43). This inference is supported by the evidence in Figures 57 and 58 which shows significant low bias in the mean and variance of the ensemble of downscaled MOGREPS-R forecasts.

Figures 56 and 59 demonstrate that both ensemble configurations of blended forecasts produce too much precipitation. The frequency distribution plots in Figures 42a and 42b indicate that this excess of

© Crown copyright 2010

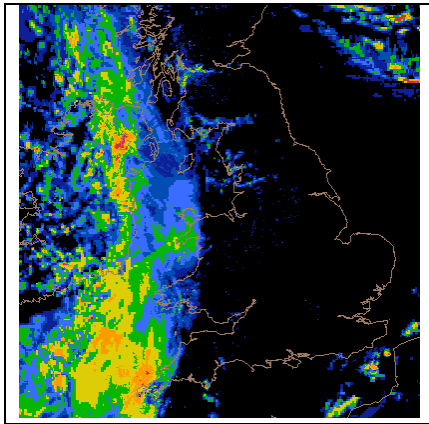	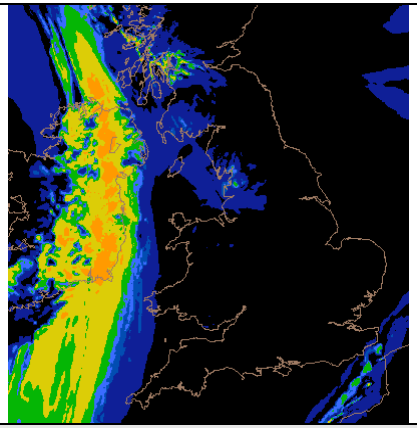	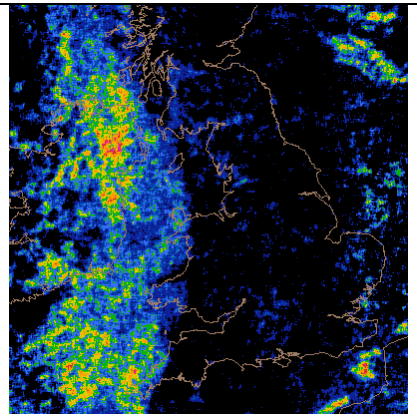	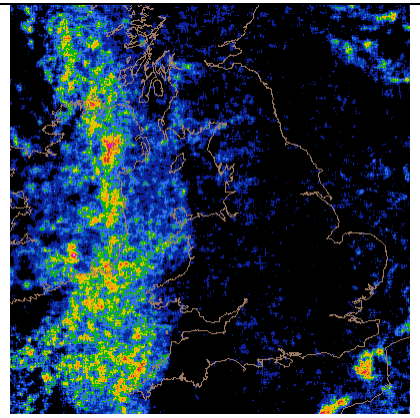
UKPP rain analysis valid at 1315 GMT on 29/10/2008	**T+7 h 15 min UKV control forecast valid at 1330 GMT on 29/10/2008**	**Member 1 of a T+15 min blend of an extrapolation nowcast, a UKV control forecast and non-parametric noise valid at 1315 GMT on 29/10/2008**	**Member 2 of a T+15 min blend of an extrapolation nowcast, a UKV control forecast and non-parametric noise valid at 1315 GMT on 29/10/2008**
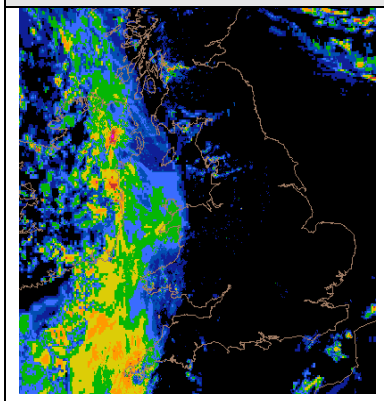	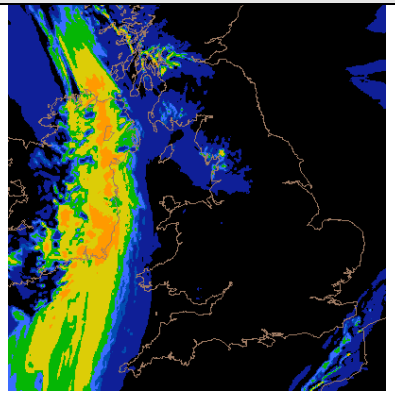	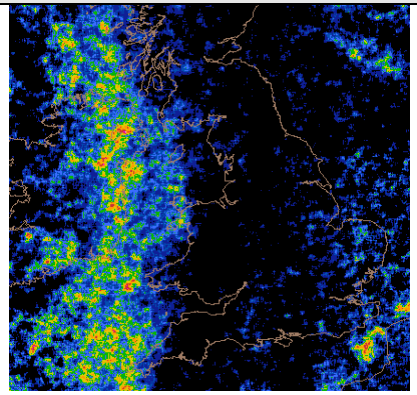	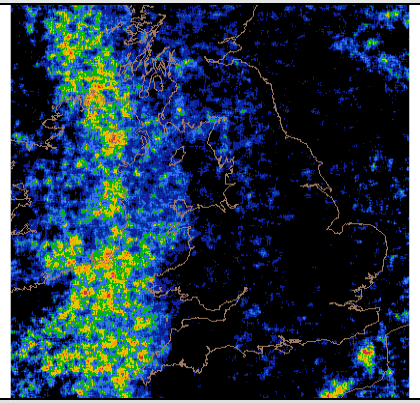
UKPP rain analysis valid at 1330 GMT on 29/10/2008	**T+7 h 30 min UKV control forecast valid at 1330 GMT on 29/10/2008**	**Member 1 of a T+30 min blend of an extrapolation nowcast, a UKV control forecast and non-parametric noise valid at 1330 GMT on 29/10/2008**	**Member 2 of a T+30 min blend of an extrapolation nowcast, a UKV control forecast and non-parametric noise valid at 1330 GMT on 29/10/2008**

© Crown copyright 2010

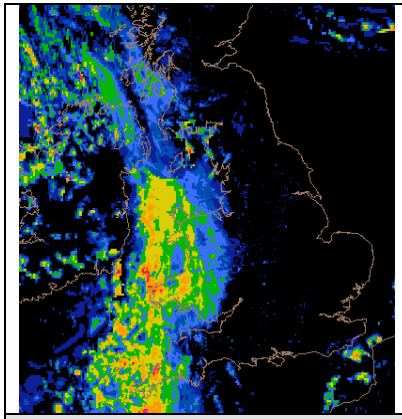	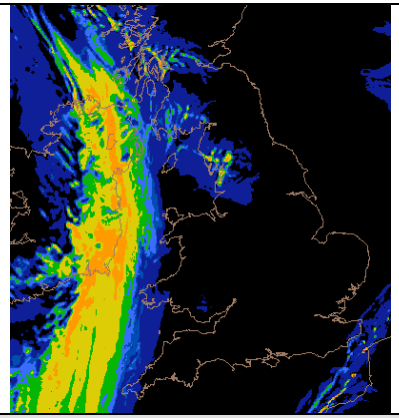	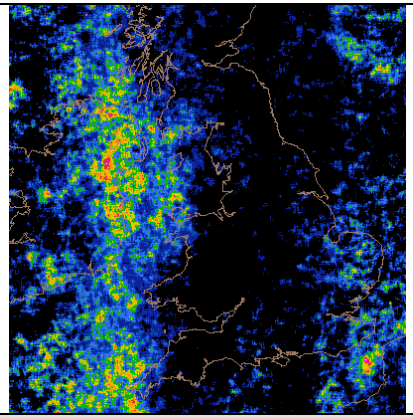	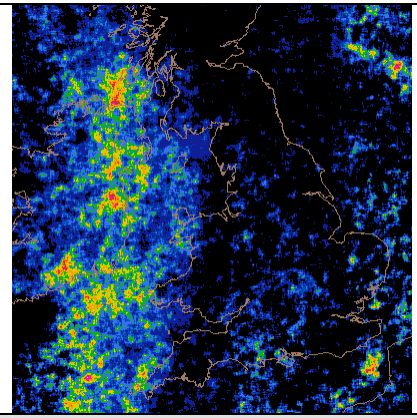
UKPP rain analysis valid at 1400 GMT on 29/10/2008	**T+8 h UKV control forecast valid at 1400 GMT on 29/10/2008**	**Member 1 of a T+1 h blend of an extrapolation nowcast, a UKV control forecast and non-parametric noise valid at 1400 GMT on 29/10/2008**	**Member 2 of a T+1 h blend of an extrapolation nowcast, a UKV control forecast and non-parametric noise valid at 1400 GMT on 29/10/2008**
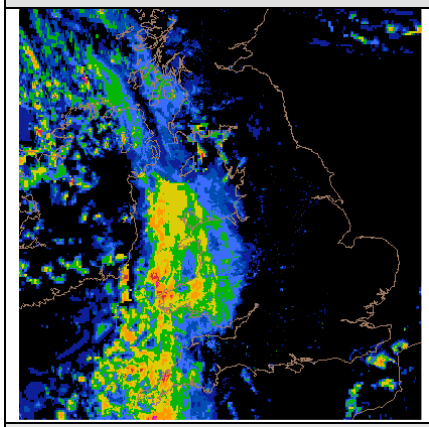	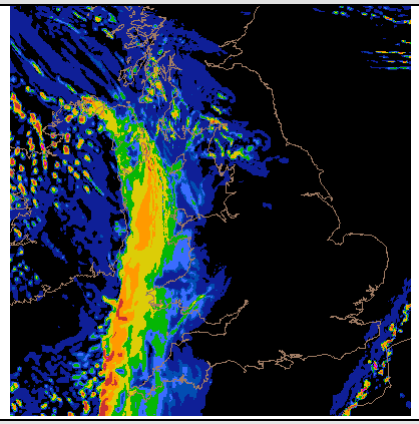	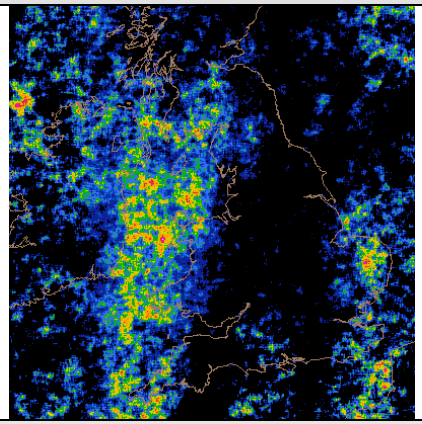	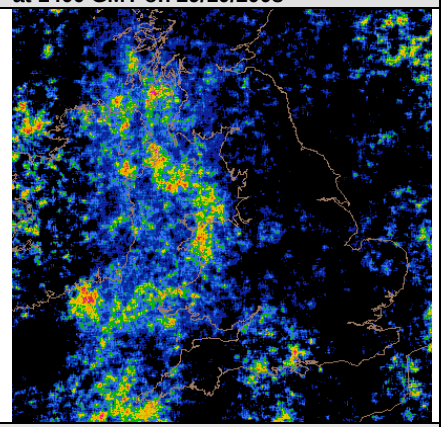
UKPP rain analysis valid at 1600 GMT on 29/10/2008	**T+10 h UKV control forecast valid at 1600 GMT on 29/10/2008**	**Member 1 of a T+3 h blend of an extrapolation nowcast, a UKV control forecast and non-parametric noise valid at 1600 GMT on 29/10/2008**	**Member 2 of a T+3 h blend of an extrapolation nowcast, a UKV control forecast and non-parametric noise valid at 1600 GMT on 29/10/2008**

© Crown copyright 2010

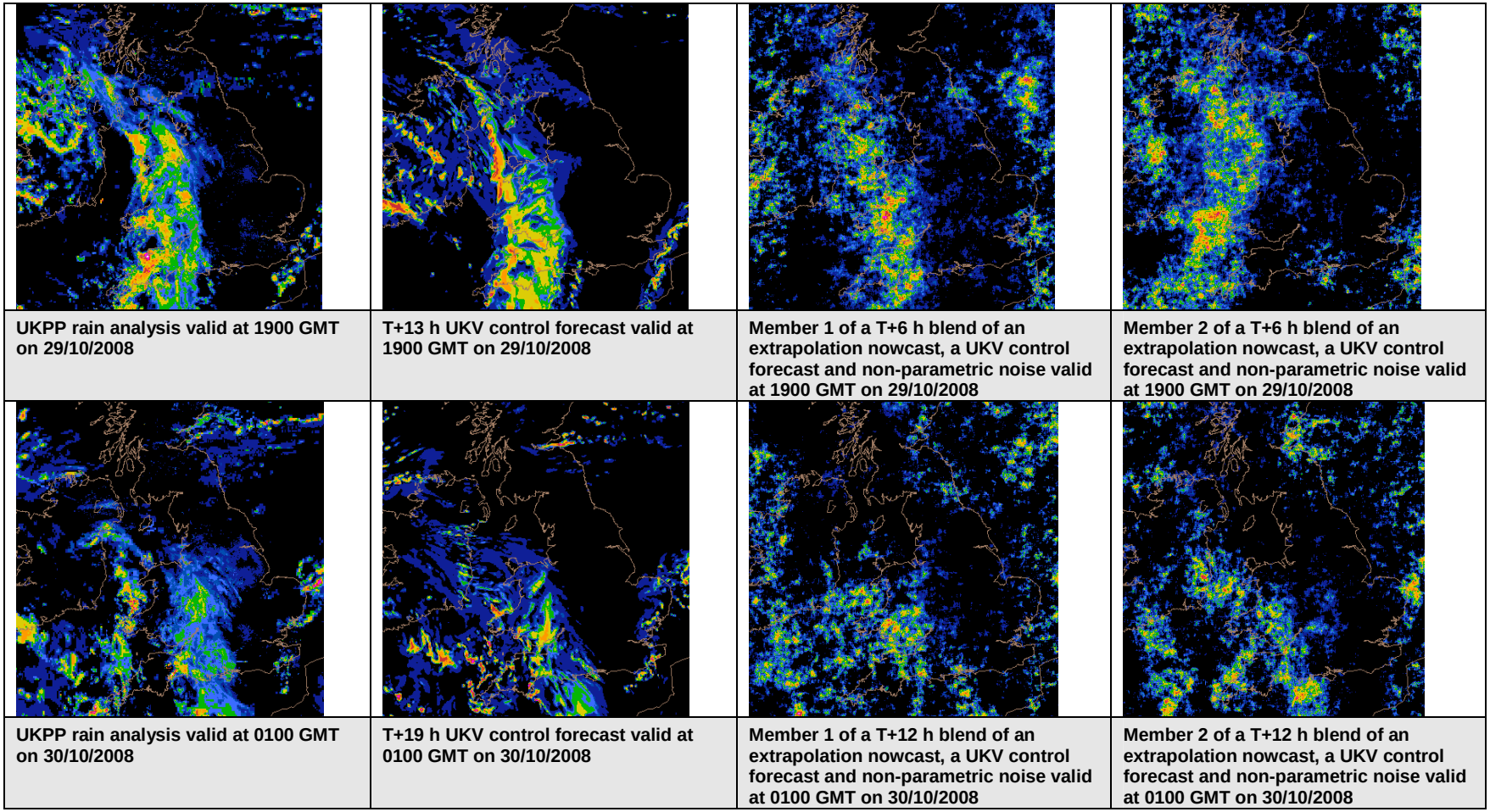

UKPP rain analysis valid at 1900 GMT on 29/10/2008	T+13 h UKV control forecast valid at 1900 GMT on 29/10/2008	Member 1 of a T+6 h blend of an extrapolation nowcast, a UKV control forecast and non-parametric noise valid at 1900 GMT on 29/10/2008	Member 2 of a T+6 h blend of an extrapolation nowcast, a UKV control forecast and non-parametric noise valid at 1900 GMT on 29/10/2008
UKPP rain analysis valid at 0100 GMT on 30/10/2008	T+19 h UKV control forecast valid at 0100 GMT on 30/10/2008	Member 1 of a T+12 h blend of an extrapolation nowcast, a UKV control forecast and non-parametric noise valid at 0100 GMT on 30/10/2008	Member 2 of a T+12 h blend of an extrapolation nowcast, a UKV control forecast and non-parametric noise valid at 0100 GMT on 30/10/2008

Figure 52a Selected steps in two members of a blended ensemble forecast of precipitation rate, comprising an extrapolation nowcast, UKV control forecast and non-parametric noise, run from 1300 GMT on 29/10/2008. The UKPP rain analysis used as the starting point for the extrapolation nowcast is also shown, as well corresponding forecast steps from the associated UKV control member forecast (data time 0600 GMT, 29/10/2008).

© Crown copyright 2010

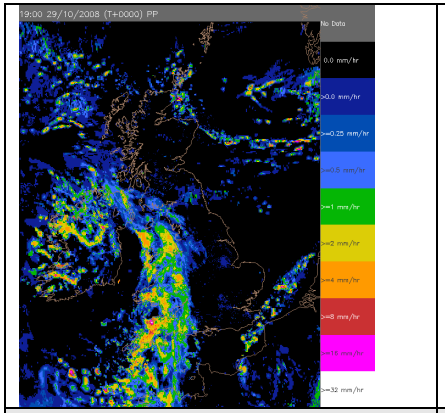	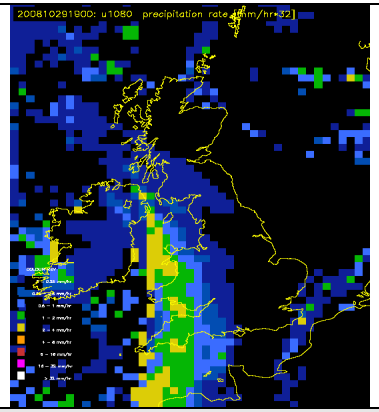	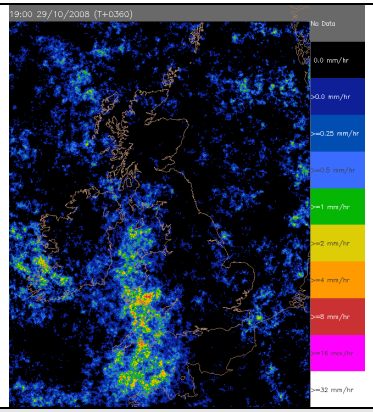	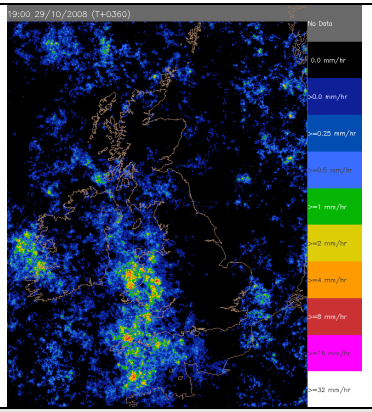
UKPP rain analysis valid at 1900 GMT on 29/10/2008	**MOGREPS-R T+13 h forecast valid at 1900 GMT on 29/10/2008**	**Member 1 of a T+13 h MOGREPS-R downscale ensemble forecast valid at 1900 GMT on 29/10/2008**	**Member 2 of a T+13 h MOGREPS-R downscale ensemble forecast valid at 1900 GMT on 29/10/2008**
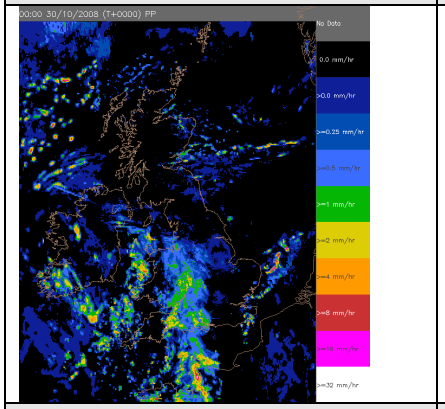	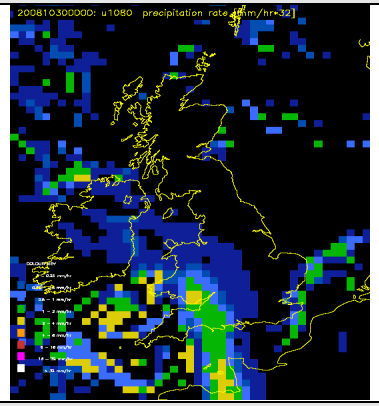	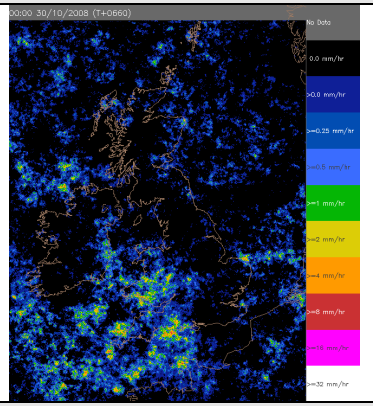	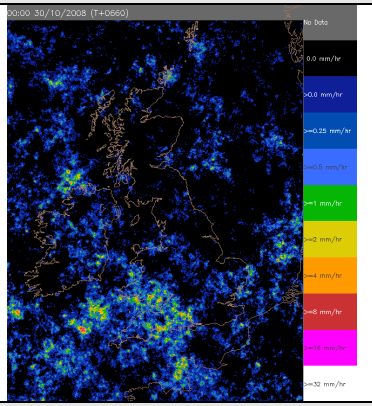
UKPP rain analysis valid at 0000 GMT on 30/10/2008	**MOGREPS-R T+18 h forecast valid at 0000 GMT on 30/10/2008**	**Member 1 of a T+18 h MOGREPS-R downscale ensemble forecast valid at 0000 GMT on 30/10/2008**	**Member 2 of a T+18 h MOGREPS-R downscale ensemble forecast valid at 0000 GMT on 30/10/2008**

Figure 52b Selected forecast steps in two members of a blended ensemble forecast of precipitation rate, comprising a MOGREPS-R control forecast and parametric noise, run from 1300 GMT on 29/10/2008 (3rd column from left). A corresponding sequence of UKPP rain analyses and forecasts steps from the associated MOGREPS-R control forecast (data time 0600 GMT, 29/10/2008) are also shown for comparison.

© Crown copyright 2010

precipitation is mainly very light (< 1/16 mm/h). Small errors in the power spectra of the noise fields can generate spurious areas of drizzle. This behaviour can result in quite significant biases in raining fraction in the blended forecast fields.

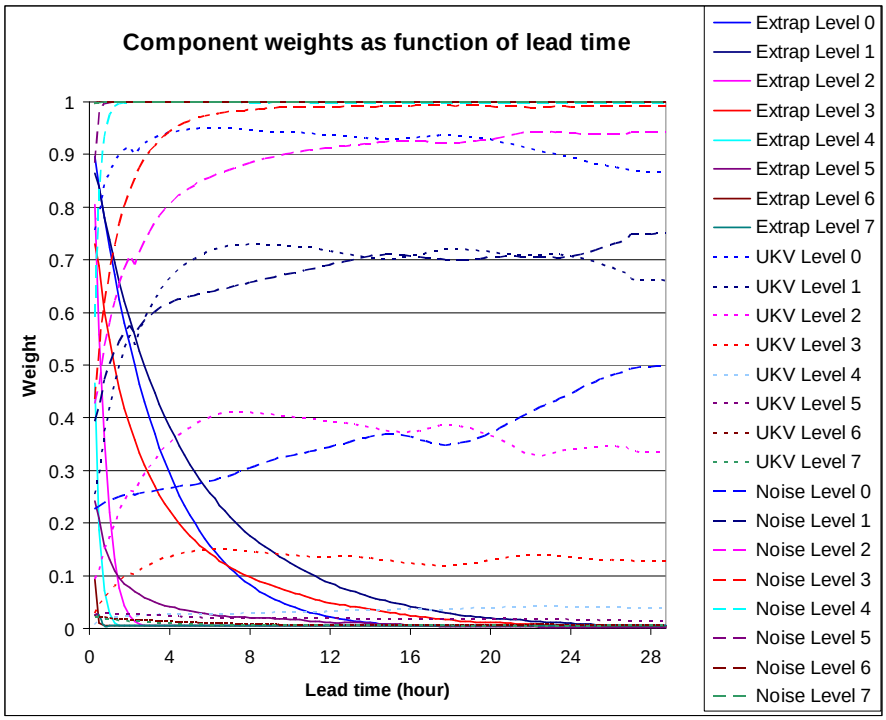

Figure 53 A plot of the weights assigned to the extrapolation and UKV forecast components and noise as a function of lead time in the blended ensemble forecast, excerpts of which are shown in Figure 52a.

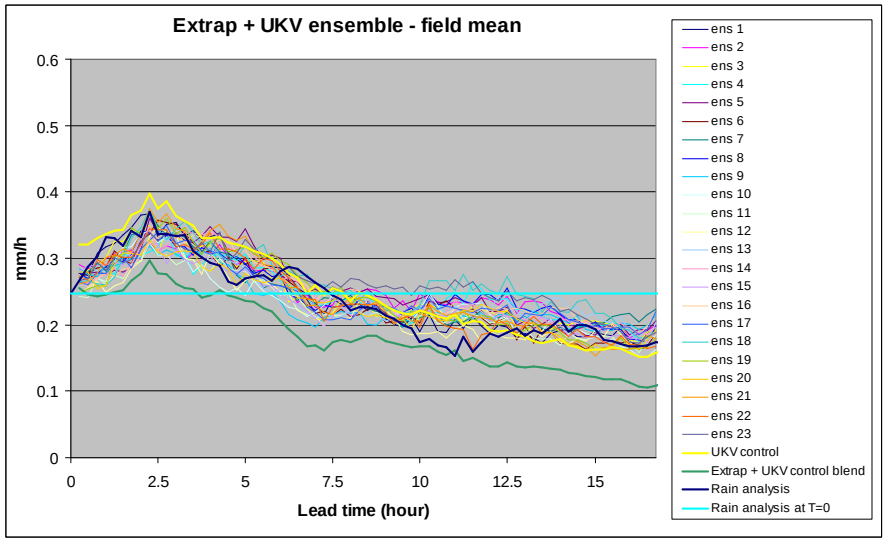

Figure 54 Time evolution of the field mean of UKPP rain analyses, a UKV control member forecast (data time 0600 GMT on 29/10/2008), and blended ensemble forecasts (data time 1300 GMT on 29/10/2008) comprising extrapolation, UKV and non-parametric noise. The forecast lead times on the X axis are those of the blended forecasts (run from 1300 GMT).

© Crown copyright 2010

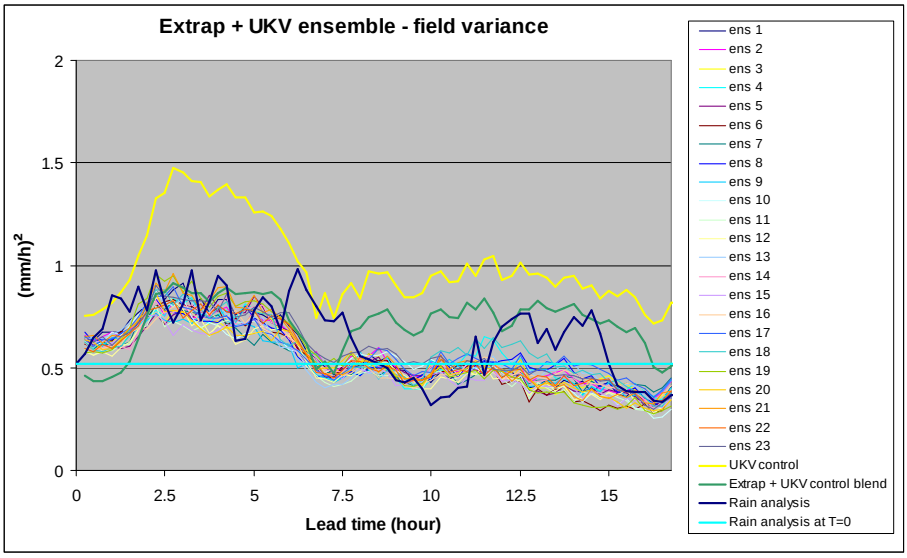

Figure 55 Time evolution of the field variance of UKPP rain analyses, a UKV control member forecast (data time 0600 GMT on 29/10/2008), and blended ensemble forecasts (data time 1300 GMT on 29/10/2008) comprising extrapolation, UKV and non-parametric noise. The forecast lead times on the X axis are those of the blended forecasts (run from 1300 GMT).

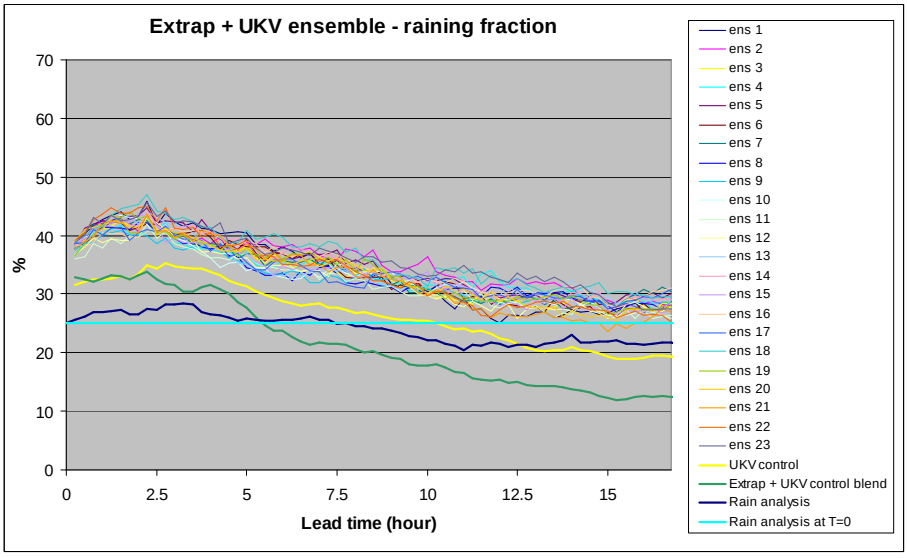

Figure 56 Time evolution of the field raining fraction of UKPP rain analyses, a UKV control member forecast (data time 0600 GMT on 29/10/2008), and blended ensemble forecasts (data time 1300 GMT on 29/10/2008) comprising extrapolation, UKV and non-parametric noise. The forecast lead times on the X axis are those of the blended forecasts (run from 1300 GMT).

© Crown copyright 2010

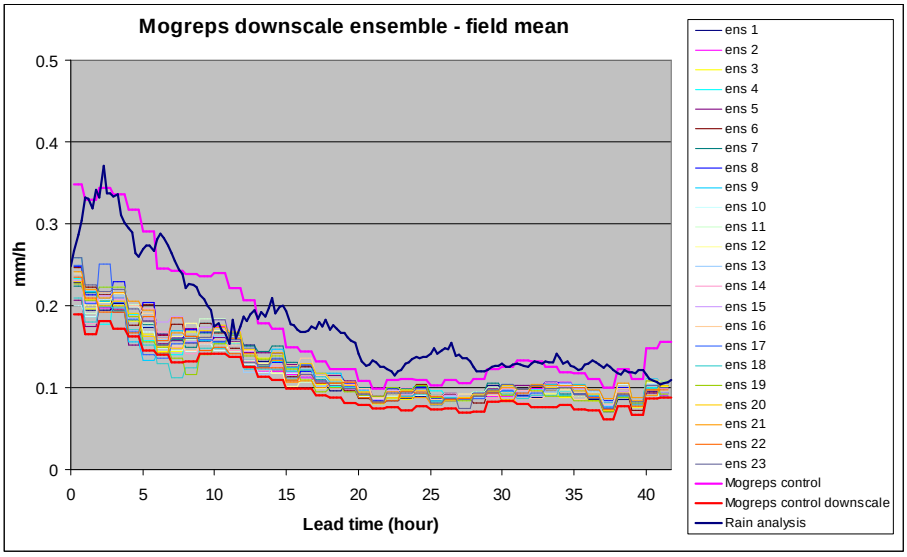

Figure 57 Time evolution of the field mean of UKPP rain analyses, a MOGREPS-R control member forecast (data time 0600 GMT on 29/10/2008), and control and ensemble blended forecasts (data time 1300 GMT on 29/10/2008) comprising MOGREPS-R and parametric noise. The forecast lead times on the X axis are those of the blended forecasts (run from 1300 GMT).

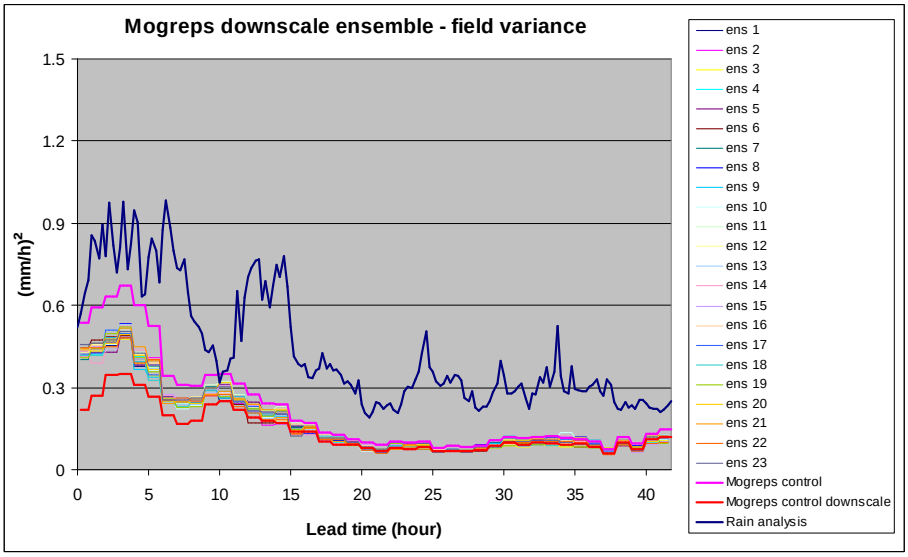

Figure 58 Time evolution of the field variance of UKPP rain analyses, a MOGREPS-R control member forecast (data time 0600 GMT on 29/10/2008), and control and ensemble blended forecasts (data time 1300 GMT on 29/10/2008) comprising MOGREPS-R and parametric noise. The forecast lead times on the X axis are those of the blended forecasts (run from 1300 GMT).

© Crown copyright 2010

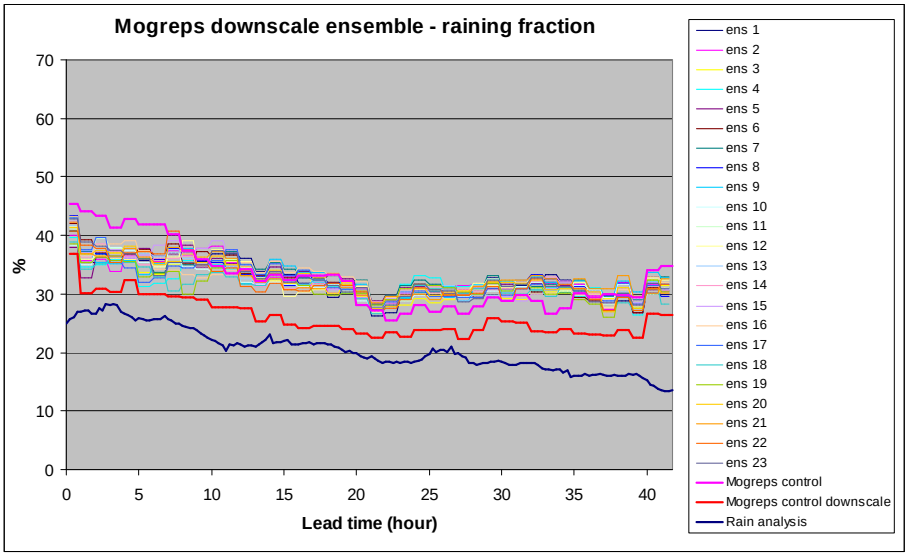

Figure 59 Time evolution of the field raining fraction of UKPP rain analyses, a MOGREPS-R control member forecast (data time 0600 GMT on 29/10/2008), and control and ensemble blended forecasts (data time 1300 GMT on 29/10/2008) comprising MOGREPS-R and parametric noise. The forecast lead times on the X axis are those of the blended forecasts (run from 1300 GMT).

5.4.5. Can the blending algorithms generate skilful blended control and ensemble forecasts?

Requirements

In this section the skill of the control member and ensemble blended forecasts is reviewed with the aid of the various verification statistics described in section 5.4.3. Two aspect of forecast skill are considered here.

Firstly, it must be demonstrated that the blended forecasts are at least as skilful as their components. Since the blending is performed on a hierarchy of scales, it is appropriate to evaluate the skill of the blends on the same hierarchy of scales. The Fractions Skill Score is employed here.

Secondly, it must be shown that the blended ensemble forecasts have the following attributes:

1) reliability – the forecast probabilities of events are similar to the observed frequencies of those same events);

2) resolution or sharpness – the forecast probabilities exhibit a range of values other than climatology;

3) an ability to predict the skill of the control member – they should exhibit an increase (decrease) in spread when the control member is less (more) skilful; this implies that the spread about the ensemble mean should increase (decrease) with increasing (decreasing) error in the ensemble mean.

© Crown copyright 2010

The focus of this verification is mostly on the performance of blended ensembles generated from a single (control) member of a UKV or MOGREPS-R ensemble forecast. In an operational environment, multiple blended ensemble members will be generated from a number of UKV or MOGREPS-R forecast realisations selected by clustering techniques.

Are the scale selective blended forecasts optimal over a range of scales

In a cascade of blended forecasts, noise is injected at each level to represent the fraction of the variance in the rain analysis not explained by the component forecasts models (extrapolation, UKV and MOGREPS-R) at that level (scale). If the skill of each of these models has been estimated successfully, and the noise has the appropriate space-time statistical properties, then the perturbations applied to each cascade level should not degrade the skill of the blended forecast at that level (scale). The Fractions Skill Score is a suitable tool for exploring forecast skill as a function of scale. A selection of FSS statistics representative of the typical performance of the blended forecasts are presented below.

Control member blended forecasts

Figures 60a and 60b compare the Fractions Skill Score of a UKV control member forecast (data time 0600 GMT on 29/10/2008) with that of a blended control member forecast (data time 0600 GMT on the same day) combining this UKV forecast with an extrapolation nowcast and non-parametric noise (bottom two cascade levels only). The statistics shown relate to the 75^{th} percentile of 60 minute accumulation. This threshold corresponds to an accumulation of about 0.5 mm/h. Performance is assessed on the hierarchy of scales represented by the cascade model and is measured relative to quality controlled 60 minute radar accumulations.

On average one would expect forecast skill to decline with decreasing scale and this is generally observed. There is a substantial increase in the performance of the UKV forecast at scales below 256 km prior to T+12 h (Figure 60a). This is due to the development of precipitation and its advection into the verification area during the forecast period. The decline in skill at the same scales beyond T+12 h is a result of increasing forecast error and decreasing precipitation amount.

The performance of the blended control member forecast in Figure 60b shows enhanced skill at short lead times. This is because the influence of the extrapolation nowcast is dominant in the first few hours. By T+6h, the handover to the UKV forecast is largely complete, and the FSS as function of scale is similar to that shown in Figure 60a. At longer range, the skill of the blended forecast is somewhat inferior to that of the UKV at all scales. This is due to the effects of the radar based non-parametric noise injected into the bottom two cascade levels and small biases introduced when collapsing the blended cascades.

© Crown copyright 2010

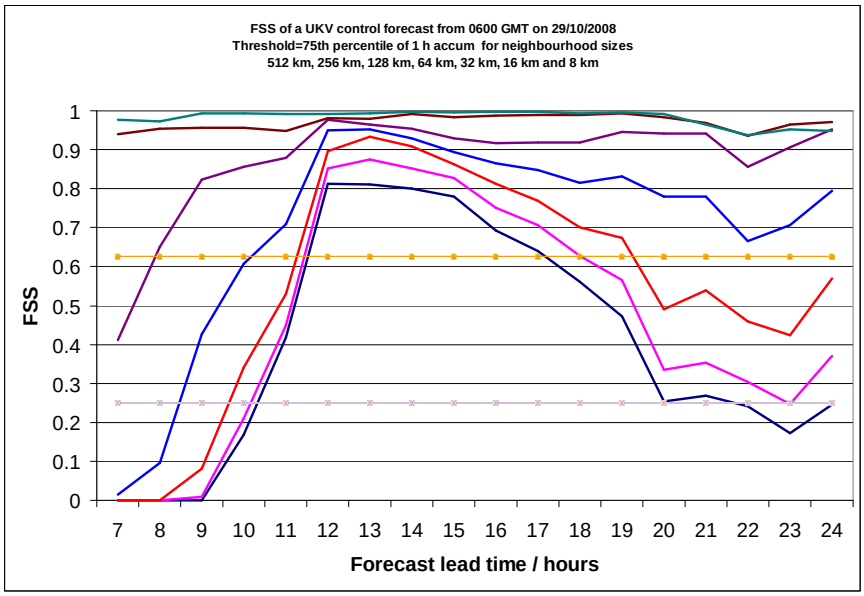

Figure 60a The Fractions Skill Score of a UKV control member forecast (data time 0600 GMT on 29/10/2008) for the 75th percentile of 1h accumulation, measured on the hierarchy of scales represented by the cascade model (512 km – green, 256 km – brown, 128 km – navy blue, 64 km – red, 32 km – purple, 16 km – pink, 8 km – dark blue) using quality controlled radar as the reference. The first time step shown (T+7 h) corresponds to the data time of the blended forecast for which FSS statistics are shown in 94b. The target skill level is the horizontal orange line; the skill of a random forecast is the horizontal pink line.

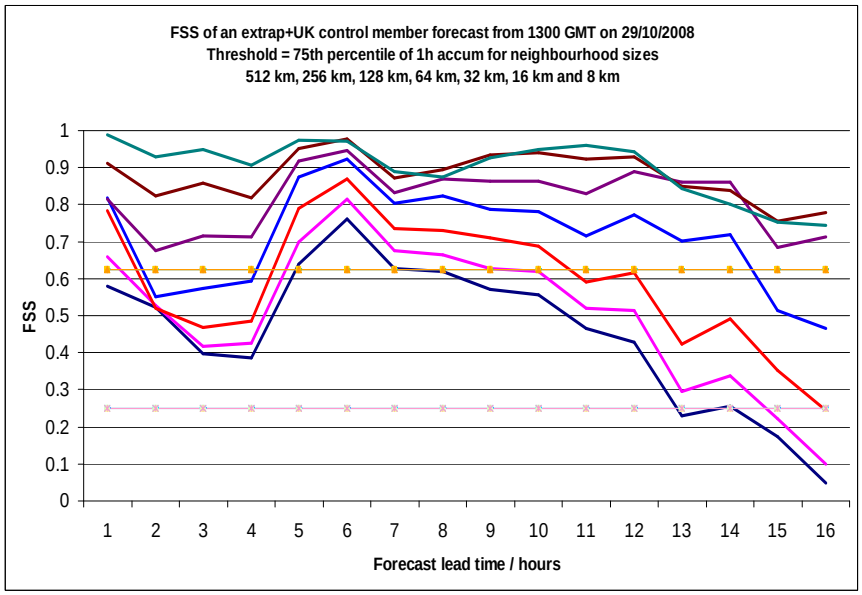

Figure 60b The FSS of a blended forecast combining an extrapolation nowcast from 1300 GMT on 29/10/2008 with a UKV control member forecast from 0600 GMT on 29/10/2008. Scores are presented for the hierarchy of scale represented by the

© Crown copyright 2010

cascade model. Forecast lead time is relative the start of the blend (1300 GMT).

Similar statistics have been compiled for MOGREPS-R control member forecasts and their downscaled counterparts. These are discussed in the following section.

Ensembles of blended forecasts

Figures 61b-d demonstrate the skill of an ensemble of blended forecasts comprising an extrapolation nowcast, UKV control member forecast and non-parametric noise. These should be compared with the relevant lines in Figure 60a. The FSSs of the ensemble of blended forecasts (including the blended control member) at the 512 km scale show little spread and are similar to the equivalent scores for the blended control forecast and UKV control forecast. At the 128 km and 32 km scales, the ensemble spread of the FSS increases and there a one or two outliers with much reduced at longer range. The median skill of the blended ensembles remains comparable with the UKV forecast at each scale.

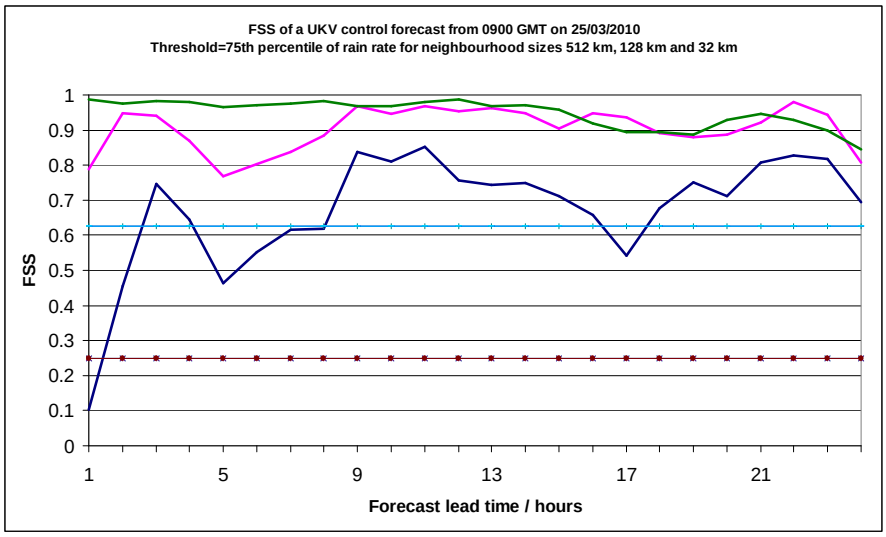

Figure 61a The Fractions Skill Score of a UKV control member forecast (data time 0900 GMT on 25/03/2010) for the 75th percentile of 1h accumulation, measured at the 512 km (green), 128 km (pink) and 32 km (dark blue) scales using quality controlled radar as the reference. The forecast lead time shown is relative to the data time of the model forecast. The target skill level is the horizontal light blue line; the skill of a random forecast is the horizontal brown line.

© Crown copyright 2010

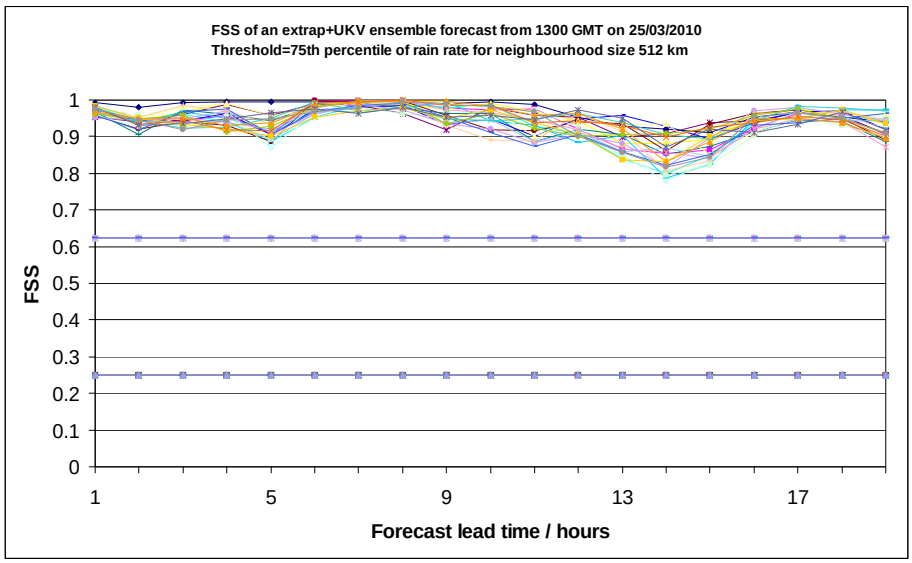

Figure 61b The FSSs of an ensemble of blended forecasts combining an extrapolation nowcast from 1300 GMT on 25/03/2010 with a UKV control member forecast from 0900 GMT on 25/03/2010 and non-parametric noise. Scores for the 75th percentile of 1 h accumulation and a 512 km scale are shown. Forecast lead time is relative the start of the blend (1300 GMT). Horizontal lines representing the target skill level and skill of a random forecast are shown for reference.

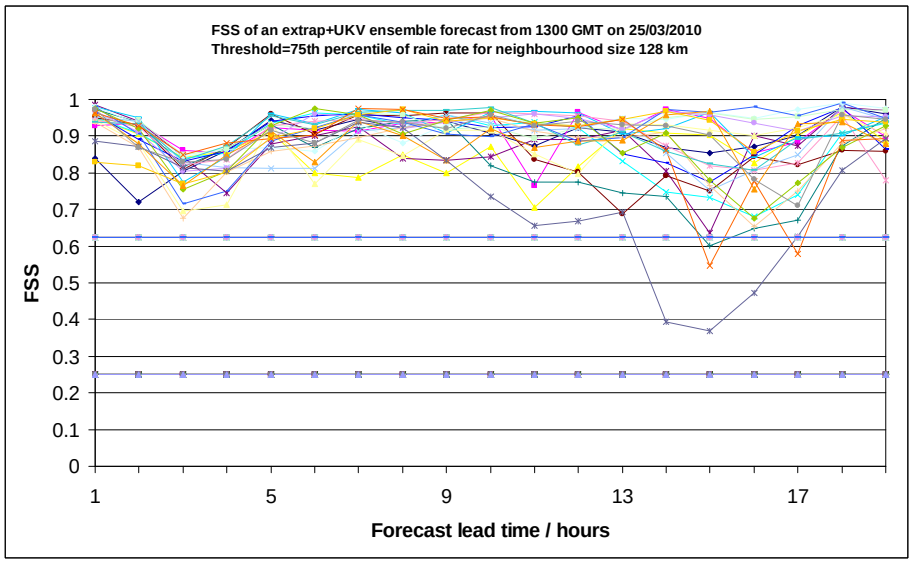

Figure 61c The FSSs of an ensemble of blended forecasts combining an extrapolation nowcast from 1300 GMT on 25/03/2010 with a UKV control member forecast from 0900 GMT on 25/03/2010 and non-parametric noise. Scores for the 75th percentile of 1 h accumulation and a 128 km scale are shown. Forecast lead time is relative the start of the blend (1300 GMT).

© Crown copyright 2010

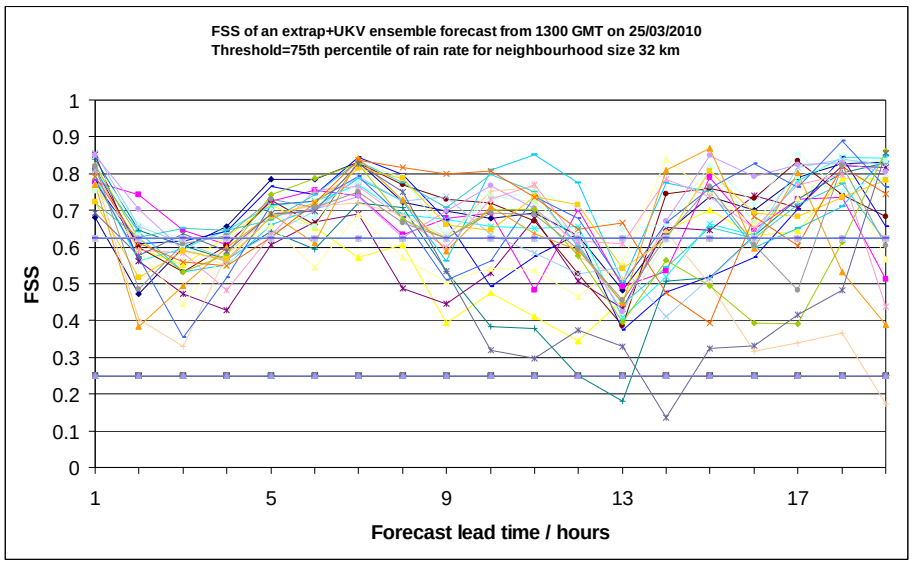

Figure 61d The FSSs of an ensemble of blended forecasts combining an extrapolation nowcast from 1300 GMT on 25/03/2010 with a UKV control member forecast from 0900 GMT on 25/03/2010 and non-parametric noise. Scores for the 75th percentile of 1 h accumulation and a 32 km scale are shown. Forecast lead time is relative the start of the blend (1300 GMT).

Figures 62a-d compare the skill a MOGREPS-R control member forecast with that of an equivalent downscale ensemble forecast including the control member. The FSS exhibits similar behaviour as a function of verification scale to that described in relation to Figures 61b-d. The downscale ensembles show comparable levels of skill to the MOGREPS-R forecast and their increased horizontal resolution (hence sample size) reduces some of the noisiness seen the scores in Figure 62a. The sharp decline in performance beyond T+14h in Figures 62c-d is due to a decrease in the extent of forecast precipitation within the verification area. Similar behaviour has been demonstrated at higher thresholds (e.g. the 95th percentile of 1 h accumulation) but statistics are not shown.

© Crown copyright 2010

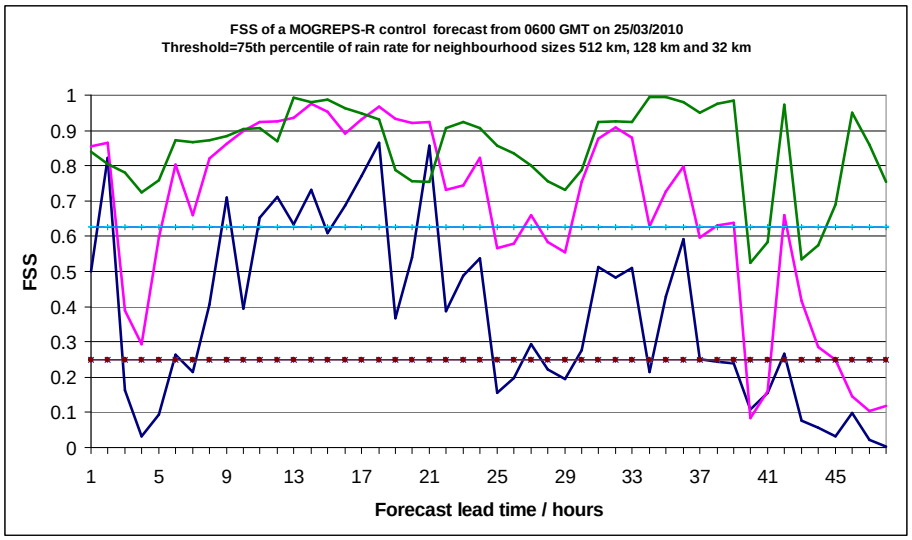

Figure 62a The Fractions Skill Score of a MOGREPS control member forecast (data time 0600 GMT on 25/03/2010) for the 75th percentile of 1h accumulation, measured at the 512 km (green), 128 km (pink) and 32 km (dark blue) scales using quality controlled radar as the reference. The target skill level is the horizontal light blue line; the skill of a random forecast is the horizontal brown line.

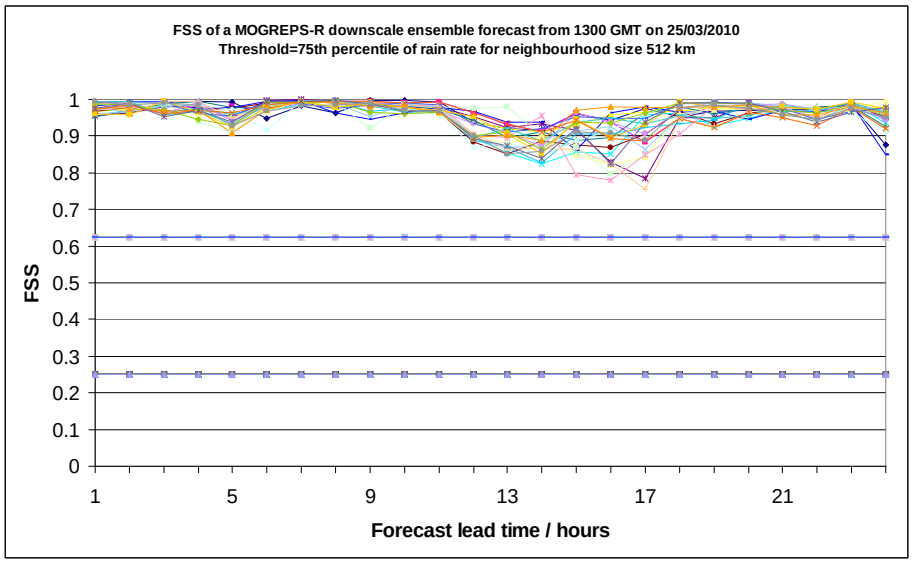

Figure 62b The FSSs of a MOGREPS-R downscale ensemble from 1300 GMT on 25/03/2010. Scores for the 75th percentile of 1 h accumulation and a 512 km scale are shown. Forecast lead time is relative the start of the blend (1300 GMT). Horizontal lines representing the target skill level and skill of a random forecast are shown for reference.

© Crown copyright 2010

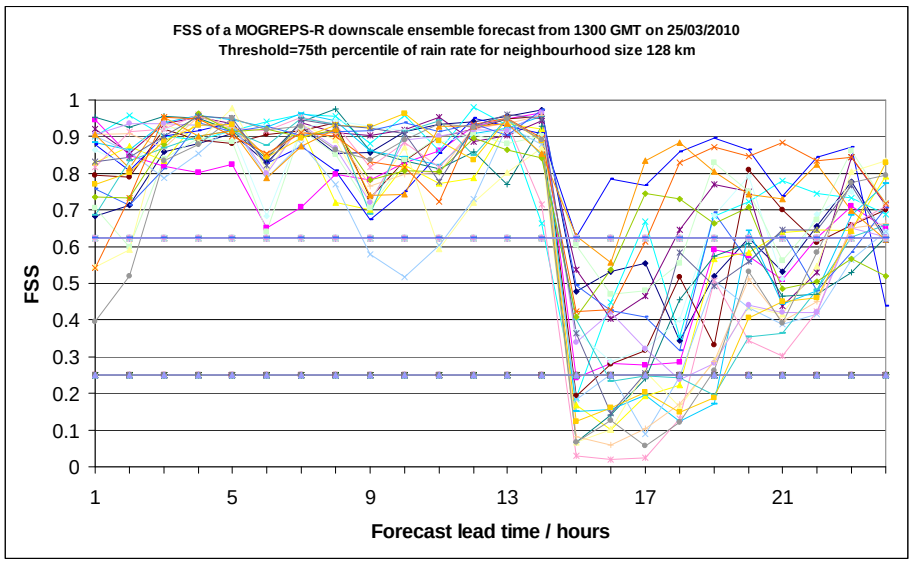

Figure 62c The FSSs of a MOGREPS-R downscale ensemble from 1300 GMT on 25/03/2010. Scores for the 75th percentile of 1 h accumulation and a 32 km scale are shown. Forecast lead time is relative the start of the blend (1300 GMT).

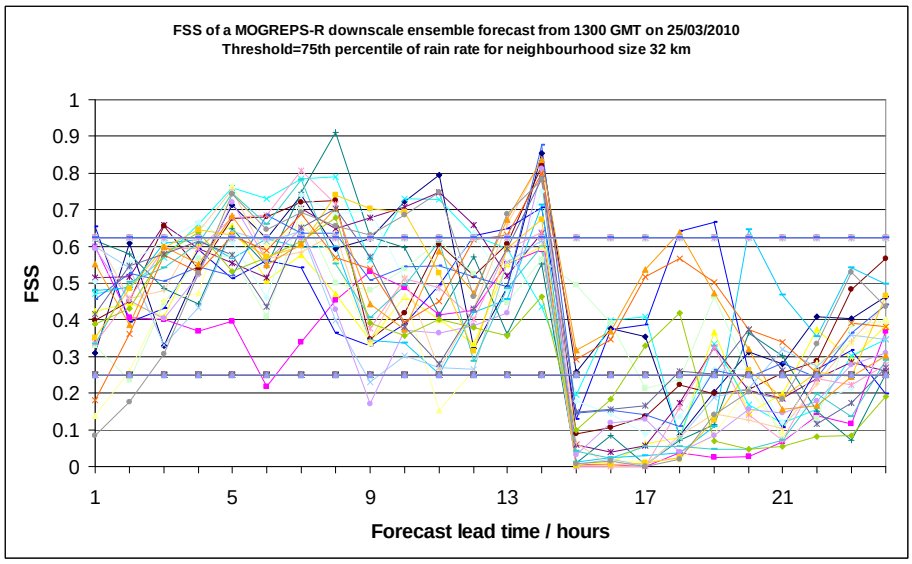

Figure 62d The FSSs of a MOGREPS-R downscale ensemble from 1300 GMT on 25/03/2010. Scores for the 75th percentile of 1 h accumulation and a 32 km scale are shown. Forecast lead time is relative the start of the blend (1300 GMT).

© Crown copyright 2010

Are the ensembles of blended forecasts well calibrated and do they demonstrate useful skill

Overview

The case study verification reviewed below compares the performances of the two configurations of blended ensembles generated from UKV and MOGREPS-R control member forecasts with those of associated UKV and MOGREPS-R ensembles supplied by the *Convective-scale Ensembles Project*.

Normally, ensemble verification scores would be compiled over a large number of events to provide an indication of performance averaged of a range of meteorological conditions. However, given the limited number of case studies available, this investigation is confined to comparing case study average performance of the blended ensembles relative to their associated NWP model ensembles. This is a stringent comparison since the blended ensembles are perturbed realisations of a single (control) member NWP model forecast.

The focus of the statistics presented is on forecast performance beyond T+6h. Ensemble verification for very short range blended forecasts (< 6 h ahead) has been found to be slightly inferior to that of STEPS. This is attributed to the fact that the perturbations applied to the extrapolation velocities in STEPS are disabled in the extrapolation based blending algorithm. This is by design. In an operational environment, the velocity perturbations will come from blending the extrapolation nowcast with selected members of a UKV ensemble of precipitation forecasts.

Reliability (Attributes) plots

Figure 63a shows a reliability plot for a threshold of 0.25 mm/h for an ensemble blending an extrapolation nowcast and UKV control forecast. These statistics have been compiled using data for the two case studies for which UKV ensembles were available – 05/09/2008 and 29/10/2008. Figure 63b shows a comparable reliability plot derived from these UKV ensemble forecasts (data times 0600 GMT on 05/09/2008 and 29/10/2008). The forecast lead times in both diagrams are relative to the data time of the UKV ensemble forecast.

In Figure 63a the plotted curves tend to follow the diagonal, perfect reliability line quite closely, implying that the blended forecast ensembles are reasonably well calibrated for precipitation rates in excess of 0.25 mm/h. However, Figure 63b suggests that the UKV ensembles may be over spread since the reliability curves are consistently above the perfect reliability line, except at high probabilities.

The inset histograms in both figures demonstrate the frequency of use of each probability category (i.e. the forecast sample size in each category). These show a tendency for most samples to fall into the lower probability bins.

© Crown copyright 2010

Reliability diagrams for higher thresholds (not shown) are noisier due to reduced sample sizes. They also exhibit inferior calibration. This is related to the inappropriate use of spatially homogeneous noise in cases involving co-existing frontal and showery precipitation. The performance of the extrapolation and UKV based ensembles described here is fairly typical of their performance overall, although enhanced levels of performance have been found in cases involving a uniform precipitation regime (e.g. 25/03/2010).

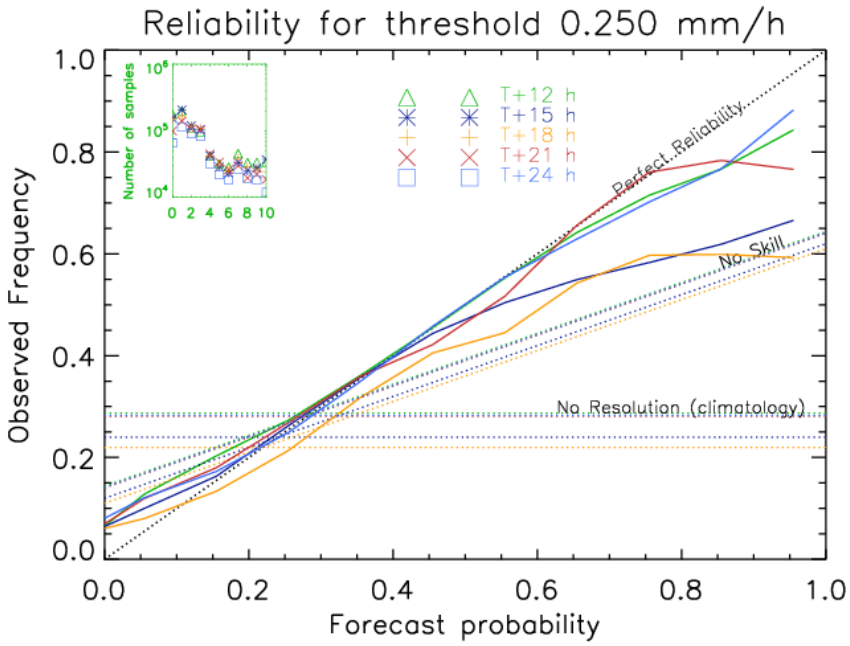

Figure 63a Reliability (attributes) diagram for 23 member ensembles blending an extrapolation nowcast and UKV control member precipitation forecast. The reliability curves show the relationship between forecast probability and radar observed frequency as a function of forecast lead time for precipitation rates > 0.25 mm/h. Statistics were compiled using data from 05/09/2008 and 29/10/2008.

© Crown copyright 2010

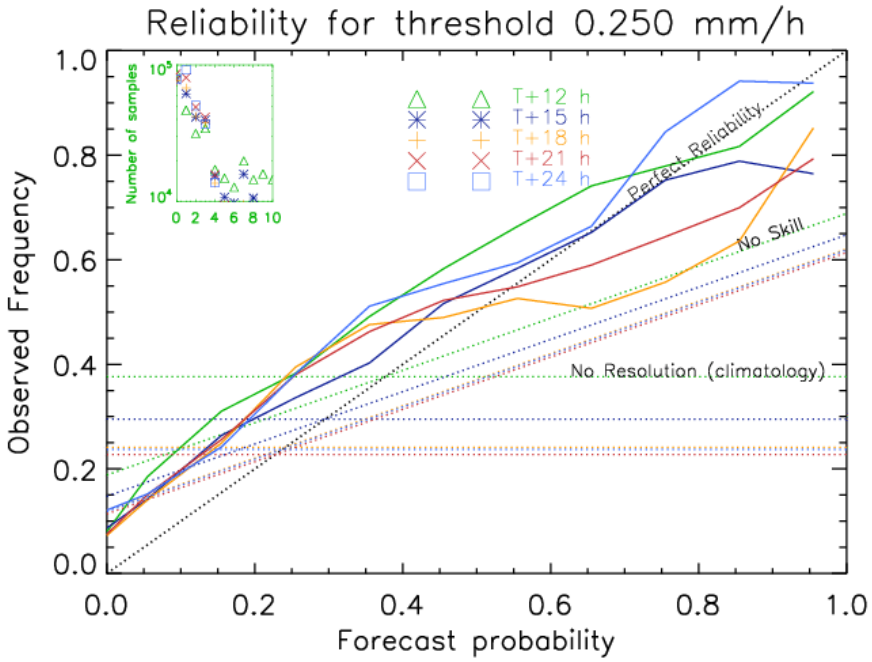

Figure 63b Reliability (attributes) diagram for 23 member UKV ensemble precipitation forecasts. The reliability curves show the relationship between forecast probability and radar observed frequency as a function of forecast lead time for precipitation rates > 0.25 mm/h. Statistics were compiled using data from 05/09/2008 and 29/10/2008.

Figure 64a shows a reliability diagram for a threshold of 0.25 mm/h compiled from MOGREPS-R downscale ensemble forecasts for 0600 GMT on 05/09/2008 and 29/10/2008. A comparable reliability diagram for the raw MOGREPS-R ensemble runs from the same cases is shown in Figure 64b.

In both figures the plotted lines tend to follow the diagonal, perfect reliability line quite closely at low probabilities but then tend to fall below the line at higher probabilities. Both ensembles are over confident since the forecast probabilities tend to be too small at low observed frequencies and too large a higher observed frequencies.

Reliability diagrams for higher thresholds (not shown) exhibit poor resolution and increased under sampling. This reflects the negative bias in the representation of higher precipitation rates. The performance of the MOGREPS-R downscale ensembles as a whole has been shown to be quite variable, depending on the accuracy of the modelled MOGREPS-R power spectrum employed by the parametric noise generator and on the nature of the precipitation. Reliability statistics compiled for case studies 3 and 5 (19/11/2009 and 25/03/2010) are superior at higher precipitation thresholds.

© Crown copyright 2010

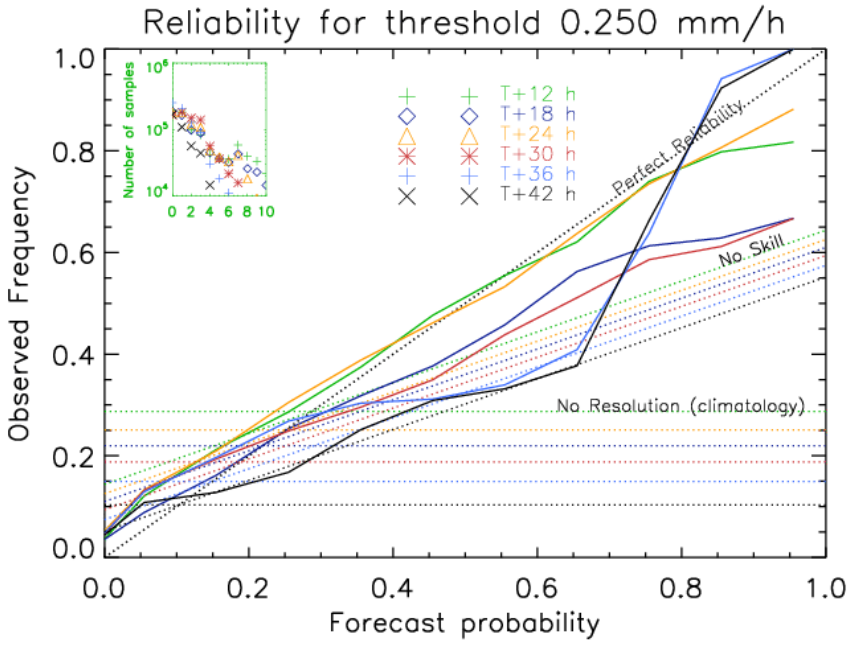

Figure 64a Reliability (attributes) diagram for 23 member MOGREPS-R downscale ensemble precipitation forecasts. The reliability curves show the relationship between forecast probability and radar observed frequency as a function of forecast lead time for precipitation rates > 0.25 mm/h. Statistics were compiled using data from 05/09/2008 and 29/10/2008.

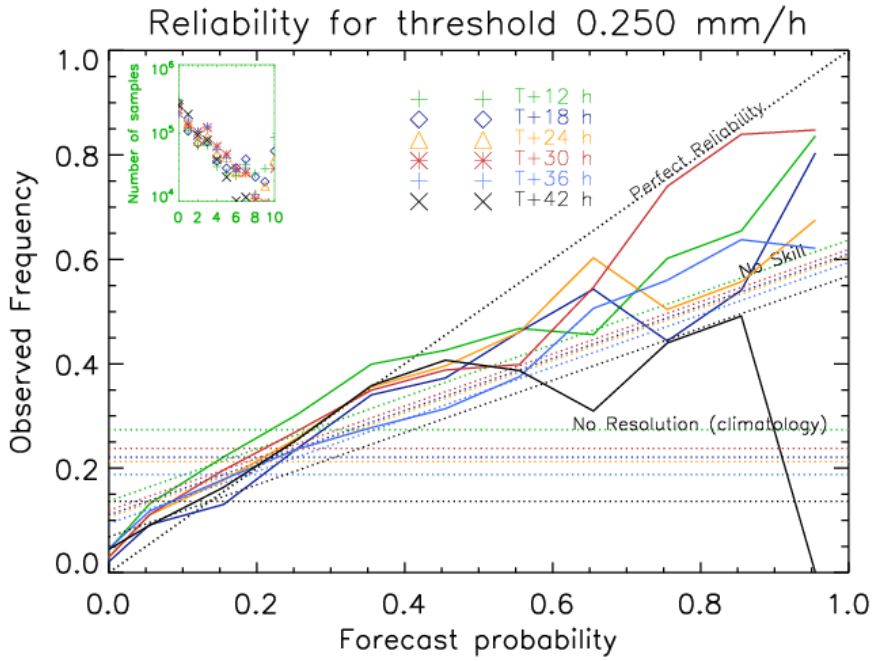

Figure 64b Reliability (attributes) diagram for 23 member MOGREPS-R ensemble precipitation forecasts. The reliability curves show the relationship between forecast probability and radar observed frequency as a function of forecast lead time for precipitation rates > 0.25 mm/h. Statistics were compiled using data from 05/09/2008 and 29/10/2008.

© Crown copyright 2010

Brier Skill Score, resolution and reliability scores

Figures 65a-c show the BSS, resolution score and reliability score for an ensemble forecast blending an extrapolation nowcast and UKV control forecast. Statistics have been compiled using case study data from 05/09/2008 and 29/10/2008. Figures 65d-f are comparable plots from a UKV ensemble forecast generated using data sets for the same case studies. The forecast lead times in all figures are relative to the data time of the UKV ensemble forecast.

Both the blended and UKV ensembles exhibit skill over and above climatology (represented by a BSS = 0.0) for precipitation thresholds < 2 mm/h (Figures 65a and 65d). Performances above this threshold are no better than climatology. Figures 65b and 65e show that resolution dominates the BSS indicating that both ensembles can be considered to be reliable in general terms.

These results are encouraging. For these two case studies at least, they demonstrate that the performance of ensembles of blended forecasts generated from the UKV control forecast are comparable with those of the full UKV ensemble forecast.

The reliability score is a penalty function for departure from perfect reliability. Thus, low values of the score are desirable for a well calibrated ensemble. One would expect the reliability score to increase and become noisier at higher precipitation rate thresholds because reliable forecasts of intense precipitation are generally more difficult to achieve and the samples sizes involved will be smaller. Figures 65c and 65f largely confirm these expectations.

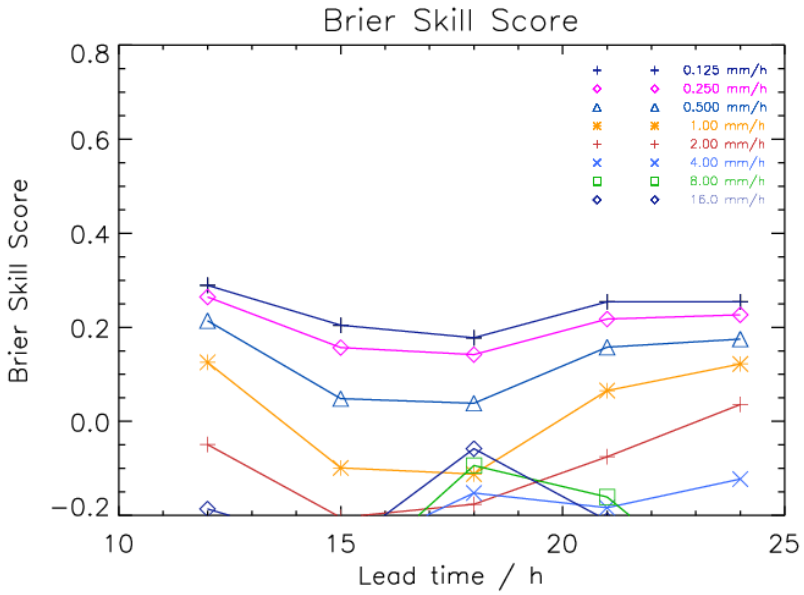

Figure 65a Brier Skill Score as a function of precipitation rate threshold for a 23 member ensemble blending an extrapolation nowcast and UKV control member precipitation. Quality controlled radar estimates of precipitation rate are used as the reference. Statistics are based upon data from 05/09/2008 and 29/10/2008.

© Crown copyright 2010

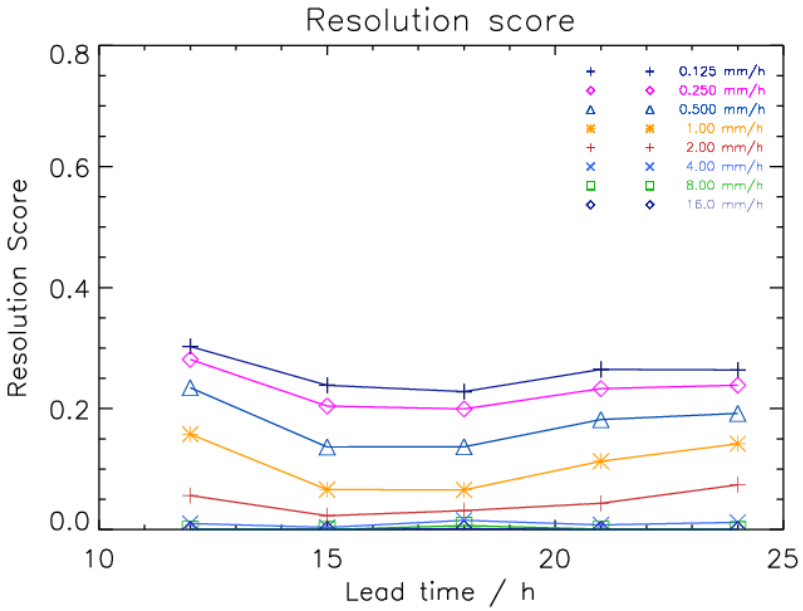

Figure 65b Resolution Score as a function of precipitation rate threshold for a 23 member ensemble blending an extrapolation nowcast and UKV control member precipitation forecast. Quality controlled radar estimates of precipitation rate are used as the reference. Statistics are based upon data from 05/09/2008 and 29/10/2008.

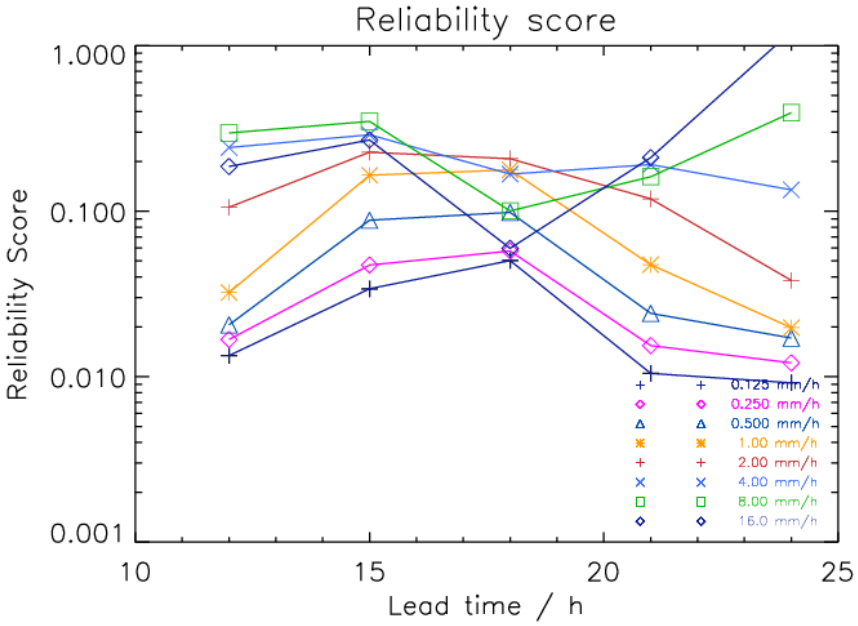

Figure 65c Reliability Score as a function of precipitation rate threshold for a 23 member ensemble blending an extrapolation nowcast and UKV control member precipitation forecast. Quality controlled radar estimates of precipitation rate are used as the reference. Statistics are based upon data from 05/09/2008 and 29/10/2008.

© Crown copyright 2010

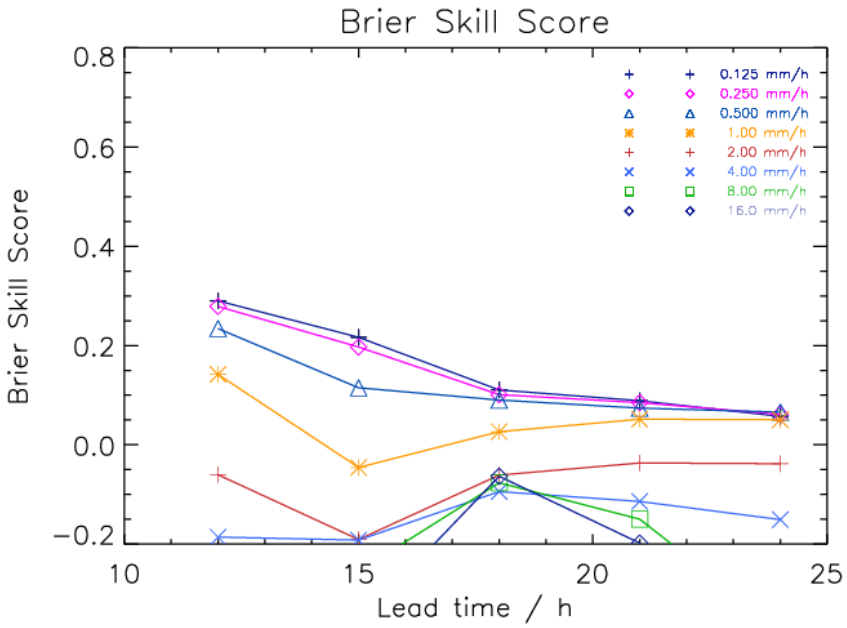

Figure 65d Brier Skill Score as a function of precipitation rate threshold for a 23 member UKV ensemble forecast. Quality controlled radar estimates of precipitation rate are used as the reference. Statistics are based upon data from 05/09/2008 and 29/10/2008.

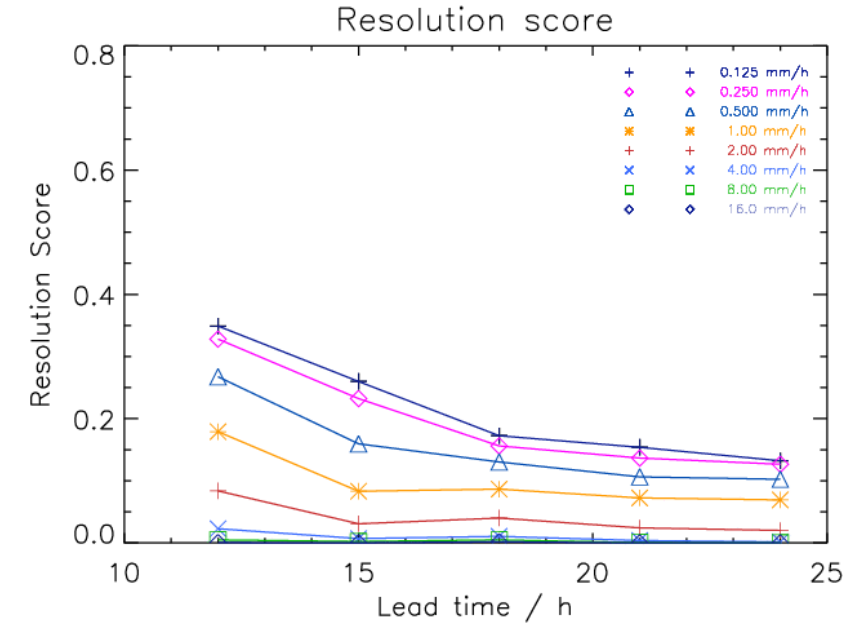

Figure 65e Resolution Score as a function of precipitation rate threshold for a 23 member UKV ensemble forecast. Quality controlled radar estimates of precipitation rate are used as the reference. Statistics are based upon data from 05/09/2008 and 29/10/2008.

© Crown copyright 2010

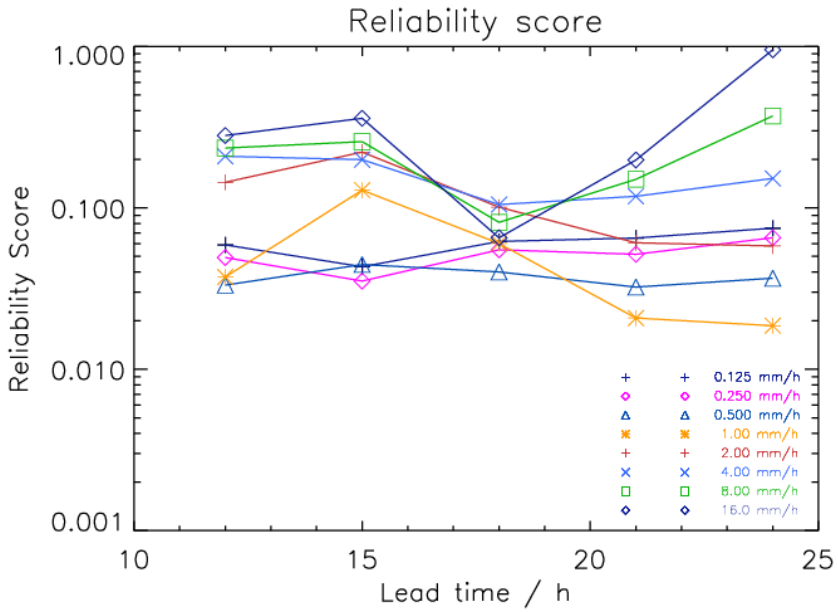

Figure 65f Reliability Score as a function of precipitation rate threshold for a 23 member UKV ensemble forecast. Quality controlled radar estimates of precipitation rate are used as the reference. Statistics are based upon data from 05/09/2008 and 29/10/2008.

Equivalent BSS statistics for 1 h precipitation accumulation, compiled using Met Office and EA hourly rain gauge reports, are shown in Figures 66a and 66b. Though noisier due to the smaller sample sizes, the results are comparable with those for rain rate shown in Figures 65a and 65d.

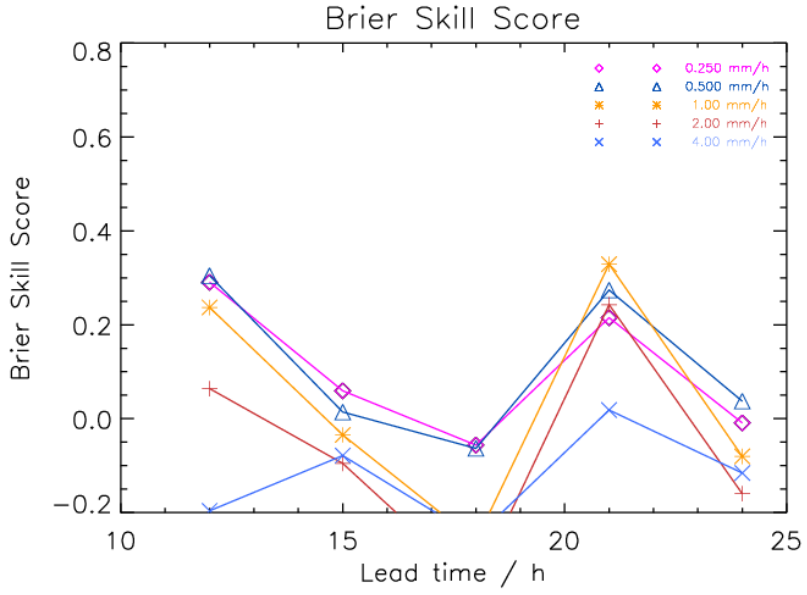

Figure 66a Brier Skill Score as a function of precipitation accumulation threshold for a 23 member ensemble blending an extrapolation nowcast and UKV control member precipitation forecast. Met Office and EA rain gauges are used as the reference. Statistics are based upon data from 05/09/2008 and 29/10/2008.

© Crown copyright 2010

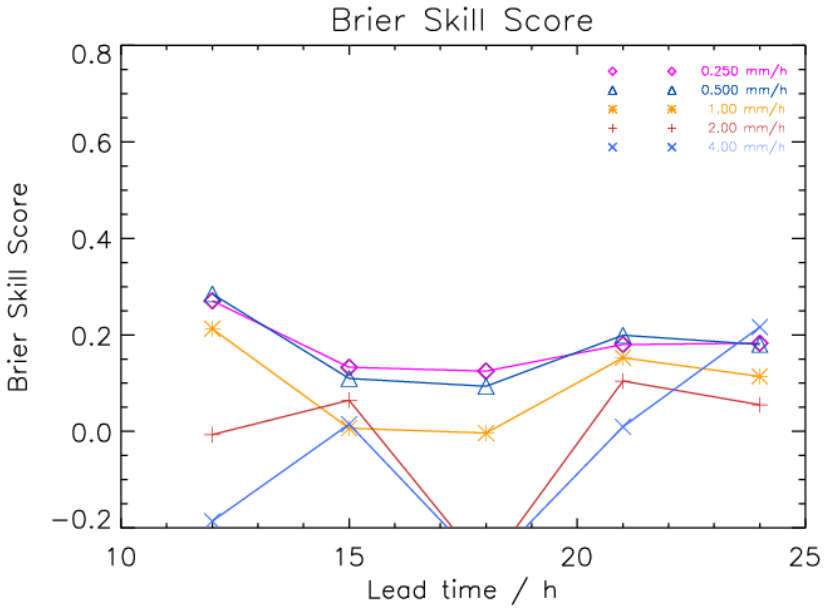

Figure 99b Brier Skill Score as a function of precipitation accumulation threshold for a 23 member UKV ensemble forecast. Met Office and EA rain gauges are used as the reference. Statistics are based upon data from 05/09/2008 and 29/10/2008.

Plots of BSS, resolution and reliability scores for the MOGREPS-R ensemble precipitation forecast and associated downscale ensemble for the same event (29/10/2008) are not reproduced here. The skill of the former is comparable with the UKV ensemble precipitation forecast at thresholds < 2 mm/h. The performance of the downscale ensemble was found to be inferior and this was attributed to two factors: errors in the modelled power spectra of the MOGREPS-R precipitation forecasts and the use of spatially homogenous noise to represent both frontal precipitation and showers.

ROC plots

The plots of Relative Operating Characteristic shown in Figure 67a demonstrate the relationship between the *Hit Rate* and the *False Alarm Rate* for a range of confidence levels for an ensemble of blended forecasts comprising an extrapolation nowcast and UKV control forecast. The statistics are based upon case study data for 05/09/2008 and 29/10/2008. Each ROC curve represents ensemble performance at a different threshold precipitation rate. The coloured symbols denote the skill of the blended control member (deterministic) forecast. Similar ROC plots for the corresponding UKV ensemble forecast are displayed in Figure 67b.

The area between each ROC curve and the dashed, diagonal no-skill line is a measure of forecast skill at the associated threshold precipitation rate. In the case of the blended ensembles it is apparent that skill decreases more rapidly with increasing threshold than would be expected. For a skilful ensemble not subject to threshold dependent errors, the ROC curves for the various thresholds should lie on a single line. This is not the case in Figure 67a.

© Crown copyright 2010

These rate dependent errors imply problems in representing the distribution of precipitation rates ≥ 2.0 mm/h. A similar performance issue was described earlier. It probably originates from the use of a single, spatially homogenous noise distribution to perturb both frontal and showery precipitation areas in the extrapolation and UKV control forecasts. This type of behaviour is not seen in cases involving precipitation fields with more uniform distributions (see Figure 68). Thus, if performance issues relating to the use spatially homogeneous noise can be resolved, there is the prospect of delivering blended ensemble forecasts with useful levels of skill at all thresholds in cases involving co-existing frontal and showery precipitation.

It is notable that the ROC curves for the UKV ensemble forecast (Figure 67b) appear to suffer from similar rate dependent errors. This suggests that the rate dependent deterioration in performance described above may originate, at least in part, from performance characteristics of the UKV model. Nonetheless, the skill of the UKV ensemble forecast at a given threshold is superior to the blended ensemble forecast, as expected.

Figures 69a and 69b are ROC plots for the same blended and UKV ensemble precipitation forecasts but these relate to the performance of hourly accumulation forecasts, assessed using Met Office and Environment Agency rain gauges. The curves are not smooth, indicating that the sample sizes are small. However, the results are encouraging since they appear consistent with those in Figures 67a-b, hence do not challenge the overall conclusion that both ensemble forecasts are skilful.

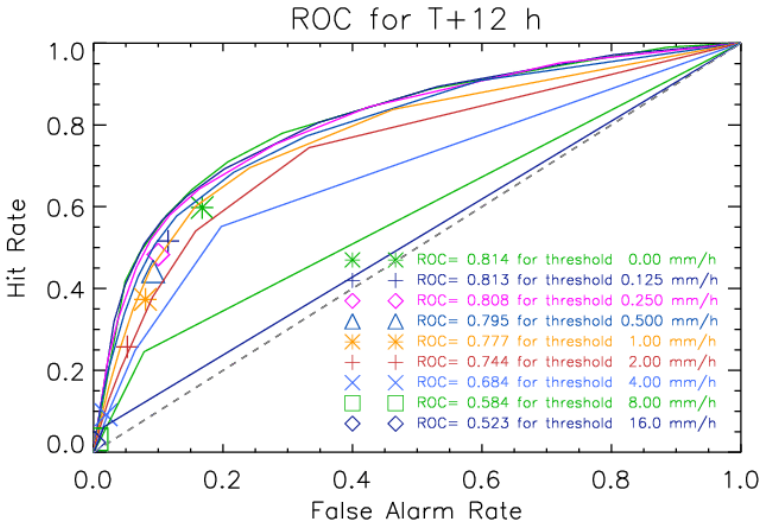

Figure 67a Relative Operating Characteristic as a function of precipitation rate threshold for a T+12 h 23 member ensemble blending an extrapolation nowcast and UKV control member precipitation forecast. The symbols indicate the performance of the control member. Quality controlled radar estimates of precipitation rate are used as the reference. Statistics are based upon data from 05/09/2008 and 29/10/2008.

© Crown copyright 2010

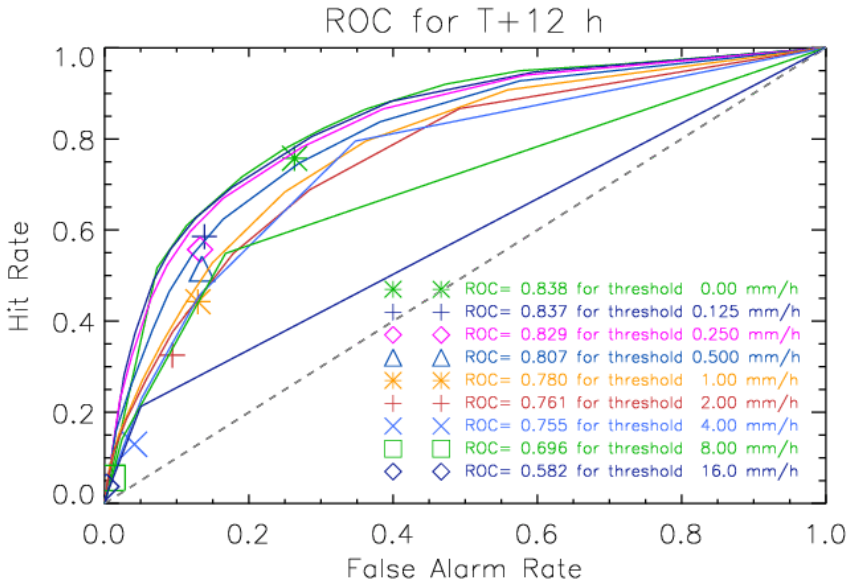

Figure 67b Relative Operating Characteristic as a function of precipitation rate threshold for a 23 member UKV ensemble forecast. The symbols indicate the performance of the control member. Quality controlled radar estimates of precipitation rate are used as the reference. Statistics are based upon data from 05/09/2008 and 29/10/2008.

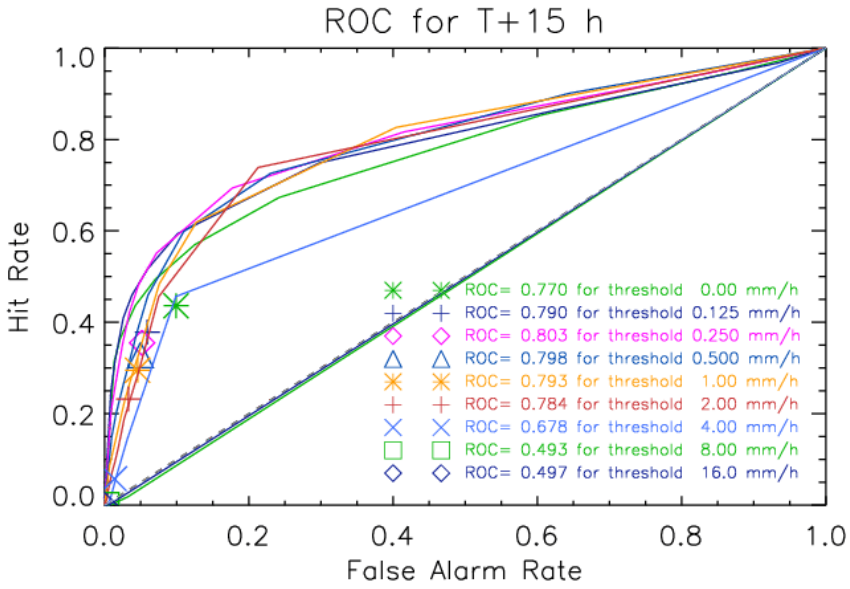

Figure 68 Relative Operating Characteristic as a function of precipitation rate threshold for a T+15 h 23 member ensemble blending an extrapolation nowcast and UKV control member precipitation forecast from 1300 GMT on 25/03/2010. The symbols indicate the performance of the control member. Quality controlled radar estimates of precipitation rate are used as the reference.

© Crown copyright 2010

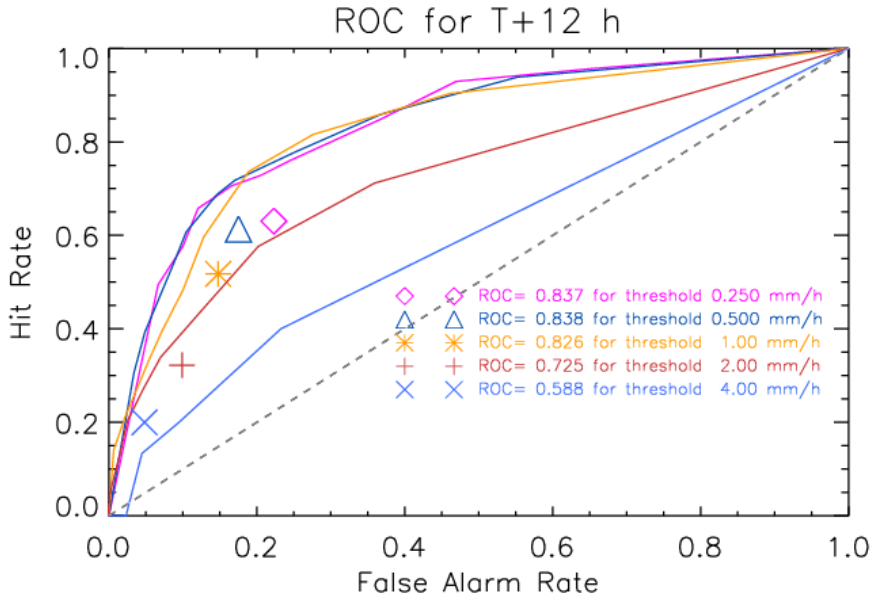

Figure 69a Relative Operating Characteristic as a function of precipitation accumulation threshold for a T+12 h 23 member ensemble blending an extrapolation nowcast and UKV control member precipitation forecast. The symbols indicate the performance of the control member. Met Office and EA rain gauges are used as the reference. Statistics are based upon data from 05/09/2008 and 29/10/2008.

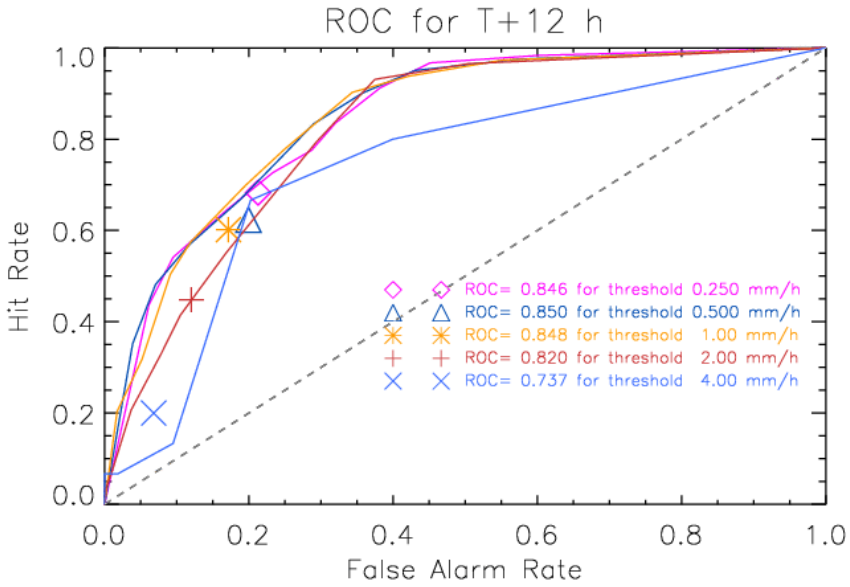

Figure 69b Relative Operating Characteristic as a function of precipitation rate threshold for a 23 member UKV ensemble forecast. The symbols indicate the performance of the control member. Met Office and EA rain gauges are used as the reference. Statistics are based upon data from 05/09/2008 and 29/10/2008.

© Crown copyright 2010

ROC plots for the MOGREPS-R ensemble precipitation forecast and associated downscale ensemble for the same events are not reproduced here. The skill of the former is comparable with the UKV ensemble precipitation forecast at thresholds < 2 mm/h. The performance of the downscale ensemble was found to be inferior and this was attributed to errors in the modelled power spectra of the MOGREPS-R precipitation forecasts and the use of spatially homogenous noise to represent both frontal precipitation and showers.

Spread-skill

The spread-skill verification discussed in this section focuses on a comparison of average ensemble spread and skill as a function of forecast lead time for several case studies.

Figures 70a-b are plots of the spread-skill relationship for a 23 member ensemble of blended forecasts of precipitation rate and 1 hour accumulation, incorporating an extrapolation nowcast and UKV control member forecast and run from 1300 GMT on 29/10/2008. Figure 70a presents statistics for precipitation rate derived using quality controlled radar data as the reference; Figure 70b displays similar statistics for 1 hour accumulation derived using Met Office and Environment Agency rain gauge reports.

Each plot contains six lines: two relate to the RMS error of the ensemble mean (brown line) and blended control member forecast (blue line); two relate to the spread about the ensemble mean (red) and about the blended control (purple); the remaining two describe the bias in the ensemble mean (green) and the bias in the blended control (yellow), both measured relative to the reference observation.

For a skilful ensemble forecast, the spread about the ensemble mean should be less than the spread about the control. Similarly, the error in the ensemble mean (in this case measured relative to radar) should be less than the error in the control. In these respects, one can conclude that the ensemble of blended forecasts evaluated in Figure 70a is skilful.

For the ensemble to be capable of predicting the skill of the control member, the spread about the ensemble mean should equal the error in the ensemble mean (after accounting for observation error). This is not the case early on the forecast sequence in Figure 70a when the ensemble spread is larger than the error. However, beyond T+7h the spread-skill relationship is reasonably close. Note though that no allowance is made for observation error in this comparison. Allowing for this error should tend to reduce the estimated forecast error thereby increasing the observed disparity between spread and skill in the first 6 hours.

Although the statistics shown in Figure 70b are based upon a relative modest sample size due to the limited number of gauge observations, it is encouraging that they also show a reasonable correspondence between ensemble spread and error.

© Crown copyright 2010

Comparable statistics for the UKV ensemble forecast run from 0600 GMT on 29/10/2008 are shown in Figures 71a-b. These show similar behaviours to those described for the ensemble of blended forecasts above. However, both radar and gauge based verification demonstrates that the UKV ensemble forecast is over spread. This finding is consistent with the reliability curves shown in Figure 63b.

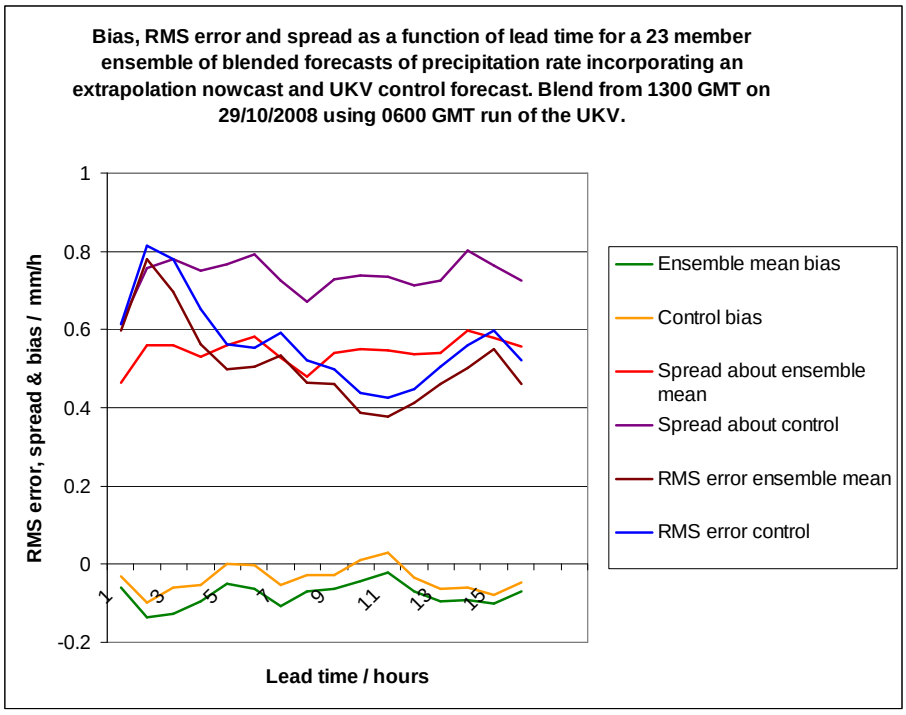

Figure 70a Spread-skill relationship as a function of lead time for a 23 member ensemble of blended forecasts of precipitation rate incorporating an extrapolation nowcast and UKV control forecast (data time 0600 GMT 29/10/2008), run from 1300 GMT on 29/10/2008. Performance is measured relative to quality controlled radar data. No account is taken of radar observation error.

© Crown copyright 2010

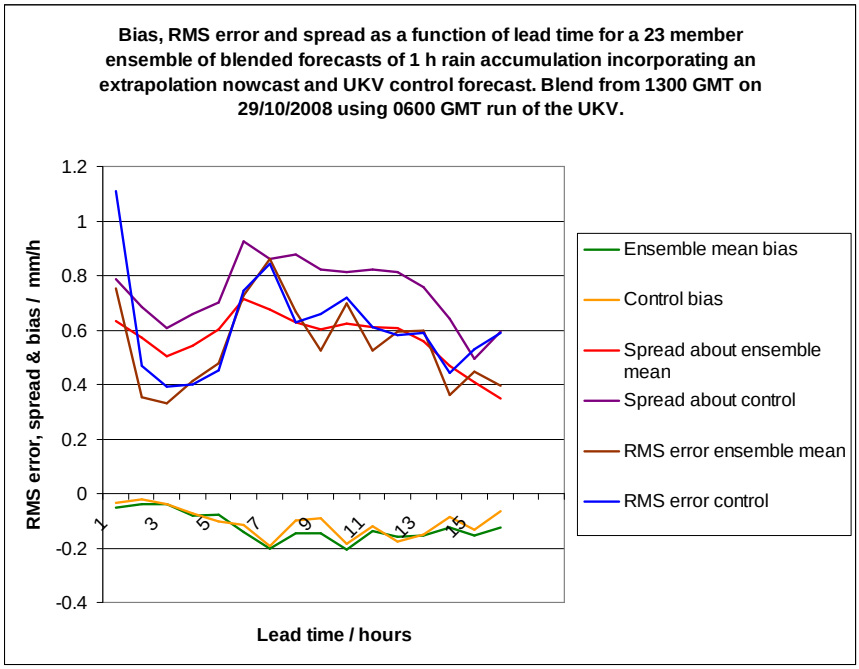

Figure 70b Spread-skill relationship as a function of lead time for a 23 member ensemble of blended forecasts of 1 hour rain accumulation incorporating an extrapolation nowcast and UKV control forecast (data time 0600 GMT 29/10/2008), run from 1300 GMT on 29/10/2008. Performance is measured relative to quality controlled Met Office and Environment Agency rain gauges. No account is taken of observation error.

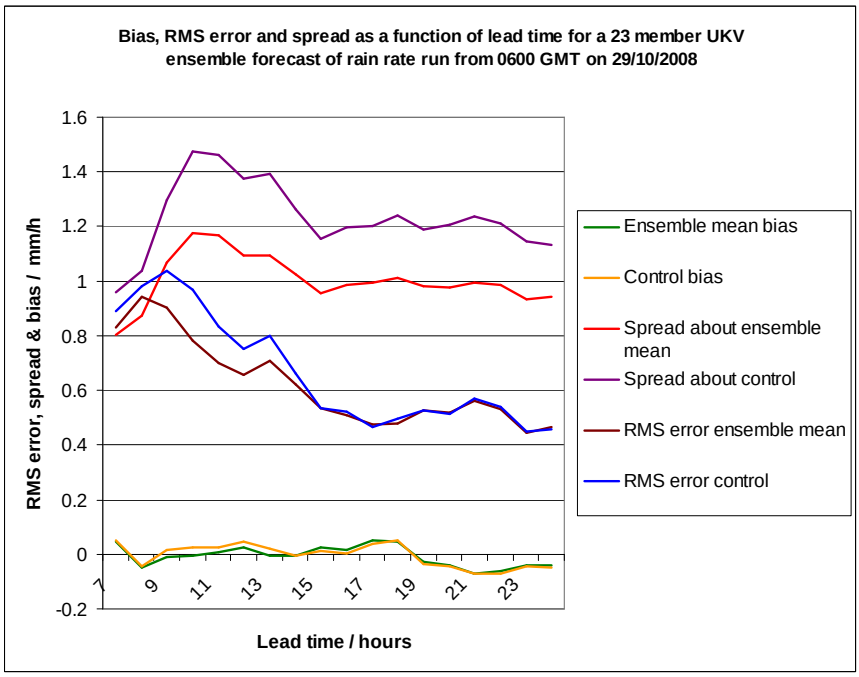

Figure 71a Spread-skill relationship as a function of lead time for a 23 member UKV ensemble forecast of precipitation rate run from 0600 GMT on 29/10/2008. Performance is measured relative to quality controlled radar data. No account is taken of radar observation error.

© Crown copyright 2010

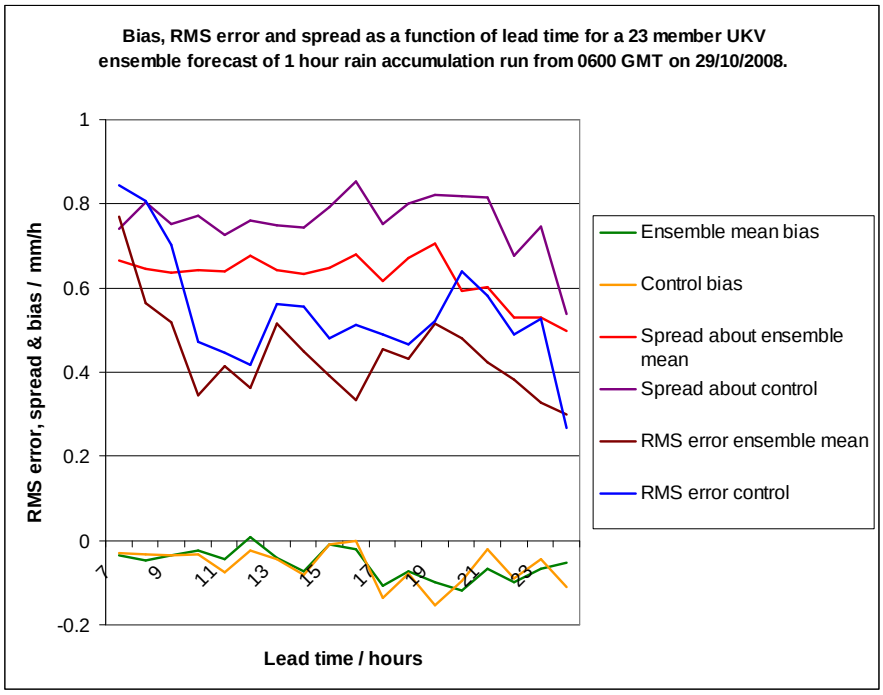

Figure 71b Spread-skill relationship as a function of lead time for a 23 member UKV ensemble forecast of 1 hour rain accumulation run from 0600 GMT on 29/10/2008. Performance is measured relative to quality controlled Met Office and Environment Agency rain gauges. No account is taken of observation error.

Figures 72a-b and 73a-b show equivalent spread-skill plots for 05/09/2008 (case study 1). In common with 29/10/2008, the 23 member ensemble of blended forecasts is skilful because the errors in the ensemble mean measured relative to radar and rain gauge are generally less than or equal those in the control member forecast. Also, broadly speaking, the ensemble spread follows the ensemble error (both decrease with lead time), although the spread tends to be somewhat larger than the error.

Similarly, the spread-skill statistics for the 23 member UKV ensemble forecast shown Figures 73a-b, demonstrate that the ensemble is over spread. In common with the case study 2 (29/10/2008), it is thought that this behaviour originates from the convective scales. However, this hypothesis needs further investigation, possibly by evaluating the spread-skill relationship on each cascade level rather than for the fields as a whole.

Spread-skill plots for the MOGREPS-R ensembles and their downscaled counterparts for case studies 1 and 2 are not reproduced here. As might be expected, the MOGREPS-R ensemble forecasts show an excess of spread at short lead times, similar to that seen for the UKV ensembles. However, the spread-skill of the downscale ensembles is generally good despite the performance issues identified in relation to the parametric noise generation model.

© Crown copyright 2010

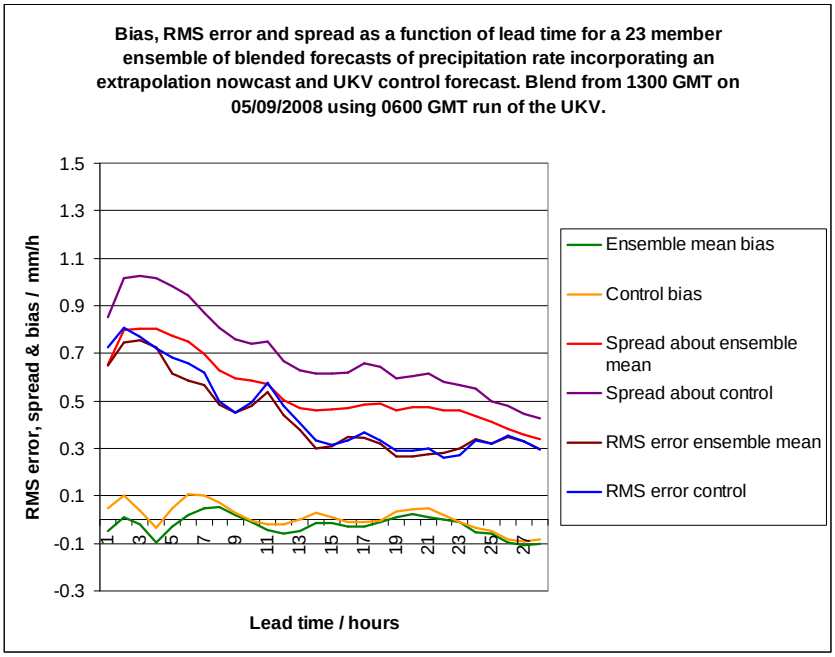

Figure 72a Spread-skill relationship as a function of lead time for a 23 member ensemble of blended forecasts of precipitation rate incorporating an extrapolation nowcast and UKV control forecast (data time 0600 GMT 05/09/2008), run from 1300 GMT on 05/09/2008. Performance is measured relative to quality controlled radar data. No account is taken of radar observation error.

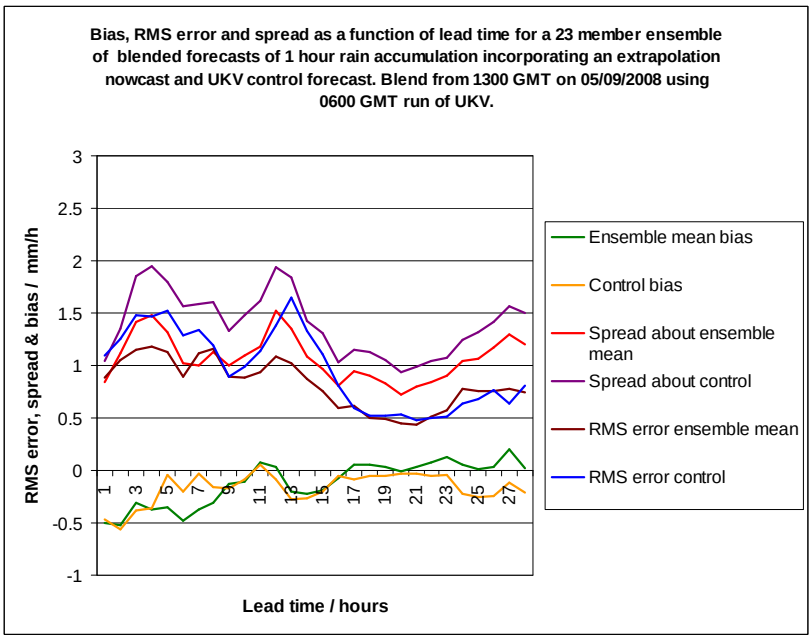

Figure 72b Spread-skill relationship as a function of lead time for a 23 member ensemble of blended forecasts of 1 hour rain accumulation incorporating an extrapolation nowcast and UKV control forecast (data time 0600 GMT 05/09/2008), run from 1300 GMT on 05/09/2008. Performance is measured relative to quality controlled Met Office and Environment Agency rain gauges. No account is taken of observation error.

© Crown copyright 2010

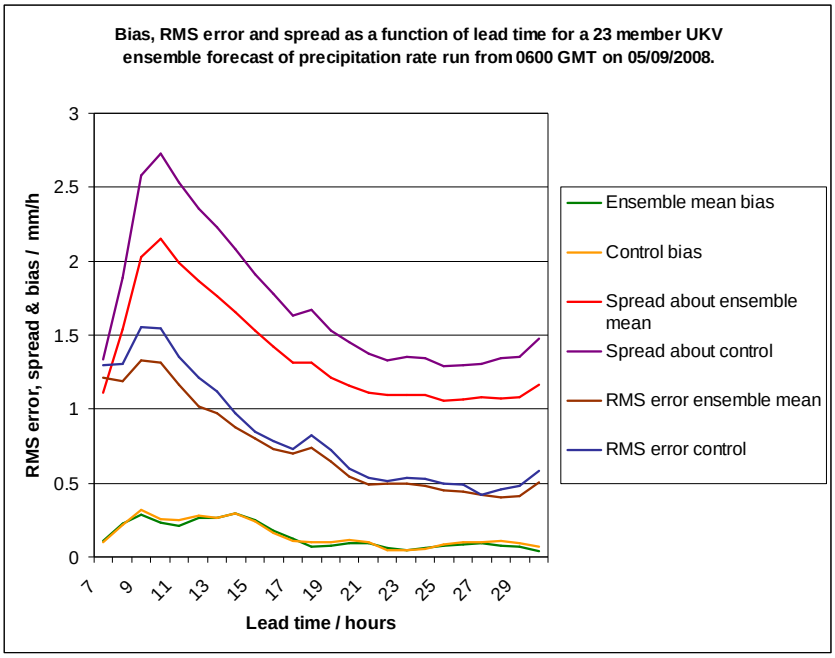

Figure 73a Spread-skill relationship as a function of lead time for a 23 member UKV ensemble forecast of precipitation rate run from 0600 GMT on 05/09/2008. Performance is measured relative to quality controlled radar data. No account is taken of radar observation error.

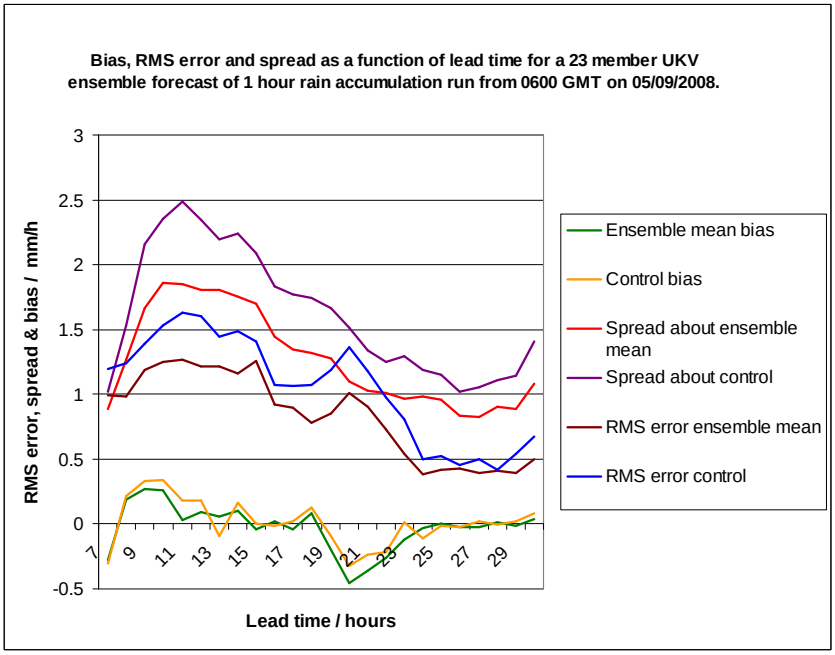

Figure 73b Spread-skill relationship as a function of lead time for a 23 member UKV ensemble forecast of 1 hour rain accumulation run from 0600 GMT on 05/09/2008. Performance is measured relative to quality controlled Met Office and Environment Agency rain gauges. No account is taken of observation error.

© Crown copyright 2010

6. Summary

Formulation and behaviour of the various blending algorithm configurations

A number of alternative blending algorithm configurations have been proposed according to the resolution and range of the available NWP model forecasts. These include a downscaled MOGREPS-R precipitation forecast, a blend of a deterministic extrapolation nowcast, a UKV (control or ensemble) forecast and noise, and a blend incorporating all these components.

These blended forecast configurations all exploit a cascade modelling framework because this provides an effective means of modelling the spatial and temporal scaling properties of precipitation fields. The form of cascade model utilised is a multiplicative, bounded, log-normal cascade comprising 8 levels, representing scales that are powers of two (4km, 8km, …, 512 km). The bottom level of the cascade represents the residual variability in the decomposed field.

A blended forecast is constructed as a weighted combination of its cascade decomposed component forecasts and noise. The weight assigned to a given forecast component on a given cascade level (scale) is a function of its skill, estimated as the fraction of the variance it explains in the equivalent cascade level field of a decomposed UKPP rain analysis. Current estimates of skill, derived by cross correlating the forecast components with a recent UKPP rain analysis are relaxed to climatologies, estimated from a month's worth of model forecasts and rain analyses. The weights allow for the fact that the forecast components are not independent.

In a blended forecast, the noise replaces extrapolated and NWP model predicted precipitation structures as they lose skill and adds variance (structure) at scales where the NWP model forecast components are deficient. Owing to the dynamic scaling properties of the precipitation fields, the noise will saturate the bottom level of the cascade first (the smallest represented scale) and then extend its influence to the levels (scales) above. This process is constrained by the predictive skill of the extrapolation and NWP model forecasts.

Formulation of the noise generators

Two, alternative noise generators have been evaluated. These originate from STEPS and are referred to as the parametric and non-parametric noise generators.

The parametric model assumes that the Power Spectral Density of the target precipitation field can be approximated by a power law relationship between frequency and PSD. This approach has the advantage that the variance (variability) at any given spatial scale can be inferred even if there is insufficient information in the target field at this scale. However, the power law assumption provides only an approximation of the PSD of the true distribution and this may introduce structures into the resulting noise fields that are not seen in reality.

The *non-parametric* noise generation method uses the FFT of the target distribution as a filter to replicate its precise Power Spectral Density and any anisotropy in the target field. This technique can only be used if the target field has the horizontal resolution required of the noise fields (2 km).

© Crown copyright 2010

A forecast sequence of noise fields is generated using a hierarchy of second order Auto-Regressive (AR-2) models. These impose the appropriate temporal scaling behaviour on the noise. The noise is advected with velocities which reflect the radar inferred motion in the short range, and the apparent motion of the NWP model precipitation forecasts at longer range.

Both noise generators produce spatially homogenous noise. In cases where a precipitation field contains frontal precipitation and showers, the noise generators will produce synthetic fields that are a composite of these two distributions.

Forecast evaluation – method of approach

The decision to use two noise generation methods, according to whether the target distribution for the noise has the required horizontal resolution (non-parametric) or not (parametric), has favoured the evaluation of several blended forecasts, one incorporating an extrapolation nowcast, a UKV control forecast and non-parametric noise, the other incorporating a MOGREPS-R control forecast and parametric noise. The evaluation of a blend incorporating all components was not considered beneficial since the UKV ensemble forecasts supplied by the *Convective-scale Ensembles Project* were downscale ensembles with very similar synoptic and mesoscale evolution to their driving MOGREPS-R forecasts.

The limited availability of these UKV ensembles has meant that the case study oriented evaluation of the blending algorithm has been based, in part, on several extreme precipitation events (5 September 2008 and 29 October 2008) under investigation by the CEP, but also on a selection of more recent precipitation events for which archives of operational forecast data, including control runs of the UKV and MOGREPS-R ensembles, are available. The number of case studies has been restricted to 5 chiefly because of constraints on computer resources and time.

The project has sought to answer the following four questions.

1) *Can time series of ensembles of synthetic, 2 km precipitation fields be generated whose spatial statistical properties reliably evolve from a target distribution based on quality controlled radar to spectra based on a UKV forecast sequence?*

2) *Can plausible, synthetic, 2km precipitation fields be generated using power spectra inferred from 24 km resolution MOGREPS-R forecasts. If not, are there suitable alternative target distributions which can be used instead?*

3) Can plausible, seamless, 2km resolution precipitation forecasts be generated from the two configuration of blending algorithm under investigation?

4) Can skilful, well calibrated ensembles of blended precipitation forecasts with useful resolution be generated using multiple realisations of noise to perturb and downscale the forecast components?

© Crown copyright 2010

Performance of the noise generators

Tests on the non-parametric noise generator have shown it to be capable of producing a time series of synthetic precipitation fields whose statistical properties evolve reliably and seamlessly from a distribution with spatial statistical properties inferred from radar to a distribution with the statistical properties derived from a high resolution UM precipitation forecast.

Small errors in the power spectra of the synthetic precipitation fields result from an imperfect representation of all frequencies by the cascade model whose eight levels are constructed using a filter based upon a Gaussian window. These imperfections do not have a significant, deleterious impact on the generated noise fields.

The non-parametric algorithm replicates any anisotropy in the target precipitation field in its synthetic realisations. This may be of benefit when linear features such as frontal precipitation bands dominate a target field.

Tests on a parametric noise generator, designed for downscaling coarse resolution (24 km) MOGREP-R precipitation forecasts, have involved examining the goodness of fit of a power law representation of the power spectra of selected MOGREPS-R precipitation forecasts and scrutiny of the resulting synthetic fields. Case study investigations suggest that this parametric technique is not sufficiently robust to be used as an operational MOGREPS-R downscaler.

Alternative approaches to downscaling MOGREPS-R precipitation forecasts warrant further investigation. These include the use of non-parametric noise with a power spectrum derived from selected UKPP precipitation fields representative of frontal precipitation or showers. However, the optimal solution would be to extend the range of the control run of the UKV model.

Frontal and convective precipitation fields exhibit quite different structures over a range of scales. Both non-parametric and parametric noise generation techniques produce noise fields with spatially homogeneous statistical properties. When the target field contains a mixture of frontal and convective precipitation, the resulting synthetic fields will contain features which are a composite of these two regimes. This may result in the generation of unrealistic precipitation features in blended forecasts incorporating noise.

Performance characteristics of the source models

Although not able to generate realistic looking convective precipitation fields as a result of its coarse resolution, an inter-comparison of model performance (Pierce *et al*., 2008) has demonstrated that MOGREPS-R can identify regions at risk from heavy convective rainfall up to two days in advance.

In agreement with the findings of the *Storm scale numerical modelling* project, case study investigations have shown that high resolution runs of the UM (UKV) in which convection is resolved explicitly are capable of generating precipitation fields which exhibit structures similar to those seen in radar data over a wide range of spatial scales.

© Crown copyright 2010

Radar based UKPP analyses of precipitation rate and corresponding UKV and MOGREPS-R forecasts of precipitation rate often exhibit different distributions. For example, the UKV and MOGREPS-R models have a tendency to produce substantial areas of precipitation with rates < 1/16 mm/h – much more than is typically found in the radar based UKPP rain analyses. Reality probably lies somewhere in between: the radar is likely to under observe drizzle from low level stratus, but equally, the large areas of very light precipitation in the UKV may be an artefact of the behaviour of sub-grid scale parameterisations.

UKV forecasts exhibit a tendency to over predict heavy convective precipitation relative to radar. This is thought to have contributed to an excess of spread in two experimental UKV ensemble forecasts. Verification of these ensembles demonstrated that the spread about the ensemble mean was larger than the error in the ensemble mean measured relative to radar and rain gauge.

Performance of the control member blended forecasts

Case studies have demonstrated that the blending algorithm configuration combining an extrapolation nowcast, a UKV control forecast and non-parametric noise (restricted to the bottom two cascade levels) is capable of producing plausible high resolution precipitation forecasts which evolve seamlessly from a UKPP rain analysis to the UKV forecast. However, small biases introduced when collapsing the blended cascade level fields can remove areas of very light precipitation. This can result is quite significant reductions in raining fraction and associated small changes in the field variance and mean of the blended forecasts.

The injection of non-parametric noise into the bottom two levels of the cascade tends to introduce rather uniform and unrealistic looking fine scale precipitation structures. The purpose of this modification was to make the handover from the UKV control forecast to the downscaled MOGREPS-R control forecast smoother. This problem can probably be resolved by adding small amounts of noise to cascade levels above to avoid any sharp discontinuities between levels.

The MOGREPS-R downscaler has met with limited success. In some cases (25/03/2010 and 05/09/2008) the scheme has demonstrated some skill in generating distributions of the precipitation rate that correct some of the deficiencies in MOGREPS-R control member precipitation fields, for example, the inability of the model to represent the extremes of the distribution and its tendency to over predict raining fraction. However, on other occasions (17/02/2010) the injection of parametric noise into the bottom four cascade levels has produced unrealistic fine scale structures and has not improved the representation of high precipitation rates.

These performance issues probably originate from two sources: the use of spatially homogenous noise with an inappropriate power spectrum; the restriction of injected noise to the bottom four cascade levels only. The latter technique may produce sharp discontinuities between the 32 km and 64 km scales in the cascade. This can be remedied by adding small amounts of noise to the cascade levels above.

© Crown copyright 2010

The performances of ensembles of blended forecasts

The capacity of the blending algorithms to generate skilful, well calibrated ensembles will depend on two factors. Firstly, the space-time statistical properties of blends of model forecast precipitation and noise must be similar to those of the model forecast precipitation and noise alone. Secondly, estimates of the skill of the component forecasts used to compute the weights assigned to the noise and model forecasts in the blends must not deviate significantly from their true skill. Both these conditions must be met if skilful, blended ensemble precipitation forecasts are to be produced.

In two cases involving co-existing frontal and convective precipitation, the performances of 23 member ensembles of blended forecasts generated from UKV and MOGREPS-R control forecasts have been shown to be comparable with those of equivalent UKV and MOGREPS-R ensemble forecasts. This is an encouraging result because, in these cases, the performance of both configurations of blended forecasts is known to be degraded by the use of spatially homogeneous noise.

Nonetheless, reliability diagrams, BSS decomposition statistics and ROC plots demonstrate that these blended ensembles produce reliable probabilities at low precipitation rate and accumulation thresholds. They also exhibit skill relative to within-sample climatologies and an equivalent, blended control member forecast. Furthermore, spread-skill plots for both configurations of blended ensemble indicate a close correspondence between spread and error in the ensemble mean.

For uniform regime precipitation events performance is improved at higher rate and accumulation thresholds.

© Crown copyright 2010

7. Conclusions

7.1. Achievements

Algorithm design, formulation and calibration

The case study investigations presented in this report have shown that radar inferred distributions of precipitation rate can differ significantly from those of corresponding MOGREPS-R and UKV forecasts.

Specifically, the NWP model forecasts often produce substantial areas of precipitation with rates < 1/16 mm/h. In addition, UKV forecasts can produce concentrations of uniformly high precipitation rate not seen in the quality controlled radar data. These are generally associated with resolved convection.

These differences pose several challenges for the blending algorithms. Firstly, it is difficult to produce a seamless blended forecast of uniform character when the underlying characteristics of the component forecasts may be different. Secondly, it is challenging to preserve areas of very light precipitation originating from the NWP model forecasts because small biases introduced when collapsing the blended cascades tend to remove these.

Software design and functionality

A number of configurations of blending algorithm have been coded in object-oriented C++ using classes and inheritance to simplify the code design and make the software as generic as possible.

The code base developed by the project is both flexible and powerful, allowing modifications to existing algorithm configurations to be made quickly and efficiently and new configurations to be built using existing code.

The software has the following capabilities:

- it can generate time series of noise fields using either the non-parametric or parametric noise generators, or a combination of the two;
- it can blend any given combination of model precipitation forecasts regardless of resolution provided the data are re-projected on to the post-processing domain;
- it can generate forecast blends with and without noise.

Performance of the noise generators

It has been demonstrated that the non-parametric noise generation algorithm can produce a time series of noise fields whose spatial statistical properties reliably and seamlessly evolve from those of a radar based UKPP rain analysis to those of a high resolution UM precipitation forecast.

© Crown copyright 2010

This algorithm can replicate the anisotropic properties of a target precipitation field in all realisations of its synthetic precipitation fields. This helps to improve the realism of perturbed forecasts containing bands or lines of precipitation.

Performance of two configurations of blended forecasts

A case study oriented appraisal of two configurations of blending algorithm has shown that they are capable of producing plausible, seamless blended control member and ensemble precipitation forecasts in situations where the precipitation fields are uniform in character. These forecasts demonstrate comparable skill to their constituent model forecasts on a hierarchy of scales over a range of precipitation rate and accumulation thresholds, implying that their calibration is good.

Verification of ensembles of blended forecasts generated from the control runs of the UKV and MOGREPS-R models has shown that they exhibit skill relative to their blended control members and relative to within-sample climatologies. For the two cases studies for which MOGREPS-R and UKV forecast ensembles were available, the performances of the blended ensembles were comparable with those of the ensemble NWP model forecasts. This is despite the fact that both case studies involved co-existing frontal and convective precipitation and some other aspects of the performance of the blended forecasts were degraded as result of this spatial heterogeneity.

Spread-skill verification from the same two case studies suggests that the spread of the blended ensembles may be usefully employed to predict the skill of the blended control member forecast.

7.2. Challenges

Impact of differing radar and model forecast distributions of precipitation rate

The case study investigations presented in this report have shown that radar inferred distributions of precipitation rate can differ significantly from those of corresponding MOGREPS-R and UKV forecasts.

Specifically, the NWP model forecasts often produce substantial areas of precipitation with rates < 1/16 mm/h. In addition, UKV forecasts can produce concentrations of uniformly high precipitation rate not seen in the quality controlled radar data. These are generally associated with resolved convection.

These differences pose several challenges for the blending algorithms. Firstly, it is difficult to produce a seamless blended forecast of uniform character when the underlying characteristics of the component forecasts may be different. Secondly, it is challenging to preserve areas of very light precipitation originating from the NWP model forecasts because small biases introduced when collapsing the blended cascades tend to remove these.

© Crown copyright 2010

Impact of co-existing widespread precipitation and showers

Underpinning the design of the various blending algorithm configurations is the assumption that a field of precipitation rate can be modelled effectively using a single, spatially homogeneous distribution. Case study investigations have shown this approach to be inadequate when frontal and convective precipitation co-exist. Widespread precipitation and showers often exhibit quite different power spectra and space-time statistical properties as demonstrated in the interim report on the performance of the various forecast models (Pierce *et al*., 2008).

Formulation and use of the noise in the blending

Both non-parametric and parametric noise generation algorithms produce synthetic precipitation fields with spatially uniform statistical properties. In cases where frontal and convective precipitation coexist, each noise realisation will contain features that are a composite of two distinct distributions and will therefore look like neither. Unrealistic intensification or weakening of the blended forecast precipitation fields can be produced when the noise is used to perturb the extrapolation and NWP forecast components.

It should be possible to remedy this deficiency by maintaining two noise distributions, one representative of typical widespread precipitation, the other of showers.

The reliability of the parametric noise generator used for downscaling MOGREPS-R precipitation forecasts is not on a par with that of the non-parametric scheme. The power law approximation of the power spectra of MOGREPS-R precipitation forecasts can produce noise fields with deviant spatial characteristics.

The restriction of noise to the lowest few cascade levels in the blended control forecasts can introduce implausible small scale precipitation features. This may be due in part to the spatial homogeneity of the noise. However, the discontinuity caused by constraining the noise to specific cascade levels is likely to be a contributory factor. This might be remedied by allowing the weight on the noise to decay exponentially up the cascade.

Evaluation of the blended forecasts

The evaluation of two configurations of the blending algorithm has been limited to a small number of cases studies, partly due to the limited availability of UKV ensemble forecasts, but also due to constraints on time and computer resources. There is a need for a further, more extensive evaluation of blending algorithm performance once recommended improvements have been made.

© Crown copyright 2010

8. Recommendations

The performances of the *non-parametric* noise generator and blended forecasts incorporating non-parametric noise are encouraging and justify further R&D to address outstanding issues related to the noise formulation, choice of target distribution for noise generation and cascade design. The implementation of a blended control and ensemble forecast with a range similar to that of the UKV (36 hours) is achievable with modest additional investment.

With some enhancement to the formulation of the non-parametric noise, it is expected that at least one configuration of the blending algorithm – a combination of non-parametric noise, an extrapolation nowcast and UKV forecast – will perform on a par with the Short Term Ensemble Prediction System. It is recommended that improvements to the non-parametric noise generator be made in the remaining months of FY 10/11 with a view to conducting an operational trial of this blended forecast configuration in spring 2011.

Given the above mentioned enhancement of the non-parametric noise generator, it should be straightforward to implement a MOGREPS-R downscaler with satisfactory levels of performance. This would be limited to the range of the UKV because the latter is required to provide a suitable target distribution for the noise.

This project has identified systematic discrepancies between UKV forecast distributions of precipitation rate and those inferred from weather radar. There is evidence to suggest that these discrepancies may have been the cause of excessive ensemble spread in two experimental UKV ensemble precipitation forecasts supplied by the Convective-scale Ensembles Project. This finding warrants further investigation.

© Crown copyright 2010

9. References

Bishop, C. H., Etherton, B. J., and S. J. Majumdar, 2001. Adaptive sampling with the ensemble transform Kalman filter. Part 1: theoretical aspects. *Mon. Wea. Rev.*, **129**, 420–436.

Bowler, N. E., Dando, M., Beare, S., and K. Mylne, 2007. The MOGREPS short-range ensemble prediction system: Verification report. Trial performance of MOGREPS January 2006 – March 2007. *Forecasting Research Technical Report No. 503*, Met Office, pp 60.

Bowler, N. E., Pierce, C. E., and A. W. Seed, 2006. STEPS: A probabilistic precipitation forecasting scheme which merges an extrapolation nowcast with downscaled NWP. *Q. J. R. Meteorol. Soc*., **132**, 2127–2155.

Davies, T.; M. J. P. Cullen, A. J. Malcolm, M. H. Mawson, A. Staniforth, A. A.White, and N. Wood, 2005. A new dynamical core for the Met Office's global and regional modelling of the atmosphere. *Q. J. R. Meteorol. Soc*., **131**, 1759–1782.

Edwards, J.M. Slingo, A., 1996. Studies with a flexible new radiation code. Part I. Choosing a configuration for a large-scale model. *Q. J. R. Meteorol. Soc*., **122**, 689–719.

Essery, R., M. Best, and P. Cox, 2001. MOSES 2.2 Technical Documentation, Hadley Centre Technical Report No. 30, Met Office Hadley Centre.

Germann, U., and Zawadzki, I., 2002. Scale dependency of the predictability of precipitation from continental radar images. Part 1: description of the methodology. *Mon. Wea. Rev.*, 130(12), 2859–2873.

Golding, B., Clark, P., and May, B., 2005. Boscastle flood: meteorological analysis of the conditions leading to flooding on 16 August 2004. *Weather*, **60**, 230–235.

Gregory, D. and P. R. Rowntree, 1990. A Mass Flux Convection Scheme with Representation of Cloud Ensemble Characteristics and Stability-Dependent Closure.
Mon. Wea. Rev., 118 1483-1506

Harris, D., Foufoula-Georgiou, E., Droegemeier, K. K. and J. L. Levit, 2001. Multiscale statistical properties of a high-resolution precipitation forecast, *J. Hydrometeorol.*,**2**, 406-418.

Lock, A. P., A. R. Brown, M. R. Bush, G. M. Martin, and R. N. B. Smith, 2000. A New Boundary Layer Mixing Scheme. Part 1: Scheme Description and Single-Column Model Tests. *Mon. Wea. Rev*., **128**, 3187–3199.

Marsan, D. amd D. Schertzer, 1996. Causal space-time multi-fractal processes: predictability and forecasting rain fields. *J. Geophys. Res*., 101(D21), 26333-26346.

© Crown copyright 2010

Hoskins, B. J., Robertson, A. W., and M. E. McIntyre, 1985. On the use and significance of isentropic potential vorticity maps. *Q. J. R. Meteorol. Soc*., **111** (470), 877–946.

Joss, J., and A. Waldvogel, 1990. Precipitation measurement and hydrology. *Radar in Meteorology*, D. Atlas, Ed., Amer. Meteorol. Soc., 577-606.

Lovejoy, S., Duncan, M. R., and D. Schertzer, 1996. Scalar multi-fractal radar observer's problem. *J. Geophys. Res. (Atmos.)*, **101** (D21), 26479**–**26491.

Mallat, S.G., 1989. A theory for multi-resolution signal decomposition: the wavelet representation. *Pattern Analysis and Machine Intelligence*, **11**(7), 674 – 693.

Menabde, M., Seed, A. W., Harris, D, and Austin, G. L, 1999. Multiaffine random field model of rainfall. *Wat. Res. Res.*, **35**, No. 2, 509**–**514.

Perica, S. and E. Foufoula-Georgiou, 1996. Model for multiscale disaggregation of spatial rainfall based on coupling meteorological and scaling descriptions. *J. Geophys. Res*.,**101**(D21),26347-26361.

Pierce, C. E., 2007. Downscaling of MOGREPS NAE ensembles, and blending with stochastic extrapolation and 1.5 km UM ensembles. *Unpublished discussion paper produced for the Blending convective scale NWP with ensemble nowcasting project, Met Office,* pp 22*.*

Pierce, C. E., and A. Singleton, 2007. Performance evaluation of the Short-Term Ensemble Prediction System (STEPS) and UK NWP model for the Environment Agency: Scale selective verification for November 2007. *Unpublished monthly verification report for the Environment Agency.*

Roberts, N., 2005. Final report for the storm scale modelling project. *R&D Technical Report FD2207/TR of the Joint Defra/EA Flood and Coastal Erosion Risk Management R&D Programme*, *January 2005*.

Pierce, C. E., Singleton, A., and A. C. Bennett, 2008. Inter-comparison of model performance on a selection of convective precipitation events and implications for a blending algorithm. *Unpublished paper produced for the Blending convective scale NWP with ensemble nowcasting project, Met Office,* pp 70*.*

Roberts, N., 2006. Simulation of extreme rainfall events using the Unified Model with a grid spacing of 12, 4 and 1 km. *Modelling extreme rainfall events project: stage 1 report. Forecast Research Technical Report 486, Met Office, April 2006*, pp 49.

Roberts, N. M., and H. W. Lean, 2008. Scale selective verification of rainfall accumulations from high resolution forecasts of convective events. *Mon. Wea. Rev*., **136**, 78–97.

Schertzer, D., Lovejoy, S., Schmitt, F., Chigirinskaya, Y. and D. Marsan, 1997. Multi-fractal cascade dynamics and turbulent intermittency. *Fractals*, 5, 427-471.

Seed, A., 2003. A dynamic and spatial scaling approach to advection forecasting. *J. Appl. Meteorol.*, **42**, No. 3, 381**–**388.

© Crown copyright 2010

Venugopal, V. E., Foufoula-Georgiou, E. and V. Sapozhnikov, 1999. Evidence of dynamic scaling in space-time rainfall. *J. Geophys. Res*., 104 (D24), 31599–31610.

Wang, X. G. and C. H. Bishop, 2003. A comparison of breeding and ensemble transform Kalman filter ensemble forecast schemes. *J. Atmos. Sci*., **60**, 1140–1158.

Wilson, D. R., and S. P. Ballard, 1999. A microphysically based precipitation scheme for the UK Meteorological Office Unified Model. *Q. J. R. Meteorol. Soc*., **125**, 1607–1636.

Zawadzki, I., Morneau, J. and R. Laprise, 1994. Predictability of precipitation patterns: an operational approach. *J. Appl. Meteorol*.,**33**,1562-1571.

© Crown copyright 2010

10. Appendices

10.1. Appendix A.1 Case study oriented verification for the control member blended forecasts

Case study 1 – 05/09/2008

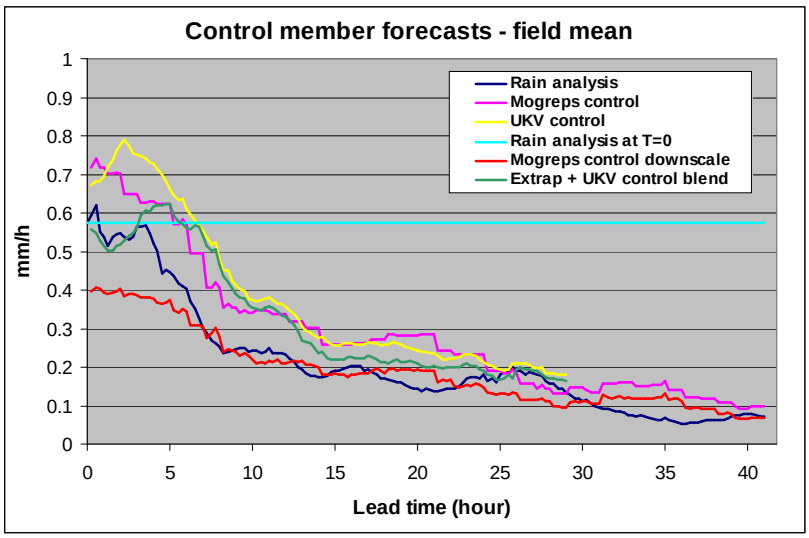

Figure A1.1 Time evolution of the field mean of UKPP rain analyses, MOGREPS-R and UKV control member forecasts and the two configurations of blended forecast for 05/09/2008. The forecast lead times on the X axis are those of the blended forecasts (run from 1300 GMT on 05/09/2008). The UKV and MOGREPS-R forecasts were run from 0600 GMT on 05/09/2008.

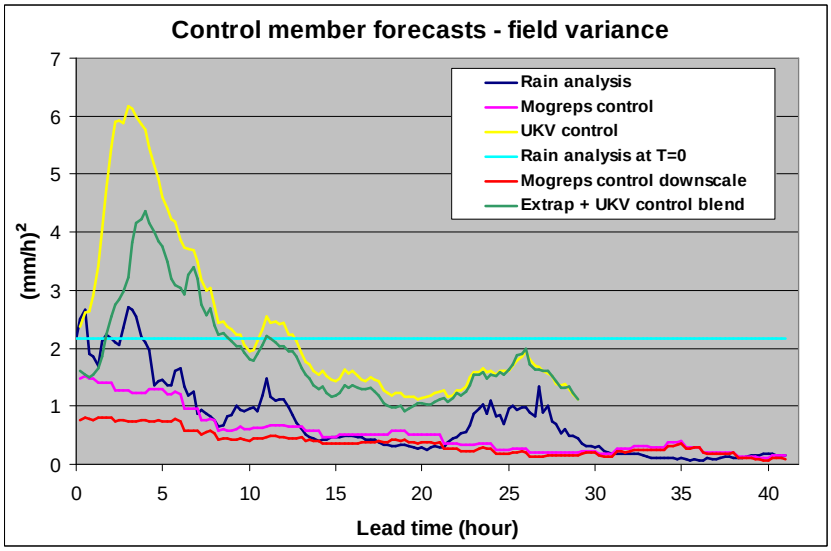

Figure A1.2 Time evolution of the field variance of UKPP rain analyses, MOGREPS-R and UKV control member forecasts and the two configurations of blended forecast for 05/09/2008. The forecast lead times on the X axis are those of the blended forecasts (run from 1300 GMT on 05/09/2008).

© Crown copyright 2010

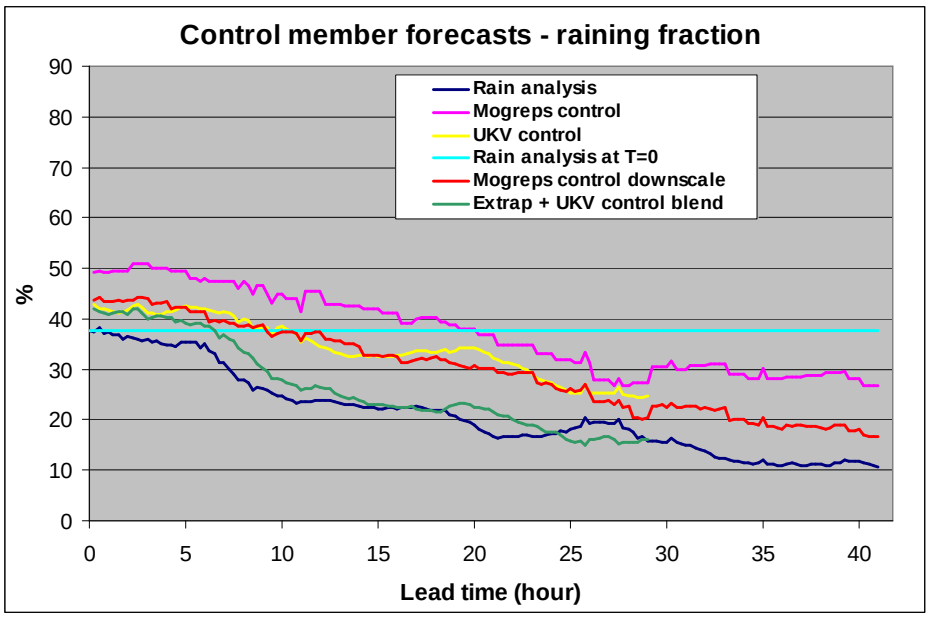

Figure A1.3 Time evolution of the raining fraction of UKPP rain analyses, MOGREPS-R and UKV control member forecasts and the two configurations of blended forecast for 05/09/2008. The forecast lead times on the X axis are those of the blended forecasts (run from 1300 GMT on 05/09/2008).

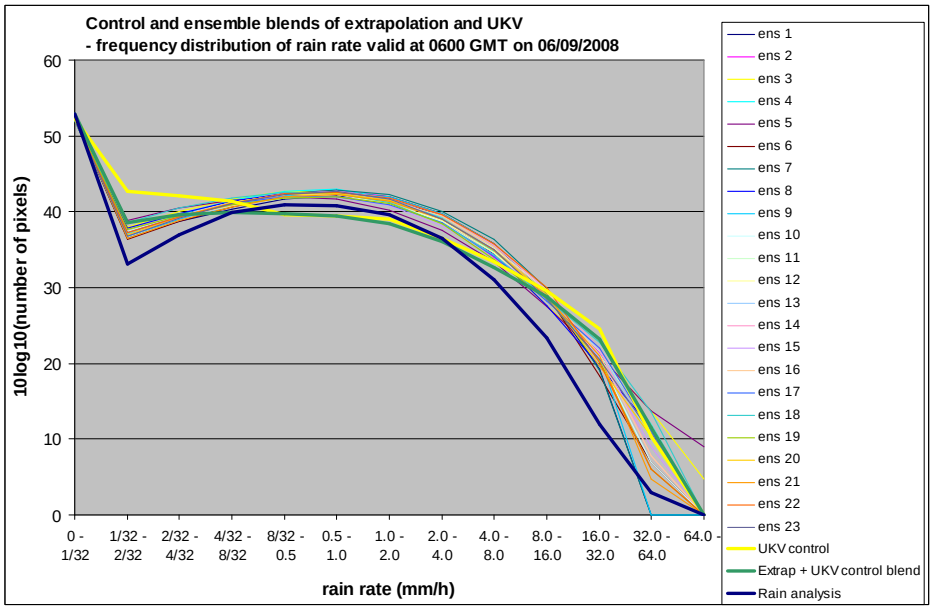

Figure A1.4 Frequency distributions of precipitation rate for a UKPP rain analysis, a 2 km resolution UKV control member forecast, and a blended control forecast and 23 member ensemble forecast incorporating an extrapolation nowcast and UKV control forecast, all valid at 0600 GMT on 06/09/2008. The blended forecasts were run from 0600 GMT on 06/09/2008 and the UKV control forecast from 0600 GMT on the previous day. The validation area is the UK radar composite.

© Crown copyright 2010

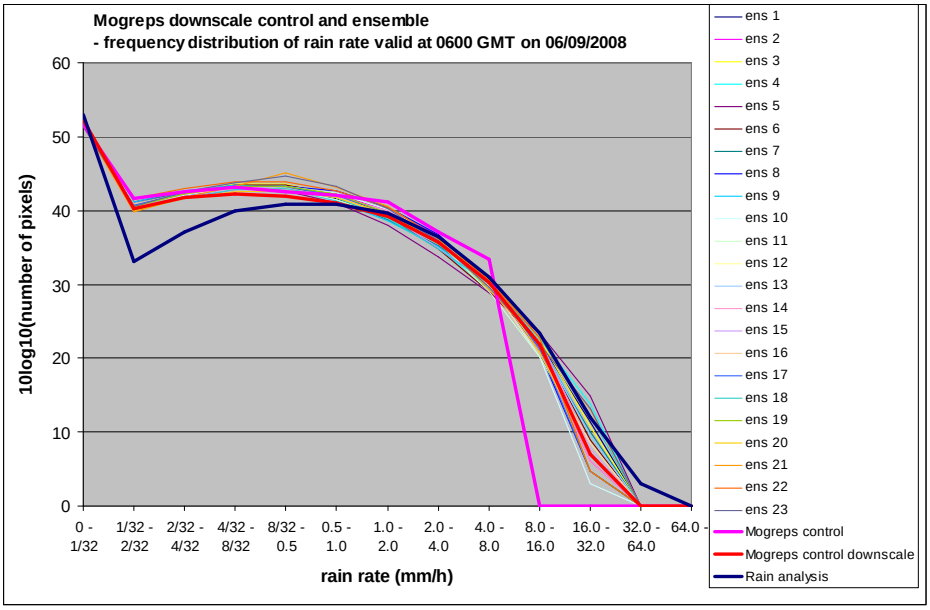

Figure A1.5 Frequency distributions of precipitation rate for a UKPP rain analyses, a 24 km resolution MOGREPS-R control member and its downscaled counterpart, and 23 members of a downscaled MOGREPS-R control forecast, all valid at 0600 GMT on 06/09/2008. The MOGREPS-R control forecast was run from 0600 GMT on 05/09/2008. The validation area is the UK radar composite.

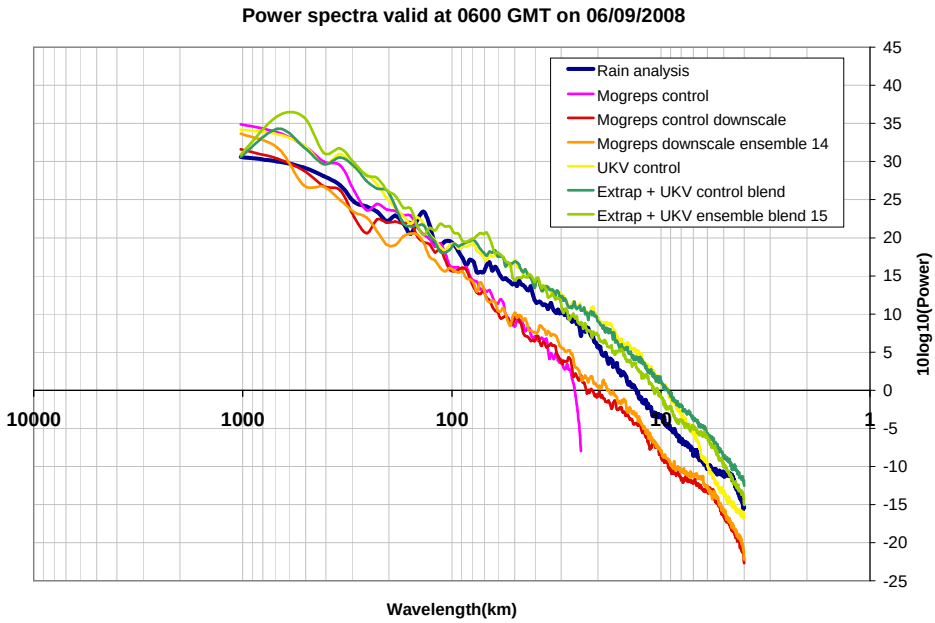

Figure A1.6 Power spectra for a UKPP rain analysis, MOGREPS-R (T+24 h) and UKV (T+24h) control member forecasts and the two configurations of blended forecasts (T+16 h) all valid at 0600 GMT on 06/09/2008.

© Crown copyright 2010

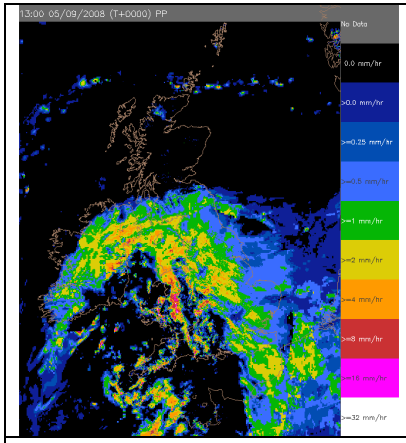	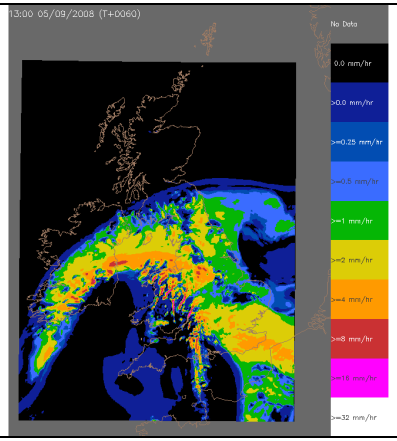	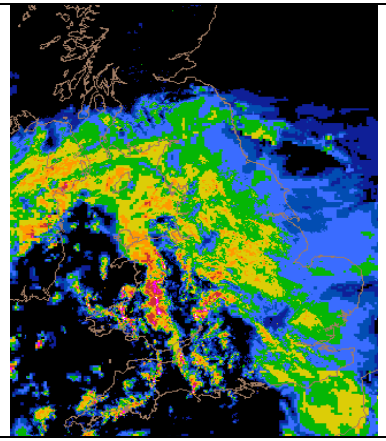	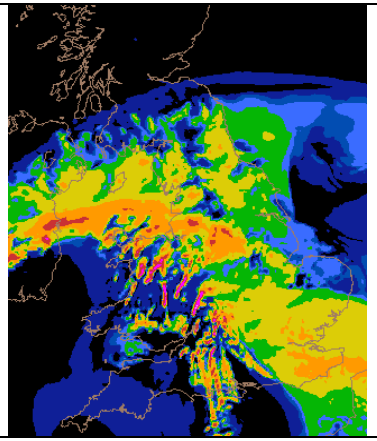
UKPP rain analysis valid at 1300 GMT on 05/09/2008	**UKV T+7h forecast valid at 1300 GMT on 05/09/2008**	**T+15 min blend of an extrapolation nowcast, a UKV control forecast and non-parametric noise valid at 1315 GMT on 05/09/2008**	**UKV T+7h 15 min forecast valid at valid at 1315 GMT on 05/09/2008**
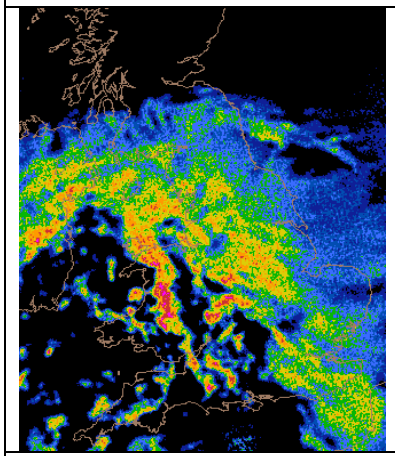	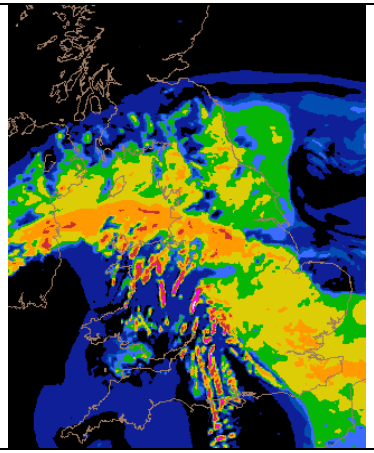	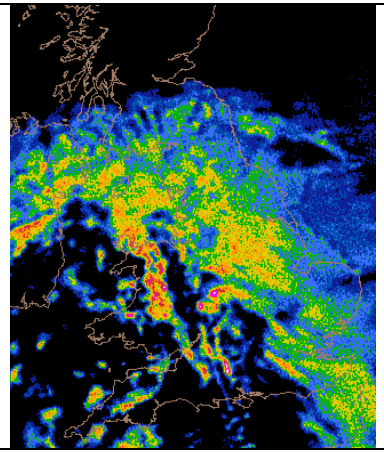	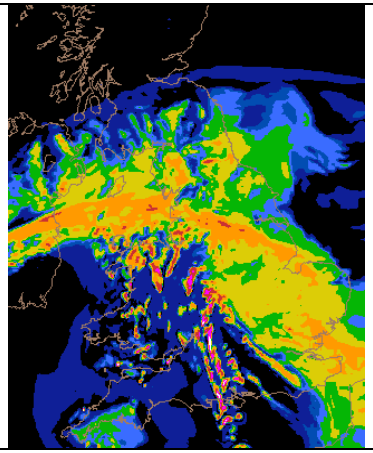
T+30 min blend of an extrapolation nowcast, a UKV control forecast and non-parametric noise valid at 1330 GMT on 05/09/2008	**UKV T+7h 30 min forecast valid at valid at 1330 GMT on 05/09/2008**	**T+1 h blend of an extrapolation nowcast, a UKV control forecast and non-parametric noise valid at 1400 GMT on 05/09/2008**	**UKV T+8 h forecast valid at 1400 GMT on 05/09/2008**

© Crown copyright 2010

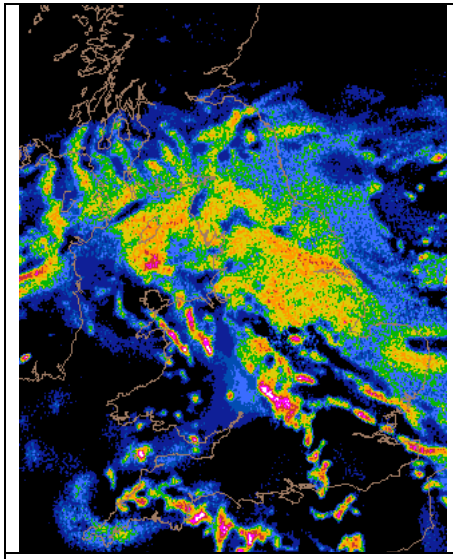

T+3 h blend of an extrapolation nowcast, a UKV control forecast and non-parametric noise valid at 1600 GMT on 05/09/2008

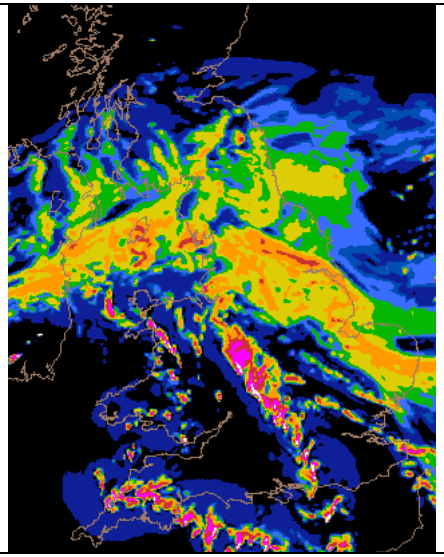

UKV T+10 h forecast valid at 1600 GMT on 05/09/2008

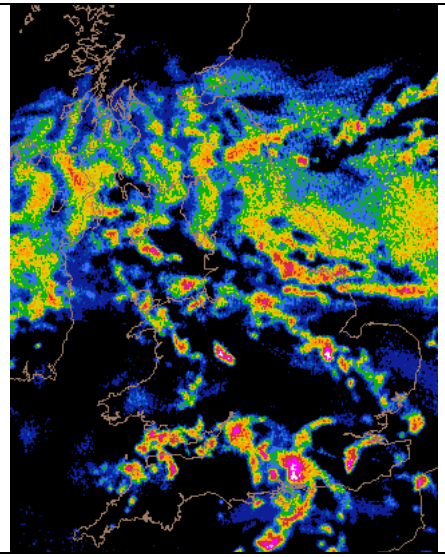

T+6 h blend of an extrapolation nowcast, a UKV control forecast and non-parametric noise valid at 1900 GMT on 05/09/2008

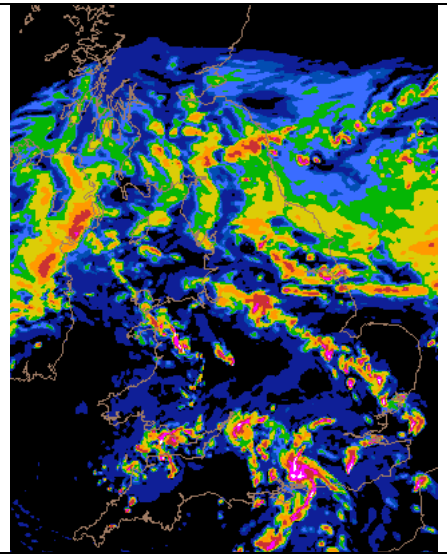

UKV T+13 h forecast valid at 1900 GMT on 05/09/2008

Figure A1.7a Selected steps in a blended, control member forecast of precipitation rate, comprising an extrapolation nowcast, UKV control forecast and non-parametric noise (confined to scales ≤ 8 km), run from 1300 GMT on 05/09/2008. The UKPP rain analysis used as the starting point for the extrapolation nowcast is also shown, as well corresponding forecast steps from the associated UKV control member forecast (data time 0600 GMT, 05/09/2008).

© Crown copyright 2010

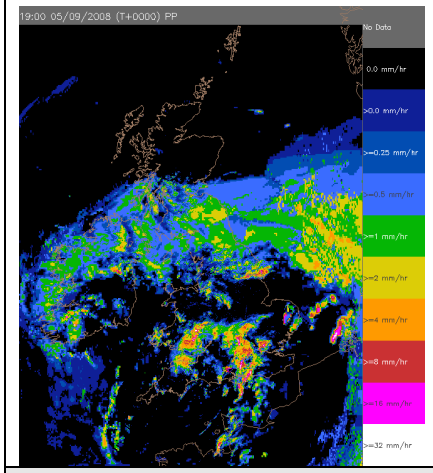

UKPP rain analysis valid at 1900 GMT on 05/09/2008

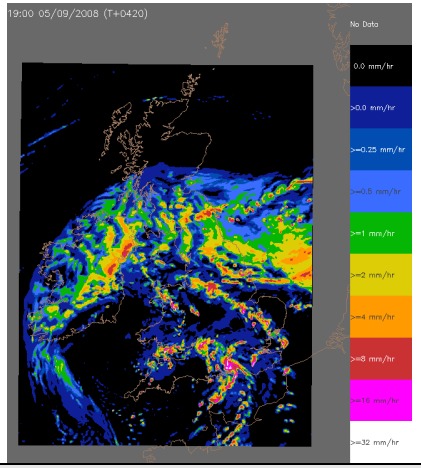

T+13 h UKV control forecast valid at 1900 GMT on 05/09/2008

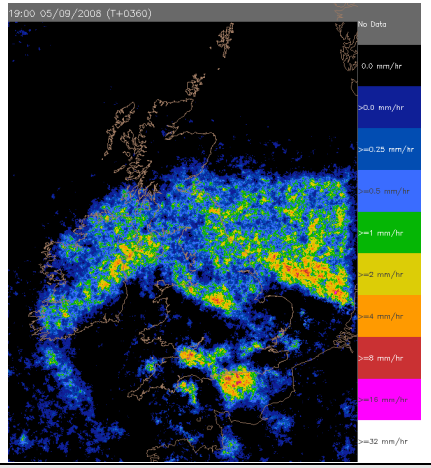

T+13 h MOGREPS-R downscale forecast valid at 1900 GMT on 05/09/2008

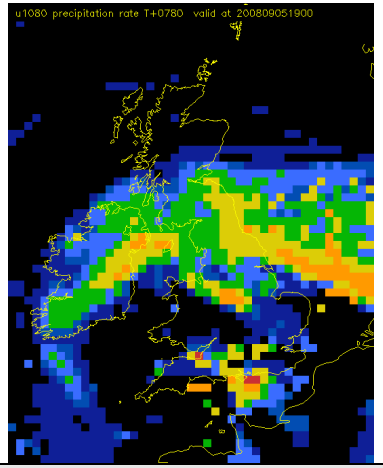

T+13 h MOGREPS-R forecast valid at 1900 GMT on 05/09/2008

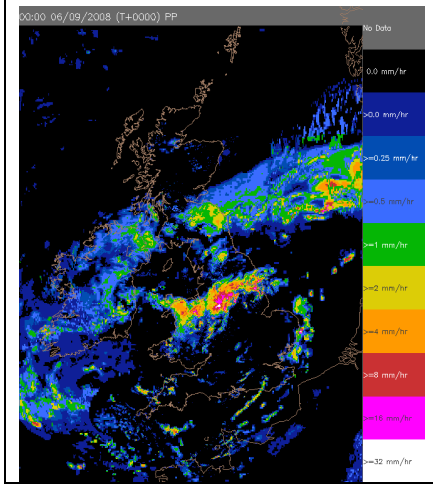

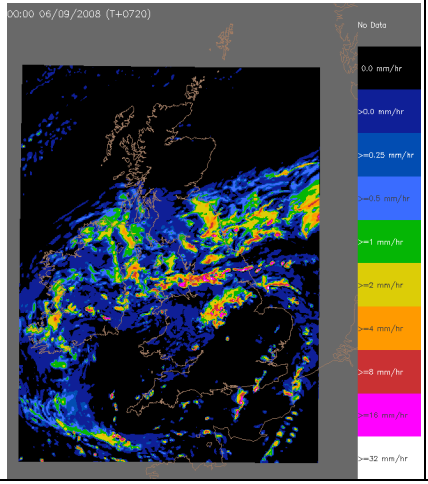

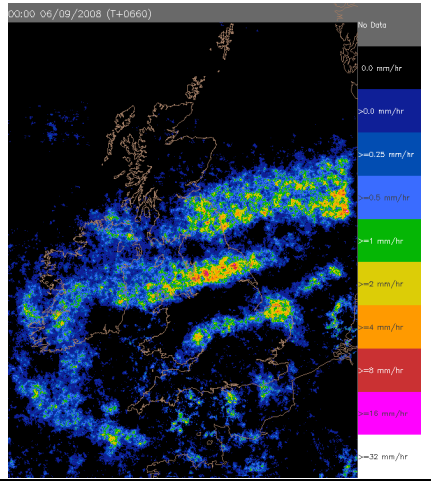

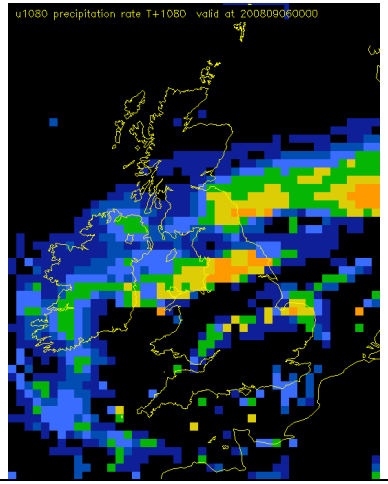

© Crown copyright 2010

UKPP rain analysis valid at 0000 GMT on 06/09/2008	T+18 h UKV control forecast valid at 0000 GMT on 06/09/2008	T+18 h MOGREPS-R downscale forecast valid at 0000 GMT on 06/09/2008	T+18 h MOGREPS-R forecast valid at 0600 GMT on 06/09/2008
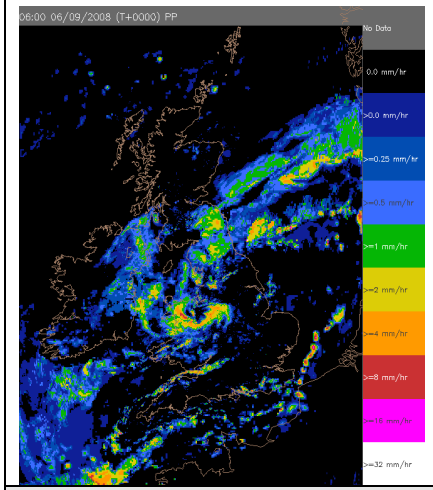	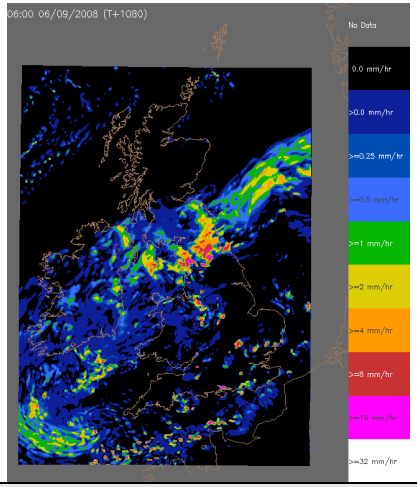	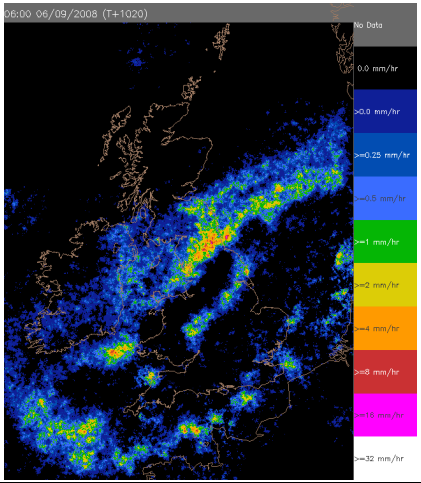	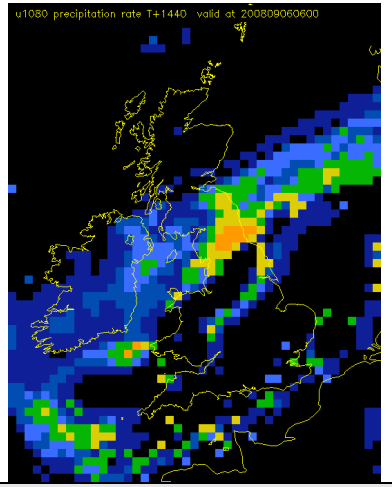
UKPP rain analysis valid at 0600 GMT on 06/09/2008	T+24 h UKV control forecast valid at 0600 GMT on 06/09/2008	T+24 h MOGREPS-R downscale forecast valid at 0600 GMT on 06/09/2008	T+24 h MOGREPS-R forecast valid at 0600 GMT on 06/09/2008

Figure A1.7b Selected forecast steps in a blended, control member forecast of precipitation rate, comprising a MOGREPS-R control forecast and parametric noise (confined to scales ≤ 64 km), run from 1300 GMT on 05/09/2008 (3rd column from left). A corresponding sequence of UKPP rain analyses and forecasts steps from the associated MOGREPS-R control forecast (data time 0600 GMT, 05/09/2008) and UKV control forecast (data time 0600 GMT, 05/09/2008) are also shown for comparison.

© Crown copyright 2010

Case study 3 – 19/11/2009

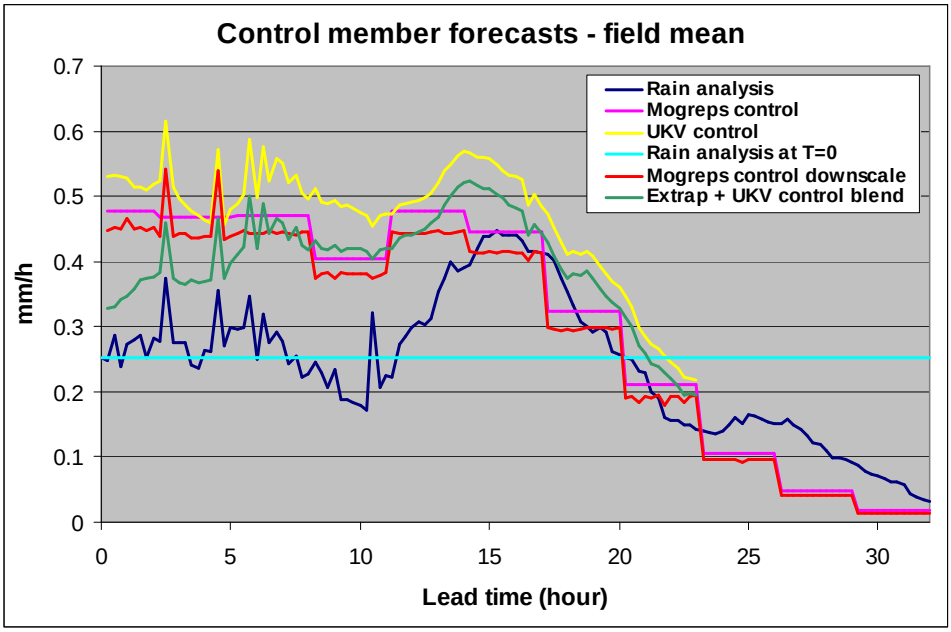

Figure A1.8 Time evolution of the field mean of UKPP rain analyses, MOGREPS-R and UKV control member forecasts and the two configurations of blended forecast for 19/11/2009. The forecast lead times on the X axis are those of the blended forecasts (run from 1000 GMT on 19/11/2009). The UKV and MOGREPS-R forecasts were run from 2100 GMT and 1800 GMT respectively on 18/11/2009.

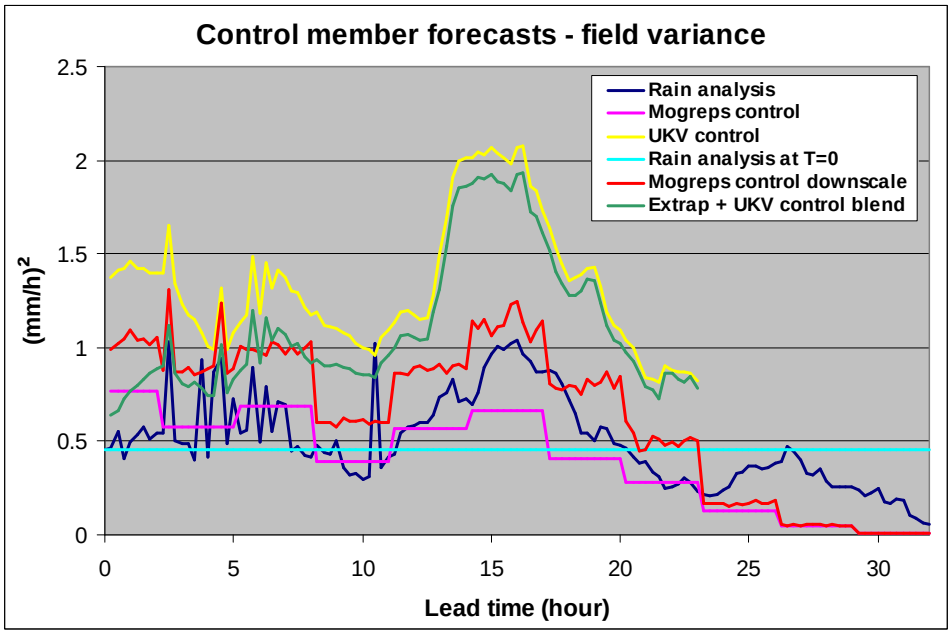

Figure A1.9 Time evolution of the field variance of UKPP rain analyses, MOGREPS-R and UKV control member forecasts and the two configurations of blended forecast for 19/11/2009. The forecast lead times on the X axis are those of the blended forecasts (run from 1000 GMT on 19/11/2009).

© Crown copyright 2010

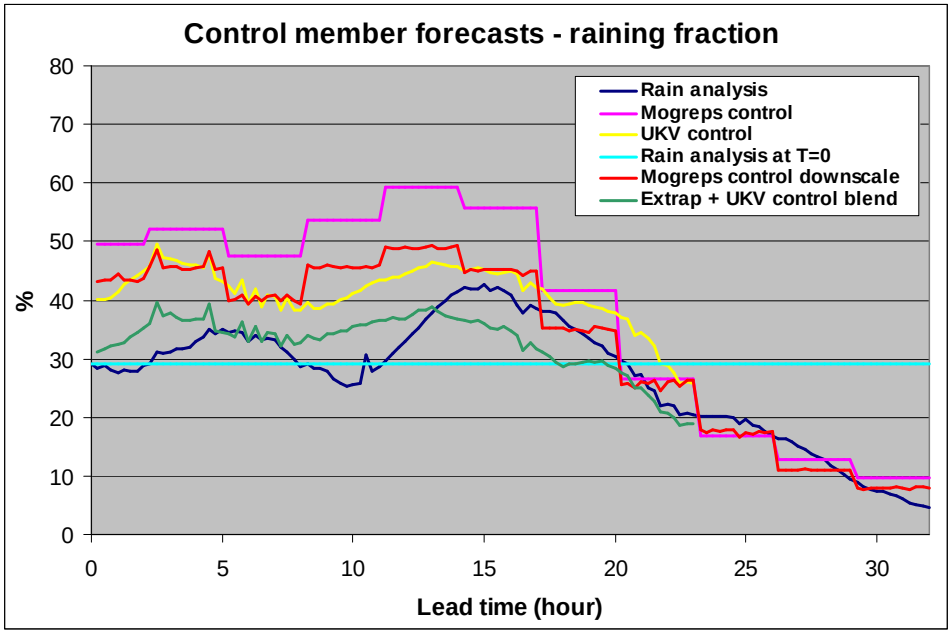

Figure A1.10 Time evolution of the raining fraction of UKPP rain analyses, MOGREPS-R and UKV control member forecasts and the two configurations of blended forecast for 19/11/2009. The forecast lead times on the X axis are those of the blended forecasts (run from 1000 GMT on 19/11/2009).

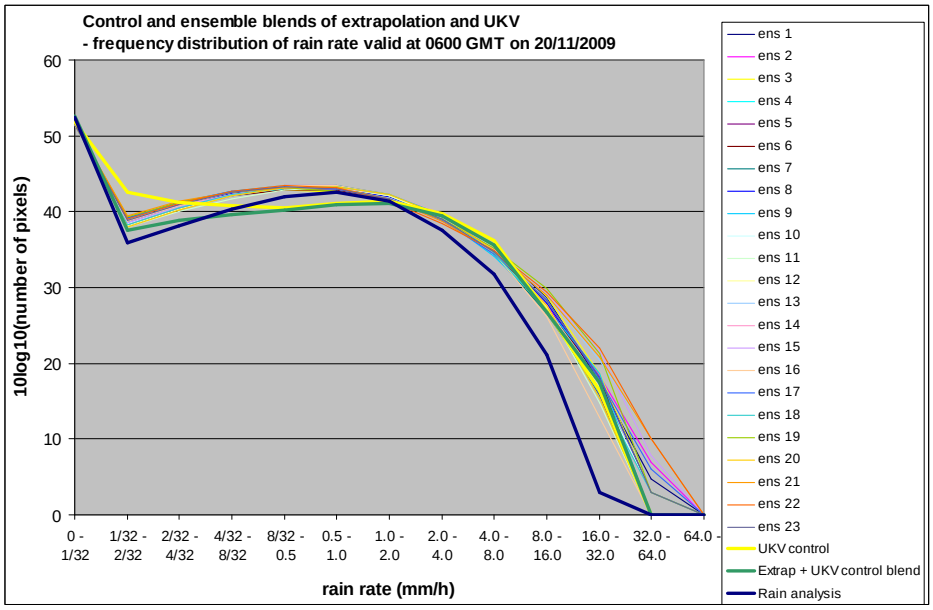

Figure A1.11 Frequency distributions of precipitation rate for a UKPP rain analysis, a 2 km resolution UKV control member forecast, and a blended control forecast and 23 member ensemble forecast incorporating an extrapolation nowcast and UKV control forecast, all valid at 0600 GMT on 20/11/2009. The blended forecasts were run from 0900 GMT on 19/11/2009 and the UKV control forecast from 2100 GMT on the previous day. The validation area is the UK radar composite.

© Crown copyright 2010

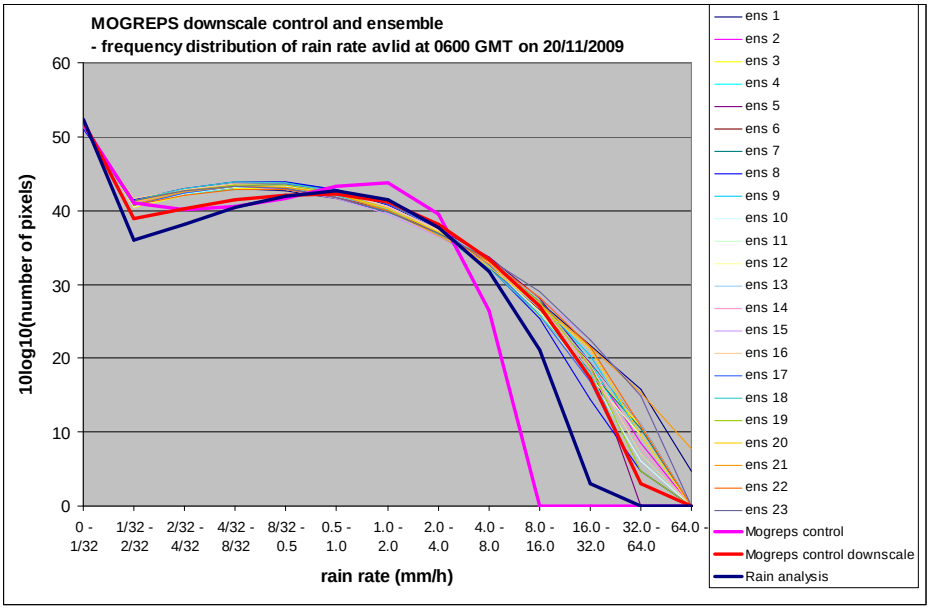

Figure A1.12 Frequency distributions of precipitation rate for a UKPP rain analyses, a 24 km resolution MOGREPS-R control member and its downscaled counterpart, and 23 members of a downscaled MOGREPS-R control forecast, all valid at 0600 GMT on 20/11/2009. The MOGREPS-R control forecast was run from 1800 GMT on 18/11/2009. The validation area is the UK radar composite.

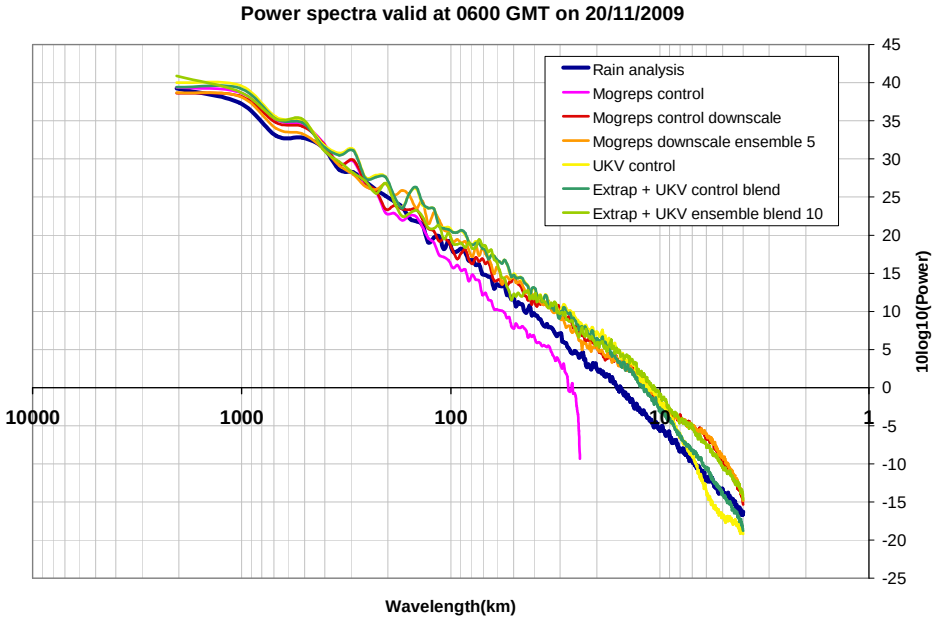

Figure A1.13 Power spectra for a UKPP rain analysis, MOGREPS-R (T+36 h) and UKV (T+33h) control member forecasts and the two configurations of blended forecasts (T+20 h) all valid at 0600 GMT on 20/11/2009.

© Crown copyright 2010

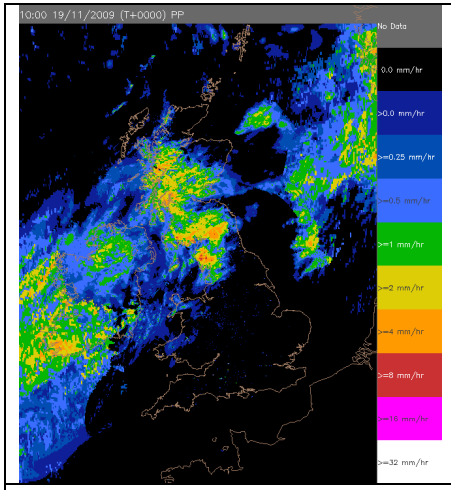	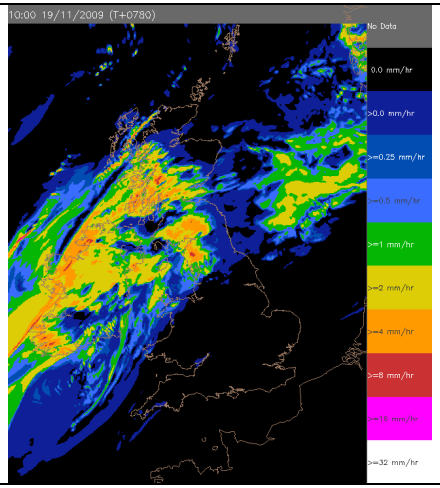	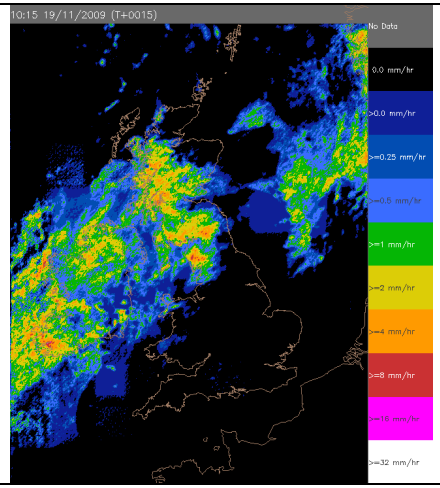	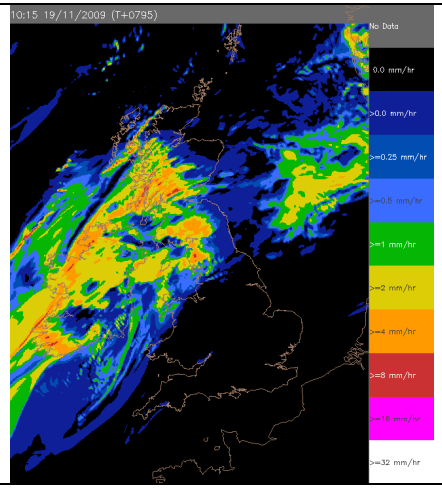
UKPP rain analysis valid at 1000 GMT on 19/11/2009	**T+13h UKV forecast valid at 1000 GMT on 19/11/2009**	**T+15 min blend of an extrapolation nowcast, a UKV control forecast and non-parametric noise valid at 1015 GMT on 19/11/2009**	**T+13h 15 min UKV forecast valid at 1015 GMT on 19/11/2009**
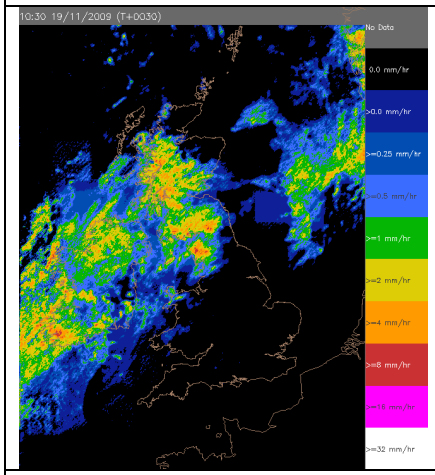	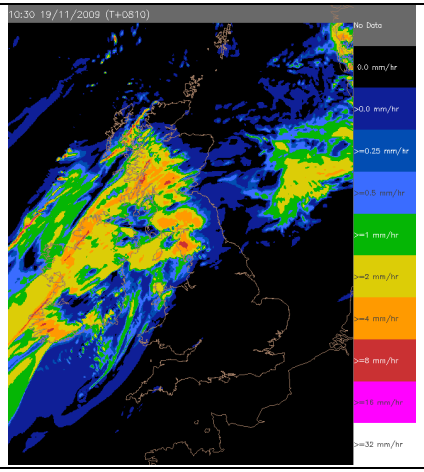	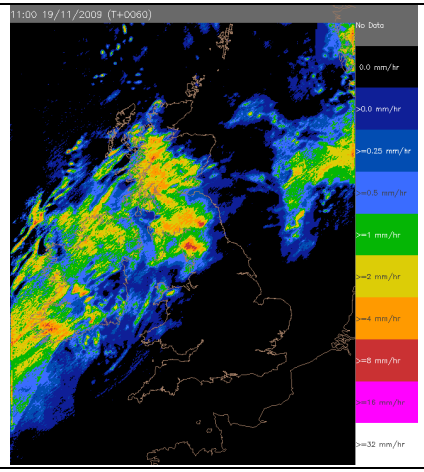	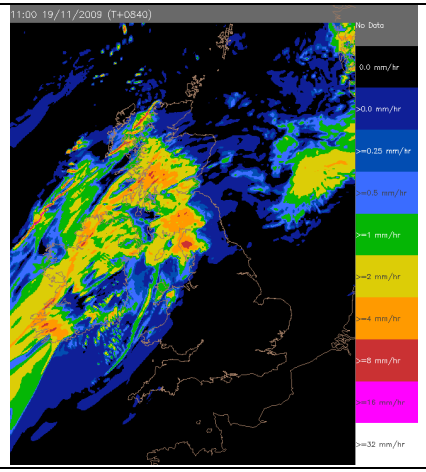
T+30 min blend of an extrapolation nowcast, a UKV control forecast and non-parametric noise valid at 1030 GMT on 19/11/2009	**T+13h 30 min UKV forecast valid at 1030 GMT on 19/11/2009**	**T+1 h blend of an extrapolation nowcast, a UKV control forecast and non-parametric noise valid at 1100 GMT on 19/11/2009**	**T+14 h UKV forecast valid at 1100 GMT on 19/11/2009**

© Crown copyright 2010

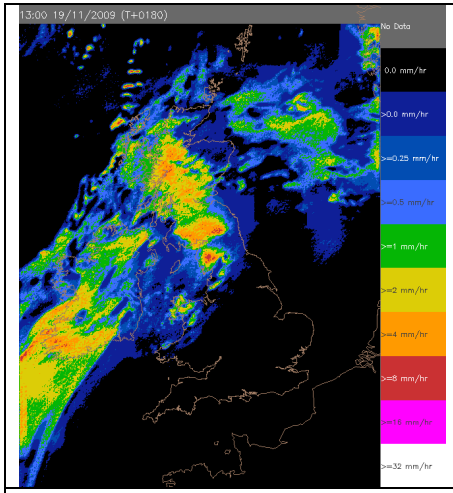	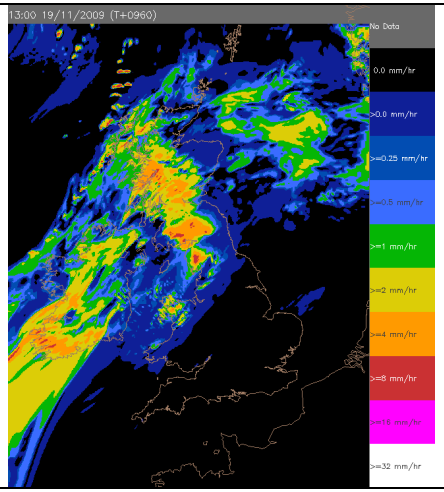	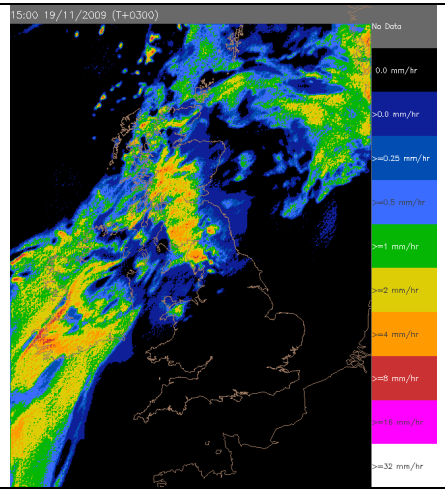	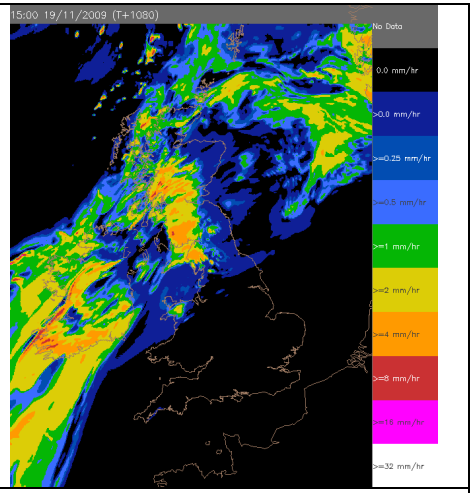
T+3 h blend of an extrapolation nowcast, a UKV control forecast and non-parametric noise valid at 1300 GMT on 19/11/2009	**T+16 h UKV forecast valid at 1300 GMT on 19/11/2009**	**T+5 h blend of an extrapolation nowcast, a UKV control forecast and non-parametric noise valid at 1500 GMT on 19/11/2009**	**T+18 h UKV control forecast valid at 1500 GMT on 19/11/2009**

Figure A1.14a Selected steps in a blended, control member forecast of precipitation rate, comprising an extrapolation nowcast, UKV control forecast and non-parametric noise (confined to scales ≤ 8 km), run from 1000 GMT on 19/11/2009. The UKPP rain analysis used as the starting point for the extrapolation nowcast is also shown, as well corresponding forecast steps from the associated UKV control member forecast (data time 2100 GMT, 18/11/2009).

© Crown copyright 2010

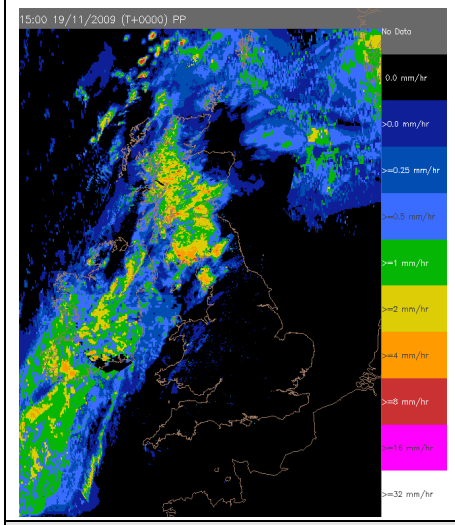

UKPP rain analysis valid at 1500 GMT on 19/11/2009

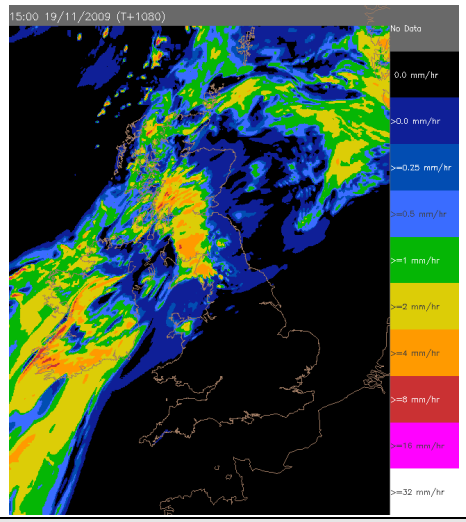

T+18 UKV control forecast valid at 1500 GMT on 19/11/2009

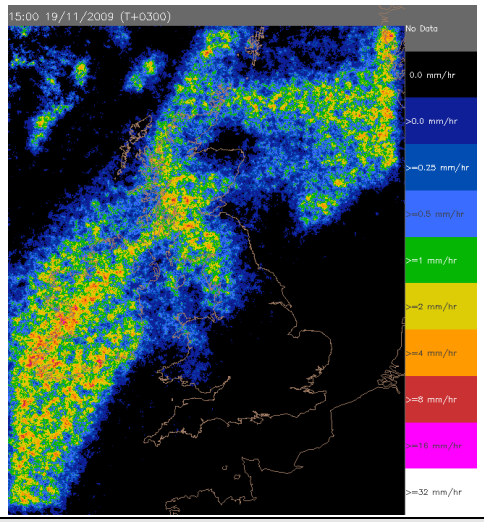

T+21 h MOGREPS-R downscale forecast valid at 1500 GMT on 19/11/2009

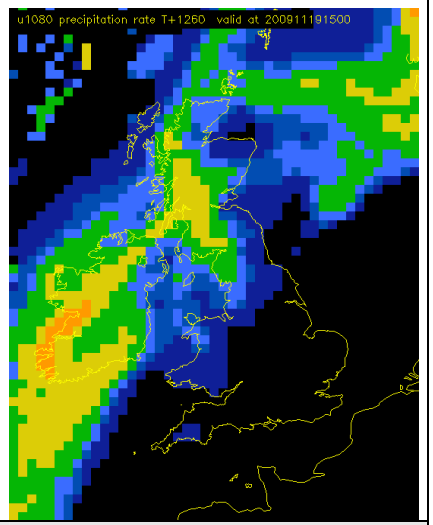

T+21 h MOGREPS-R forecast valid at 1500 GMT on 19/11/2009

© Crown copyright 2010

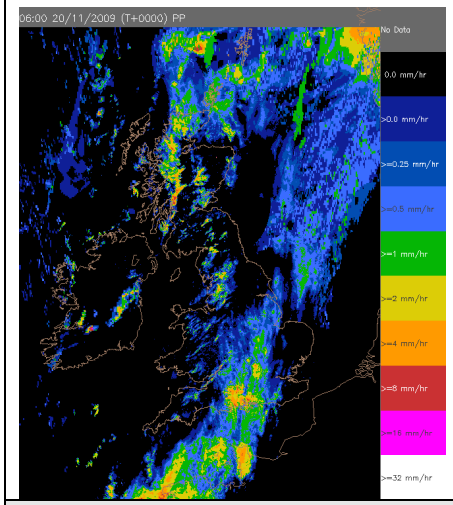

UKPP rain analysis valid at 0600 GMT on 20/11/2009

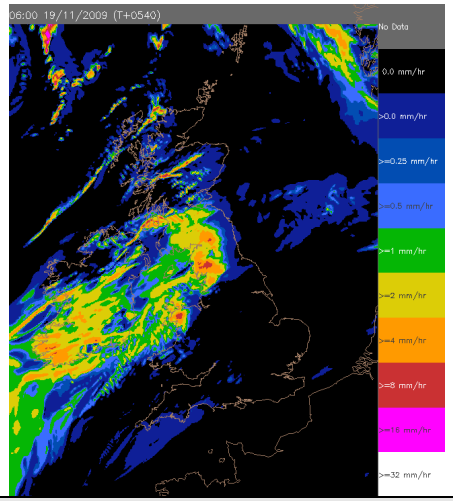

T+33 UKV control forecast valid at 0600 GMT on 20/11/2009

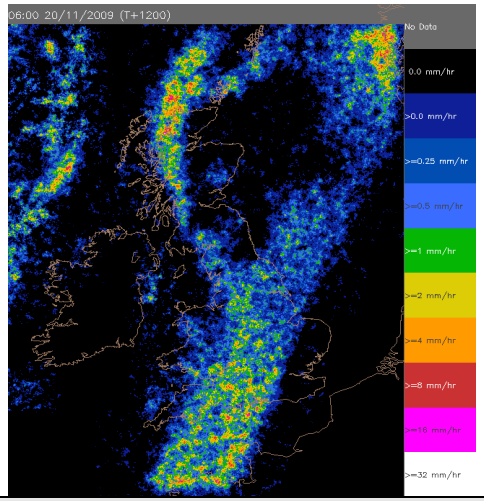

T+36 h MOGREPS-R downscale forecast valid at 0600 GMT on 20/11/2009

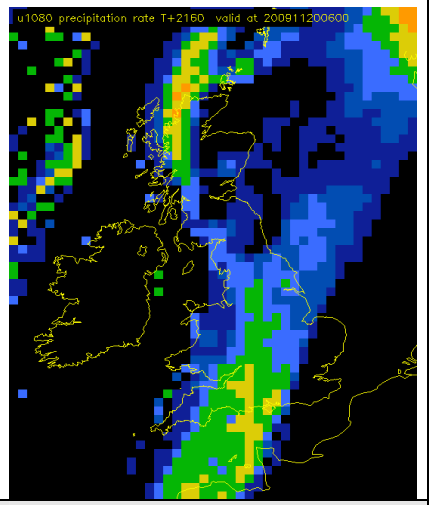

T+36 h MOGREPS-R forecast valid at 0600 GMT on 20/11/2009

Figure A1.14b Selected forecast steps in a blended, control member forecast of precipitation rate, comprising a MOGREPS-R control forecast and parametric noise (confined to scales ≤ 64 km), run from 1000 GMT on 19/11/2009 (3rd column from left). A corresponding sequence of UKPP rain analyses and forecasts steps from the associated MOGREPS-R control forecast (data time 1800 GMT, 18/11/2009) and UKV control forecast (data time 2100 GMT, 18/11/2009) are also shown for comparison.

© Crown copyright 2010

Case study 4 – 17/02/2010

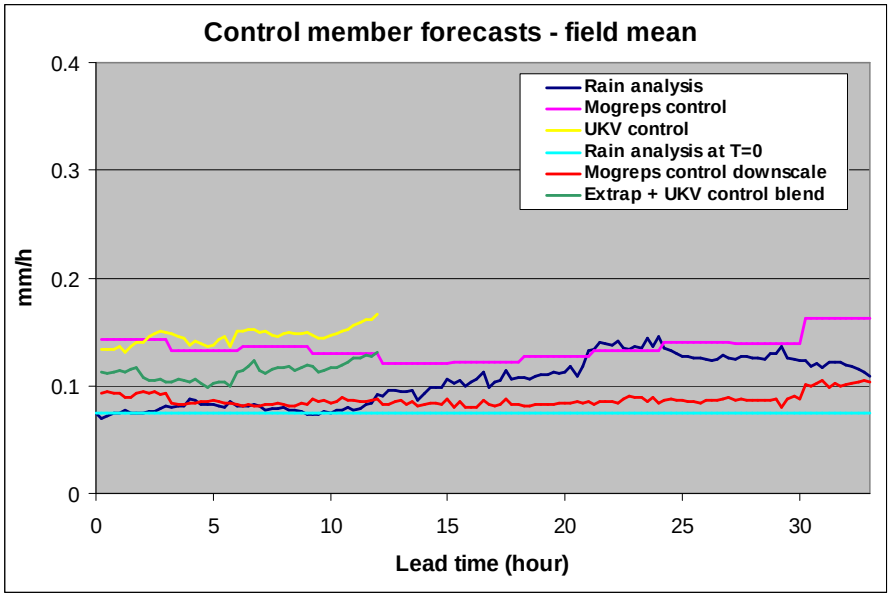

Figure A1.15 Time evolution of the field mean of UKPP rain analyses, MOGREPS-R and UKV control member forecasts and the two configurations of blended forecast for 17/02/3010. The forecast lead times on the X axis are those of the blended forecasts (run from 0900 GMT on 17/02/2010). The UKV and MOGREPS-R forecasts were run from 2100 GMT and 1800 GMT respectively on 16/02/2010.

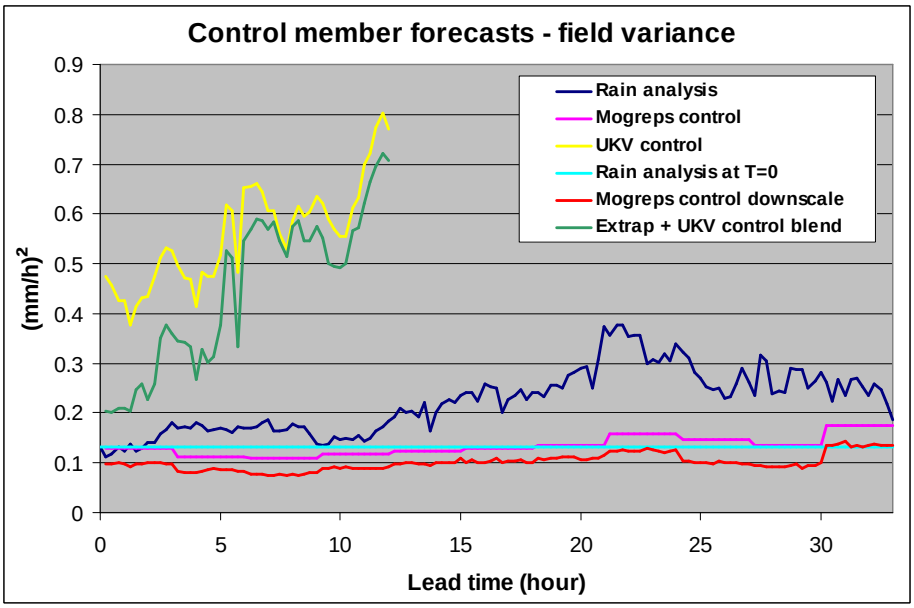

Figure A1.16 Time evolution of the field variance of UKPP rain analyses, MOGREPS-R and UKV control member forecasts and the two configurations of blended forecast for 17/02/2010. The forecast lead times on the X axis are those of the blended forecasts (run from 0900 GMT on 17/02/2010).

© Crown copyright 2010

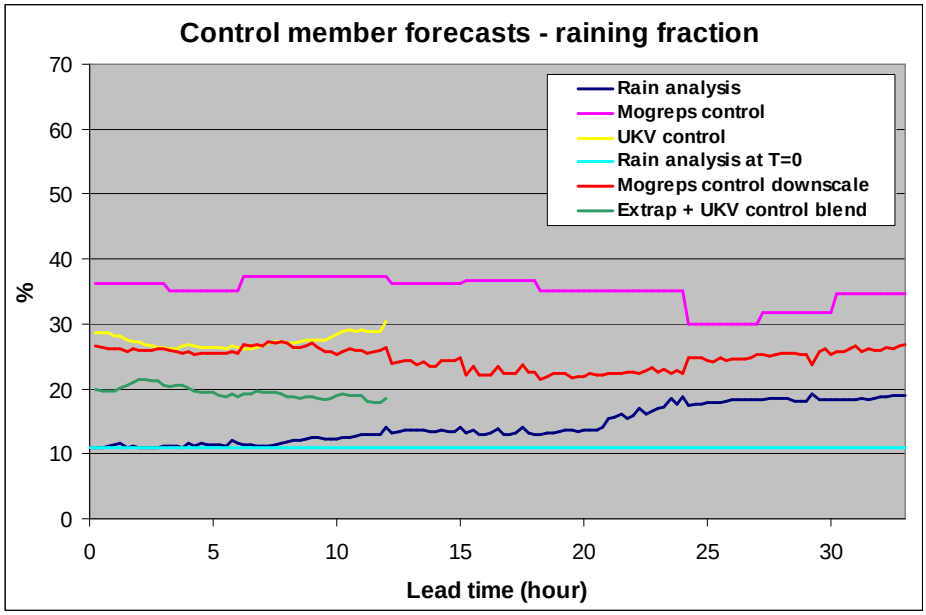

Figure A1.17 Time evolution of the raining fraction of UKPP rain analyses, MOGREPS-R and UKV control member forecasts and the two configurations of blended forecast for 17/02/2010. The forecast lead times on the X axis are those of the blended forecasts (run from 0900 GMT on 17/02/2010).

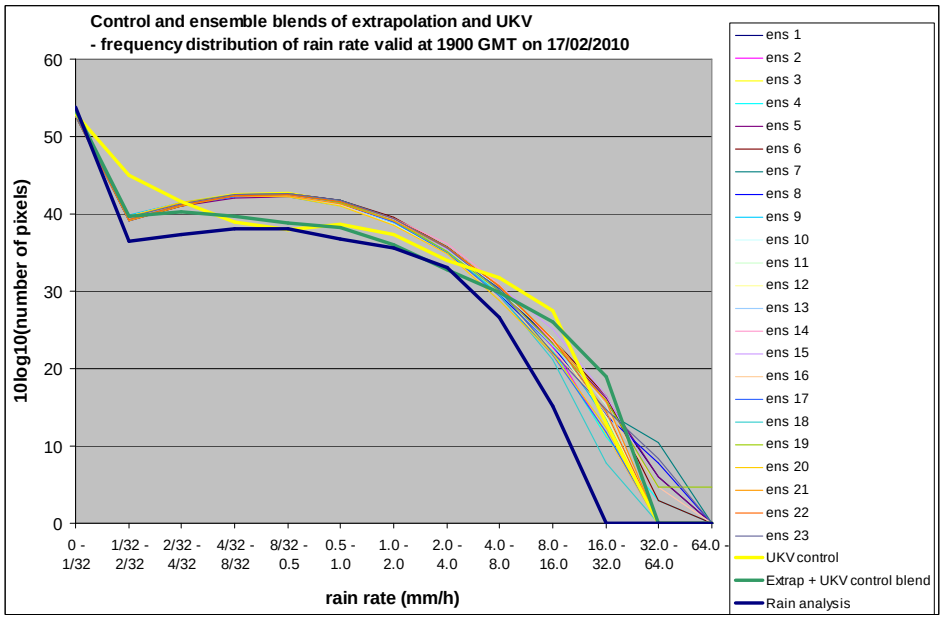

Figure A1.18 Frequency distributions of precipitation rate for a UKPP rain analysis, a 2 km resolution UKV control member forecast, and a blended control forecast and 23 member ensemble forecast incorporating an extrapolation nowcast and UKV control forecast, all valid at 1900 GMT on 17/02/2010. The blended forecasts were run from 0900 GMT on 17/02/2010 and the UKV control forecast from 2100 GMT on the previous day. The validation area is the UK radar composite.

© Crown copyright 2010

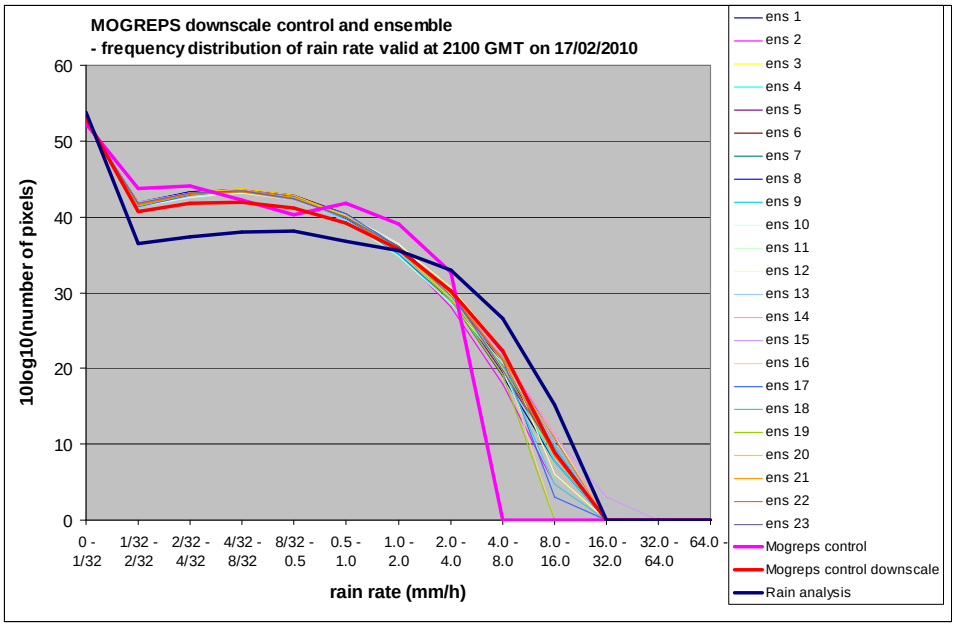

Figure A1.19 Frequency distributions of precipitation rate for a UKPP rain analyses, a 24 km resolution MOGREPS-R control member and its downscaled counterpart, and 23 members of a downscaled MOGREPS-R control forecast, all valid at 2100 GMT on 17/02/2010. The MOGREPS-R control forecast was run from 1800 GMT on 16/02/2010. The validation area is the UK radar composite.

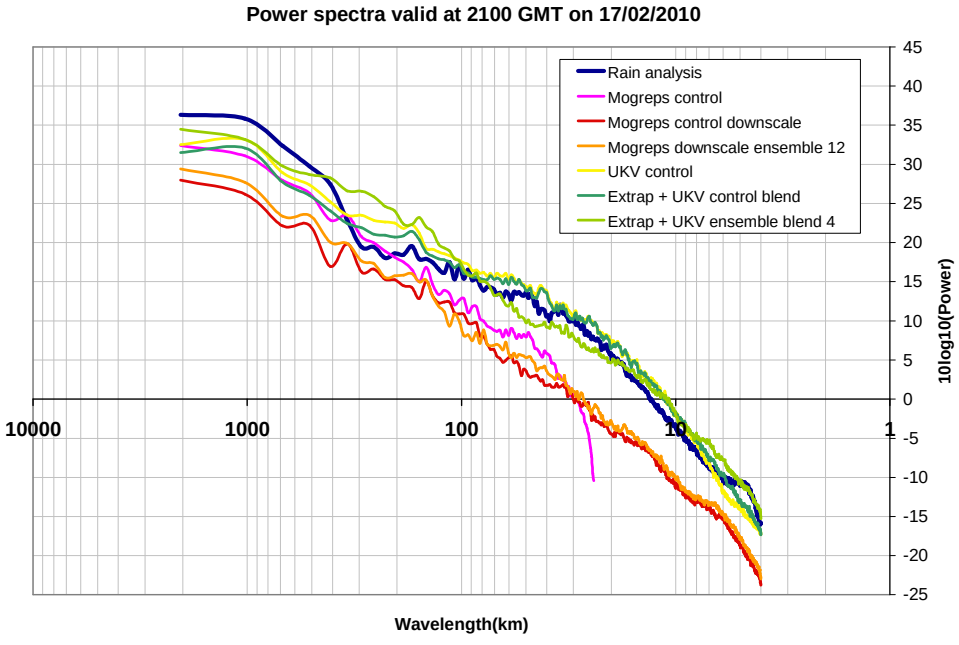

Figure A1.20 Power spectra for a UKPP rain analysis, MOGREPS-R (T+27 h) and UKV (T+24h) control member forecasts and the two configurations of blended forecasts (T+12 h) all valid at 2100 GMT on 17/02/2010.

© Crown copyright 2010

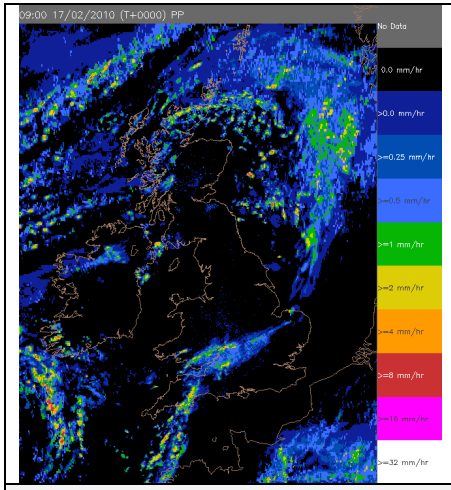	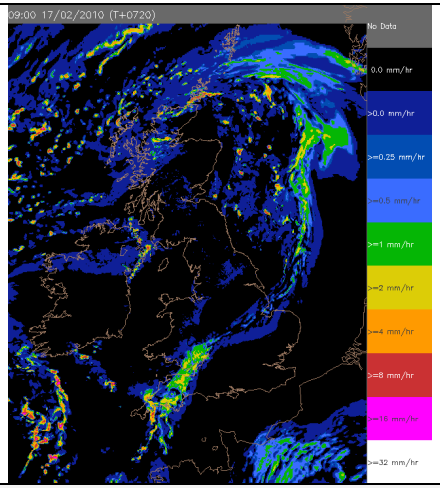	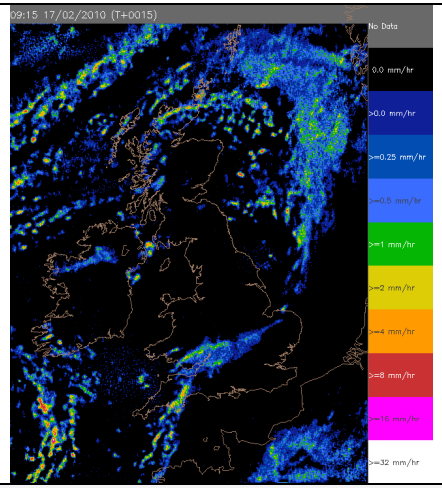	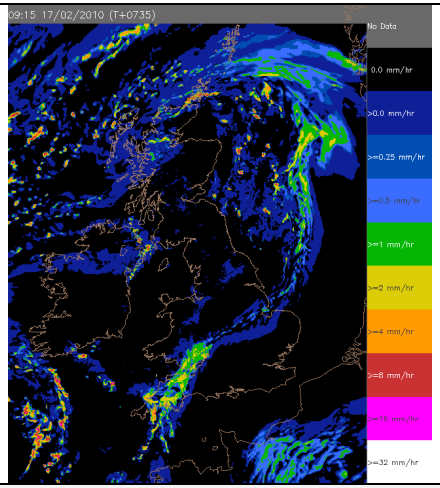
UKPP rain analysis valid at 0900 GMT on 17/02/2010	**T+12h UKV forecast valid at 0900 GMT on 17/02/2010**	**T+15 min blend of an extrapolation nowcast, a UKV control forecast and non-parametric noise valid at 0915 GMT on 17/02/2010**	**T+12h 15 min UKV forecast valid at 0915 GMT on 17/02/2010**
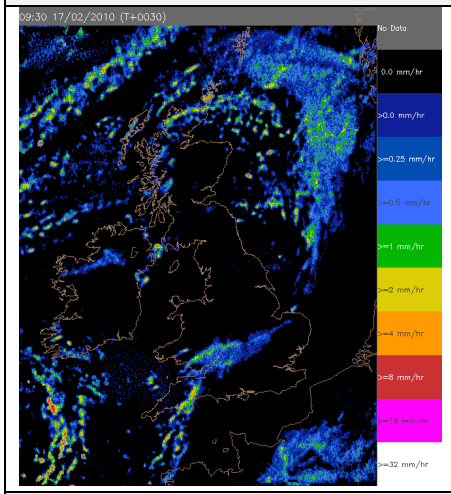	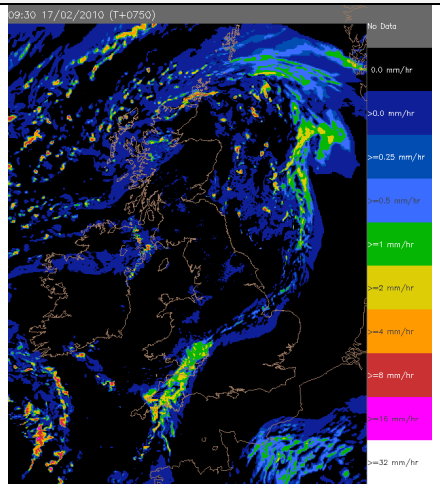	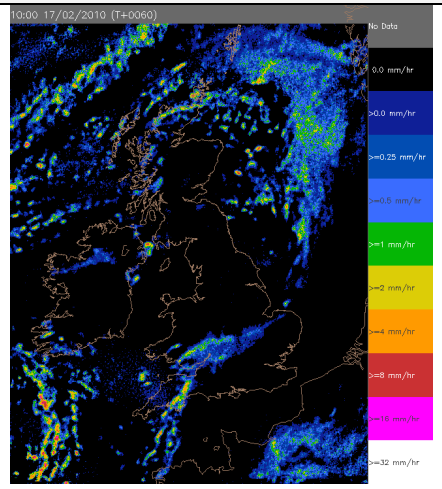	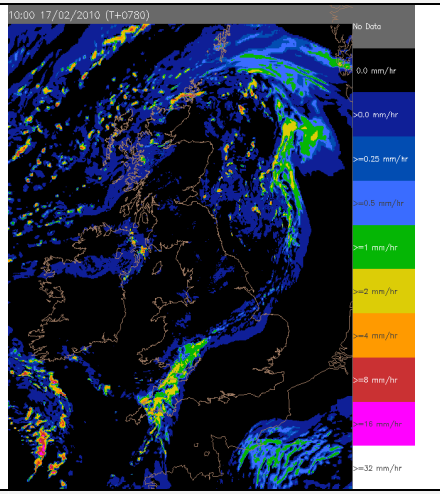
T+30 min blend of an extrapolation nowcast, a UKV control forecast and non-parametric noise valid at 0930 GMT on 17/02/2010	**T+12h 30 min UKV forecast valid at 0930 GMT on 17/02/2010**	**T+1 h blend of an extrapolation nowcast, a UKV control forecast and non-parametric noise valid at 1000 GMT on 17/02/2010**	**T+13 h UKV forecast valid at 1000 GMT on 17/02/2010**

© Crown copyright 2010

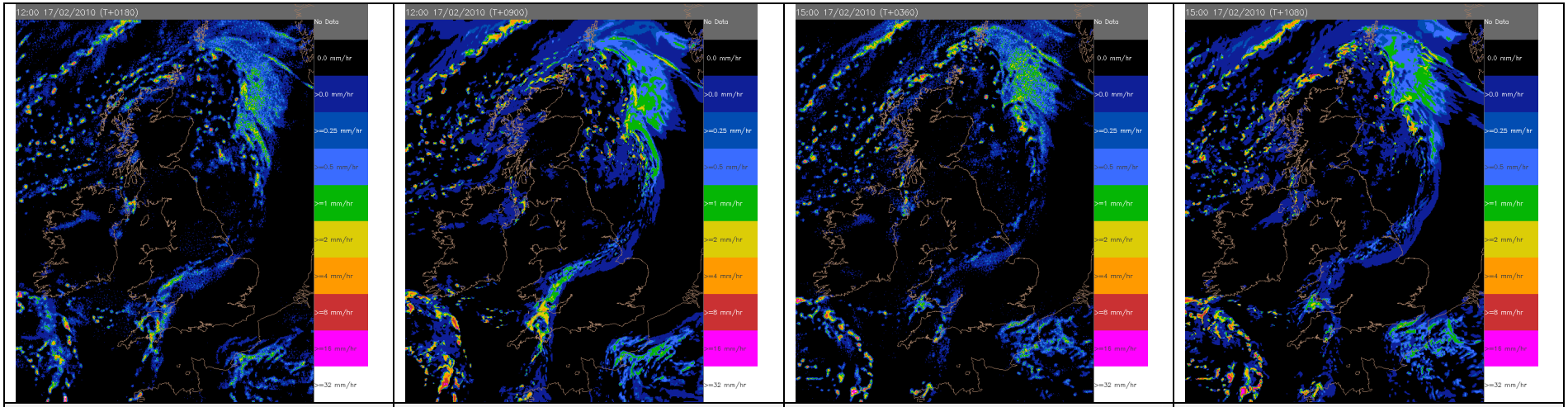

T+3 h blend of an extrapolation nowcast, a UKV control forecast and non-parametric noise valid at 1200 GMT on 17/02/2010	**T+13 h UKV forecast valid at 1200 GMT on 17/02/2010**	**T+6 h blend of an extrapolation nowcast, a UKV control forecast and non-parametric noise valid at 1500 GMT on 17/02//2010**	**T+16 h UKV control forecast valid at 1500 GMT on 17/02/2010**

Figure A1.21a Selected steps in a blended, control member forecast of precipitation rate, comprising an extrapolation nowcast, UKV control forecast and non-parametric noise (confined to scales ≤ 8 km), run from 0900 GMT on 17/02/2010. The UKPP rain analysis used as the starting point for the extrapolation nowcast is also shown, as well corresponding forecast steps from the associated UKV control member forecast (data time 2100 GMT, 16/02/2010).

© Crown copyright 2010

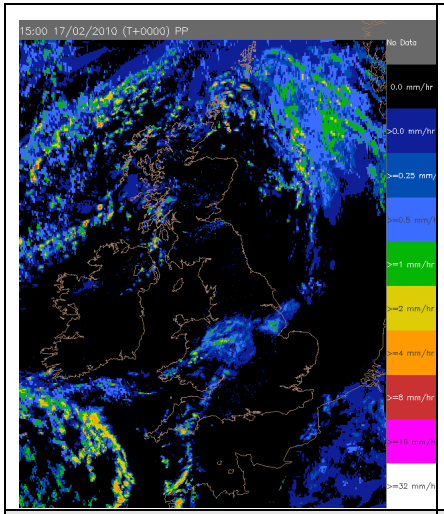

UKPP rain analysis valid at 1500 GMT on 17/02/2010

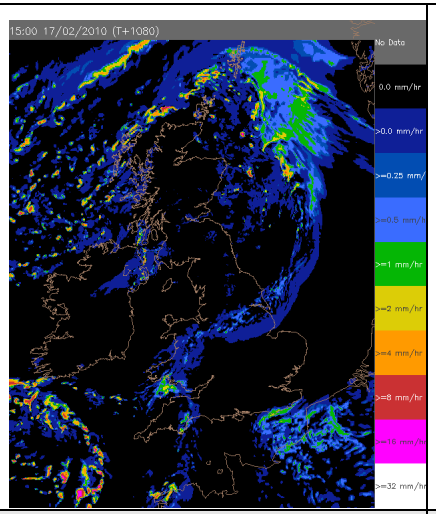

T+18 UKV control forecast valid at 1500 GMT on 17/02/2010

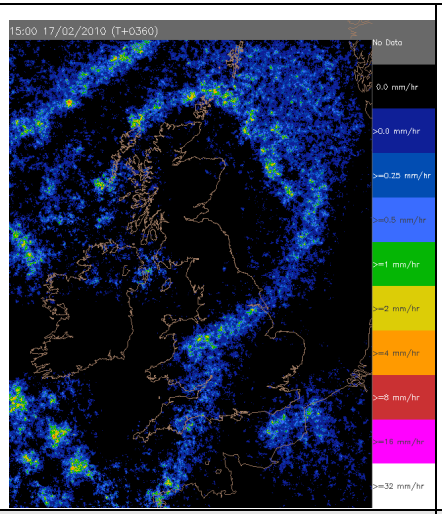

T+21 h MOGREPS-R downscale forecast valid at 1500 GMT on 17/02//2010

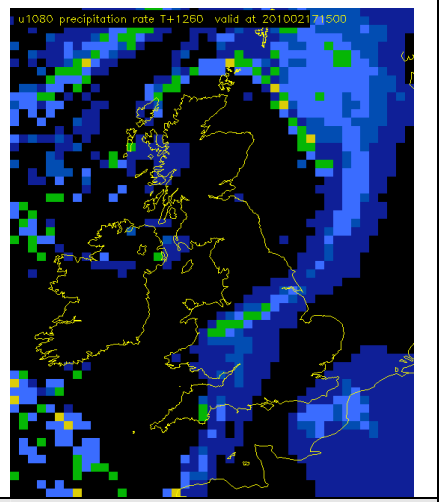

T+21 h MOGREPS-R forecast valid at 1500 GMT on 17/02/2010

© Crown copyright 2010

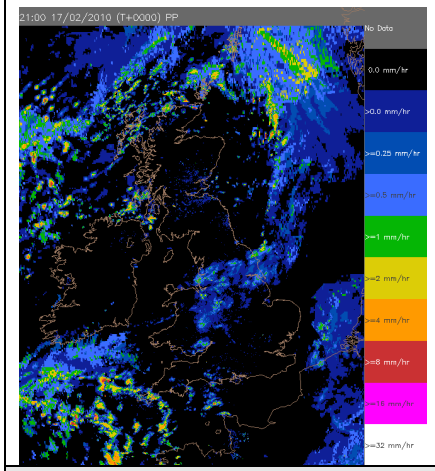

UKPP rain analysis valid at 2100 GMT on 17/02/2010

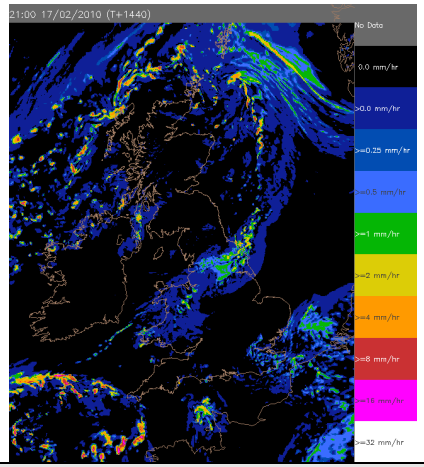

T+24 UKV control forecast valid at 2100 GMT on 17/02/2010

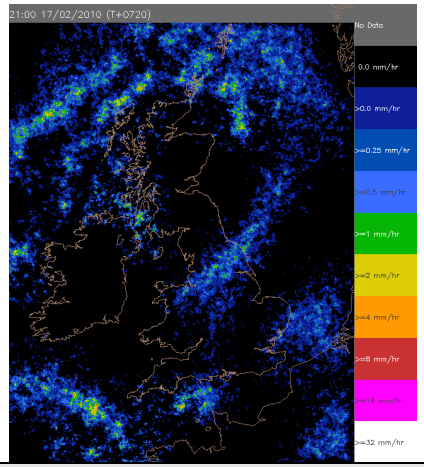

T+27h MOGREPS-R downscale forecast valid at 2100 GMT on 17/02//2010

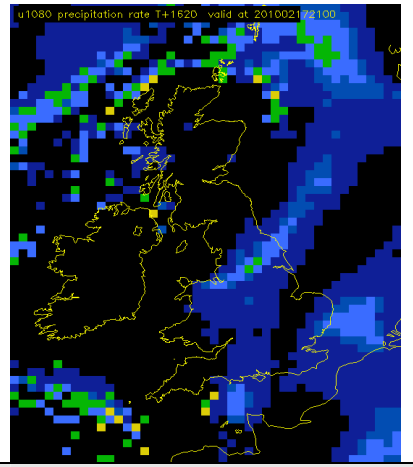

T+27h MOGREPS-R forecast valid at 2100 GMT on 17/02//2010

Figure A1.21b Selected forecast steps in a blended, control member forecast of precipitation rate, comprising a MOGREPS-R control forecast and parametric noise (confined to scales ≤ 64 km), run from 0900 GMT on 17/02/2010 (3rd column from left). A corresponding sequence of UKPP rain analyses and forecasts steps from the associated MOGREPS-R control forecast (data time 1800 GMT, 16/02/2010) and UKV control forecast (data time 2100 GMT, 16/02/2010) are also shown for comparison.

© Crown copyright 2010

10.2. Appendix A.2 Case study oriented verification for ensembles of blended forecasts

Case study 1 – 05/09/2008

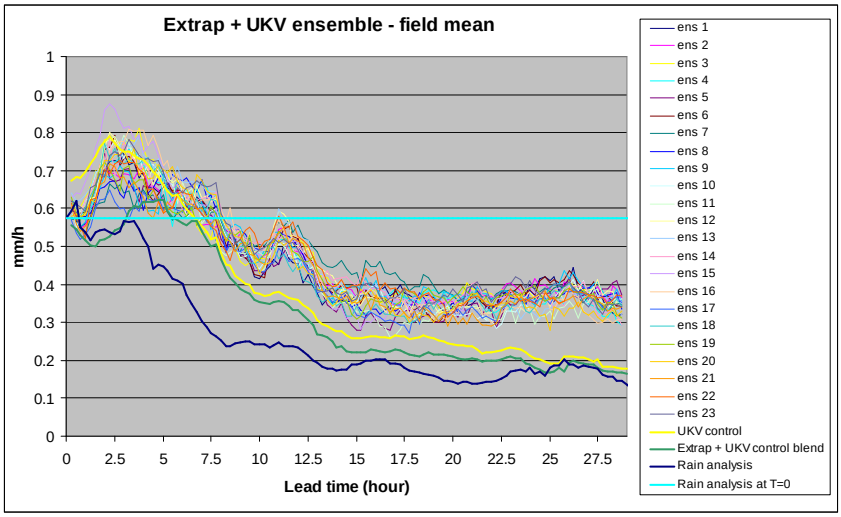

Figure A2.1 Time evolution of the field mean of UKPP rain analyses, a UKV control member forecast (data time 0600 GMT on 05/09/2008), and blended ensemble forecasts (data time 1300 GMT on 05/09/2008) comprising extrapolation, UKV and non-parametric noise. The forecast lead times on the X axis are those of the blended forecasts (run from 1300 GMT).

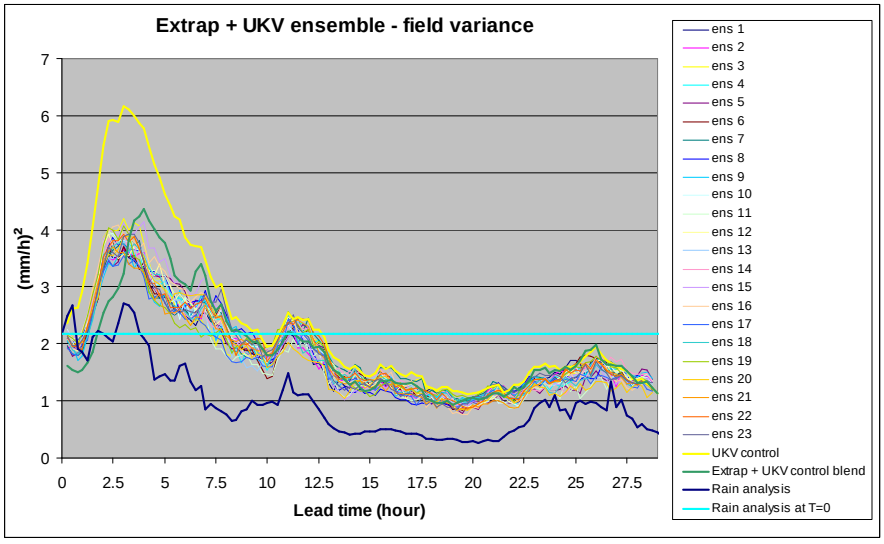

Figure A2.2 Time evolution of the field variance of UKPP rain analyses, a UKV control member forecast (data time 0600 GMT on 05/09/2008), and blended ensemble forecasts (data time 1300 GMT on 05/09/2008) comprising extrapolation, UKV and non-parametric noise. The forecast lead times on the X axis are those of the blended forecasts (run from 1300 GMT).

© Crown copyright 2010

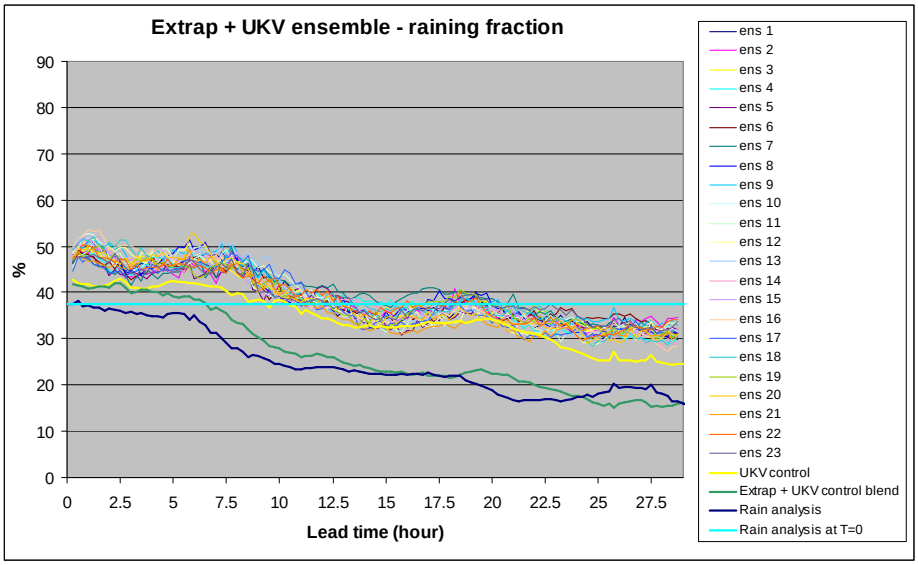

Figure A2.3 Time evolution of the field raining fraction of UKPP rain analyses, a UKV control member forecast (data time 0600 GMT on 05/09/2008), and blended ensemble forecasts (data time 1300 GMT on 05/09/2008) comprising extrapolation, UKV and non-parametric noise. The forecast lead times on the X axis are those of the blended forecasts (run from 1300 GMT).

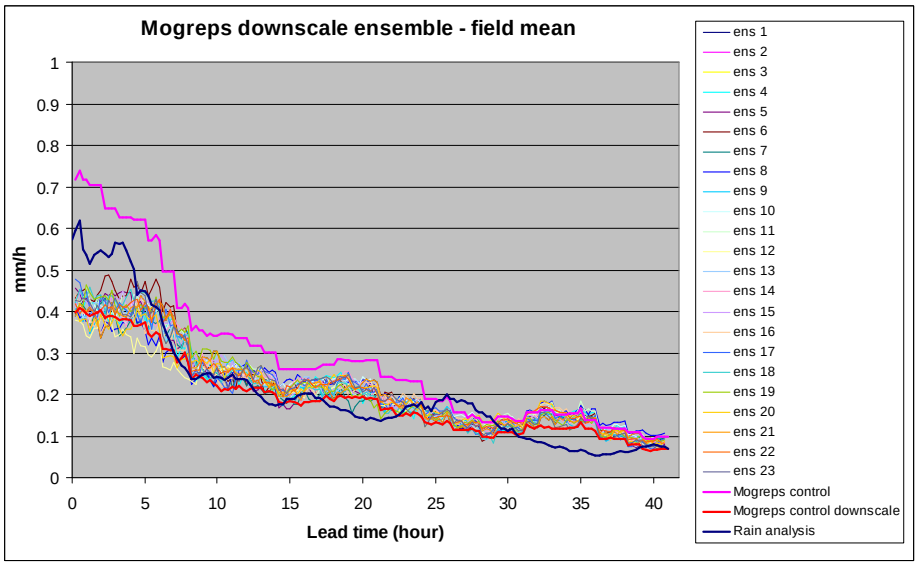

Figure A2.4 Time evolution of the field mean of UKPP rain analyses, a MOGREPS-R control member forecast (data time 0600 GMT on 05/09/2008), and control and ensemble blended forecasts (data time 1300 GMT on 05/09/2008) comprising MOGREPS-R and parametric noise. The forecast lead times on the X axis are those of the blended forecasts (run from 1300 GMT).

© Crown copyright 2010

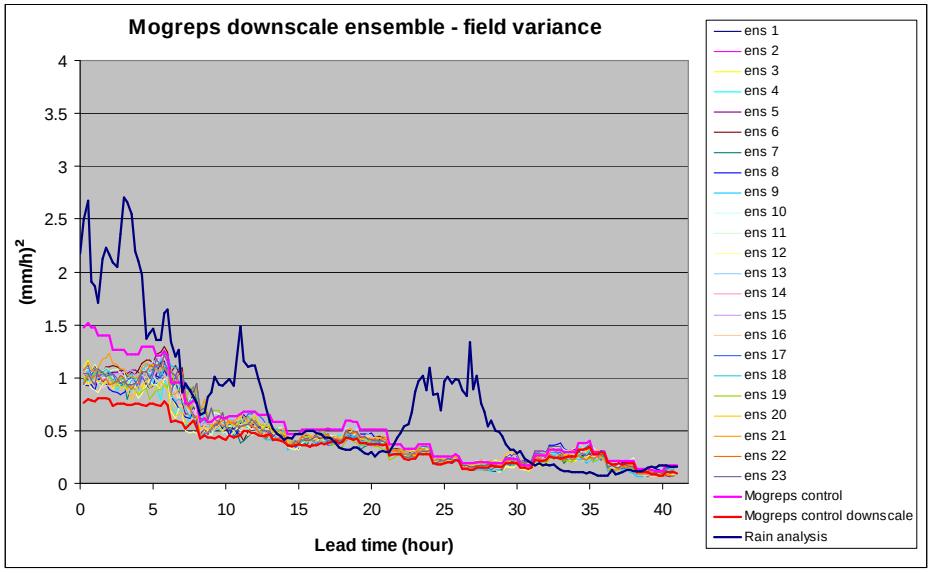

Figure A2.5 Time evolution of the field variance of UKPP rain analyses, a MOGREPS-R control member forecast (data time 0600 GMT on 05/09/2008), and control and ensemble blended forecasts (data time 1300 GMT on 05/09/2008) comprising MOGREPS-R and parametric noise. The forecast lead times on the X axis are those of the blended forecasts (run from 1300 GMT).

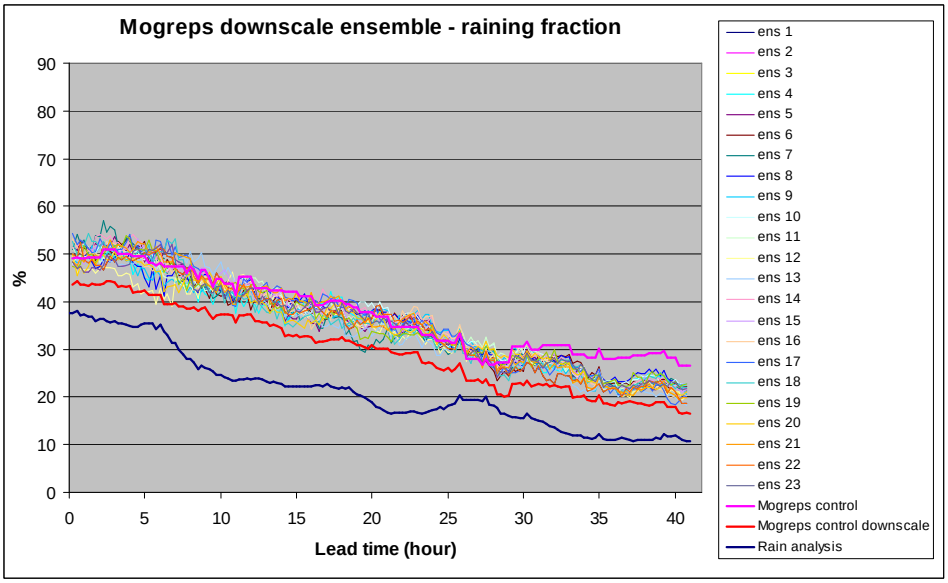

Figure A2.6 Time evolution of the field raining fraction of UKPP rain analyses, a MOGREPS-R control member forecast (data time 0600 GMT on 05/09/2008), and control and ensemble blended forecasts (data time 1300 GMT on 05/09/2008) comprising MOGREPS-R and parametric noise. The forecast lead times on the X axis are those of the blended forecasts (run from 1300 GMT).

© Crown copyright 2010

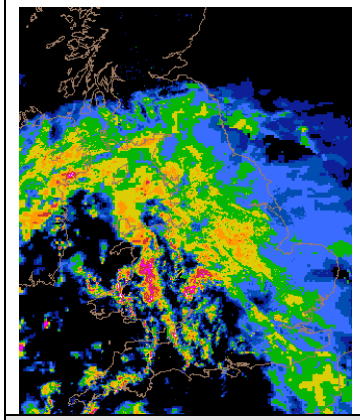	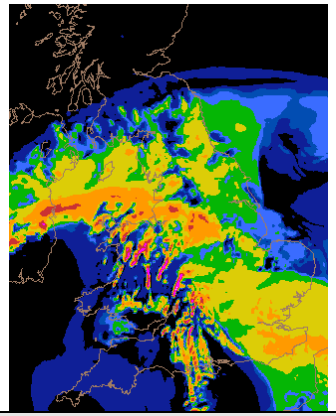	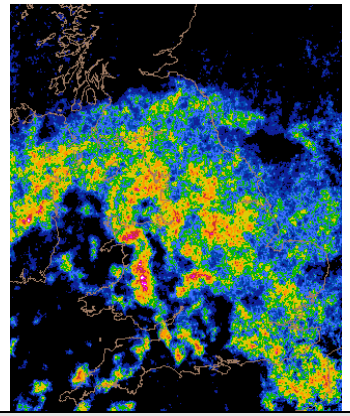	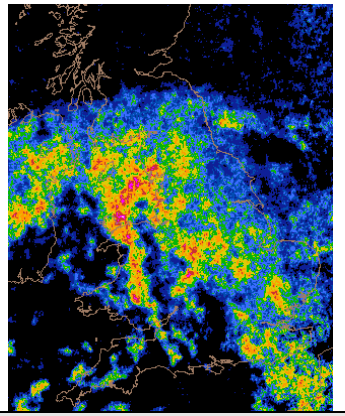
UKPP rain analysis valid at 1315 GMT on 05/09/2008	**T+7 h 15 min UKV control forecast valid at 1330 GMT on 05/09/2008**	**Member 1 of a T+15 min blend of an extrapolation nowcast, a UKV control forecast and non-parametric noise valid at 1315 GMT on 05/09/2008**	**Member 2 of a T+15 min blend of an extrapolation nowcast, a UKV control forecast and non-parametric noise valid at 1315 GMT on 05/09/2008**
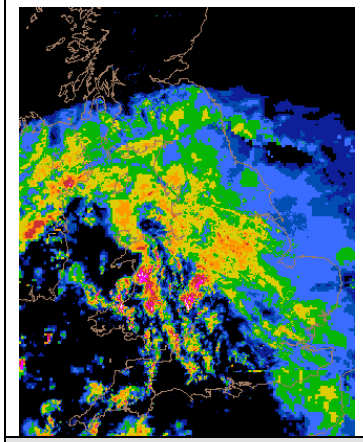	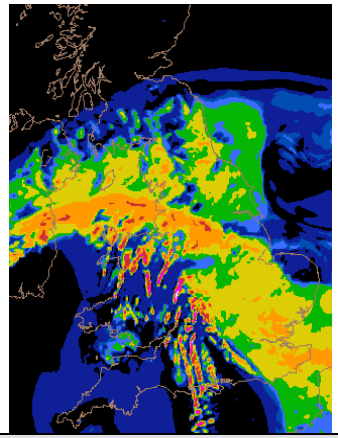	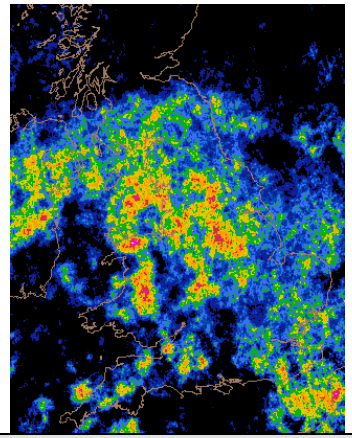	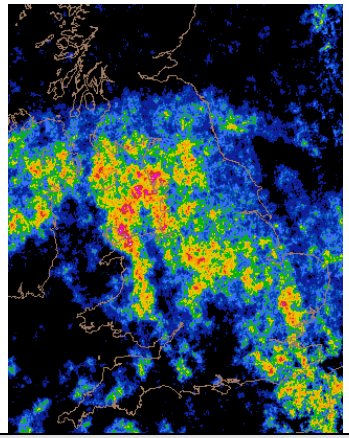
UKPP rain analysis valid at 1330 GMT on 05/09/2008	**T+7 h 30 min UKV control forecast valid at 1330 GMT on 05/09/2008**	**Member 1 of a T+30 min blend of an extrapolation nowcast, a UKV control forecast and non-parametric noise valid at 1330 GMT on 05/09/2008**	**Member 2 of a T+30 min blend of an extrapolation nowcast, a UKV control forecast and non-parametric noise valid at 1330 GMT on 05/09/2008**

© Crown copyright 2010

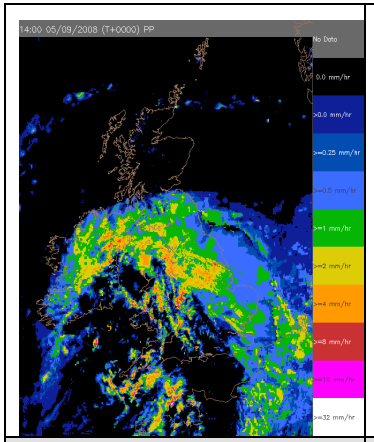

UKPP rain analysis valid at 1400 GMT on 05/09/2008

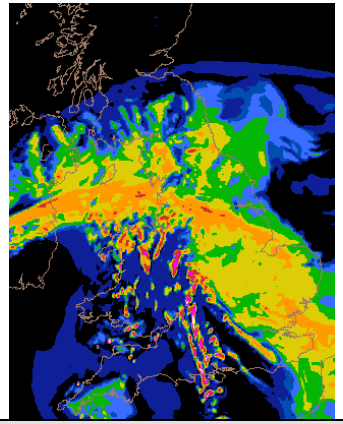

T+8 h UKV control forecast valid at 1400 GMT on 05/09/2008

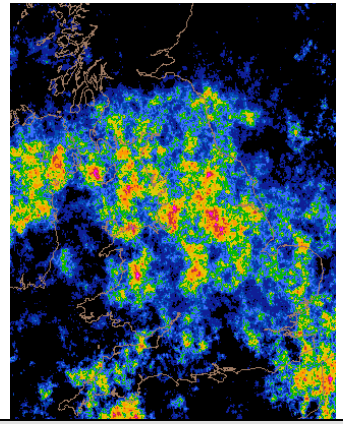

Member 1 of a T+1 h blend of an extrapolation nowcast, a UKV control forecast and non-parametric noise valid at 1400 GMT on 05/09/2008

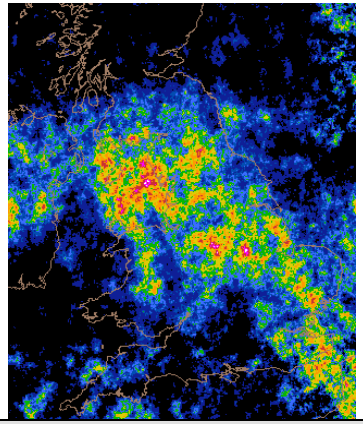

Member 2 of a T+1 h blend of an extrapolation nowcast, a UKV control forecast and non-parametric noise valid at 1400 GMT on 05/09/2008

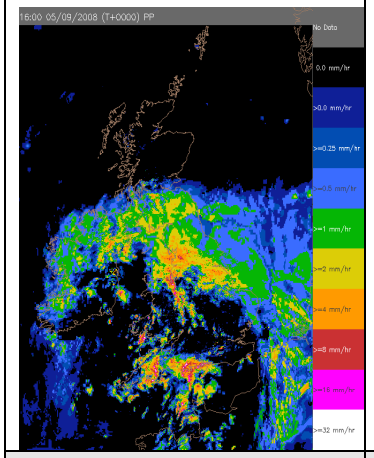

UKPP rain analysis valid at 1600 GMT on 05/09/2008

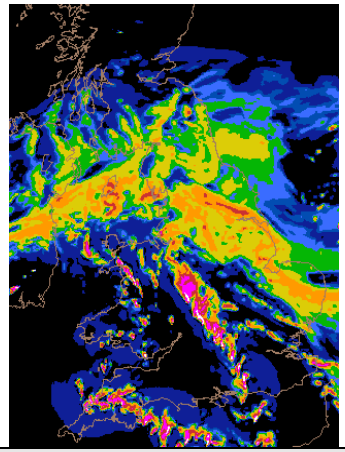

T+10 h UKV control forecast valid at 1600 GMT on 05/09/2008

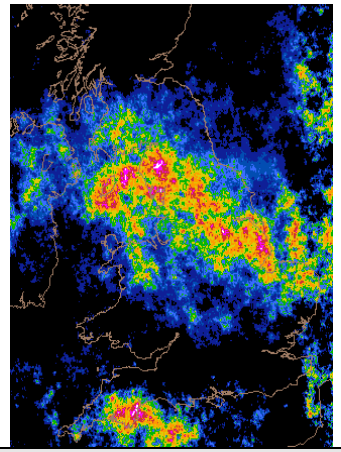

Member 1 of a T+3 h blend of an extrapolation nowcast, a UKV control forecast and non-parametric noise valid at 1600 GMT on 05/09/2008

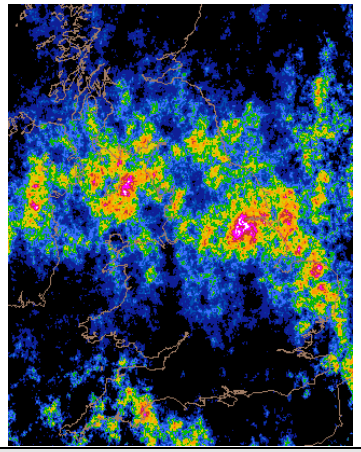

Member 2 of a T+3 h blend of an extrapolation nowcast, a UKV control forecast and non-parametric noise valid at 1600 GMT on 05/09/2008

© Crown copyright 2010

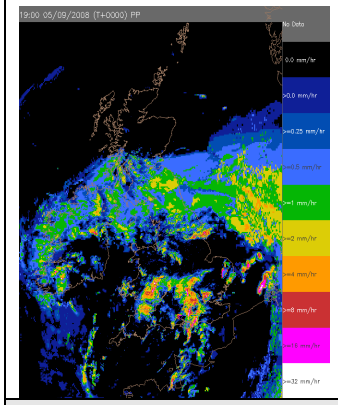	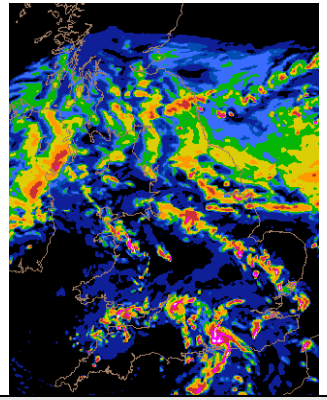	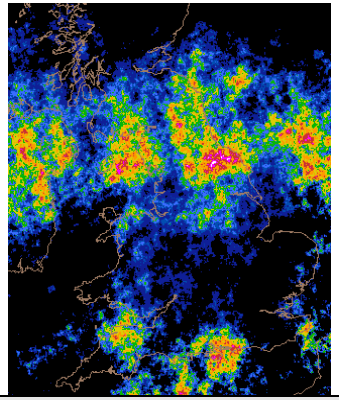	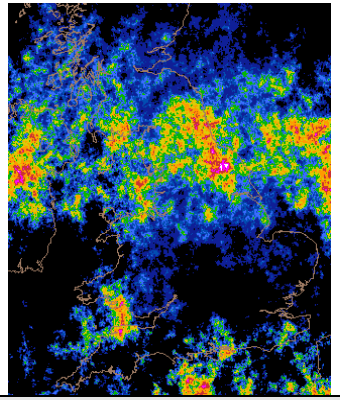
UKPP rain analysis valid at 1900 GMT on 05/09/2008	**T+13 h UKV control forecast valid at 1900 GMT on 05/09/2008**	**Member 1 of a T+6 h blend of an extrapolation nowcast, a UKV control forecast and non-parametric noise valid at 1900 GMT on 05/09/2008**	**Member 2 of a T+6 h blend of an extrapolation nowcast, a UKV control forecast and non-parametric noise valid at 1900 GMT on 05/09/2008**
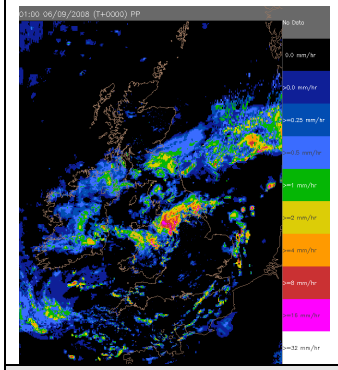	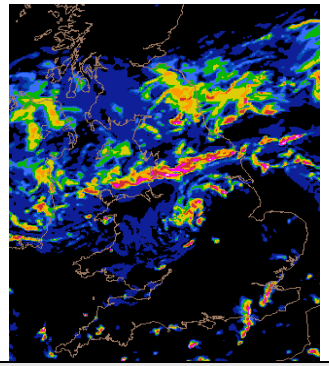	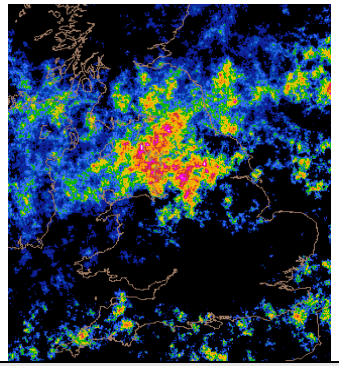	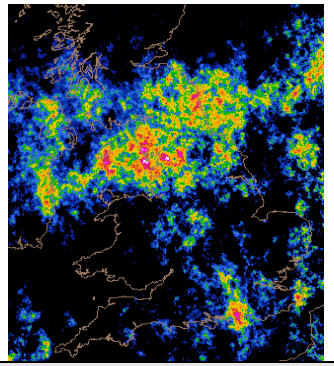
UKPP rain analysis valid at 0100 GMT on 05/09/2008	**T+19 h UKV control forecast valid at 0100 GMT on 05/09/2008**	**Member 1 of a T+12 h blend of an extrapolation nowcast, a UKV control forecast and non-parametric noise valid at 0100 GMT on 05/09/2008**	**Member 2 of a T+12 h blend of an extrapolation nowcast, a UKV control forecast and non-parametric noise valid at 0100 GMT on 05/09/2008**

A2.7a Selected steps in two members of a blended ensemble forecast of precipitation rate, comprising an extrapolation nowcast, UKV control forecast and non-parametric noise, run from 1300 GMT on 29/10/2008. The UKPP rain analysis used as the starting point for the extrapolation nowcast is also shown, as well corresponding forecast steps from the associated UKV control member forecast (data time 0600 GMT, 29/10/2008).

© Crown copyright 2010

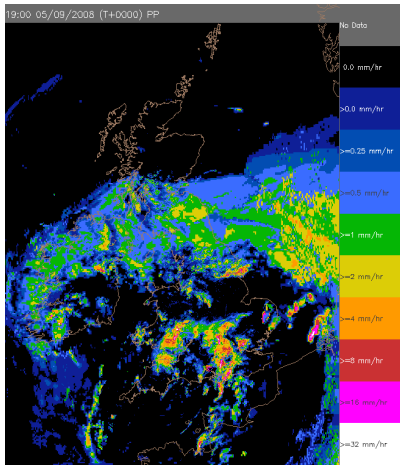

UKPP rain analysis valid at 1900 GMT on 05/09/2008

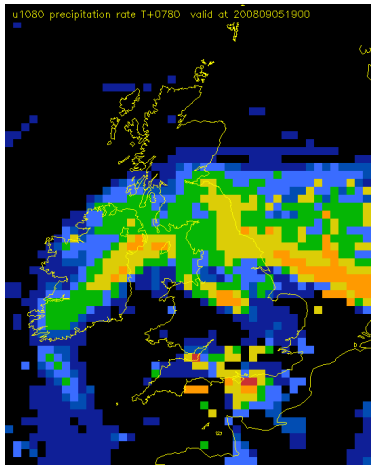

MOGREPS-R T+13 h forecast valid at 1900 GMT on 05/09/2008

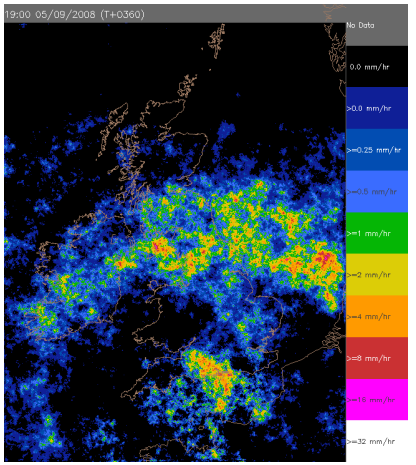

Member 1 of MOGREPS-R T+13 h downscale ensemble forecast valid at 1900 GMT on 05/09/2008

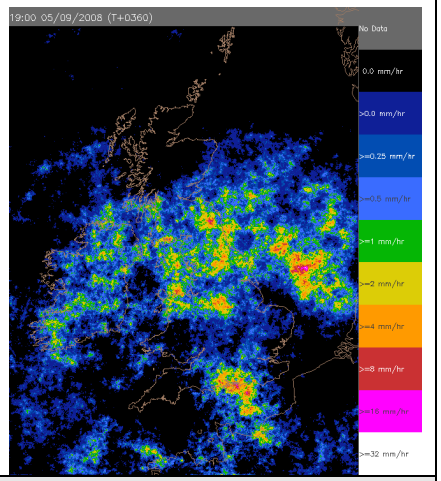

Member 2 of MOGREPS-R T+13 h downscale ensemble forecast valid at 1900 GMT on 05/09/2008

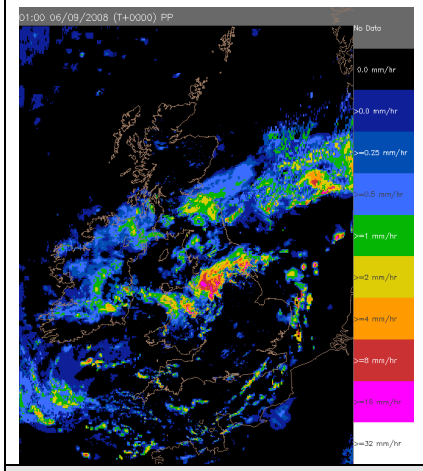

UKPP rain analysis valid at 0100 GMT on 06/09/2008

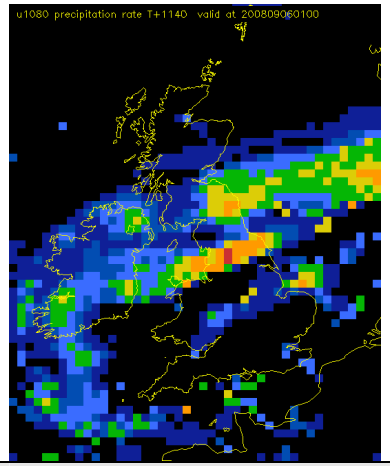

MOGREPS-R T+19 h forecast valid at 0100 GMT on 06/09/2008

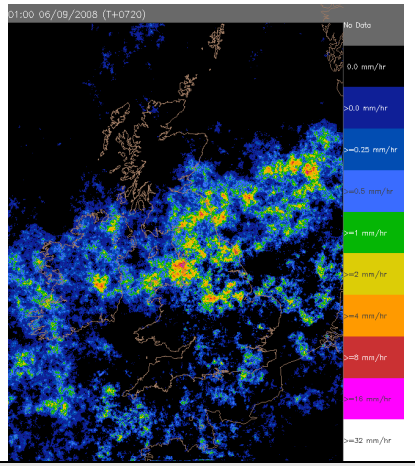

Member 1 of MOGREPS-R T+19 h downscale ensemble forecast valid at 0100 GMT on 06/09/2008

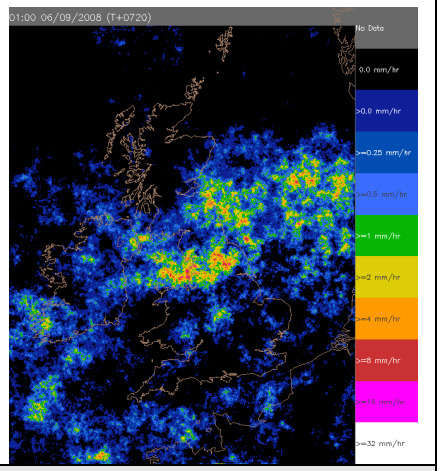

Member 2 of MOGREPS-R T+19 h downscale ensemble forecast valid at 0100 GMT on 06/09/2008

© Crown copyright 2010

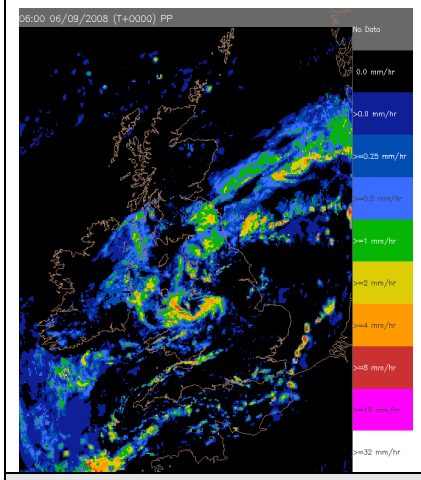

UKPP rain analysis valid at 0600 GMT on 06/09/2008

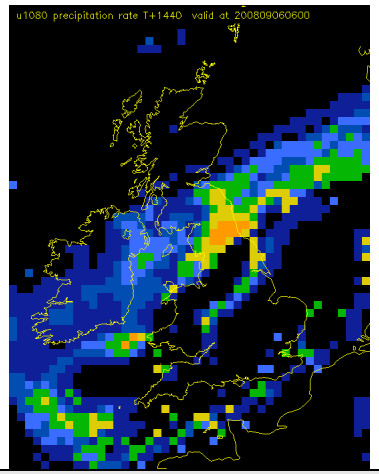

MOGREPS-R T+24 h forecast valid at 0600 GMT on 06/09/2008

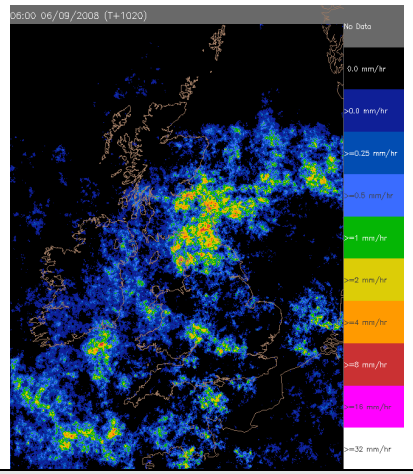

Member 1 of MOGREPS-R T+24 h downscale ensemble forecast valid at 0600 GMT on 06/09/2008

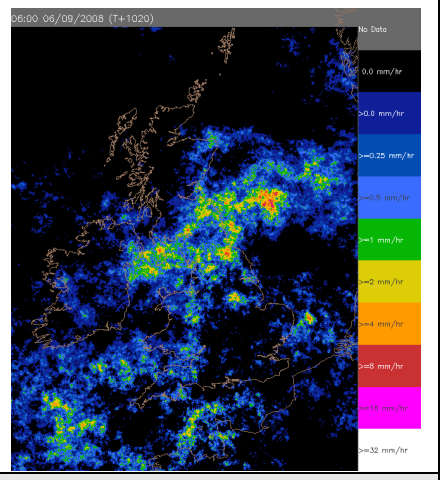

Member 2 of MOGREPS-R T+24 h downscale ensemble forecast valid at 0600 GMT on 06/09/2008

A2.7b Selected forecast steps in two members of a blended ensemble forecast of precipitation rate, comprising a MOGREPS-R control forecast and parametric noise, run from 1300 GMT on 05/09/2008 (3rd column from left). A corresponding sequence of UKPP rain analyses and forecasts steps from the associated MOGREPS-R control forecast (data time 0600 GMT, 05/09/2008) are also shown for comparison.

© Crown copyright 2010

Case study 3 – 19/11/2009

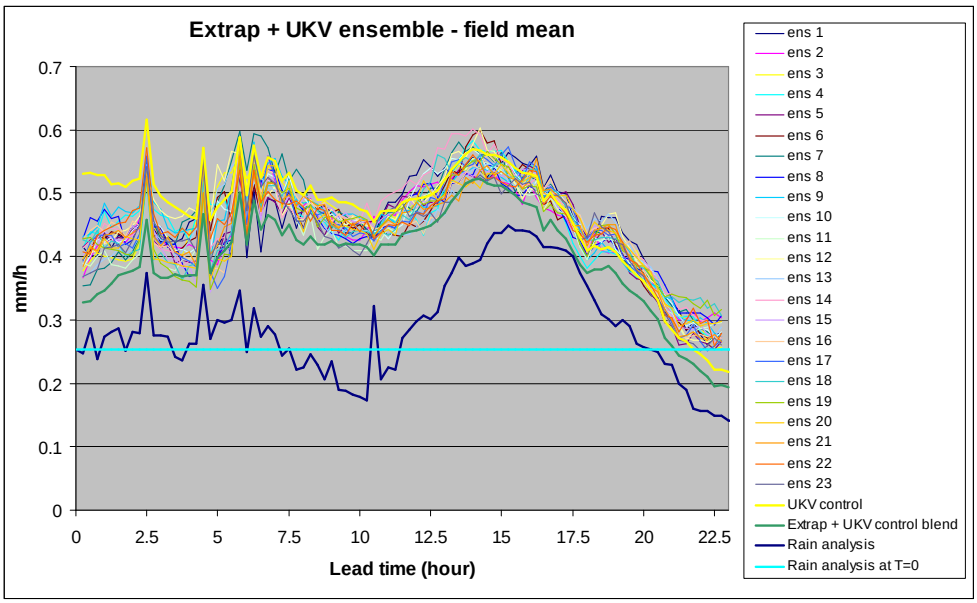

Figure A2.8 Time evolution of the field mean of UKPP rain analyses, a UKV control member forecast (data time 2100 GMT on 18/11/2009), and blended ensemble forecasts (data time 1000 GMT on 19/11/2009) comprising extrapolation, UKV and non-parametric noise. The forecast lead times on the X axis are those of the blended forecasts (run from 1000 GMT).

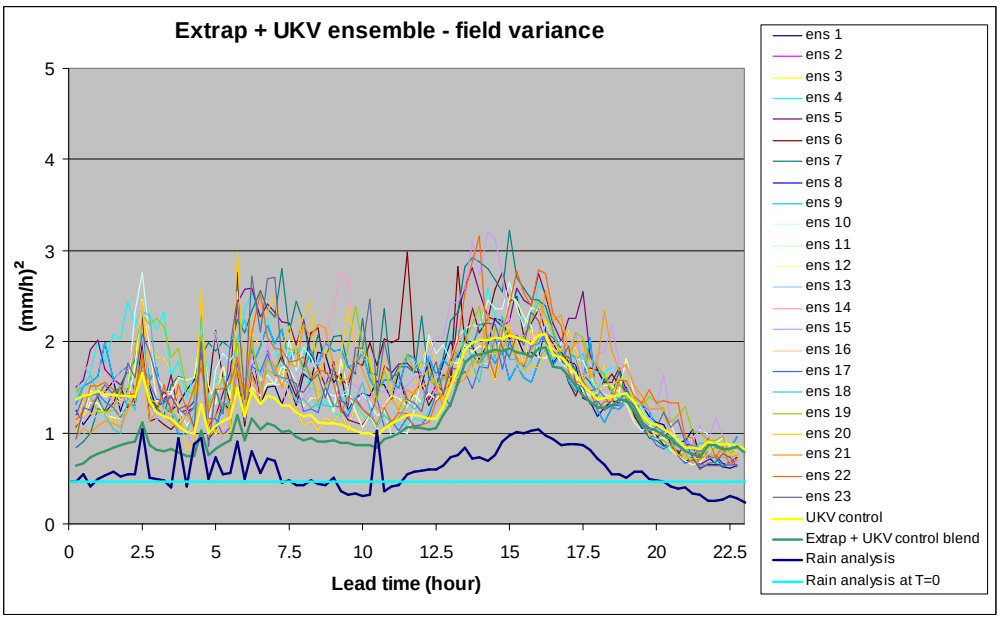

Figure A2.9 Time evolution of the field variance of UKPP rain analyses, a UKV control member forecast (data time 2100 GMT on 18/11/2009), and blended ensemble forecasts (data time 1000 GMT on 19/11/2009) comprising extrapolation, UKV and non-parametric noise. The forecast lead times on the X axis are those of the blended forecasts (run from 1000 GMT).

© Crown copyright 2010

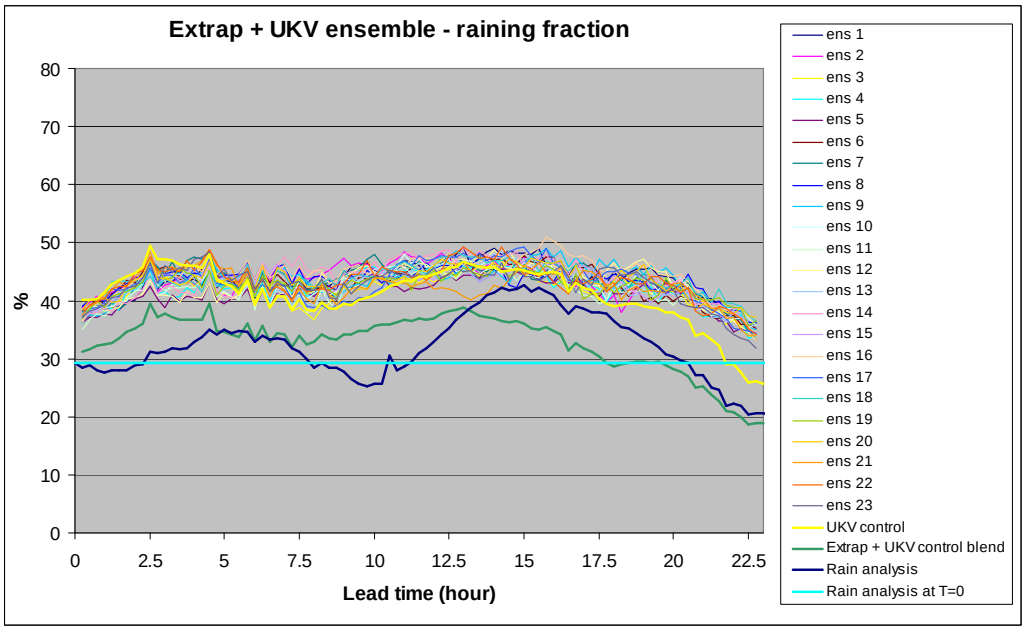

Figure A2.10 Time evolution of the field raining fraction of UKPP rain analyses, a UKV control member forecast (data time 2100 GMT on 18/11/2009), and blended ensemble forecasts (data time 1000 GMT on 19/11/2009) comprising extrapolation, UKV and non-parametric noise. The forecast lead times on the X axis are those of the blended forecasts (run from 1000 GMT).

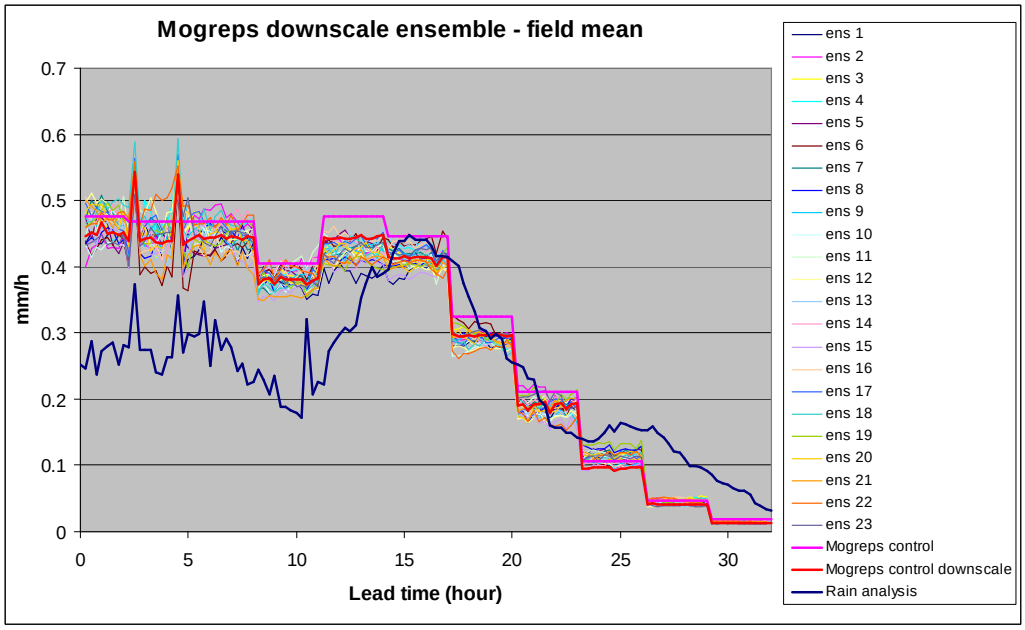

Figure A2.11 Time evolution of the field mean of UKPP rain analyses, a MOGREPS-R control member forecast (data time 1800 GMT on 18/11/2009), and control and ensemble blended forecasts (data time 1000 GMT on 19/11/2009) comprising MOGREPS-R and parametric noise. The forecast lead times on the X axis are those of the blended forecasts (run from 1000 GMT).

© Crown copyright 2010

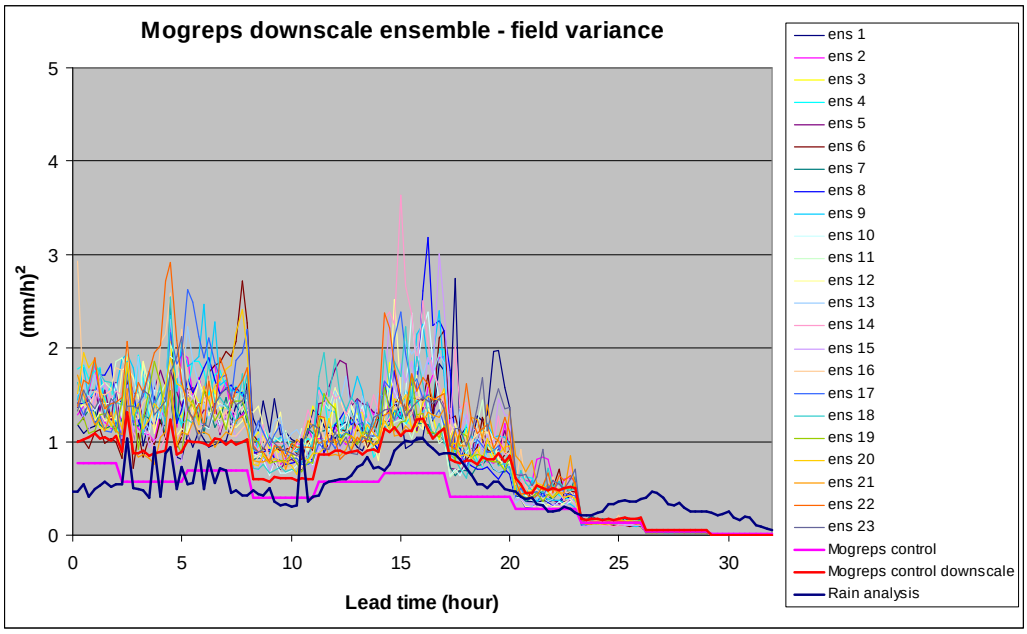

Figure A2.12 Time evolution of the field variance of UKPP rain analyses, a MOGREPS-R control member forecast (data time 1800 GMT on 18/11/2009), and control and ensemble blended forecasts (data time 1000 GMT on 19/11/2009) comprising MOGREPS-R and parametric noise. The forecast lead times on the X axis are those of the blended forecasts (run from 1000 GMT).

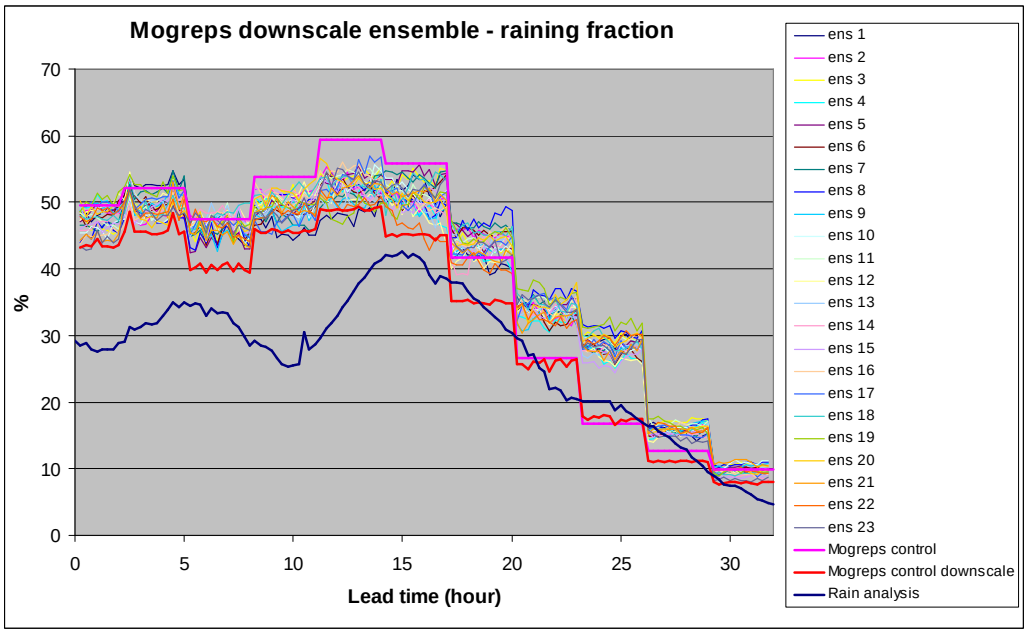

Figure A2.13 Time evolution of the field raining fraction of UKPP rain analyses, a MOGREPS-R control member forecast (data time 1800 GMT on 18/11/2009), and control and ensemble blended forecasts (data time 1000 GMT on 19/11/2009) comprising MOGREPS-R and parametric noise. The forecast lead times on the X axis are those of the blended forecasts (run from 1000 GMT).

© Crown copyright 2010

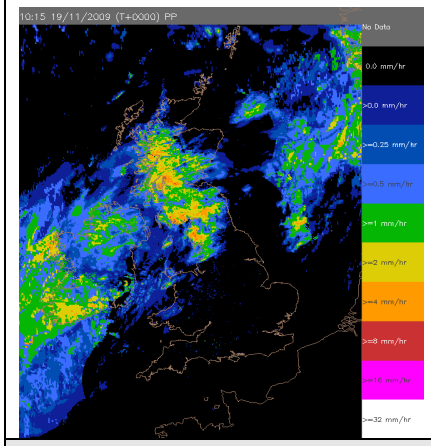	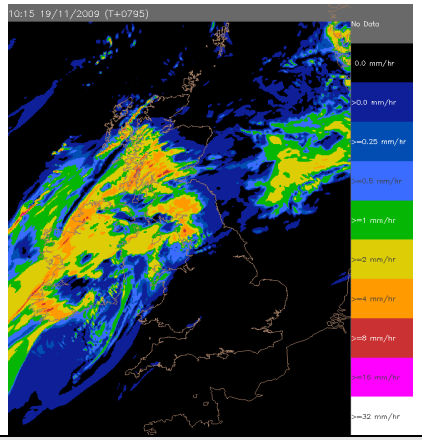	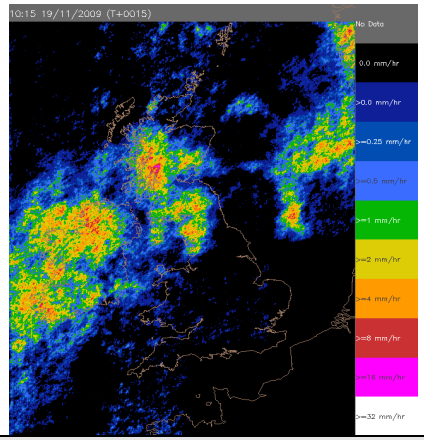	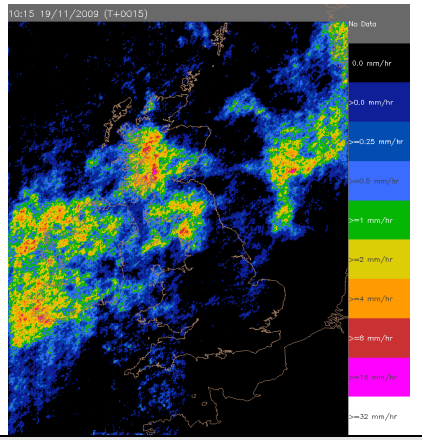
UKPP rain analysis valid at 1015 GMT on 19/11/2009	**T+13 h 15 min UKV control forecast valid at 1015 GMT on 19/11/2009**	**Member 1 of a T+15 min blend of an extrapolation nowcast, a UKV control forecast and non-parametric noise valid at 1015 GMT on 19/11/2009**	**Member 2 of a T+15 min blend of an extrapolation nowcast, a UKV control forecast and non-parametric noise valid at 1015 GMT on 19/11/2009**
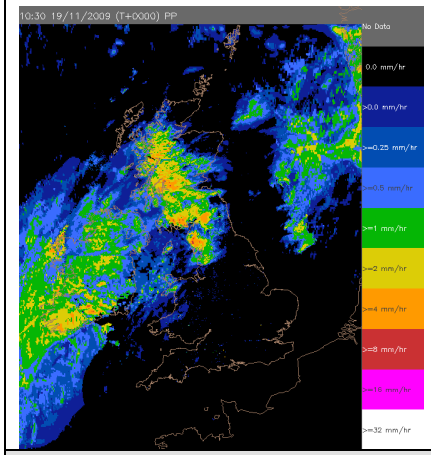	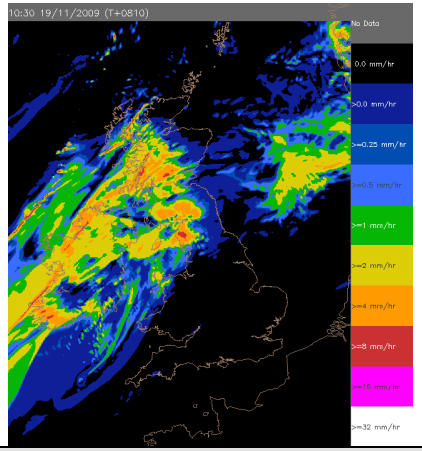	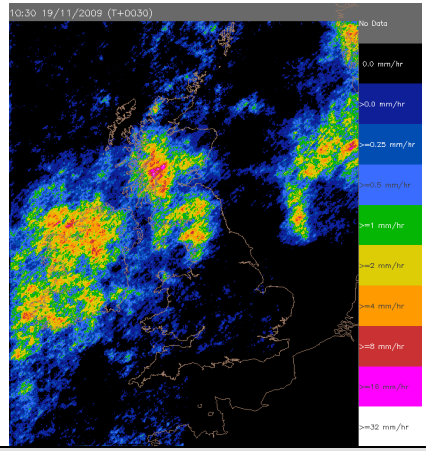	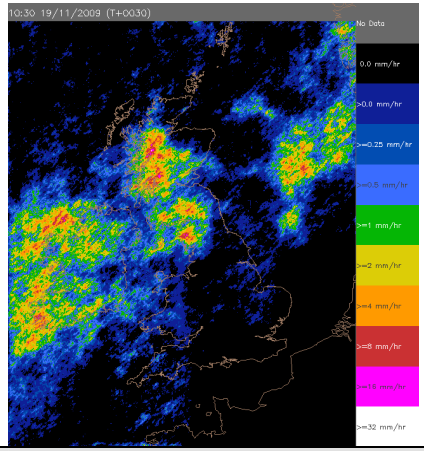
UKPP rain analysis valid at 1030 GMT on 19/11/2009	**T+13 h 30 min UKV control forecast valid at 1030 GMT on 19/11/2009**	**Member 1 of a T+30 min blend of an extrapolation nowcast, a UKV control forecast and non-parametric noise valid at 1030 GMT on 19/11/2009**	**Member 2 of a T+30 min blend of an extrapolation nowcast, a UKV control forecast and non-parametric noise valid at 1030 GMT on 19/11/2009**

© Crown copyright 2010

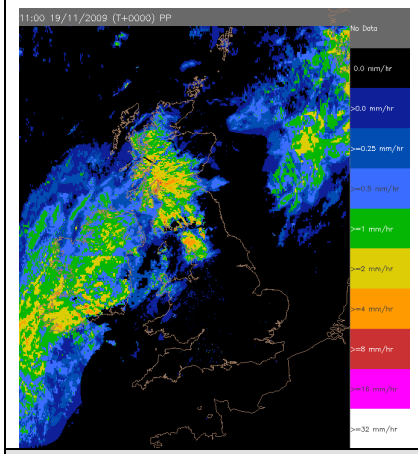	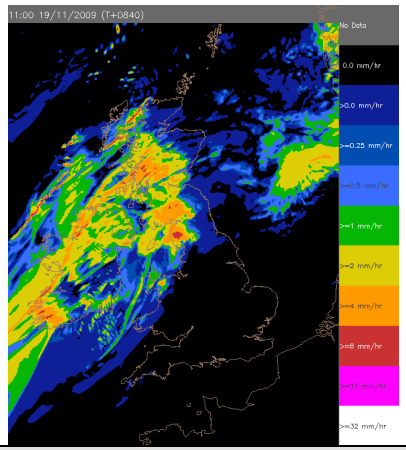	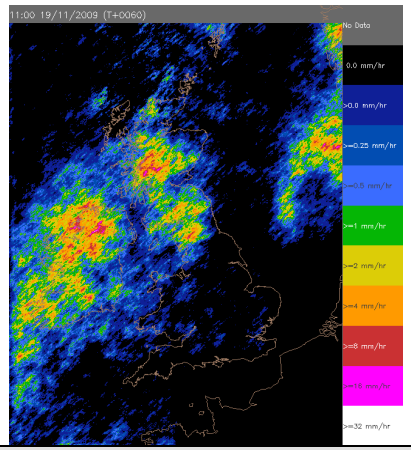	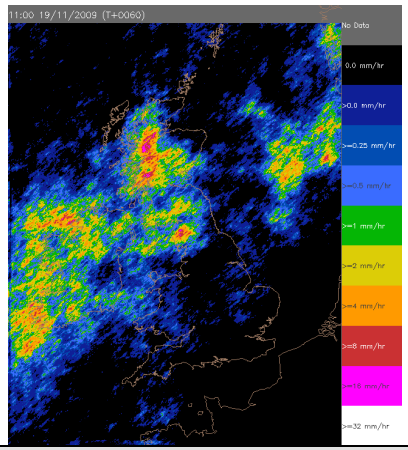
UKPP rain analysis valid at 1100 GMT on 19/11/2009	**T+14 h UKV control forecast valid at 1100 GMT on 19/11/2009**	**Member 1 of a T+1 h blend of an extrapolation nowcast, a UKV control forecast and non-parametric noise valid at 1100 GMT on 19/11/2009**	**Member 2 of a T+1 h blend of an extrapolation nowcast, a UKV control forecast and non-parametric noise valid at 1100 GMT on 19/11/2009**
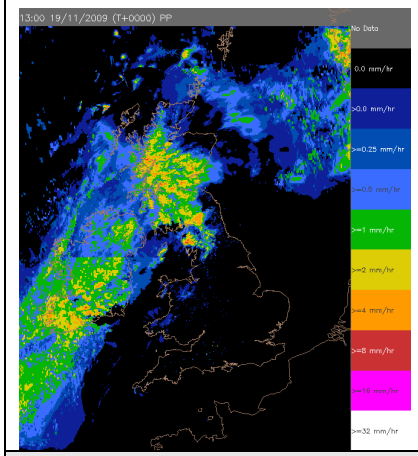	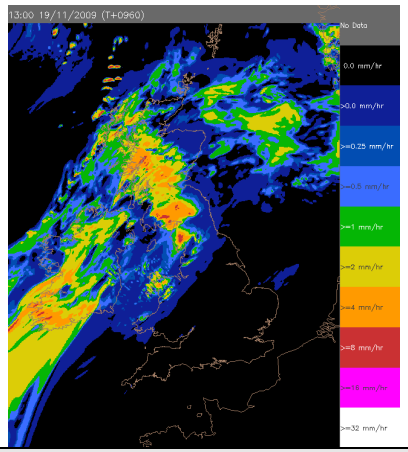	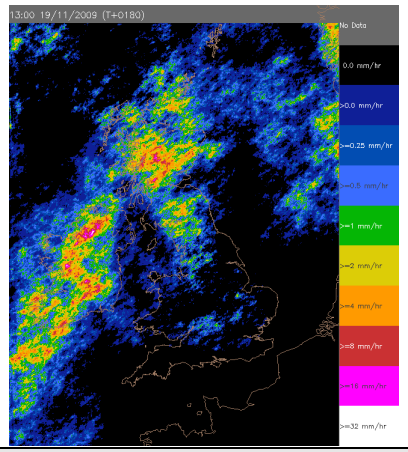	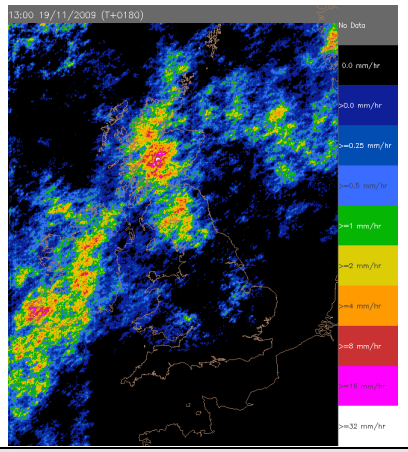
UKPP rain analysis valid at 1300 GMT on 19/11/2009	**T+16 h UKV control forecast valid at 1300 GMT on 19/11/2009**	**Member 1 of a T+3 h blend of an extrapolation nowcast, a UKV control forecast and non-parametric noise valid at 1300 GMT on 19/11/2009**	**Member 2 of a T+3 h blend of an extrapolation nowcast, a UKV control forecast and non-parametric noise valid at 1300 GMT on 19/11/2009**

© Crown copyright 2010

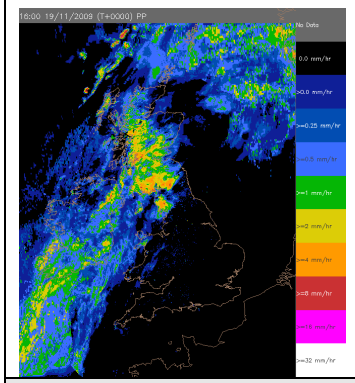

UKPP rain analysis valid at 1600 GMT on 19/11/2009

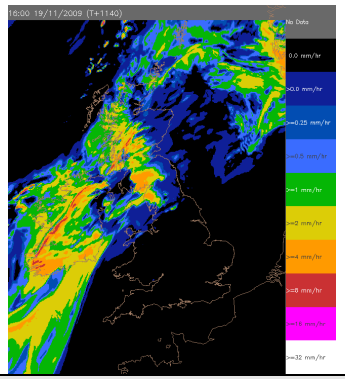

T+19 h UKV control forecast valid at 1600 GMT on 19/11/2009

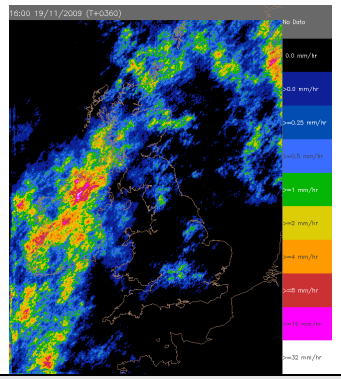

Member 1 of a T+6 h blend of an extrapolation nowcast, a UKV control forecast and non-parametric noise valid at 1600 GMT on 19/11/2009

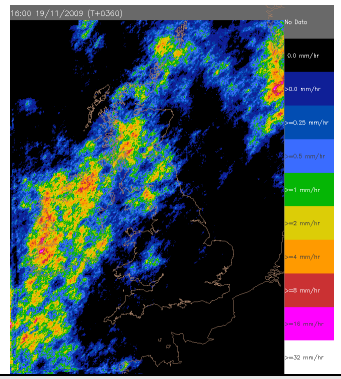

Member 2 of a T+6 h blend of an extrapolation nowcast, a UKV control forecast and non-parametric noise valid at 1600 GMT on 19/11/2009

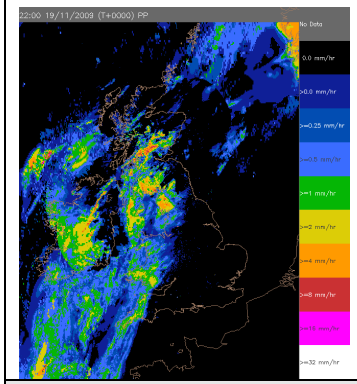

UKPP rain analysis valid at 2200 GMT on 19/11/2009

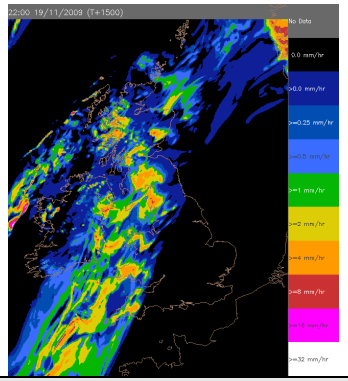

T+25 h UKV control forecast valid at 2200 GMT on 19/11/2009

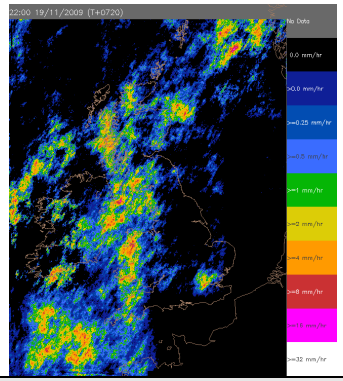

Member 1 of a T+12 h blend of an extrapolation nowcast, a UKV control forecast and non-parametric noise valid at 2200 GMT on 19/11/2009

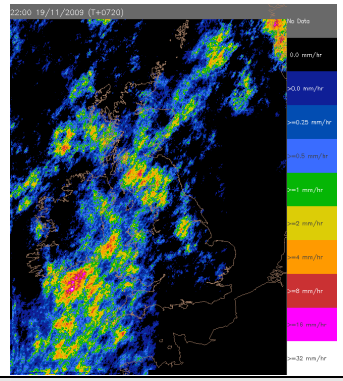

Member 2 of a T+12 h blend of an extrapolation nowcast, a UKV control forecast and non-parametric noise valid at 2200 GMT on 19/11/2009

Figure A2.14a Selected steps in two members of a blended ensemble forecast of precipitation rate, comprising an extrapolation nowcast, UKV control forecast and non-parametric noise, run from 1000 GMT on 19/11/2009. The UKPP rain analysis used as the starting point for the extrapolation nowcast is also shown, as well corresponding forecast steps from the associated UKV control member forecast (data time 2100 GMT, 18/11/2009).

© Crown copyright 2010

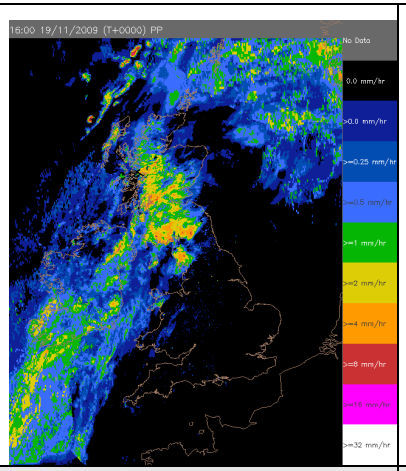

UKPP rain analysis valid at 1600 GMT on 19/11/2009

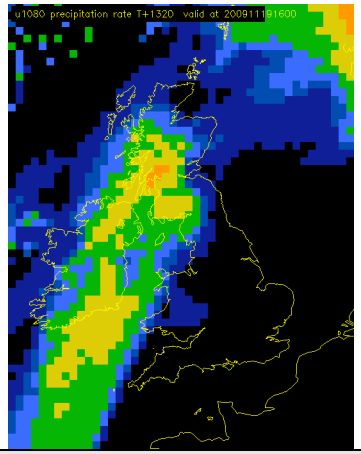

T+22 h MOGREPS-R control forecast valid at 1600 GMT on 19/11/2009

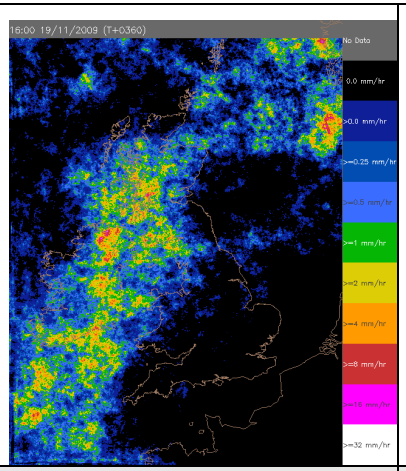

Member 1 of a T+22 h MOGREPS-R downscale ensemble forecast valid at 1600 GMT on 19/11/2009

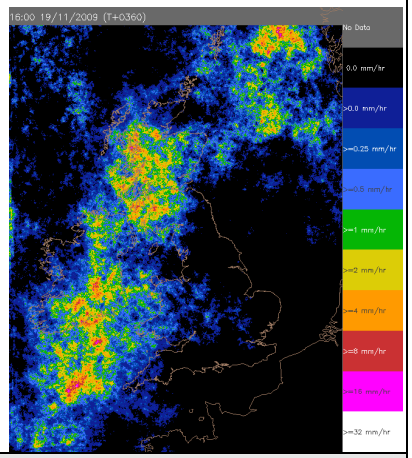

Member 2 of a T+22 h MOGREPS-R downscale ensemble forecast valid at 1600 GMT on 19/11/2009

© Crown copyright 2010

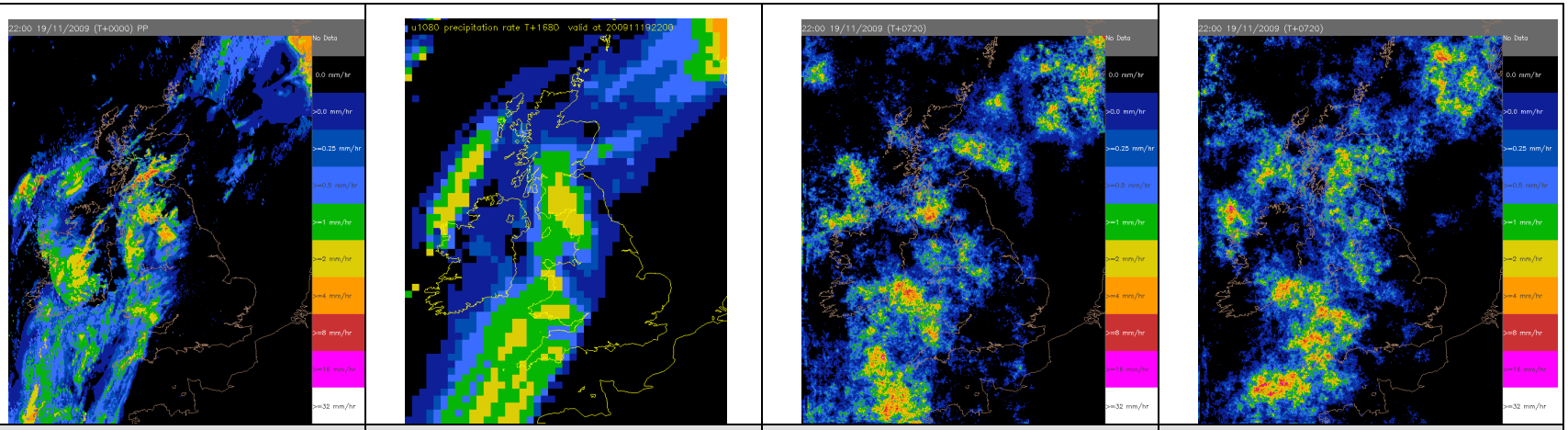

UKPP rain analysis valid at 2200 GMT on 19/11/2009	**T+28 h MOGREPS-R control forecast valid at 2200 GMT on 19/11/2009**	**Member 1 of a T+28 h MOGREPS-R downscale ensemble forecast valid at 2200 GMT on 19/11/2009**	**Member 2 of a T+22 h MOGREPS-R downscale ensemble forecast valid at 2200 GMT on 19/11/2009**

Figure A2.14b Selected forecast steps in two members of a blended ensemble forecast of precipitation rate, comprising a MOGREPS-R control forecast and parametric noise, run from 1000 GMT on 19/11/2009 (3rd column from left). A corresponding sequence of UKPP rain analyses and forecasts steps from the associated MOGREPS-R control forecast (data time 1800 GMT, 18/11/2009) are also shown for comparison.

© Crown copyright 2010

Case study 4 – 17/02/2010

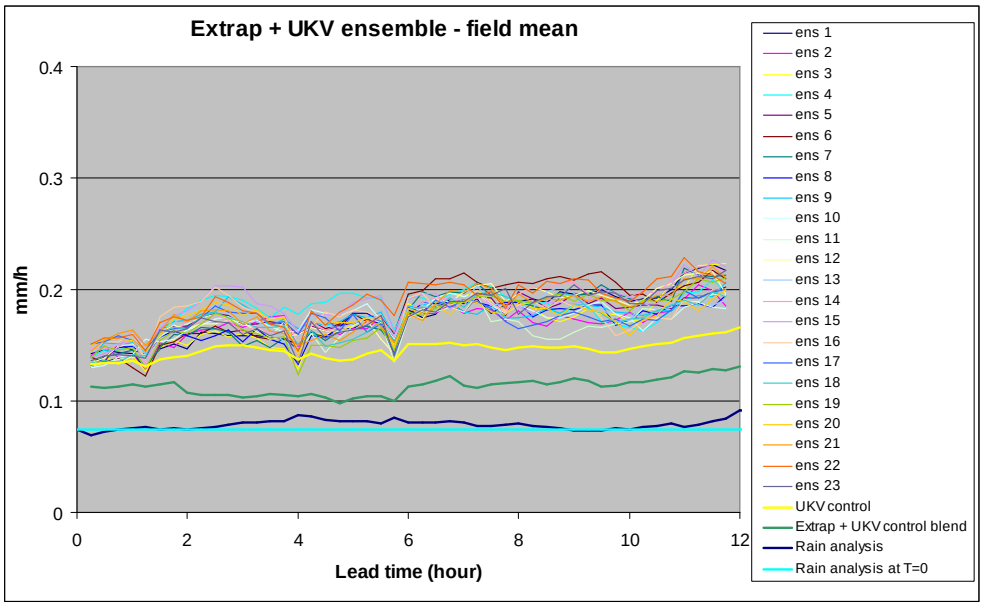

Figure A2.15 Time evolution of the field mean of UKPP rain analyses, a UKV control member forecast (data time 2100 GMT on 16/02/2010), and control and ensemble blended forecasts (data time 0900 GMT on 17/02/2010) comprising extrapolation, UKV and non-parametric noise. The forecast lead times on the X axis are those of the blended forecasts (run from 0900 GMT).

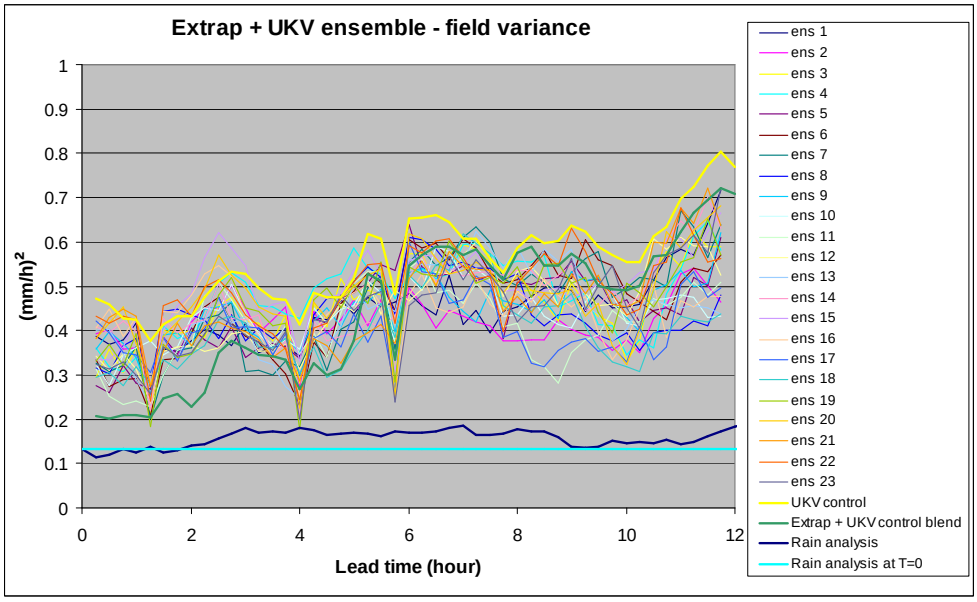

Figure A2.16 Time evolution of the field variance of UKPP rain analyses, a UKV control member forecast (data time 0900 GMT on 17/02/2010), and control and ensemble blended forecasts (data time 1300 GMT on 17/02/2010) comprising extrapolation, UKV and non-parametric noise. The forecast lead times on the X axis are those of the blended forecasts (run from 0900 GMT).

© Crown copyright 2010

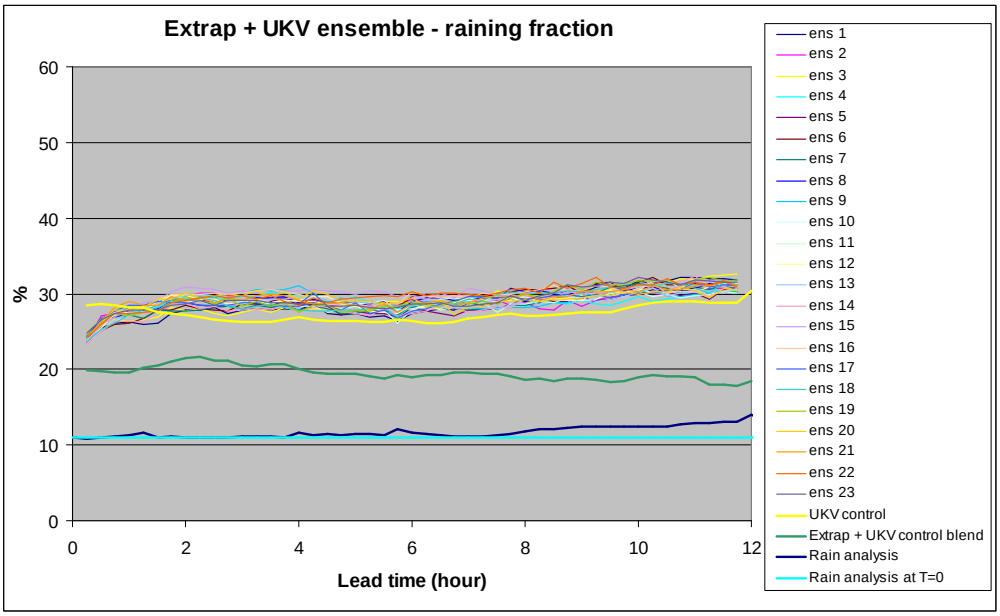

Figure A2.17 Time evolution of the field raining fraction of UKPP rain analyses, a UKV control member forecast (data time 0900 GMT on 17/02/2010), and control and ensemble blended forecasts (data time 0900 GMT on 17/02/2010) comprising extrapolation, UKV and non-parametric noise. The forecast lead times on the X axis are those of the blended forecasts (run from 0900 GMT).

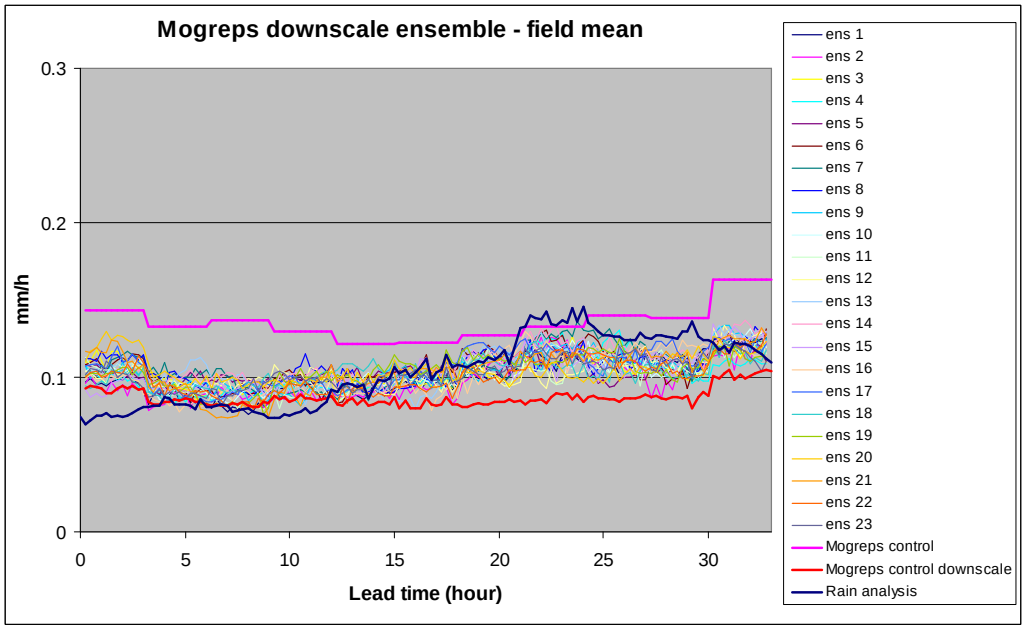

Figure A2.18 Time evolution of the field mean of UKPP rain analyses, a MOGREPS-R control member forecast (data time 1800 GMT on 16/02/2010), and control and ensemble blended forecasts (data time 0900 GMT on 17/02/2010) comprising MOGREPS-R and parametric noise. The forecast lead times on the X axis are those of the blended forecasts (run from 0900 GMT).

© Crown copyright 2010

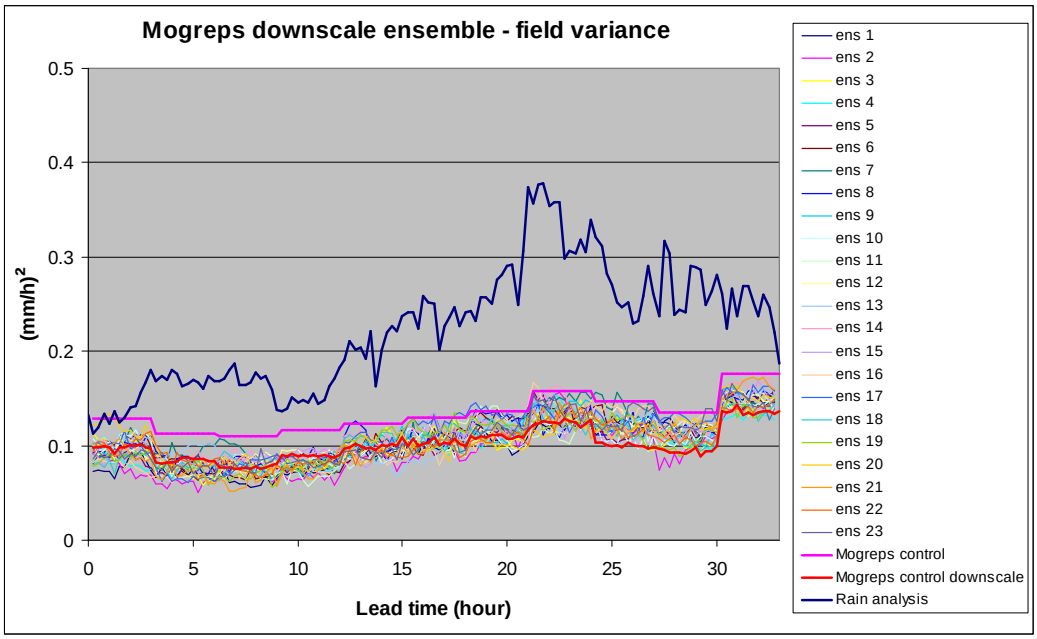

Figure A2.19 Time evolution of the field variance of UKPP rain analyses, a MOGREPS-R control member forecast (data time 1800 GMT on 16/02/2010), and control and ensemble blended forecasts (data time 0900 GMT on 17/02/2010) comprising MOGREPS-R and parametric noise. The forecast lead times on the X axis are those of the blended forecasts (run from 0900 GMT).

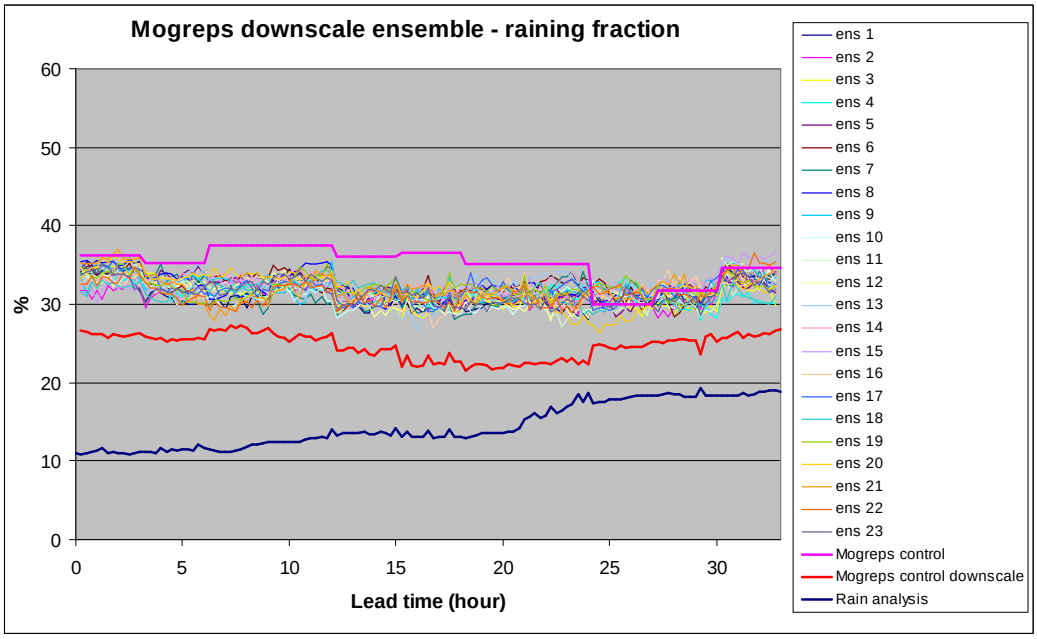

Figure A2.20 Time evolution of the field raining fraction of UKPP rain analyses, a MOGREPS-R control member forecast (data time 1800 GMT on 16/02/2010), and control and ensemble blended forecasts (data time 0900 GMT on 17/02/2010) comprising MOGREPS-R and parametric noise. The forecast lead times on the X axis are those of the blended forecasts (run from 0900 GMT).

© Crown copyright 2010

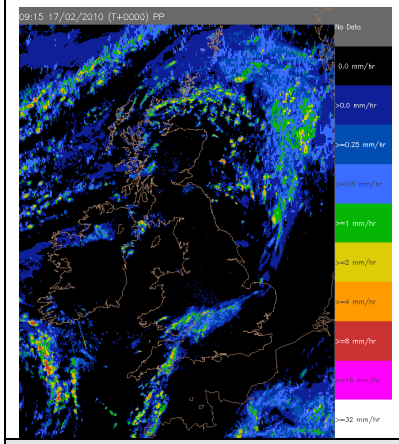	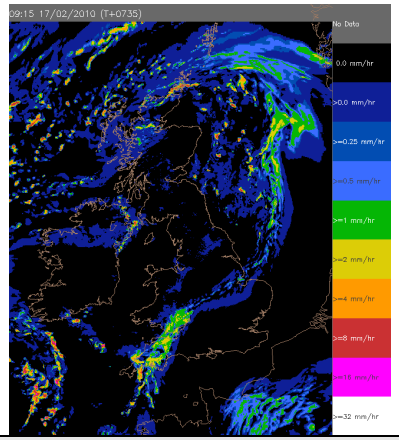	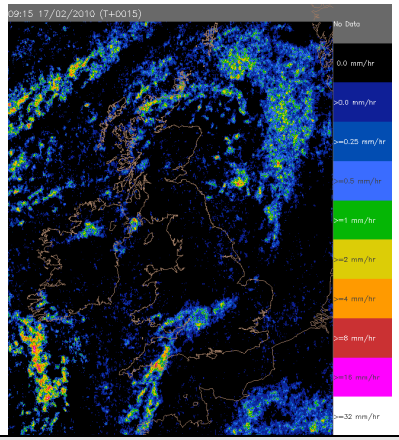	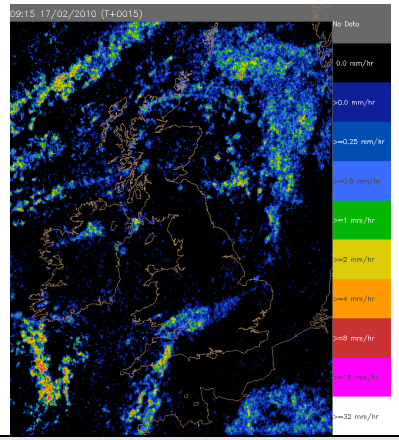
UKPP rain analysis valid at 0915 GMT on 17/02/2010	**T+12 h 15 min UKV control forecast valid at 0915 GMT on 17/02/2010**	**Member 1 of a T+15 min blend of an extrapolation nowcast, a UKV control forecast and non-parametric noise valid at 0915 GMT on 17/02/2010**	**Member 2 of a T+15 min blend of an extrapolation nowcast, a UKV control forecast and non-parametric noise valid at 0915 GMT on 17/02/2010**
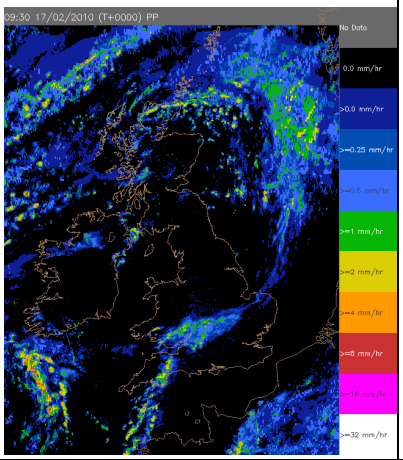	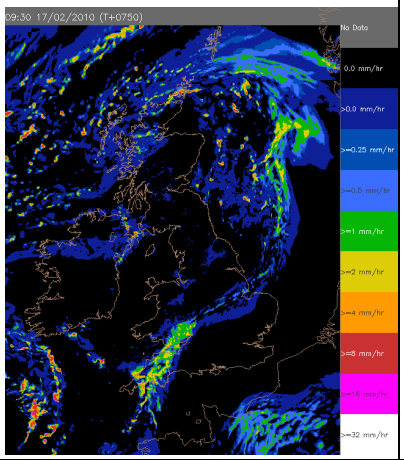	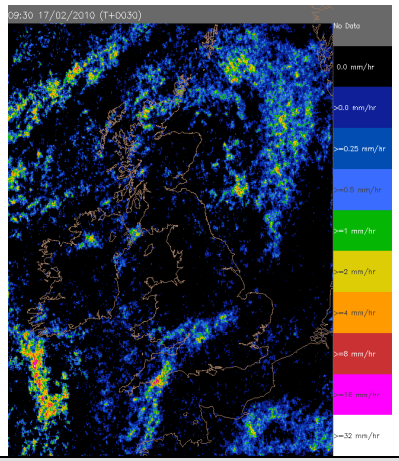	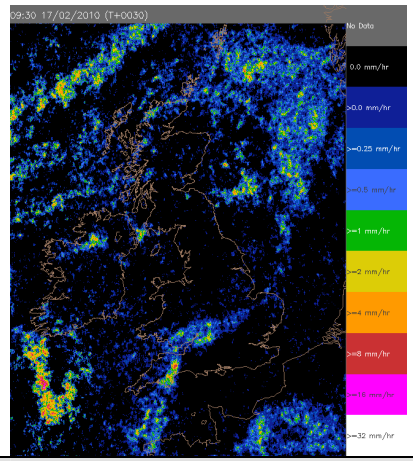
UKPP rain analysis valid at 0930 GMT on 17/02/2010	**T+12 h 30 min UKV control forecast valid at 0930 GMT on 17/02/2010**	**Member 1 of a T+30 min blend of an extrapolation nowcast, a UKV control forecast and non-parametric noise valid at 0930 GMT on 17/02/2010**	**Member 2 of a T+30 min blend of an extrapolation nowcast, a UKV control forecast and non-parametric noise valid at 0930 GMT on 17/02/2010**

© Crown copyright 2010

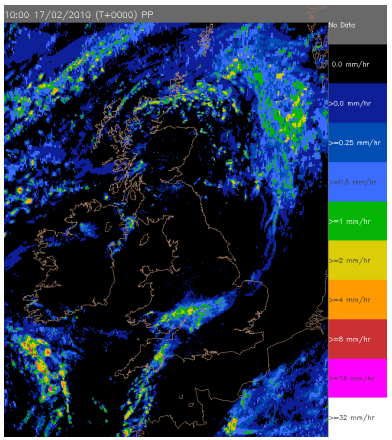	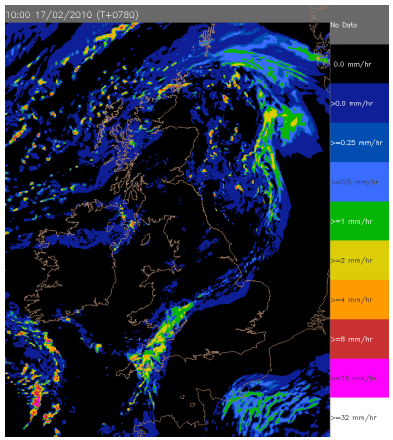	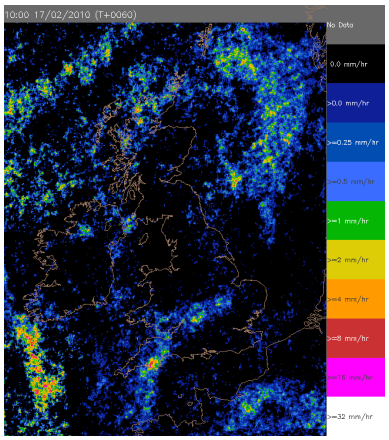	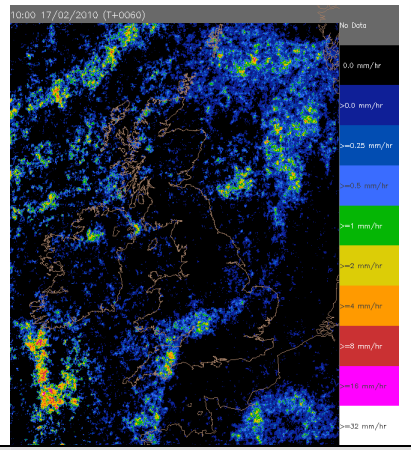
UKPP rain analysis valid at 1000 GMT on 17/02/2010	**T+13 h UKV control forecast valid at 1000 GMT on 17/02/2010**	**Member 1 of a T+1 h blend of an extrapolation nowcast, a UKV control forecast and non-parametric noise valid at 1000 GMT on 17/02/2010**	**Member 2 of a T+1 h blend of an extrapolation nowcast, a UKV control forecast and non-parametric noise valid at 1000 GMT on 17/02/2010**
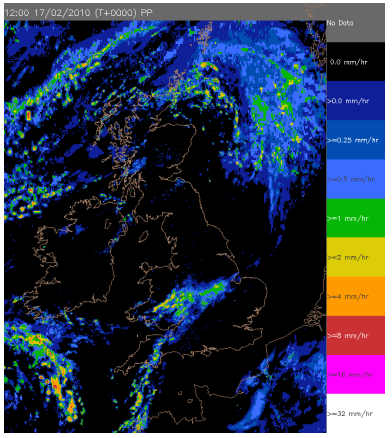	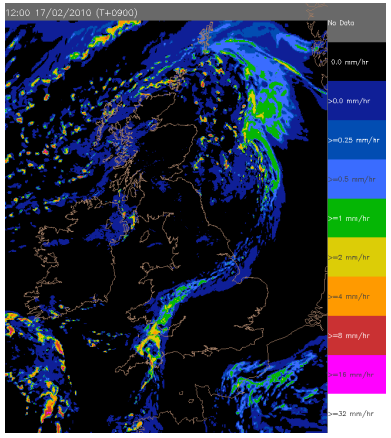	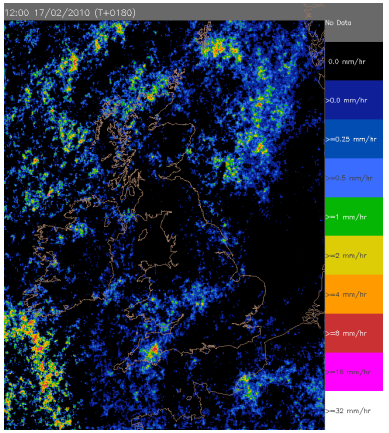	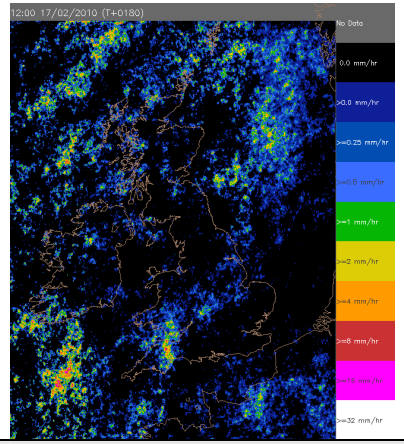
UKPP rain analysis valid at 1200 GMT on 17/02/2010	**T+15 h UKV control forecast valid at 1200 GMT on 17/02/2010**	**Member 1 of a T+3 h blend of an extrapolation nowcast, a UKV control forecast and non-parametric noise valid at 1200 GMT on 17/02/2010**	**Member 2 of a T+3 h blend of an extrapolation nowcast, a UKV control forecast and non-parametric noise valid at 1200 GMT on 17/02/2010**

© Crown copyright 2010

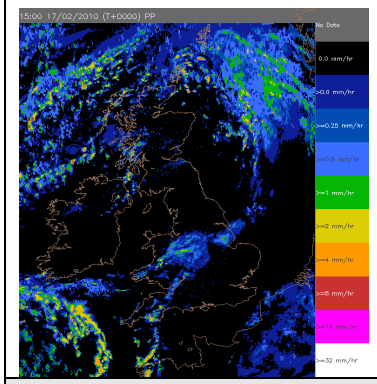

UKPP rain analysis valid at 1500 GMT on 17/02/2010

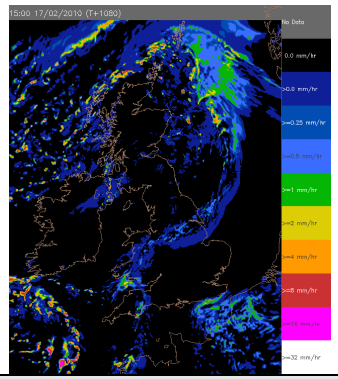

T+18 h UKV control forecast valid at 1500 GMT on 17/02/2010

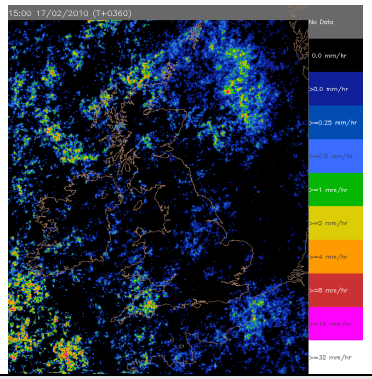

Member 1 of a T+6 h blend of an extrapolation nowcast, a UKV control forecast and non-parametric noise valid at 1500 GMT on 17/02/2010

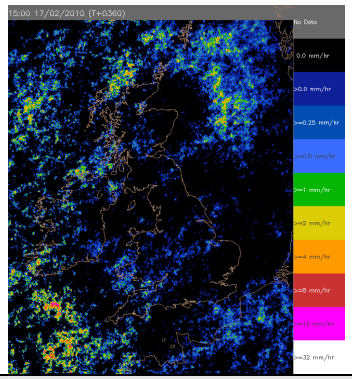

Member 2 of a T+6 h blend of an extrapolation nowcast, a UKV control forecast and non-parametric noise valid at 1500 GMT on 17/02/2010

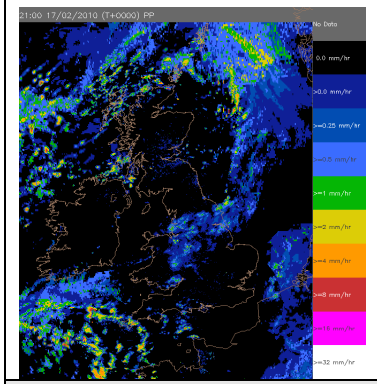

UKPP rain analysis valid at 2100 GMT on 17/02/2010

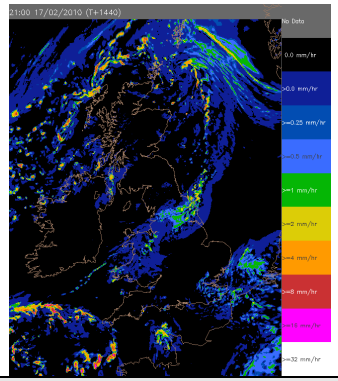

T+24 h UKV control forecast valid at 2100 GMT on 17/02/2010

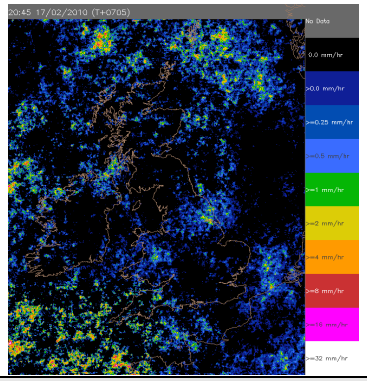

Member 1 of a T+12 h blend of an extrapolation nowcast, a UKV control forecast and non-parametric noise valid at 2100 GMT on 17/02/2010

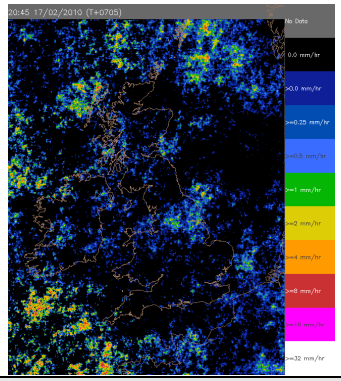

Member 2 of a T+12 h blend of an extrapolation nowcast, a UKV control forecast and non-parametric noise valid at 2100 GMT on 17/02/2010

Figure A2.21a Selected steps in two members of a blended ensemble forecast of precipitation rate, comprising an extrapolation nowcast, UKV control forecast and non-parametric noise, run from 0900 GMT on 17/02/2010. The UKPP rain analysis used as the starting point for the extrapolation nowcast is also shown, as well corresponding forecast steps from the associated UKV control member forecast (data time 2100 GMT, 16/02/2010).

© Crown copyright 2010

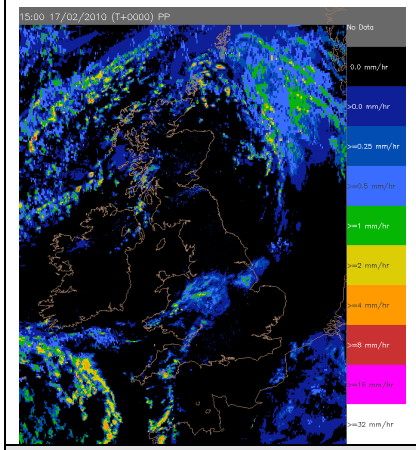	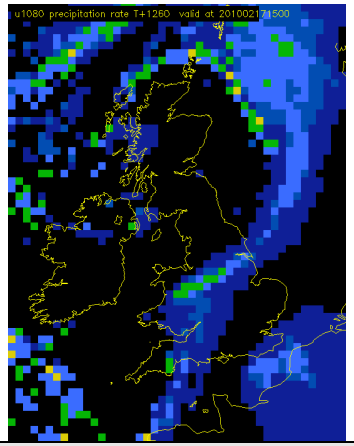	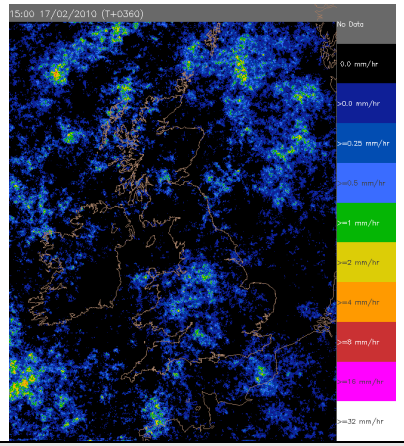	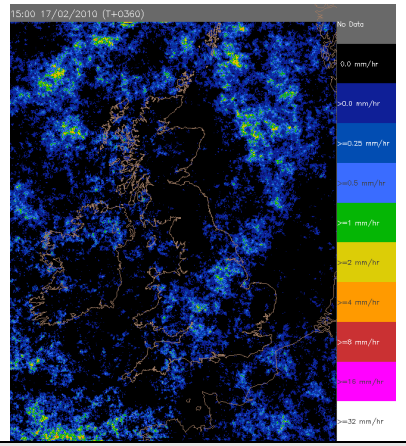
UKPP rain analysis valid at 1500 GMT on 17/02/2010	**T+21 h MOGREPS-R control forecast valid at 1500 GMT on 17/02/2010**	**Member 1 of a T+21 h MOGREPS-R downscale ensemble forecast valid at 1500 GMT on 17/02/2010**	**Member 2 of a T+21 h MOGREPS-R downscale ensemble forecast valid at 1500 GMT on 17/02/2010**

© Crown copyright 2010

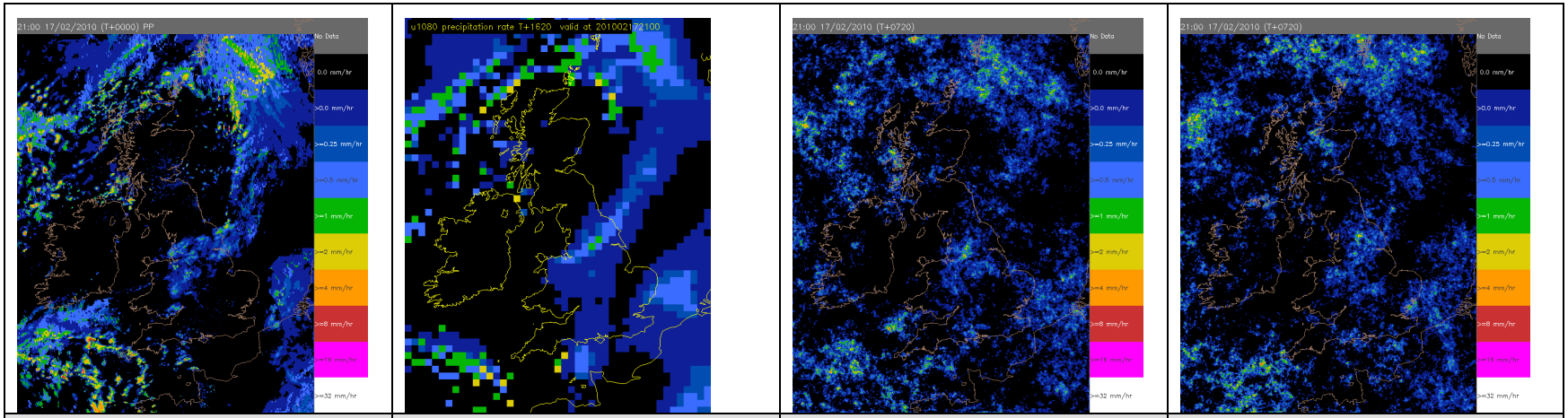

UKPP rain analysis valid at 2100 GMT on 17/02/2010	**T+27 h MOGREPS-R control forecast valid at 2100 GMT on 17/02/2010**	**Member 1 of a T+27 h MOGREPS-R downscale ensemble forecast valid at 2100 GMT on 17/02/2010**	**Member 2 of a T+21 h MOGREPS-R downscale ensemble forecast valid at 2100 GMT on 17/02/2010**

Figure A2.21b Selected forecast steps in two members of a blended ensemble forecast of precipitation rate, comprising a MOGREPS-R control forecast and parametric noise, run from 0900 GMT on 17/02/2010 (3rd column from left). A corresponding sequence of UKPP rain analyses and forecasts steps from the associated MOGREPS-R control forecast (data time 1800 GMT, 16/02/2010) are also shown for comparison.

© Crown copyright 2010

Met Office:
FitzRoy Road, Exeter
Devon, EX1 3PB
UK

Tel: +44(0)1392 885680
Fax: +44(0)1392 885681
enquiries@metoffice.gov.uk
www.metoffice.gov.uk